ANALYTICA CHIMICA ACTA

International monthly devoted to all branches of analytical chemistry
Revue mensuelle internationale consacrée à tous les domaines de la chimie analytique
Internationale Monatsschrift für alle Gebiete der analytischen Chemie

ELSEVIER SCIENTIFIC PUBLISHING COMPANY

AMSTERDAM

Anal. Chim. Acta, Vol. 82, No. 1, 1–230, March 1976
Published monthly

ANALYTICA CHIMICA ACTA

Publication Schedule for 1976

Vol. 81, No. 1	January 1976	
Vol. 81, No. 2	February 1976	**(completing Vol. 81)**
Vol. 82, No. 1	March 1976	
Vol. 82, No. 2	April 1976	**(completing Vol. 82)**
Vol. 83	May 1976	**(complete in one issue)**
Vol. 84, No. 1	June 1976	
Vol. 84, No. 2	July 1976	**(completing Vol. 84)**
Vol. 85, No. 1	August 1976	
Vol. 85, No. 2	September 1976	**(completing Vol. 85)**
Vol. 86	October 1976	**(complete in one issue)**
Vol. 87, No. 1	November 1976	
Vol. 87, No. 2	December 1976	**(completing Vol. 87)**

Subscription price for 1976 (covering November '75/December '76, Vols. 80–87): Dfl. 840.00 plus Dfl. 96.00 postage. Subscribers in the U.S.A. and Canada receive their copies by airmail. Additional charges for airmail to other countries are available on request. For advertising rates apply to the publishers.

Subscriptions should be sent to:
Elsevier Scientific Publishing Company, P.O. Box 211, Amsterdam, The Netherlands.

GENERAL INFORMATION

Languages

Papers will be published in English, French or German.

Detailed information

Authors should consult Vol. 73, p. 435 for detailed instructions. Reprints of this information are obtainable from Dr. Macdonald or from: Elsevier Editorial Services Ltd., Mayfield House, 256 Banbury Road, Oxford (Great Britain).

Submission of papers

Papers should be sent to:

Prof. Philip W. West,
Coates Chemical Laboratories,
College of Chemistry and Physics,
Louisiana State University,
Baton Rouge 3,
La. 70803 (U.S.A.)

or to:

Dr. A.M.G. Macdonald,
Department of Chemistry,
The University,
P.O. Box 363
Birmingham B15 2TT (Great Britain)

Reprints

Fifty reprints will be supplied free of charge. Additional reprints (minimum 100) can be ordered at quoted prices. They must be ordered on order forms which are sent together with the proofs.

Wilson and Wilson's

Comprehensive Analytical Chemistry

edited by **G. SVEHLA**, Reader in Analytical Chemistry,
The Queen's University of Belfast.

Volume IV - INSTRUMENTATION FOR SPECTROSCOPY
ANALYTICAL ATOMIC ABSORPTION AND FLUORESCENCE SPECTROSCOPY
DIFFUSE REFLECTANCE SPECTROSCOPY

1975 392 pages
US $51.95/Dfl. 125.00 (Subscription price: US $44.25/Dfl. 106.00)
ISBN 0-444-41163-1

Volume IV in the series "Comprehensive Analytical Chemistry" features spectroscopy as its theme.
The book is divided into three main sections. The first part deals with instrumentation and aims at assisting the spectroscopist in the selection of the correct instruments and experimental conditions for measurement. The second section — Analytical Atomic Absorption and Fluorescence Spectroscopy, as well as the last part — Diffuse Reflectance Spectroscopy, cover modern techniques widely used in analytical laboratories. Extensive lists of references are provided as a guide for the search of further information.

From Reviews of Earlier Volumes:

"I warn every practising analytical chemist and every chemical librarian that he had better become resigned to purchasing each volume as it appears."
— Science

"There is no doubt whatsoever that an authoritative book of this nature will find its way on to the bookshelves of all institutions dealing with either the practise or teaching of analytical chemistry and will retain its status as a unique 'vade mecum' for many years to come."
— Nature

Elsevier
P.O. Box 211
Amsterdam, The Netherlands

1595 E

Isotopes in Organic Chemistry

edited by E. BUNCEL, Queen's University, Kingston, Ontario, Canada, and C.C. LEE, University of Saskatchewan, Saskatoon, Saskatchewan, Canada.
with a foreword by LARS MELANDER

Volume 1:
Isotopes in Molecular Rearrangements

1975. 318 pages. US $ 41.75/Dfl. 100.00. ISBN 0-444-41223-9

The value of the series of which the present work is the first volume lies in theaid that the surveys it contains will offer the research worker, and, equally important, the stimulus it provides for further research. As a whole, it will highlight the use and value of isotopes in diverse areas of organic chemistry, while each volume, containing a number of articles by experts in the field, will be devoted to one major area of current interest. An Editorial Advisory Board advises on the selection of topics.

Five active research workers in the field contributed to the present book, covering the broad area of isotopes in molecular rearrangements. The topics dealt with include the chemistry of carbonium ions, carbanions, photochemical studies, mass spectral fragmentations, and pericyclic reactions, with emphasis on isotope effects, labelling studies, reaction mechanisms, etc., in the overall context of molecular rearrangements. Lecturers, students and research workers in the field will particularly welcome this indispensable reference source and can certainly look forward to many useful future volumes in the series. Volumes 2 and 3, now in preparation, are entitled "Isotopes in Hydrogen Transfer Processes" and "Carbon-13 in Organic Chemistry" respectively.

ELSEVIER SCIENTIFIC PUBLISHING COMPANY

P.O.Box 211, Amsterdam, The Netherlands

Distributed in the U.S.A. and Canada by:
American Elsevier Publishing Company, Inc.,
52 Vanderbilt Ave., New York, N.Y. 10017

1670 E

Surface Properties of Materials

Proceedings of the Conference on Surface Properties of Materials, University of Missouri-Rolla, 24-27 June, 1974

edited by LEONARD L. LEVENSON, University of Missouri-Rolla, Rolla, Missouri, U.S.A.

Reprinted from the journal *Surface Science, Vol. 48, No. 1*

1975. 304 pages. US $ 37.50/Dfl. 90.00.
ISBN 0-7204-0327-8

Surfaces possess a variety of properties which make them important in many areas of science and technology such as solid state physics, chemistry, chemical and electrical engineering, biology and medicine. A number of methods have been developed to characterize surfaces and much can be learned about them from the way in which particles such as electrons, photons and molecules are scattered, adsorbed or transmitted.

The participants of the conference have contributed to the advancement and application of these techniques, among them being Dr. Pierre Auger, who describes the circumstances of his discovery of the Auger effect and expounds his views on subsequent applications.

The papers presented in these proceedings, which include detailed theoretical and experimental treatments of particle-surface interactions, are indicative of the rapid changes taking place in the whole field of surface science. Auger electron, photoemission, appearance potential, ion scattering, secondary ion emission, infra-red and other spectroscopies are constantly evolving and theoretical treatments are becoming more successful in accounting for and often predicting experimental results.

north-holland P.O. BOX 211 AMSTERDAM THE NETHERLANDS

1673 NH

Distributed in the U.S.A. and Canada by
American Elsevier Publishing Company, Inc., 52 Vanderbilt Avenue, New York, N.Y. 10017

ANALYTICA CHIMICA ACTA
Vol. 82 (1976)

ANALYTICA CHIMICA ACTA

International monthly devoted to all branches of analytical chemistry
Revue mensuelle internationale consacrée à tous les domaines de la chimie analytique
Internationale Monatsschrift für alle Gebiete der analytischen Chemie

ELSEVIER SCIENTIFIC PUBLISHING COMPANY

AMSTERDAM

PRINTED IN THE NETHERLANDS

Analytica Chimica Acta, 82 (1976) 1—17

STANDARDIZATION OF METHODS FOR THE DETERMINATION OF TRACES OF SOME VOLATILE CHLORINATED ALIPHATIC HYDROCARBONS IN AIR AND WATER BY GAS CHROMATOGRAPHY*

The Bureau International Technique des Solvants Chlorés, B.I.T.-S.C., 49 Square Marie-Louise, Bruxelles 4 (Belgium)

(Received 16th June 1975)

SUMMARY

Methods are described for the routine determination of some volatile chlorinated aliphatic hydrocarbons in environmental samples of air and water. The procedures are based on gas chromatography with electron-capture detection. The chlorinated compounds are determined in the ranges 1—100 ng l^{-1} of air and 0.01—10 $\mu g\ kg^{-1}$ of water. The overall repeatability of both methods is 20 % relative. The procedures are easily adapted to the determination of other volatile halogenated materials.

In the past few years there has been concern over the environmental effects of the release of organic chlorine compounds such as the chlorinated pesticides and polychlorinated biphenyls (PCB). This has led to the question of the extent to which industrial chlorinated solvents such as 1,1,1-trichloroethane, trichloroethylene and perchloroethylene, might also be entering the environment. Despite the recovery of solvents, there are handling losses and these are reflected by the world production capacities. Certain other products such as chloroform and carbon tetrachloride are important, but their use as intermediates means that their losses are smaller. However, from processes using intermediates, by-products arise which include tetrachloro-, pentachloro- and hexachloroethanes as well as chlorinated butadienes. In the past these by-products have found their way into the environment, although they are now largely destroyed or reused.

To obtain data on the existing distribution of chlorinated solvents, the European manufacturers have been co-operating via the Bureau International Technique des Solvants Chlorés (B.I.T.-S.C.) in the development of general methods for the determination of chlorinated solvents at trace concentrations.

Compared with the extensive analytical literature on pesticides and PCB, there have been few publications on measurements of traces of chlorinated solvents. All have used gas chromatography in order to separate the

---

*A report prepared by the Analysis Working Group of the Bureau International Technique des Solvants Chlorés. The members of the Working Group responsible for its preparation were A. A. Deetman, P. Demeulemeester, M. Garcia, G. Hauck, J. I. Hollies, D. Krockenberger, D. E. Palin, H. Prigge, L. Rohrschneider, L. Schmidhammer.

compounds, usually in conjunction with an electron capture detector (e.c.d.) to achieve partial selectivity for organo-chlorine compounds and the sensitivity necessary to measure concentrations approaching ca. 1 ng l^{-1} in air and 0.01 μg kg^{-1} in water.

For air samples, preconcentration by adsorption on charcoal has been used [1, 2] followed by heating and desorption into a cold trap filled with chromatographic packing which was subsequently purged into a chromatograph. However, recovery of adsorbates from charcoal, either by heating or solvent extraction, is uncertain so that thermally stable porous polymers have been tried instead [3], sometimes with the chromatograph combined with a mass spectrometer [4]. The latter approach, whilst very effective, is expensive and requires very good chromatographic separation. Carbon tetrachloride has been measured in air [5, 6] with a novel e.c.d. capable of coulometric measurements [7, 8]; the absolute response of this detector avoids the need for regular calibration but it is not available commercially. A variation, with two ^{63}Ni e.c. detectors connected in series, has been used recently to measure halocarbons including carbon tetrachloride, trichloroethylene, perchloroethylene and 1,1,1-trichloroethane [9]. A simpler method in which air was sampled with a gas syringe and injected via a sample loop into a conventional e.c.d. gas chromatograph has been used for fluorocarbons [10], and was chromatographically suitable for carbon tetrachloride, trichloroethylene and perchloroethylene.

For water samples, a procedure has been employed based on sparging the sample with highly purified inert gas followed by trapping and gas chromatography, analogous to trapping in air analysis [1, 2]. However, a limiting factor was that compounds which boil considerably above 100 °C could not be determined [11]. A different approach was to pass the water through a bed of activated carbon which was subsequently extracted exhaustively in a Soxhlet, and the extract was evaporated and analysed; this measured perchloroethylene and hexachloroethane but the results were uncertain quantitatively [12]. A method has been published by which the water sample was codistilled with cyclohexane, and the organic phase was then injected into an e.c.d. gas chromatograph but the method description was incomplete [13]. Extraction with n-pentane followed by gas chromatography has also been used [14], but although the extraction was easy and effective, the chromatographic conditions described were time-consuming and unsuitable for compounds heavier than perchloroethylene.

DEVELOPMENT OF THE METHODS

For general routine methods, gas chromatography with e.c.d. was the obvious technique: the options lay in the sample handling/pretreatment and in the chromatographic conditions. For air, direct sampling into a flask and syringe injection into the chromatograph was preferred to trapping, because for sampling and calibration the same simple glassware could be used and the

chromatographic results were easy to reproduce. Peak retentions were also more certain because in trapping procedures desorption times are not very reproducible and peak broadening may also occur. For water, headspace procedures were considered but rejected as unsuitable for the less volatile polychlorinated compounds. Instead, solvent extraction was selected; trials showed that 95 % of chlorinated compounds could be recovered in a single extraction, and n-pentane was chosen as the solvent, for it could be obtained readily in sufficient purity without further treatment. To dry the extract, anhydrous sodium sulphate was found to be effective. Furthermore, this drying agent could be freed from electron-capturing contaminants by heating [15], and did not adsorb the chlorinated compounds.

For both air and water, the methods specify temperature programming; this is to achieve reasonably short chromatogram times and to sharpen the peaks for ease and precision of measurement. No single column was found to be adequate for all the compounds named, so that two columns are named, one containing Apiezon-L for air analysis, the other containing Dexsil-300 for water. Under the specified conditions all the compounds are separated, with the exception of carbon tetrachloride and 1,1,1-trichloroethane which are resolved only on the Apiezon-L column. Therefore this column is given as an option for the analysis of water with the proviso that it is not suitable for samples containing the less volatile compounds ('heavies'). Whilst Apiezon-L and Dexsil-300 columns are recommended for general use, other columns may be as suitable. The methods can be adapted readily to suit widely differing sample compositions by altering the column geometry and packing. For example, natural waters which have been treated with chlorine may contain chlorobromomethanes [16] which can interfere with the determination of chloroform and trichloroethylene. In this event it is advisable to augment the analysis by repeating the chromatography with a column containing Oxydipropionitrile packing which will separate the bromine compounds from the chlorinated solvents. In general, when the identity of a peak is doubtful, it is advantageous to chromatograph the sample on several different columns.

The type of detector specified, ^{63}Ni, is suitable for the operating temperature (300 °C) specified in order to avoid condensation by 'heavies' and other contaminants which could reduce its sensitivity. Tritiated titanium detectors cannot be used at this temperature [17]. The methods also specify tests, to check the detector sensitivity, and if needed, decontamination procedures. These measures also help to achieve sufficient linearity to avoid having to match closely the concentrations of the calibration standards to the samples, a tedious or hit-and-miss problem.

Some difficulties may arise from contamination. Therefore the methods describe means of checking that the materials, reagents and apparatus are free from contamination, the prime offenders being grease and cutting oil. In particular the water method specifies a glove-box for sample preparation. In general, it is wise to exclude chlorinated solvents from the laboratory and if

the ambient air is suspect, to blanket the inject port of the chromatograph with clean nitrogen.

The layout of the following methods is based on the recommendations of the International Organisation for Standardisation [18].

METHOD A. DETERMINATION OF TRACE VOLATILE CHLORINATED ALIPHATIC HYDROCARBONS IN AIR BY GAS CHROMATOGRAPHY

Scope and field of application

The method covers the determination in air of the compounds chloroform, carbon tetrachloride, 1,1,1-trichloroethane, trichloroethylene, and perchloroethylene in the concentration range 1—100 ng l^{-1} for each compound.

Principle

A 250-ml sample is collected in a glass flask. A 2-ml portion is taken from the flask by means of a gas-tight syringe and injected directly into the gas chromatograph fitted with a 3 m (5-mm i.d.) stainless steel or glass column packed with 15 % Apiezon-L on Chromosorb-P (150—180 μm) and a ^{63}Ni electron-capture detector. The carrier gas is purified nitrogen at 50 ml min^{-1}. The oven is maintained at 70 °C for 6 min and then temperature-programmed at 10 °C min^{-1} up to 150 °C and held. The concentrations of the chlorinated hydrocarbons are determined by comparison of peak areas in the sample chromatogram with those of external standards.

Materials

Nitrogen supply. Nitrogen is purified by passing through a 2 m (15-mm i.d.) tube packed with activated charcoal followed by a 200 mm (40-mm i.d.) tube packed with 5A molecular sieve.

Carrier gas. Nitrogen is initially purified as for the above nitrogen supply and then passed through an oxygen trap mounted inside the chromatograph oven (e.g. Alltech Associates "Oxy-Trap" No. 4002).

Calibration compounds. Chloroform, carbon tetrachloride, 1,1,1,-trichloroethane, trichloroethylene, and perchloroethylene (Pfaltz and Bauer, Inc.; purity > 99.0 %) were used. Each must give only one peak when used as a standard in the method described.

Solvent for preparation of calibration standard solutions. n-Pentane (laboratory-reagent grade) must be checked as being free from interfering impurities when used in the preparation of standards by the method described.

Column packing materials. Chromosorb-P (150—180 μm, equivalent to British Standard mesh 85—100: see BS 410 and ISO/TC 24) and Apiezon-L, both available commercially, are used. The ready prepared packing containing 15 % of Apiezon-L is also suitable.

Apparatus

Gas chromatograph. A single-column, temperature-programmed instrument fitted with a ^{63}Ni electron-capture detector is suitable. Although it is not essential, it is advantageous if the instrument is also fitted with a flame ionization detector (f.i.d.) connected to the column via an effluent splitter. (This is valuable for the analysis of samples which contain excessively high concentrations of electron-capturing compounds, or compounds with low electron-capture sensitivity.) Several suitable chromatographs are available commercially.

Injection devices. Samples are injected with either 2-ml gas-tight syringes, e.g. (Precision Sampling Syringe type 030034 or 050034), or with 10-μl or 50-μl liquid syringes, e.g. Hamilton. The septa for the chromatograph are of the silicone rubber, high-temperature type.

Columns. The stainless steel or glass columns, (3-m long, 5-mm i.d., 6.4-mm o.d.) may be of any shape suitable for the chromatograph oven. Stainless steel columns are pretreated by washing the empty column with acetone and drying by air blowing. A glass column may be used without pretreatment.

To pack one column, weigh out 30 g of Chromosorb-P (150—180 μm) and 5.3 g of Apiezon-L. Dissolve the Apiezon-L in 20 ml of toluene. Stir this into the Chromosorb-P which has been slurried in 80 ml of toluene. Heat gently under a ventilated hood, and stir to remove the solvent until the powder is dry and free-flowing. Sieve the powder and retain the fraction sized between 150 and 180 μm. Alternatively, use the equivalent commercially available packing. Pack the column under a pressure of 1—2 bar to obtain maximum packing density.

For conditioning, connect the column directly to the injection port, without a sample vaporizer, and condition at 260 °C for 24 h, using the nitrogen carrier gas.

Detector. The electron-capture detector, with a ^{63}Ni source of activity at least 10 mCi must be capable of being heated to 350 °C.

Recorder. The recorder should be of the potentiometric type adjustable to 10 mV full scale deflection (f.s.d.) with a 20-cm chart width, a chart speed adjustable to 10 mm min^{-1}, a 1-s response time, a deadband $\geqslant$ 0.3 % f.s.d., and a linearity $\leqslant$ 0.5 % f.s.d. A 2-pen recorder is used for simultaneous e.c.d. and f.i.d. measurements.

Peak integration. A transparent ruler with mm graduations and a small drawing board for triangulation measurements are required. An electronic integrator should not be used, because most electronic integrators do not have the sophisticated base-line tracking facilities that would be required to follow the chromatograms adequately.

Flask for collection of air samples and preparation of calibration standards (Fig. 1). A 250-ml round-bottom flask is fitted with a Drechsel-type head with PTFE-plug taps on each arm (e.g. "Interflon"), and an additional side-arm equipped with an injection port fitted with a septum made of silicone rubber with a PTFE backing disc: this disc must be replaced after each use.

Accessories. A portable suction diaphragm pump with a pumping rate of at least 3 l min^{-1} (e.g. a Casella personal sampler, Model C) is required.

Sampling

Before using the sampling flask (Fig. 1), thoroughly purge with purified nitrogen and then check that it is free from contaminants by analysing the nitrogen it contains by the method described later. At the site of sampling, open both taps and connect the diaphragm pump to arm A of the flask. Draw air through the flask for 3—5 min, then disconnect the pump, and close

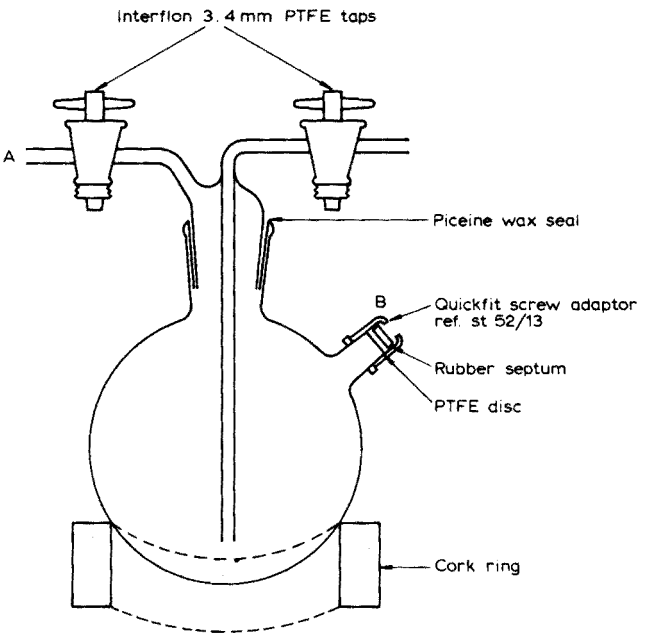

Fig. 1. Air sampling flask.

both taps securely. Store the sample in the dark at a temperature not greater than 25 °C, and analyse the contents as soon as possible but not later than after three days.

Setting the optimal conditions for the method

Check that the septum of the injection port is leak-free, using a proprietary leak test solution. Set the purified nitrogen carrier gas flow at 50 ml min^{-1}. Set the following temperature programme: initial isothermal period 6 min at 70 °C, then programme at 10 °C min^{-1} up to 150 °C and hold at this temperature for 15 min (or a longer period as required to elute any heavy impurities).

As a programming test, determine the time that the chromatograph takes to cool down sufficiently between successive programmed chromatograms to achieve repeatable retention times. For this purpose, run the programme indicated above. Switch off the oven heater, and leave the fan running and the oven door open for a period of, say, 30 minutes. Close the oven door and monitor the oven temperature for 5 min with a mercury thermometer. Note the stabilization temperature. If this temperature is not 60 °C or less, repeat the above procedure, leaving the oven door open for a further period as required. Note the time that results in a stabilization temperature of 60 °C and allow at least this time between successive runs in the recommended procedure.

Set the detector controls as follows:

Detector oven temperature	300 °C	
Pulse interval	500 μs	typically
Pulse width	0.75 μs	
Pulse amplitude	fixed in the range 47—60 V	
Amplifier attenuation	set to obtain suitable recorder deflection, typically × 500 to × 2000 ($5 \cdot 10^{-10}$ A to $2 \cdot 10^{-9}$ A f.s.d.)	
Purge gas	nitrogen at a flowrate found by trial and error to achieve minimum peak distortion and broadening consistent with acceptable detector sensitivity (see below).	

Set the recorder chart speed at 10 mm min^{-1}, and the range at 10 mV f.s.d.

Calibration and preparation of standards

The external standard method is used with calibration checks at least every three days. Standards (5 ng l^{-1}) for each compound in air are required for measurement of detector sensitivities. Standards of other concentrations are required for calibration within the range of concentration for each compound found in samples.

Prepare a standard solution (400 $\mu g\ l^{-1}$) in n-pentane for each compound as follows: by means of the 10-μl syringe, add a volume of the calibration compound equivalent to 10 mg (see list of densities, Table 1) to about 5 ml of n-pentane in a 10-ml graduated flask, make up to the mark with n-pentane, and mix. Take 10 μl of this solution and similarly dilute to 25 ml with n-pentane. Prepare these standard solutions freshly each week.

To prepare gaseous mixtures of standards, calculate the volumes of the standard solutions in n-pentane that must be injected, in turn, into the 250-ml calibration flask (Fig. 1), using the expression: $v = 0.63C'$, where v μl is the volume of the standard solution in n-pentane of an individual compound and C' is the required concentration (in ng l^{-1}) of that compound in air. For example, the most dilute mixture of standards required — that for the sensitivity test (see below) — is of concentration 5 ng l^{-1}, for each compound, for which the required volume of each standard solution in n-pentane is 3.1 μl. Take the calibration flask, fit a clean PTFE backing disc in its injection port (Fig. 1, arm B) and inject the calculated volumes of standard solutions in n-pentane using the 10-μl or 50-μl syringe as appropriate.

TABLE 1

Compounds determined by methods A and B: typical parameters

Compound	Density (20 °C)	Method A (for air)		Method B (for water)	
		Rel. retention	Detection limit (ng/l^{-1})	Rel. retention[a]	Detection limit[b] ($\mu g\ kg^{-1}$)
Chloroform	1.470	0.59	1.5	0.50	0.080
1,1,1-Trichloroethane	1.338	0.70	0.5	0.69	
Carbon tetrachloride	1.552	0.82	0.2		0.025
Trichloroethylene	1.459	1.00	1.0	1.00	0.050
Perchloroethylene	1.619	1.40	1.0	1.93	0.025
1,1,1,2-Tetrachloroethane	1.583			2.21	0.035
1,1,2,2-Tetrachloroethane	1.585			2.60	0.100
Pentachloroethane	1.680			2.86	0.020
Hexachloroethane	Solid			3.25	0.015
Pentachlorobutadiene	1.623			3.67	0.055
Hexachlorobutadiene	1.682			3.94	0.020

[a]The relative retentions quoted for Method B (Water) apply to the Dexsil column. With the Apiezon-L column, the relative retentions are similar to those tabulated under Method A.

[b]The detection limits quoted apply to the Dexsil column. With the Apiezon-L column, the corresponding detection limits will be broadly similar up to perchloroethylene.

Gas chromatography system tests

Standing current test on the detector. Fit an empty column in the chromatograph oven and set the oven and detector controls as follows:

Column oven temperature	150 °C
Detector oven temperature	300 °C
Pulse width	0.75 μs
Amplifier attenuation	set to give 100 % f.s.d. on the recorder at 15-μs pulse spacing.

Plot the standing current against the pulse spacing covering the typical range 15—500 μs. If the standing current at 500 μs does not fall to less than half the value at 15 μs proceed to the detector/column combination test below. If the standing current does fall to less than half that at 15 μs, the detector or the carrier gas or both are too badly contaminated for use and the following routine decontamination treatment should be applied.

Routine decontamination of the detector and carrier gas. Retain the empty column in the oven, increase the detector temperature to 350 °C and purge the chromatograph with nitrogen carrier gas for 24 h. Then check the standing current as above with the detector temperature re-set to 300 °C. If the chromatograph passes this test, proceed to the following detector/column combination test. If it fails and the standing current still indicates the presence of impurities, replace the gas purifying adsorbents and again check the standing current with the detector temperature at 300 °C. If the standing current at 500 μs is still too low replace the detector* and repeat the above standing current tests.

Standing current test on the detector/column combination. When the detector has passed the first standing current test, apply the following procedure. Retaining the empty column in the oven and using the above conditions for the detector test, set the pulse interval to 500 μs. Measure and note the standing current. Then cool the column oven, replace the empty column with the Apiezon-L column, and raise the column oven temperature to 150 °C. Allow the chromatograph to stabilise for 30 min and then measure the standing current. This value should be not less than 70 % of the previous value obtained with the empty column. If the chromatograph passes this test, carry out the following base-line stability test, but if it fails, then the column is contaminated or is bleeding excessively and should be reconditioned (see below).

Base-line stability test. If the chromatograph has passed the above detector/column combination test, record the detector signal with the prescribed maximum attenuation during the prescribed temperature programme. Measure the net base-line drift during the period of temperature rise and if this does not exceed 5 % f.s.d., proceed with the sensitivity test below. If the chromatograph fails this test recondition the column as follows.

*A contaminated detector which does not respond to the treatment described should be returned to the manufacturers for cleaning. On no account should it be dismantled in the laboratory for cleaning.

Reduction of column bleed or contamination. Disconnect the column from the detector and pass nitrogen carrier gas through it at 260 °C for 24 h. Whilst this is in progress, it is advisable to remove any contamination that may have been transmitted to the detector during the earlier tests, by purging the detector at 350 °C with nitrogen carrier gas.

After this process repeat the above standing current test and base-line stability test and if successful proceed to the sensitivity test. If the chromatograph fails either of these tests replace the column with a freshly packed, reconditioned one and repeat the tests.

Test for sensitivity to chlorinated hydrocarbons. Analyse the mixture of standards containing 5 ng l^{-1} of each compound of interest by the following recommended chromatographic procedure with the minimum prescribed attenuation. Measure the peak areas. Assuming that the smallest peak area measurable is 10 mm^2, the limits of detection should approximate to those given in Table 1.

Recording the sample chromatograms

Using the above prescribed optimal conditions, set the amplifier attenuation to the prescribed minimum and the initial isothermal temperature at 70 °C, and allow 5 min for stabilization. Flush the gas syringe with the nitrogen supply four or five times, remove a 2.0-ml aliquot from the air sample flask via the septum, inject it directly into the gas chromatograph, immediately start the temperature programme, and record the chromatogram. Figure 2 shows a typical chromatogram. When the chromatogram appears to be complete, keep the column temperature at 150 °C for at least 15 min, or a longer time if required to allow any heavy impurities to elute. Then switch off the oven heater, leave the fan running and open the oven door for the period determined previously in the programming test; then close it and reset the initial temperature. Allow 5 min for stabilization before making the next injection.

If the chromatogram shows peaks that have gone off the recorder chart scale, the amplifier attenuation should be reset to a suitably higher value and another aliquot of sample should be injected. Note the attenuation when an acceptable chromatogram has been obtained. It is advisable to run duplicate chromatograms of samples.

Recording the standard chromatogram

Inspect the sample chromatogram to decide which compounds are required and use the sensitivity data to estimate the concentrations of standards required. Preferably, these concentrations should be of the same order as in the sample and certainly not greater than by a factor of 10. Prepare a suitable gaseous calibration mixture by the procedure prescribed above.

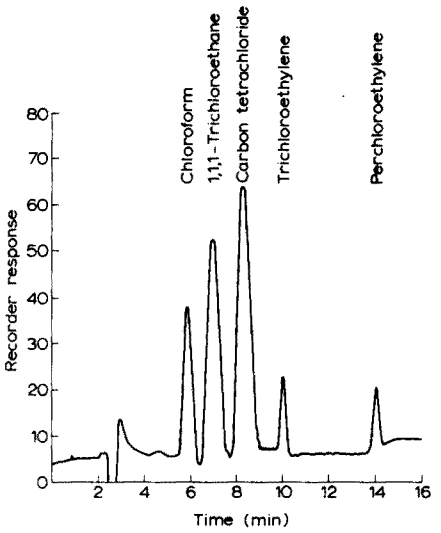

Fig. 2. Typical chromatogram of an air sample.

Chromatograph the standard mixture, following the general instructions for samples, but omit the time allowed for the elution of heavy impurities. If the standard chromatogram matches the sample qualitatively, run a duplicate chromatogram and note the attenuation. Then measure the areas of the peaks (see below). If the match is doubtful, apply the following procedure.

Confirmation of peak identity

Compare the sample chromatogram with the standard chromatogram to identify corresponding peaks. If the match between their respective retention times is doubtful, if stronger evidence of identity is required, or if interfering peaks appear, prepare sets of chromatograms of both sample and standard on several columns of differing polarity, or use a smaller diameter column or both. Use procedures analogous to those described in this method. Suitable column phases are (a) low polarity: Apiezon-L, DC 11, (b) medium polarity: S.E.30, M.S.550, Dexsil-300; (c) high polarity: PEG 20M, Oxydipropionitrile. A suitable alternative column diameter is 2-mm i.d./3.2 mm o.d.

Measurement of peak areas

Transfer the chromatograms to the drawing board and by triangulation measure the peak areas to the nearest 10 mm^2 or better. Do not include any negative peak tails in the area.

Calculation of results

The concentration of any particular compound in the sample is given by $C = C' \times A/A'$, where C and C' are the concentrations of the compound in the sample and standard, respectively (ng l^{-1}), and A and A' are the peak areas × attenuation of the compound in the sample and standard, respectively.

This simple relationship holds over the range 1—100 ng l^{-1} for each compound. Duplicate results on any one sample would be expected to agree to within 20 %.

Test report

Record the following information: (i) the results and the method of expression; (ii) any special details and any unusual features noted during the analysis; (iii) any operation not included in the method.

METHOD B. DETERMINATION OF TRACE VOLATILE CHLORINATED ALIPHATIC HYDROCARBONS IN WATER BY GAS CHROMATOGRAPHY

Scope and field of application

This method covers the determination in sea and fresh water of the compounds chloroform, carbon tetrachloride, trichloroethylene, perchloroethylene, 1,1,1,2-tetrachloroethane, 1,1,2,2-tetrachloroethane, pentachloroethane, hexachloroethane, pentachlorobutadiene, hexachlorobutadiene in the concentration range 0.01—10 μg kg^{-1}.

The column specified in this method, Dexsil-300, does not separate carbon tetrachloride from 1,1,1-trichloroethane, but these compounds can be separated by the chromatographic system of Method A. However, if the sample is thought to contain "heavies" which require purging from the column at high temperature, then the therml stability limitation of Apiezon-L makes it unsuitable and the sample must be chromatographed by Method B.

Principle

A 200-ml sample of water is extracted with n-pentane and the extract is dried with anhydrous sodium sulphate. A portion of this solution is injected into the gas chromatograph fitted with a 1.5 m (5-mm i.d.) stainless steel or glass column packed with 15 % Dexsil-300 on Diatomite-C (180—212 μm) and a ^{63}Ni electron-capture detector. The carrier gas is purified nitrogen at 50 ml min^{-1}. The oven is maintained at 65 °C for 6 min and then temperature-programmed at 10 °C min^{-1} up to 150 °C and held until hexachlorobutadiene has eluted. The column is then purged at 250 °C. The concentrations of the chlorinated hydrocarbons are determined by comparison of peak areas in the sample chromatogram with those of an external standard mixture.

Materials

The materials are as specified in Method A, with the following exceptions.

Calibration compounds. Chloroform, carbon tetrachloride, 1,1,1-trichloroethane, trichloroethylene, perchloroethylene, 1,1,1,2-tetrachloroethane, 1,1,2,2-tetrachloroethane, pentachloroethane, hexachloroethane, pentachlorobutadiene and hexachlorobutadiene (purity > 99.0 %) were used. Each gave only one peak when used as a standard in the method described.

Drying agent. Anhydrous sodium sulphate is heated at 300—350 °C overnight.

Column packing materials. Diatomite-C (180—212 μm, equivalent to British Standard mesh 72—85: see BS 410 and ISO/TC 24) and Dexsil-300, both available commercially, are used.

Apparatus

The apparatus specified for Method A is suitable with the following exceptions.

Injection device. Liquid syringes (10 μl, e.g. Hamilton) are suitable.

Columns. The stainless steel or glass columns (1.5-m long, 5-mm i.d., 6.4-mm o.d.) are pretreated as described for Method A.

To pack one column, weigh out 10.2 g of Diatomite-C (180—212 μm) and 1.8 g of Dexsil-300. Dissolve the Dexsil-300 in 10 ml of acetone: do not use chloroform, the solvent recommended by the manufacturers, because it is strongly electron capturing and would entail lengthy conditioning of the column. Stir this solution into the Diatomite-C which has been slurried in 50 ml of acetone. Heat gently under a ventilated hood and stir to remove the solvent until the powder is dry and free-flowing. Sieve the powder and retain the fraction sized between 180 and 212 μm. Pack the column as for Method A.

For conditioning, connect the column directly to the injector, without a sample vaporizer, and disconnect the detector. Condition at 350 °C for 48 h, with the nitrogen carrier gas. When not in use, keep the column purged with carrier gas.

Bottles for collection of water samples. Brown glass, ground-glass stoppered bottles (1 l) are suitable.

Glove box. This must be of sufficient size (about 0.5 m^3) to accommodate a flask shaker with a timer and fitted with nitrogen lock. Purge during use with 2000 l h^{-1} of purified nitrogen.

Other equipment needed includes separating funnels (250-ml, all-glass, with ungreased stopcocks), sample bottles (amber glass, 30-ml capacity with narrow necks), and 1-ml graduated pipettes. The serum caps to fit the sample bottles must be refluxed with n-pentane for 4 h to extract impurities.

Sampling

A fresh bottle must be used for each sample. Before use purge with purified nitrogen and stopper. Do not filter the water to be analysed; always fill the bottle fully with sample, leaving minimum ullage. Store the sample in the dark at 0—5 °C and analyse within two days.

Extraction of the sample

Carry out all the following operations inside the glove box. Accurately transfer 200 ml of sample to a 250-ml separating funnel which has been stored unstoppered in the glove-box or purged with purified nitrogen. Accurately add 10 ml of n-pentane, stopper and shake mechanically for 5 min. Allow the liquid phases to separate; do not centrifuge, as this would involve removal of the sample from the glove box and possible contamination, and could also cause warming, resulting in loss of volatiles. Run off the (lower) aqueous layer and then run the n-pentane layer into a 30-ml sample bottle containing 1 g of anhydrous sodium sulphate. Close the bottle with a clean serum cap and remove it from the glove-box.

Setting the optimal conditions for the method

Follow the general procedure for Method A, but modify where necessary as follows.

Set the following temperature programme: initial isothermal period 6 min at 65 °C, then programme at 10 °C min^{-1} up to 150 °C and hold until hexachlorobutadiene has eluted (after about 5 min). Raise the oven temperature to 250 °C and hold at that temperature for 10 min or a longer period as required to elute any heavy impurities.

For the programming test, follow the general instructions given for Method A, but use the programme prescribed above, and ensure that the stabilization temperature is not greater than 55 °C.

Calibration and preparation of standards

The external standard method is used. In the extraction stage, there is a 20-fold enrichment factor, thus, for measurement of detector sensitivities, a suitable concentration for standards in n-pentane is 2 $\mu g\ l^{-1}$ for each compound. Standards of other concentrations are required for calibration within the range of concentration for each compound found in samples.

In contrast to Method A, these should be individual solutions, not mixtures, because of the very variable composition of water samples.

Prepare a standard solution (10 $\mu g\ l^{-1}$) in n-pentane for each compound as follows: by means of the 10-μl liquid syringe add a volume of the calibration compound equivalent to 10 mg (see list of densities, Table 1); or, for solids, dissolve 10 mg in about 5 ml of n-pentane in a 10-ml graduated flask, make up to the mark with n-pentane and mix. Take 10 μl of this solution and dilute similarly to 10 ml with n-pentane. Take 100 μl of this latter solution and dilute further to 10 ml with n-pentane. Prepare these standard solutions freshly each week.

To prepare calibration solutions from the standard solutions, dilute a calculated volume of the standard solution with n-pentane. For example, to prepare the solutions (2 $\mu g\ l^{-1}$) required for the sensitivity test (see below), take 0.2 ml of the above standard solution in a 1-ml pipette and dilute to 1 ml in a graduated flask.

Gas chromatography system tests

Carry out the tests described previously for Method A with the modifications of column, temperature programming and conditioning appropriate for Method B.

Test for sensitivity to chlorinated hydrocarbons

Run chromatograms on the 2 $\mu g\ l^{-1}$ standards of each compound of interest by the following recommended procedure with the minimum prescribed attenuation, and then measure the limits of detection as described for Method A.

Recording the sample chromatogram

Using the above optimal conditions, set the amplifier attenuation (Method A) to the prescribed minimum, and the initial isothermal temperature at 65 °C, and allow 5 min for stabilization. Flush the syringe with sample solution and then fill it; discharge to the 1-μl mark and then draw back the plunger until the residual solution is in the syringe barrel. Inject this into the gas chromatograph. After withdrawing the syringe, invert it and draw back the plunger. Note the residual volume of solution in the syringe and take the difference between the first reading and this as the volume of solution injected. At the end of the chromatogram, raise the column oven temperature to 250 °C and hold for 10 min or a longer time if required to allow any heavy impurities to elute. Then, cool the oven and restabilize as described for Method A, ensuring that the stabilization temperature does not exceed 55 °C. If the chromatogram shows peaks that have gone off the scale, reset the amplifier attenuation to a suitable higher value and inject another aliquot

of sample. Note the attenuation when an acceptable chromatogram has been obtained. It is advisable to run duplicate chromatograms.

Figure 3 shows a typical chromatogram.

Recording the standard chromatograms

Select the standards and their concentrations as described for Method A. Prepare a suitable set of calibration solutions and run the chromatograms as prescribed above.

Confirm peak identity and measure peak areas as described for Method A.

Calculation of results

The concentration of any particular compound in the sample is given by the equation

$$C = \frac{10 \times C' \times A \times \mu'}{A' \times \mu \times W}$$

as the volume of sample extract is 10 ml and where, C is the concentration of the compound in the sample ($\mu g\ kg^{-1}$); C' is the concentration of the compound in the standard ($\mu g\ l^{-1}$); A and A' are the peak areas × attenuation of the compound in the sample and standard, respectively; μ and μ' are the volumes of the sample extract and the standard injected (μl), respectively; and W is the weight of the sample (g).

This simple relationship holds over the concentration range 0.01—10 $\mu g\ kg^{-1}$. Duplicate results on any one sample would be expected to agree to within 20 %.

Test reports are completed as described for Method A.

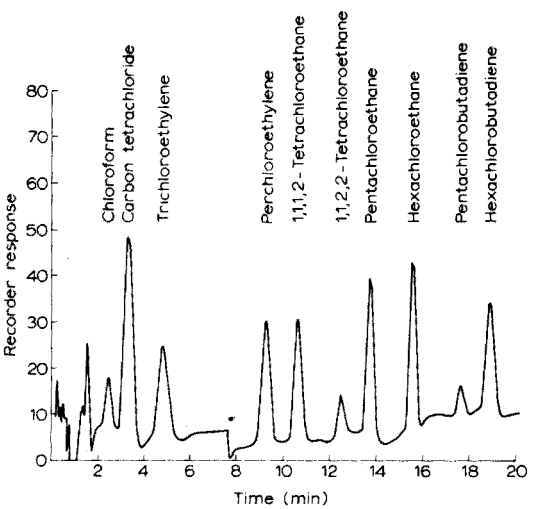

Fig. 3. Typical chromatogram of a water sample.

CONCLUSIONS

The methods use conventional commercial equipment for the routine determination of chlorinated solvents and byproducts within the concentration ranges 1—100 ng l^{-1} (air) and 0.01—10 $\mu g\ kg^{-1}$ (water). The repeatability of the results, 20 %, is quite satisfactory for making environmental surveys.

The methods can be adapted to determine other electron-capturing substances such as fluorinated aerosol propellants and fluorochlorinated solvents by straightforward modifications to the chromatography. Furthermore, the method for water can be extended to mud and fish by the substitution, at the sample pretreatment stage, of well known extraction procedures. A description of such work carried out by one of the B.I.T.-S.C. member companies is being published elsewhere [19].

REFERENCES

1 A. J. Murray and J. P. Riley, Nature (London), 242 (1973) 37.
2 A. J. Murray and J. P. Riley, Anal. Chim. Acta, 65 (1973) 261.
3 B. Versino, M. de Groot and F. Geiss, Chromatographia, 7 (1974) 302.
4 W. Bertsch, R. C. Chang and A. Zlatkis, J. Chromatogr. Sci., 12 (1974) 175.
5 J. E. Lovelock, R. J. Maggs and R. J. Wade, Nature (London), 241 (1973) 194.
6 P. E. Wilkins, R. A. Lamontagne, R. E. Larson, J. W. Swinnerton, C. R. Dickson and T. Thompson, Nature (London) Phys. Sci., 245 (1973) 45.
7 J. E. Lovelock, R. J. Maggs and E. R. Adlard, Anal. Chem., 43 (1971) 1962.
8 J. E. Lovelock, J. Chromatogr., 99 (1974) 3.
9 D. Lillian and H. B. Singh, Anal. Chem., 46 (1964) 1060.
10 N. E. Hester, E. R. Stephens and O. C. Taylor, J. Air Pollut. Contr. Ass., 24 (1974) 596.
11 J. Novak, J. Zluticky, V. Kubulka and J. Mostecky, J. Chromatogr., 76 (1973) 45.
12 R. D. Kleopfer and B. J. Fairless, Environ. Sci. Technol., 6 (1972) 1036.
13 S. Jensen, A. Jernelov, R. Lange and K. H. Palmork, Food and Agriculture Organisation of the United Nations, Report No. FIR:MP/70/E-88 (Nov. 1970).
14 F. Dietz and J. Traud, Vom Wasser, 41 (1973) 137.
15 C. S. Giam and M. K. Wong, J. Chromatogr., 72 (1972) 283.
16 J. J. Rook, J. Water Treat. Examin., 23 (1974) 234.
17 D. J. David, Gas Chromatographic Detectors, Wiley—Interscience, New York, 1974.
18 Standard Layout for a Method of Chemical Analysis by Gas Chromatography, International Standard, ISO 2718, (1972).
19 C. R. Pearson and G. McConnell, Proc. Roy. Soc. Ser. B., 189 (1975) 305.

Analytica Chimica Acta, 82 (1976) 19—27

NEUE EINHEITEN FÜR SPURENGEHALTE *

O. G. KOCH

Chemisches Laboratorium, Neunkircher Eisenwerk AG, D-668 Neunkirchen/Saar (West Germany)

(Eingegangen den 18 August 1975)

ZUSAMMENFASSUNG

Die Abgrenzung und Aufteilung des Spurenbereiches werden diskutiert und neue Einheiten für Spurengehalte vorgeschlagen. Es wird empfohlen: (1) für die Angabe von Spurengehalten als Grundlage das Mengenverhältnis von Spurenelement zu Matrix zu verwenden; (2) auf dieser Basis als Einheit die ausgeschriebene Form $a \cdot \mathrm{pp}10^{x}$ anzuwenden oder die teil-logarithmische Form $a \cdot \mathrm{pT}\ x$ oder die voll-logarithmische Form pX. Hiernach würde man z.B. 0,005 p.p.m. Cu angeben als 5 $\mathrm{pp}10^{9}$ Cu oder 5 pT 9 Cu oder pCu 8,30.

SUMMARY

Nomenclature for the demarcation and the division of the trace range is discussed and new units for trace contents are proposed. It is recommended: (1) to use the ratio of trace element to matrix as the basis for the statement of trace contents; (2) on this basis to apply as unit the full written form $a \cdot \mathrm{pp}10^{x}$, or the partial logarithmic form $a \cdot \mathrm{pT}\ x$, or the full logarithmic form pX. For example, 0.005 p.p.m. Cu is written as 5 pp 10^{9} Cu, or 5 pT 9 Cu, or pCu 8.30.

Seit den ersten Anfängen der Spurenalanyse erwiesen sich die Gehaltseinheiten Prozent (%) und part per million (p.p.m.) für die Angabe von Spurengehalten und analytischen Arbeitsbereichen als am zweckmässigsten. Sie fanden deshalb im Laufe der Jahrzehnte die häufigste Anwendung [1—4].

Mit der zunehmenden Erfassung niedrigerer Spurengehalte aufgrund der weiteren Entwicklung auf dem Gebiet der Technik und der Analysenmethoden entstehen aber gewisse Schwierigkeiten. Denn einerseits werden die Einheiten % und p.p.m. bei Konzentrationen von < 1 p.p.m. mit sinkendem Gehalt zunehmend unhandlich. Andererseits stellen sich der logischen Ableitung kleinerer Einheiten von der bekannten Einheit p.p.m. sprachliche Unterschiede entgegen, auf die noch weiter unten näher eingegangen wird. Sowohl dieser Sachverhalt als auch die Bemühungen um eine Vereinheitlichung von Einheiten und Begriffen auf internationaler Grundlage führten in letzter Zeit vor allem zu zwei Vorschlägen [5, 6] mit Einheiten für die Angabe des Arbeitsbereiches und der Gehalte sowohl in der analytischen Chemie im allgemeinen als auch in der Spurenanalyse im besonderen.

Zweifellos besteht ein Bedarf an einer Verbesserung, Erweiterung und

* Author and Editors would welcome correspondence on this paper, because of the general interest of the theme. If there is sufficient response, the correspondence will be published in a summarized form.

Vereinheitlichung der zur Zeit im Spurenbereich verwendeten Einheiten, weshalb die zur Diskussion gestellten Vorschläge [5, 6] grundsätzlich zu begrüssen sind. Ein Teil der für den Spurenbereich vorgeschlagenen Einheiten bzw. Begriffe erscheint jedoch aufgrund der bisherigen Erfahrungen nicht zweckmässig bzw. realisierbar. Auch unterscheiden sich die in beiden Vorschlägen [5, 6] für den Spurenbereich empfohlenen Einheiten erheblich. Aus diesem Grunde werden vom Autor der Inhalt der Vorschläge [5, 6] diskutiert und Gegenvorschläge unterbreitet, die zu einer Vereinheitlichung der Auffassungen führen sollen. Für die angeführten Gegenvorshläge sind allein folgende Gesichtspunkte massgebend: Zweckmässigkeit, leichte und allgemeine Verständlichkeit und Anwendbarkeit, Berücksichtigung der bisher gebräuchlichen Einheiten und Begriffe.

Kurz nach dem Erscheinen von Vorschlag 1 [5] wurden dessen Verfassern die vorliegenden Gegenvorschläge in einer kürzeren Fassung (1972) vom Autor übersandt. Später wurden davon unabhängig ähnliche Gedanken zu diesem Problem in einer anderen Zeitschrift veröffentlicht [7].

ABGRENZUNG UND AUFTEILUNG DES SPURENBEREICHES

Der von einer Analysenmethode erfassbare Gehaltsbereich kann in Prozent (Massen-%, Volumen-%, mol-%) und in anderen Einheiten ($g\,l^{-1}$, $g\,g^{-1}$ usw.) angegeben werden. Für den Bereich der Spurenanalyse ist nun die Anwendung der Einheit Massen-% besonders bei sinkenden Gehalten recht umständlich und unanschaulich, weshalb sowohl Vorschlag 1 [5] als auch Vorschlag 2 [6] den Begriff "Spur" als Einheit zur Diskussion stellen. Die Definitionen nach beiden Vorschlägen für die Einheit "Spur" zeigen aber erhebliche Unterschiede und widersprechen teilweise dem bisher gebräuchlichen Begriff "Spur", weshalb darauf näher eingegangen werden soll und ein geeigneter erscheinender Gegenvorshlag gemacht wird.

Die verschiedenen Vorschläge zur Aufteilung in Gehaltsbereiche sind in Tab. 1 zusammengefasst. Aus dieser ist ersichtlich, dass die Vorschläge 1 [5] und 2 [6] bei keinem Bestandteil übereinstimmen. Besonders krass sind die Unterschiede im Spurenbereich, wo sie 4—5 Zehnerpotenzen betragen!

In diesem Zusammenhang muss besonders auf die richtige und gebräuchliche Abgrenzung des Spurenbereiches hingewiesen werden: nach den massgebenden Kriterien (Analysentechnik, Spuren-Wirkungsbereich) stellt 0.01 % aus historischen und sachlich-praktischen Gründen am zweckmässigsten die obere Grenze des Spurenbereiches dar [1, 2, 4].

Nach Vorschlag 2 [6] (Tab. 1, Spalte 6) soll 1 % die obere Grenze des Spurenbereiches darstellen. Diese für den Spurenanalytiker unübliche und wenig zweckmässige Grenze wurde offensichtlich gewählt, damit zur besseren Verständlichkeit und leichteren Anwendbarkeit die Vorsätze "Milli-, Mikro- usw." (Tab. 1, Spalte 1) mit der zahlenmässigen Aufteilung des Spurenbereiches "10^{-3} %, 10^{-6} % usw." (Tab. 1, Spalte 6) übereinstimmen. Doch geht diese recht ungewöhnliche Abgrenzung des Spurenbereiches an den Anforderungen

TABELLE 1

Gehaltsbereiche

Bestandteil	Bereich						
	nach Vorschlag 1 [5]				nach Vorschlag 2 [6]	nach Vorschlag des Autors	
	Variante 1		Variante 2		%	%	p.p.m.
	%	p.p.m.	%	p.p.m.			
(1)	(2)	(3)	(4)	(5)	(6)	(7)	(8)
Hauptbestandteil	1—100	—	1—100	—	10—100	1—100	
Nebenbestandteil	0,1—1	—	0,1—1	—	1—10	0,01—1	
Spur	10^{-8}—10^{-2}	10^{-5}—10^{-2}	10^{-7}—10^{-2}	10^{-3}—10^{-2}	< 1	10^{-4}—10^{-2}	1—10^{2}
Millispur					10^{-3}—1	10^{-7}—10^{-4}	10^{-3}—1
Mikrospur	10^{-11}—10^{-8}	10^{-7}—10^{-4}	10^{-10}—10^{-7}	10^{-6}—10^{-3}	10^{-6}—10^{-3}	10^{-10}—10^{-7}	10^{-6}—10^{-3}
Nanospur	10^{-14}—10^{-11}	10^{-10}—10^{-7}	10^{-13}—10^{-10}	10^{-9}—10^{-6}	10^{-9}—10^{-6}	10^{-13}—10^{-10}	10^{-9}—10^{-6}
Picospur	10^{-17}—10^{-14}	10^{-13}—10^{-10}	10^{-16}—10^{-13}	10^{-12}—10^{-9}	10^{-12}—10^{-9}	10^{-16}—10^{-13}	10^{-12}—10^{-9}
Femtospur					10^{-15}—10^{-12}		
Attospur					10^{-18}—10^{-15}		

der Praxis vorbei, indem sie die für den Spurenbereich massgebenden Kriterien unberücksichtigt lässt und zu diesen im Widerspruch steht. Aus diesem Grunde ist Vorschlag 2 [6] als unzweckmässig abzulehnen.

Vorschlag 1 [5] verwendet die richtige Abgrenzung des Spurenbereiches, nämlich 0,01 % als obere Grenze. Er weist aber folgende Nachteile auf: (a) in beiden Varianten wird 0,1 % als untere Grenze für Nebenbestandteile angegeben, während diese richtig 0,01 % sein muss; (b) die Aufteilung des Spurenbereiches weist eine Lücke auf, indem in inkonsequenter Weise der Bereich "Millispur" ignoriert bzw. übersprungen wird; (c) der Vorschlag enthält zwei Varianten, so dass deren Anwendung zweifellos zu Missverständnissen führen muss.

Variante 2 (Tab. 1, Spalten 4 und 5) wurde vorgeschlagen, damit die Vorsätze "Mikro-, Nano- usw." mit der unteren Grenze des jeweiligen Spurenbereiches "10^{-6} p.p.m., 10^{-9} p.p.m. usw." übereinstimmen. Im Vergleich zu Variante 1 liegen die Spurenbereiche von Variante 2 um 1 Zehnerpotenz höher. Wegen der unter (a) bis (c) angeführten Nachteile muss auch Vorschlag 1 [5] in seiner vorliegenden Form abgelehnt werden.

Im Hinblick auf die zur Diskussion gestellten Vorschläge 1 [5] und 2 [6] sowie auf eine eventuelle, internationale Anerkennung der Einheit "Spur" wird vom Autor in Tab. 1 (Spalten 7 und 8) eine zweckmässige Aufteilung des Spurenbereiches angegeben. Diese stellt eine korrigierte und ergänzte Version der Variante 2 von Vorschlag 1 [5] dar.

Geht man davon aus, dass die vorgeschlagene Aufteilung des Spurenbereiches allgemein als zweckmässig anerkannt wird, so ist diese in Tab. 1 mit den Spalten 1, 2 und 3 in den bekannten Begriffen und Einheiten klar definiert. Ihre Einführung in der Praxis würde dann in der Anwendung der Begriffe "Spur, Millispur usw." erfolgen.

Hier muss allerdings ernsthaft die Frage gestellt werden, ob die Einführung des Begriffes "Spur" als neue Einheit und dessen Unterteilung in "Millispur, Mikrospur usw." für den Spurenbereich überhaupt ratsam und nützlich ist. Nach Ansicht des Autors erscheint dies aus zwei Gründen wenig sinnvoll. Zum einen setzt ihre Anwendung die genaue Kenntnis der schwer zu merkenden Definitionen der Begriffe "Spur, Millispur usw." voraus, wobei erfahrungsgemäss Schwierigkeiten auftreten. Zum anderen hat das Wort "Spur" bisher eine sehr breite und allgemeine Bedeutung für die verschiedensten Bereiche, worauf auch von anderer Seite hingewiesen wurde [7]. Aus diesen Gründen werden vom Autor die Verwendung des Begriffes "Spur" als Gehaltseinheit abgelehnt und statt dessen die im folgenden Abschnitt vorgeschlagenen, neuen Einheiten für die Angabe von Spurengehalten empfohlen.

EINHEITEN FÜR DIE ANGABE VON SPURENGEHALTEN

Was für den gesamten Spurenbereich benötigt wird, das ist eine von der Definition her leicht und international verständliche Einheit, die für Spurengehalte beliebiger Höhe universell anwendbar ist. Hierzu sind

Wortbegriffe weniger geeignet, viel zweckmässiger erscheint dagegen ein Zahlenbegriff.

Anwendung bekannter Einheiten

Zunächst sei versucht, Spurengehalte mit Hilfe bisher benützter Einheiten in Zahlen auszudrücken. Berücksichtigt man dabei, dass sich die Einheiten Prozent und p.p.m. — wie oben schon erwähnt — für niedrige Spurengehalte schlecht eignen, so bieten sich dafür die nachfolgenden zwei Möglichkeiten an.

(a) Nimmt man an, dass in den meisten Fällen die zur Spurenanalyse verwendete Probemenge in der Grössenordnung von 1 g liegt, so lässt sich der Spurenbereich mit der Spurenmenge in μg angeben (Tab. 2, Spalte 4). Hiernach würde man z.B. für eine Analysenmethode zur Bestimmung von 0,001—1 p.p.m. Cu in Mineralien angeben: "Die Bestimmung von Nanogramm-Mengen Kupfer in Mineralien".

(b) Eine weitere Möglichkeit ist die Angabe des Spurenbereiches in *p*%-Einheiten (Tab. 2, Spalte 5). Analog zum pH-Wert ist die vorgeschlagene Einheit *p*% der negative Logarithmus des Spurengehaltes in Prozent. Auch von anderer Seite [7] wurde die Verwendung des negativen Logarithmus des Prozentgehaltes unter Benützung des Symbols pX (X = Symbol des Elementes), z.B. für Kupfer pCu, für Spurengehalte vorgeschlagen. Für die im vorhergenden Absatz (a) als Beispiel erwähnte Analysenmethode würde man hiernach angeben: "Die Bestimmung von Kupferspuren im Bereich von *p*% 4—7 in Mineralien".

Die unter (a) und (b) angeführten zwei Möglichkeiten sind jedoch keine befriedigende Lösung, weshalb nachfolgend neue, geeignet erscheinende Einheiten definiert werden.

Definition und Anwendung neuer Einheiten

Es besteht kein Zweifel, dass die Einheit p.p.m. für die Angabe von Spurengehalten am häufigsten angewandt wird. Dies ist vor allem darauf zurückzuführen, dass das p.p.m. sich als sehr praktisch und anschaulich erwies, weil die meist auftretenden Spurengehalte mit der Einheit p.p.m. in einfachen Zahlen angegeben werden können im Gegensatz zur Prozentangabe.

Wegen der somit erwiesenen Zweckmässigkeit des p.p.m. werden deshalb in der amerikanischen Literatur für Gehalte < 1 p.p.m. fallweise die vom p.p.m. (part per million) = 10^{-4} % logisch und konsequent abgeleiteten Einheiten p.p.b. (part per billion) = 10^{-7} % und p.p.t. (part per trillion) = 10^{-10} % verwendet. Obwohl p.p.b. und p.p.t. ebenso zweckmässig erscheinen wie das p.p.m., fanden sie aber bis heute keine allgemeine Anwendung in der Literatur. Dies ist hauptsächlich auf die Unterschiede zwischen den Zahlennamen in den USA und Europa zurückzuführen. 1 US-Billion (= 10^9) entspricht der europäischen Milliarde, bzw. die europäische Billion (= 10^{12}) ist um den Faktor 10^3 grösser als die US-Billion. 1 US-Trillion (= 10^{12}) weiterhin entspricht der europäischen Billion, bzw. die europäische Trillion

TABELLE 2

Neue Einheiten für Spurengehalte

Gehalt	Einheit						
	%	p.p.m.	μg^a	$p\%^b$	$pp10^{xc}$	pT^d	pX^e
(1)	(2)	(3)	(4)	(5)	(6)	(7)	(8)
Hauptbestandteil	1—100						
Nebenbestandteil	0,01—1						
Spur	10^{-2}	10^{2}	10^{2}	2	$pp10^{4}$	4	4
	10^{-3}	10	10	3	$pp10^{5}$	5	5
	10^{-4}	1	1	4	$pp10^{6}$	6	6
	usw.	usw.	usw.	usw.	usw.	usw.	usw.
	10^{-16}	10^{-12}	10^{-12}	16	$pp10^{18}$	18	18

[a] Spurenmenge in μg bei einer Probemenge von 1 g.
[b] $p\%$ = negativer Logarithmus von %.
[c] $pp10^{x}$ = 1 part per 10^{x} parts.
[d] pT = negativer Logarithmus von 10^{x} in der Einheit $pp10^{x}$ (nach Spalte 6).
[e] Negativer Logarithmus des Gehaltes des Spurenelementes X.

(= 10^{18}) ist um den Faktor 10^{6} grösser als die US-Trillion. Diese sprachlichen Unterschiede führen unvermeidlich zu Verwechslungen und Verständigungsschwierigkeiten.

Wohl wegen dieser Schwierigkeiten wurde in einer Arbeit [8] vorgeschlagen, neben dem p.p.m. (1 p.p.m. = 10^{-4} %) als nächsttiefere Einheit das p.p.M. (1 p.p.M. = 10^{-7} %) zu verwenden. Dies ist sicherlich ein interessanter Vorschlag und ein möglicher Weg zur Vermeidung der oben erläuterten Schwierigkeiten mit der Einheit p.p.b. So brauchbar das p.p.M. auch erscheint, so beseitigt es nicht die oben genannten sprachlichen Unterschiede und bietet keine Lösung für tiefere Einheiten (d.h. für Gehalte $< 10^{-7}$ %) an. Auch kann es zu Verwechslungen kommen mit dem kleinen "m" und grossen "M", d.h. zwischen p.p.m. und p.p.M. Aus diesem Grunde ist die vorgeschlagene Einheit p.p.M. abzulehnen.

In dem früher erwähnten Vorschlag 2 [6] wird nun sogar empfohlen, die Einheiten p.p.m., p.p.b. usw. aus zwei Gründen nicht zu verwenden und sie abzuschaffen: (a) weil p.p.m.-Angaben in der Regel ohne Angabe der Relation erfolgen, d.h. es wäre nicht klar, ob es sich um Gewichts-p.p.m., Volumen-p.p.m. oder mol-p.p.m. handelt; (b) wegen der oben erwähnten sprachlichen Unterschiede.

Dem unter (a) angeführten Grund muss aber als nicht stichhaltig widersprochen werden. Die Anwendung des p.p.m. erfolgt ganz analog wie die international anerkannte und verwendete Gehaltseinheit "Prozent": ohne Zusatzinformation bedeutet sie stets Massen-%, für die anderen Relationen Volumen-% und mol-% ist stets die Zusatzinformation "Volumen-" und "mol-" erforderlich. Dasselbe gilt auch für das p.p.m.: ohne Zusatzinformation

bedeutet es stets Massen-p.p.m., für die anderen Relationen ist stets die Zusatzinformation hinzuzufügen, nämlich Volumen-p.p.m. und mol-p.p.m. Weiterhin sollte hier berücksichtigt werden, dass eine Ablehnung des p.p.m. als einer im Vergleich zum Prozent weniger exakten Einheit unlogisch erscheint. Denn zwischen Prozent und p.p.m. besteht kein grundlegender Unterschied, vielmehr ist das p.p.m. die logische Weiterentwicklung bzw. Ableitung des Prozent zu kleineren Dimensionen unter Anwendung derselben Definition. Bekanntlich bedeutet z.B. 1 % = 1 Prozent = 1 per cent = der hundertste Teil = 1 Teil von (per) 100 Teilen. Wendet man diesen Begriff in logischer Weise in Richtung kleinerer Einheiten hin an, d.h. 1 Prozent (1 per cent), 1 Promille (1 per thousand) usw., so kommt man zum 1 p.p.m. = 1 part per million = 1 Teil von 1000000 Teilen. Ersetzt man nun beim p.p.m., p.p.b. usw. das für die Ballaststoffmenge stehende Wort million, billion usw. durch die entsprechende Zahl 10^6, 10^9 usw., so entfallen die erwähnten sprachlichen Schwierigkeiten.

Den benötigten Zahlenbegriff leitet man am zweckmässigsten von dem in vorhergehenden Absatz erläuterten Zusammenhang von % und p.p.m. ab. Danach dient das Mengenverhältnis von Spurenelement zu Matrix als Grundlage für die in den folgenden Absätzen (a) bis (c) definierten neuen Einheiten für Spurengehalte.

(a) Ausgeschriebene Form. Die das Niveau des Spurenelementgehaltes bestimmende Ballaststoffmenge wird als Zahl in Zehnerpotenzen angegeben (Tab. 2, Spalte 6). Zum Beispiel.

1 p.p.m. = 1 Teil von 1000000 Teilen = 1 pp10^6 (1)

Aus Gl. (1) ergibt sich die allgemeine Form

Spurengehalt = a Teile von 10^x Teilen = $a \cdot$ pp10^x (2)

Hiernach (Tab. 2, Spalte 6) würde man z.B. für eine Analysenmethode zur Bestimmung von 0,001—1 p.p.m. Cu in Mineralien angeben: "Die Bestimmung von 1—1000 parts per 10^9 (oder 1—1000 pp10^9) Kupfer in Mineralien". Vereinzelt fand diese Einheit in ausgeschriebener Form (z.B. part per 10^9) bereits in der Literatur Anwendung [9].

(b) Teil-logarithmische Form. Das durch die Ballaststoffmenge bestimmte Zehnerpotenzniveau des Spurenelementgehaltes wird in logarithmischer Form angegeben (Tab. 2, Spalte 7). Zum Beispiel

1 p.p.m. = 1 Teil von 1000000 Teilen = $1/1000000 = 1 \cdot 10^{-6}$ (3)

Setzt man für den Faktor 10^{-6} dessen negativen Logarithmus ein und verwendet für diese Einheit ein dem pH-Wert analoges Symbol, nämlich pT (T ist vom Wort "trace=spur" abgeleitet und bedeutet hier Zehnerpotenzniveau des Spurenelementes), so lässt sich nach Gl. (3) angeben

1 p.p.m. = 1 pT 6 (4)

Aus Gl. (4) ergibt sich die allgemeine Form

$$\text{Spurengehalt} = a \text{ Teile von } 10^x \text{ Teilen} = a \cdot 1/10^x = a \cdot 10^{-x} \triangleq a \cdot (-\log 10^{-x})$$

$$= a \cdot \text{pT}\, x \quad (5)$$

a = Menge des Spurenelementes auf einem definiertem Zehnerpotenzniveau, T = Zehnerpotenzniveau des Spurenelementgehaltes, pT = negativer Logarithmus von T, x = Zahlengrösse für pT. Hervorzuheben ist hier, dass nach Gl. (3) bis (5) nur der Zehnerpotenz-Faktor (Multiplikator) logarithmiert wird, die erste Zahl a (Multiplikand) aber unverändert bleibt. Hiernach (Tab. 2, Spalte 7) würde man z.B. für eine Analysenmethode zur Bestimmung von 0,001—1 p.p.m. Cu in Mineralien angeben: "Die Bestimmung von pT 6—9 Kupfer in Mineralien".

(c) Voll-logarithmische Form. Eine weitere Möglichkeit wäre schliesslich, analog zum pH-Wert den Spurengehalt vollständig in logarithmischer Form anzugeben (Tab. 2, Spalte 8). Nach Gl. (5) ergibt sich die allgemeine Form

$$\text{Spurengehalt} = a \cdot 10^{-x} \triangleq -\log (a \cdot 10^{-x}) = \text{pX} \quad (6)$$

p = negativer Logarithmus des Spurengehaltes, X = Symbol des Spurenelementes. Diese Darstellungform hat aber den Nachteil, dass die gemessenen Spurengehalte immer in die Logarithmen umgerechnet werden müssen, im Gegensatz zu der einfachen Messung des pH-Wertes mit Hilfe eines pH-Meters ohne zusätzliche Rechenoperationen. Hiernach (Tab. 2, Spalte 8) würde man z.B. für eine Analysenmethode zur Bestimmung von 0,001—1 p.p.m. Cu in Mineralien angeben: "Die Bestimmung von pCu 6—9 in Mineralien". Auch von anderer Seite wurde die Verwendung des Symbols pX für die Angabe von Spurengehalten vorgeschlagen [7], jedoch dient dort der negative Logarithmus des Prozengehaltes als Grundlage.

SCHLUSSFOLGERUNG UND EMPFEHLUNG

Aufgrund der Erörterungen in den vorhergehenden Abschnitten erscheint es am zweckmässigsten und sinnvollsten, für die Angabe von Spurengehalten und -bereichen einen Zahlenbegriff zu verwenden. Wortbegriffe, wie z.B. Millispur, Mikrospur usw., sollten hingegen vermieden werden. Es wird daher empfohlen, dafür die im vorhergehenden Abschnitt abgeleitete Einheit in ausgeschriebener Form (a), in teil-logarithmischer Form (b) oder in voll-logarithmischer Form (c) zu verwenden

(a) $\boxed{a \cdot \text{pp}10^x}$ oder (b) $\boxed{a \cdot \text{pT}\, x}$ oder (c) $\boxed{\text{pX}}$

Beispiel:
Hiernach würde man 0,005 p.p.m. Cu angeben als (a) 5 $\text{pp}10^9$ Cu, oder (b) 5 pT 9 Cu, oder (c) pCu 8,30.

In vorliegender Form, d.h. ohne Zusatzinformation, handelt es sich stets um Massen-Gehalte. Für die anderen Relationen ist stets die Zusatzinfomation "Volumen" bzw. "mol" hinzuzufügen: $a \cdot \mathrm{pp10}^{x}$ (Vol) oder $a \cdot \mathrm{pT}\,x$ (Vol) oder pX (Vol) bzw. $a \cdot \mathrm{pp10}^{x}$ (mol) oder $a \cdot \mathrm{pT}\,x$ (mol) oder pX (mol).

Diese Definitionen erfüllen die geforderten Bedingungen und schliessen alle denkbaren Vorteile ein: sie sind als Zahlenbegriff leicht und allgemein verständlich, vermeiden die Definition von Wortbegriffen (Milli-, Mikrospur usw.) als Quelle von Missverständnissen, machen somit eine Aufteilung des Spurenbereiches mit Hilfe von Wortbegriffen überflüssig und sind auf beliebig kleine Gehalte anwendbar, wie dies aus Tab. 2 (Spalten 6—8) hervorgeht.

Die Einheit in Form (a) hat den Vorteil, dass sie leicht zu verstehen und zu merken ist, die Angabe endeutig ist und Missverständnisse nicht möglich sind. Ihre allgemeine Anwendung dürfte ausserdem keine Schwierigkeiten bereiten, da sie sich deutlich erkennbar vom vertrauten p.p.m. ableitet. Die Einheit in Form (b) hat dagegen den Vorteil der einfacheren Schreibweise, ist aber vorläufig noch neu and ungewohnt, weshalb ihre klare Definition notwendig ist. Die Einheit in Form (c) schliesslich ist einfach in der Schreibweise und vertraut wegen ihrer Analogie zum pH-Wert, hat aber den Nachteil der stets notwendigen Umrechnung in Logarithmen. Nach Ansicht des Autors sollte Form (a) oder (b) der Vorzug gegeben werden.

LITERATUR

1 O. G. Koch und G. A. Koch-Dedic, Handbuch der Spurenanalyse, Springer, Berlin, 2 Aufl. 1974.
2 G. H. Morrison, Trace analysis: Physical methods, Interscience, New York, 1965.
3 M. Pinta, Recherche et dosage des éléments traces, Dinod, Paris, 1962.
4 E. B. Sandell, Colorimetric determination of traces of metals, Interscience, New York, 3rd edn., 1959.
5 Int. Union Pure Appl. Chem., Anal. Chem. Division, Comm. Anal. Nomenclature, Recommendations on nomenclature of scales of working in analysis, IUPAC Inform. Bull. No. 18, February 1972.
6 G. Gottschalk, R. Kaiser, H. Malissa, J. Rendl, E. Schwarz v. Bergkampf, W. Simon, H. Spitzy, R. D. Werder und H. Zettler, Z. Anal. Chem., 261 (1972) 1.
7 H. Kaiser, Pure Appl. Chem., 34 (1973) 35.
8 G. Tölg, Talanta, 19 (1972) 1489.
9 P. Schiller, G. B. Cook, A. Kitzinger and E. Wölfl, Analyst (London), 97 (1972) 601.

Analytica Chimica Acta, 82 (1976) 29—35

THE POLAROGRAPHIC REDUCTION OF SOME DINITROANILINE HERBICIDES*

LLOYD M. SOUTHWICK and GUYE H. WILLIS

United States Department of Agriculture, Agricultural Research Service, P.O. Drawer U, University Station, Baton Rouge, LA 70803 (USA)

PURNENDU K. DASGUPTA and CSABA P. KESZTHELYI

The Charles Edward Coates Laboratory, Department of Chemistry, Louisiana State University, Baton Rouge, LA 70803 (USA)

(Received 30th June 1975)

SUMMARY

Polarography of 2,6-dinitroaniline herbicides in aqueous ethanol revealed a marked pH dependence of the reduction potentials. The study included the herbicides trifluralin (I), benefin (II), isopropalin (III), dinitramine (IV), nitralin (V), and oryzalin (VI), for which $E_{\frac{1}{2}}$ values (mV vs. SCE) for the first polarographic wave, at pH 1.5, 5.1, 7.4, and 9.2, respectively, were (I) −190, −430, −540, −640; (II) −190, −430, −540, −640; (III) −170, −360, −560, −650; (IV) −230, −510, −720, −810; (V) −160, −330, −540, −650; (VI) −160, −370, −540, −680.

Polarography at the dropping mercury electrode (DME) is perhaps the best established electroanalytical technique [1—4]. The very high overpotential for hydrogen discharge on mercury makes d.c. polarography [1—4] feasible for many aqueous systems in which other types of voltammetry, e.g. those employing platinum disk electrodes (PDE), are impractical. Recent advances in the development of nonaqueous solvents [5—7], while greatly extending the anodic and cathodic range of feasibility for platinum and other precious metal electrodes, by their very nature curtail the use of aqueous solvents which are encountered in biological systems or the natural environment. Consequently, electrochemical studies of aqueous systems continue to employ DME polarography.

The electrochemistry of nitroaromatic compounds has been thoroughly investigated and reported over the years. In particular, nitrobenzene and *m*-dinitrobenzene have been studied by Pearson [8] and by Dennis et al. [9], and 2,4-dinitroaniline has been examined by Holleck and Exner [10]. The newness and widespread application of the dinitroaniline herbicides (for example, in 1971 alone 25 million pounds of trifluralin were produced [11])

*Joint contribution from the Agricultural Research Service, U.S. Department of Agriculture, cooperating with the Louisiana Agricultural Experiment Station, and the Chemistry Department, Louisiana State University, Baton Rouge, Louisiana.

are an added impetus to the present study. While the literature contains information on the reductive degradation of some dinitroaniline herbicides [12—14], this is the first electrochemical investigation dealing with the compounds I—VI.

EXPERIMENTAL

A Sargent model XV polarograph* equipped with a Sargent model A *iR* compensator was used. Samples were scanned from 0 to —2.00 V, usually with small damping conditions (RC = 1 s). The instrument was checked and calibrated with standard cadmium chloride solutions in 0.2 M HCl. The experiments, conducted at ambient temperatures, were necessarily anaerobic and carried out under nitrogen. The nitrogen was first bubbled through a 40 % alcohol solution to prevent excessive alcohol evaporation from the experimental cell. A mercury column height of 35.3 cm was maintained. All the chemicals used were analytical reagent grade, except for the mercury (Sargent—Welch Scientific Company, triply distilled) and the herbicides, which were recrystallized from aqueous ethanol.

Figure 1 gives the structural formulae and nomenclature for the six herbicides studied. Pearson's work [8] with *m*-dinitrobenzene was duplicated with satisfactory agreement before the technique was extended to the new

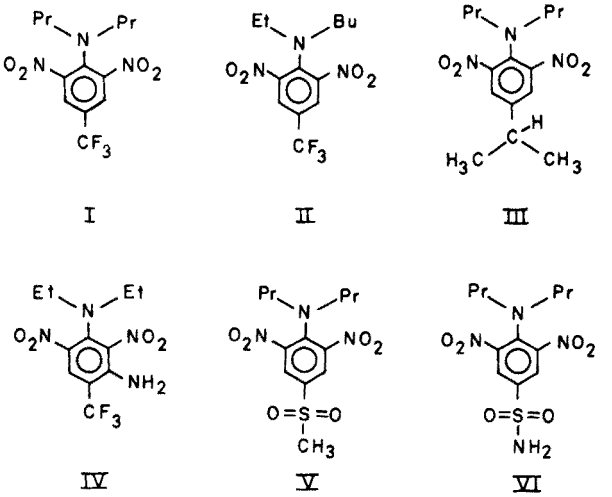

Fig. 1. Dinitroaniline herbicides studied: I, 4-(trifluoromethyl)-2,6-dinitro-*N*,*N*-dipropylaniline (trifluralin); II, *N*-butyl-*N*-ethyl-4-(trifluoromethyl)-2,6-dinitroaniline (benefin); III, 2,6-dinitro-4-isopropyl-*N*,*N*-dipropylaniline (isopropalin); IV, N^1,N^1-diethyl-4-(trifluoromethyl)-2,6-dinitro-*m*-phenylenediamine (dinitramine); V, 4-(methylsulfonyl)-2,6-dinitro-*N*,*N*-dipropylaniline (nitralin); VI, 3,5-dinitro-N^4,N^4-dipropylsulfanilamide (oryzalin).

*Mention of trade names is for convenience and does not indicate any preference of the U.S. Dept. of Agriculture.

compounds. Half-wave potentials were determined in solutions buffered at pH 1.5 (KCl—HCl), 5.1 (potassium hydrogen phthalate—NaOH), 7.4 (KH_2PO_4—NaOH), and 9.2 (borax—NaOH). Since the alcohol concentration raised the final pH by several tenths of a unit, the buffers themselves were adjusted to appropriately lower values. Poor herbicide solubility in aqueous buffered solution prevented the use of less alcohol.

The potential at which background electrolysis began was dependent on pH. At pH 1.5 electrolyte reduction occurred at −1.5V; at pH 9.2 reduction began at −1.9V.

A 100-ml ethanolic solution of the compound under study was diluted to 250 ml with 0.25 M aqueous buffer to give a 40 % ethanolic solution, $6 \cdot 10^{-5}$ M in the nitro compound and 0.15 M in buffer; 20—25 mg gelatin was added as maximum suppressor. The measured half-wave potentials are based on the top of the polarographic wave as is customary for irreversible reductions.

RESULTS

Table 1 gives the reduction potentials for *m*-dinitrobenzene and for 2,4- and 2,6-dinitroaniline. For *m*-dinitrobenzene at pH 4.1, $6 \cdot 10^{-4}$ M, 8 % ethanol, the measured half-wave potentials agree closely with Pearson's values [8] which were −250 and −420 mV. The potentials observed for *m*-dinitrobenzene in 40 % ethanol at pH 7.4 and 9.2 (Table 1) are 50 to 100 mV more negative than those reported by Pearson at these pH values in 8 % ethanol. Our data for 2,4-dinitroaniline supplement the results of Holleck and Exner [10], who reported the reduction in 20 % methanol at pH 3.1 and 11.0.

A study of concentration effects with trifluralin indicated that the reduction is not greatly concentration dependent. In 40 % ethanol at pH 1.5, one wave was discernible with both $6 \cdot 10^{-5}$ M and $6 \cdot 10^{-4}$ M solutions; the

TABLE 1

Half-wave potentials (mV vs. SCE) of nitroaromatic compounds at different pH values

	pH					
	1.5	4.1[a]	4.1[b]	5.1	7.4	9.2
m-Dinitrobenzene[a]	−120	−270	−260	−330	−450	−560
	−240	−420	−390	−510	−670	−790
2,4-Dinitroaniline[c]	−160			−380	−560	−690
	−300			−610	−790	−910
2,6-Dinitroaniline[c]	−110			−340	−460	−590
	−260			−550	−760	−880

[a] $6 \cdot 10^{-4}$ M in 40 % ethanol. At pH 1.5 an additional, ill defined wave was present at about −1000 mV.
[b] $6 \cdot 10^{-4}$ M in 8 % ethanol.
[c] $6 \cdot 10^{-5}$ M in 40 % ethanol.

measured $E_{\frac{1}{2}}$ values were −190 and −170 mV, respectively. In the same solvent at pH 9.2, two waves were distinguishable; trifluralin at the lower concentration exhibited $E_{\frac{1}{2}}$ values of −640 and −810 mV, whereas at the higher concentration the reduction occurred at −620 and −780 mV.

Table 2 presents the results obtained for the dinitroaniline herbicides in 40 % ethanol at a concentration of $6 \cdot 10^{-5}$ M.

DISCUSSION

The dinitroaniline herbicides exhibited the decrease in reduction potential with increase in pH (Table 2) that is characteristic of the polarographic reduction of the aromatic nitro group. Figure 2 illustrates this relationship between pH and $E_{\frac{1}{2}}$ for trifluralin (I).

The ease of reduction of the herbicides was similar but not identical. The greatest difference occurred with dinitramine (IV), which at every pH investigated was more difficult to reduce than the other dinitroanilines. The lower reduction potentials exhibited by dinitramine are presumably a result of the electron-donating influence of the 3-amino group.

In his study of the polarography of several aromatic nitro compounds, Pearson [8] obtained data which indicated a series of stepwise reductions of the nitro groups, first to the hydroxylamino derivatives, then to the amino compounds. This sequential reduction is shown below for *m*-dinitrobenzene, which Pearson observed was not reduced to the phenylenediamine unless the pH of the medium was below about 3. This scheme is the commonly observed pathway for polarographic reduction of the aromatic nitro group in protic solvents [5, 15].

TABLE 2

Half-wave potentials (mV vs. SCE) of dinitroaniline herbicides[a]

	pH			
	1.5	5.1	7.4	9.2
Trifluralin	−190	−430	−540	−640
			−700	−810
Benefin	−190	−430	−540	−640
			−700	−810
Isopropalin	−170	−360	−560	−650
			−720	−810
Dinitramine	−230	−510	−720	−810
				−1010
Nitralin	−160	−330	−540	−650
		−480	−710	−790
Oryzalin	−160	−370	−540	−680
		−530	−680	−810

[a] $6 \cdot 10^{-5}$ M in 40 % ethanol.

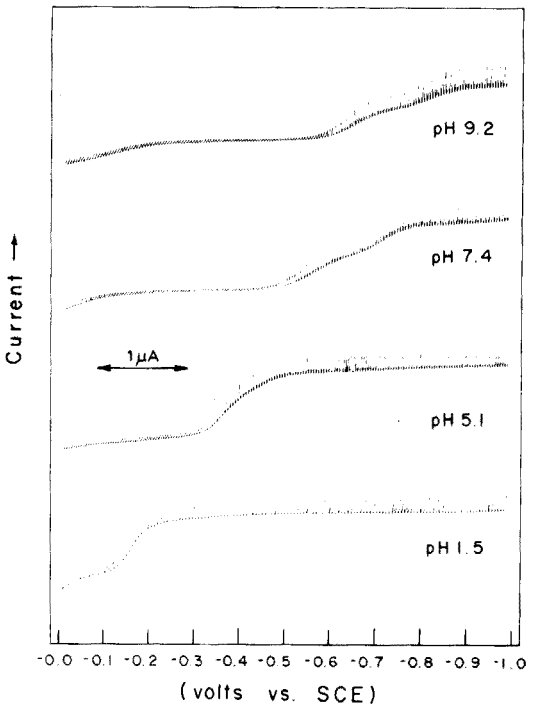

Fig. 2. Half-wave reduction potentials of $6 \cdot 10^{-5}$ M trifluralin in 40 % ethanol solution as a function of pH.

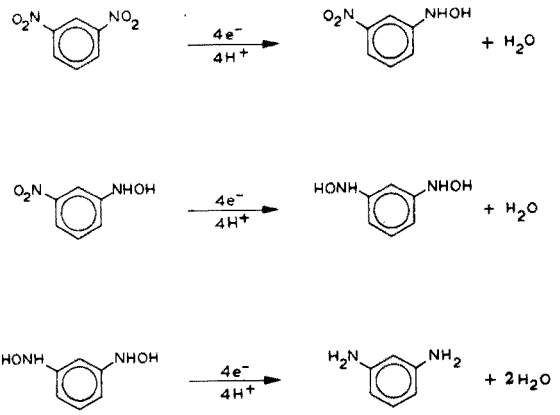

Comparing diffusion current values for *m*-dinitrobenzene with those measured for the herbicides indicated that these dinitroaniline derivatives were reduced in two 4e steps, as illustrated for trifluralin.

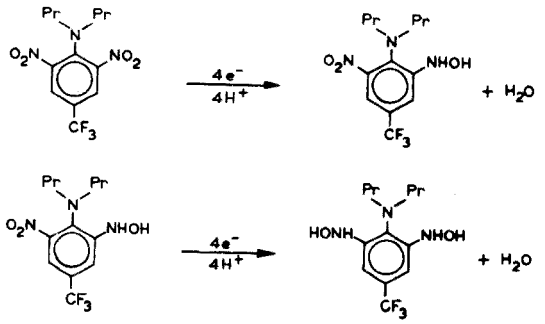

Even at the lowest pH studied the herbicides did not appear to undergo further reduction before the beginning of background electrolysis.

A prevalent environmental situation characterized by a reducing, anaerobic condition is a submerged soil or sediment, which commonly exhibits an oxidation—reduction potential of −250 to −550 mV (SCE), and occasionally of −650 mV [16]. Although the solution pH of submerged soils is usually around 7 [16] the effective pH at the surface of the soil particles is generally assumed to be lower [17]. Trifluralin is one of a number of pesticides which degrade more rapidly under anaerobic than under aerobic conditions [13]. In an anaerobic situation the initial steps of trifluralin degradation entail reduction of the nitro groups, but the literature reports concerning the chemical—biochemical nature of these steps are conflicting [14]. Our polarographic study demonstrates the relative ease of reduction of these compounds and points to the feasibility, in a submerged soil situation, of a nonbiological pathway for the initial steps in the reductive degradation of the dinitroaniline herbicides.

We thank Eli Lilly Research Laboratories, Greenfield, Indiana, U.S. Borax Research Corporation, Anaheim, California, and Shell Chemical Company, New York, New York for samples of the herbicides used. The paper was presented at the 30th Southwest Regional Meeting of the American Chemical Society, December, 1974, Houston, Texas. Partial financial support of this work by an LSU Council on Research 1974 summer faculty grant is gratefully acknowledged.

REFERENCES

1 I. M. Kolthoff and J. J. Lingane, Polarography: Polarographic Analysis and Voltammetry, Amperometric Titrations, Interscience, New York, 2nd ed., 1952.
2 L. Meites, Polarographic Techniques, Wiley—Interscience, New York, 1965.
3 J. Heyrovský and P. Zuman, Practical Polarography, Academic Press, New York, 1968.
4 H. L. Kies and M. Den Os, Anal. Chim. Acta, 67 (1973) 246.
5 C. K. Mann and K. K. Barnes, Electrochemical Reactions in Nonaqueous Systems, Dekker, New York, 1970.
6 C. P. Keszthelyi and A. J. Bard, J. Electrochem. Soc., 120 (1973) 241.

7 C. P. Keszthelyi, N. E. Tokel-Takvoryan and A. J. Bard, Anal. Chem., 47 (1975) 249.
8 J. Pearson, Trans. Faraday Soc., 44 (1948) 683.
9 S. F. Dennis, A. S. Powell and M. J. Astle, J. Amer. Chem. Soc., 71 (1949) 1484.
10 L. Holleck and H. J. Exner, Z. Electrochem., 56 (1952) 677.
11 O. Johnson, Chem. Week, 110 (June 21, 1972) 33.
12 G. W. Probst and J. B. Tepe, in P. C. Kearney and D. D. Kaufman (Eds.), Degradation of Herbicides, Dekker, New York, 1969, p. 255.
13 G. H. Willis, R. C. Wander and L. M. Southwick, J. Environ. Qual., 3 (1974) 262.
14 J. F. Parr and S. Smith, Soil Sci., 115 (1973) 55.
15 H. Lund, in M. M. Baizer (Ed.), Organic Electrochemistry, Dekker, New York, 1973, p. 315.
16 F. N. Ponnamperuma, Advan. Agron., 24 (1972) 29.
17 G. W. Bailey and J. L. White, Residue Rev., 32 (1970) 29.

Analytica Chimica Acta, 82 (1976) 37—44

A THALLIUM(I)-SELECTIVE ELECTRODE BASED ON A LIQUID ION-EXCHANGER CONTAINING 0,0′-DIDECYLDITHIOPHOSPHORIC ACID

WALENTY SZCZEPANIAK and KRZYSZTOF REN

Institute of Chemistry, Adam Mickiewicz University, 60—780 Poznań (Poland)

(Received 14th July 1975)

SUMMARY

A liquid ion-exchange electrode containing thallium(I) 0,0′-didecyldithiophosphate in chlorocyclohexane is described. Nernstian behaviour is obtained in the *p*Tl range 1—5.5, the slope of the calibration graph being 57.6 mV/decade change in activity at ionic strength 0.1. Alkali and alkaline earth metal cations do not interfere ($K_{Tl/M} < 10^{-5}$). Potentials are established rapidly, and are unaffected by pH in the range 5—12. In analytical applications direct potentiometry and potentiometric precipitation titrations with iodide or tetraphenylborate solutions are satisfactory. Various interfering ions can be masked with EDTA.

Complexes of metal cations with 0,0′-dialkyldithiophosphoric acids have found widespread technical usage, but are less known in analytical work [1]. The complexes with many bivalent transition metal ions(I) are difficultly soluble in water but readily soluble in apolar solvents. With monovalent metal cations, these acids form two kinds of compound, II and III.

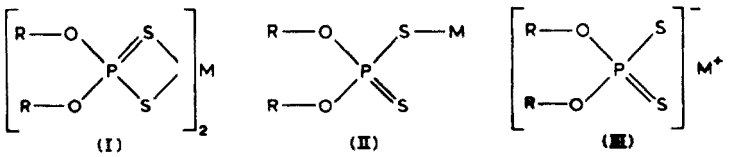

(I) (II) (III)

The covalent complexes (II), which are difficultly soluble in water, are formed by cations such as Ag(I), Tl(I) and Cu(I), whereas water-soluble salts of type III are formed with cations such as potassium(I).

In this paper, the covalent salt of thallium(I) with 0,0′-didecyldithiophosphoric acid, is proposed as the active electrode substance in a thallium(I)-selective liquid-exchanger electrode.

EXPERIMENTAL

Preparation of the liquid exchanger

The potassium salt of 0,0′-didecyldithiophosphoric acid was prepared by a procedure analogous to that used for the synthesis of lower esters [2, 3]. In the case of decanol, the reaction is

$$P_2S_5 + 4\ C_{10}H_{21}OH = 2\ (C_{10}H_{21}O)_2PSSH + H_2S$$

The acid was neutralized with potassium carbonate. The potassium salt of 0,0′-didecyldithiophosphoric acid was then purified by dissolution in acetone and precipitation with ether. After 3 recrystallizations, a crystalline product was obtained (m.p 167 °C); elemental analysis confirmed the compound to be $(C_{10}H_{21}O)_2PSSK$.

The thallium(I) salt was precipitated by addition of thallium nitrate to an aqueous—alcoholic solution of the potassium salt at pH 5.6. This salt is readily soluble in diethyl ether, which was therefore used for its extraction; the ether solution was washed twice with twice-distilled water in order to remove any traces of the potassium salt (and $TlNO_3$). After evaporation of the ether, the complex was dried in a vacuum desiccator and recrystallized twice from diethyl ether. The crystalline substance (m.p. 62 °C) was shown to be $(C_{10}H_{21}O)_2PSSTl$.

Reagents

Solutions of the cations tested were prepared from pro-analysi salts. Twice-distilled water was used. Solvents were purified by distillation.

Construction of the electrode

A Teflon body [4] was used in the electrode construction. The general principle was similar to that of the Orion liquid-exchanger electrode, i.e. an internal aqueous solution, separated from the aqueous test solution by means of a porous membrane saturated with an organic solution. The internal solution consisted of 10^{-3} M TlCl and 0.1 M KCl in a saturated solution of AgCl. The liquid ion-exchanger solution was a 0.2 M solution of $(C_{10}H_{21}O)_2PSSTl$ in chlorocyclohexane.

The porous membranes (Sartorius type SM-113-06) were silanized: the filter disks (5.5-mm diameter) were dried over Molecular Sieve 4A and then treated with a solution of trimethylchlorosilane in benzene. After careful washing in benzene and drying in a vacuum desiccator, the membranes were ready for use.

The measuring cell used was:

Ag/AgCl	internal solution	membrane	test solution	1 M KNO_3 salt bridge	1 M KCl	AgCl/Ag

E.m.f. measurements were done with an Elpo pH meter type N-512 connected to a digital readout (type V530 Meratronik, Poland); this system allowed the e.m.f. to be read to ± 0.1 mV. For recording titration curves and testing potential stabilization, the pH meter was connected to a recorder (type KSP-4, U.S.S.R) through a d.c. amplifier (type I-37, U.S.S.R).

All measurements were carried out at 20 ± 1 °C in 150-ml teflon beakers. Test solutions were stirred magnetically.

RESULTS AND DISCUSSION

The liquid ion-exchanger

The optimal composition of the liquid ion-exchanger was studied in detail. Tests were made with solutions of thallium 0,0′-didecyldithiophosphate in *n*-decanol, butyrophenone, 2-chlorotoluene, 1,1,2,2,-tetrachloroethane and chlorocyclohexane. A 0.2 M solution in chlorocyclohexane was found most suitable; other solvents were less satisfactory. The choice of the best alkyl chain length was also considered. The shorter the chain length in the 0,0′-dialkyldithiophosphoric acid, the greater the solubility of the thallium(I) salt in water but the lower the solubility in apolar solvents. For example, the diethyldithiophosphate salt has a solubility of $3.05 \cdot 10^{-3}$ mol l^{-1} in water at 25 °C, so that it cannot be used as the ion-exchanger in a liquid membrane. Thallium(I) 0,0′-didecyldithiophosphate is much less soluble in water ($4.7 \cdot 10^{-6}$ mol l^{-1} at 25 °C), and therefore provides a reasonable range of linear response of the electrode.

Linear response range

The dependence of the electrode potential on the thallium(I) concentration was tested in pure thallium nitrate solutions in the range 10^{-1}—10^{-6} M, in solutions containing both thallium(I) nitrate and 0.1 M sodium nitrate. Figure 1 shows that in both cases the electrode provides a Nernstian relationship over the pTl range 1—5.5. The slope of the linear range of the calibration graphs at 20 °C is 57.6 mV. At an ionic strength of 0.1 ($NaNO_3$), there is no statistical difference between the e.m.f.—activity relationships for solutions of $TlNO_3$, TlCl and Tl_2SO_4; in all three cases, the relationship is linear to pa_{Tl} 5.5, and the slope of the plot is 57.9 mV/*p*Tl at 20 °C, which is very near the theoretical Nernstian slope. Thus the anions nitrate, chloride and sulphate do not affect the potential of the electrode.

Effect of pH

The influence of pH over the range 2—12 on the electrode potential was tested for solutions containing 10^{-1}—10^{-5} M thallium(I) nitrate. The test solutions were prepared in 0.1 M sodium hydroxide solution, nitric acid was

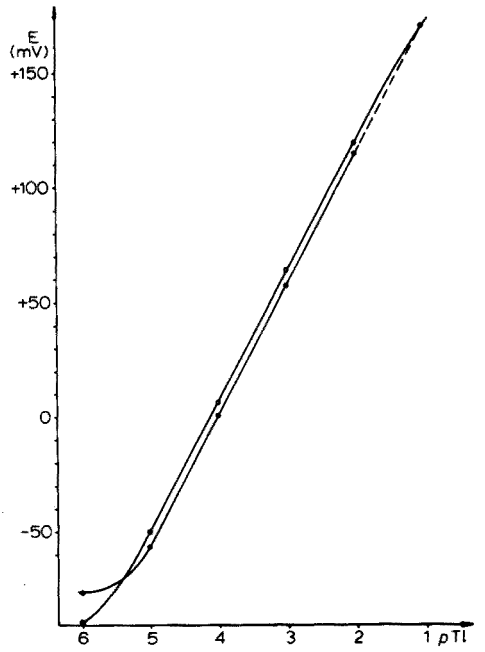

Fig. 1. Calibration curves for $TlNO_3$ (○) and $TlNO_3$ in 0.1 M $NaNO_3$ (●).

added to give the appropriate pH, and the potential was then measured. The results obtained are given in Fig. 2. The electrode shows constant potentials between pH 3 and 12 in solutions which are 10^{-1} M, 10^{-2} M or 10^{-3} M in thallium nitrate. With 10^{-4} M $TlNO_3$, constant potential is maintained in the pH range 5.5—12, whereas in 10^{-5} M $TlNO_3$, the permissible pH range is 6—12.

Dynamic response of the electrode

The dynamic response was tested for 10^{-6}—10^{-2} M thallium nitrate solutions in 0.1 M $NaNO_3$ at pH 10; the sequence of measurements was from low concentrations to high concentrations. The results (Fig. 3) show that the potential (± 0.1 mV) is established quickly, within 15—60 s depending on concentration. For an accuracy of ± 1 mV, the potential stabilization is practically immediate.

Selectivity coefficients

The selectivity coefficients were determined from measurements of the electrode potential in thallium(I) nitrate solutions with and without the diverse ion; the thallium(I) activity of the solutions was always 10^{-3} M, and constant ionic strength was maintained with sodium nitrate. The selectivity coefficients ($K_{Tl/M}$) were calculated from the formula

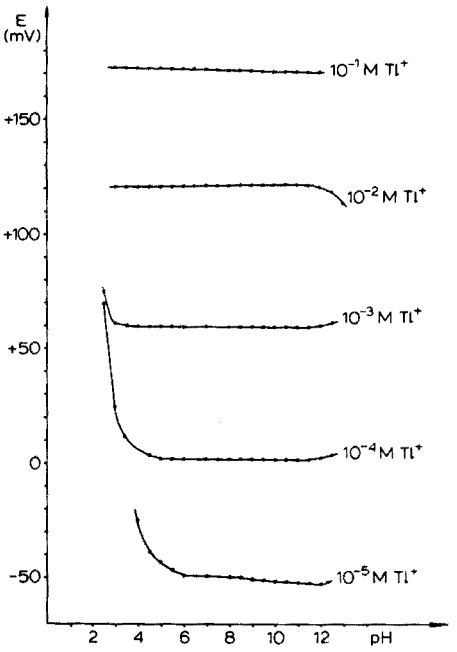

Fig. 2. The effect of pH on the response of the electrode.

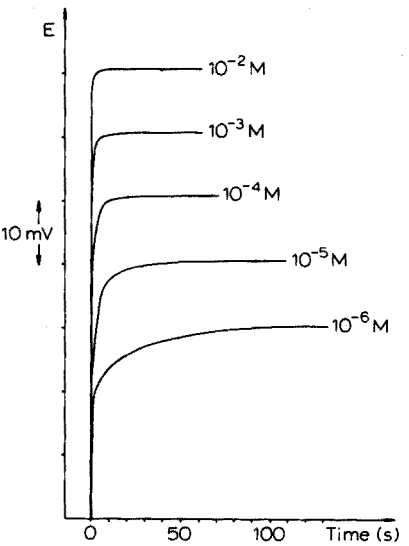

Fig. 3. Dynamic response of the thallium-selective electrode in pure $TlNO_3$ solutions.

$$K_{Tl/M} = \left\{\left[\exp\frac{(E_{Tl/M} - E_{Tl})F}{RT}\right] - 1\right\}\frac{a_{Tl}}{a_M^{\frac{1}{z}}}$$

where $E_{Tl/M}$ is the potential of the electrode immersed in a solution containing Tl(I) and M^{z+}, E_{Tl} is the potential in the Tl(I) solution, a_{Tl} and a_M^{z+} are the activities of Tl^+ and M^{z+}, respectively, and z is the valency of the M cation.

The $K_{Tl/M}$ values obtained are presented in Table 1. These values show that the electrode has a very high selectivity for thallium(I) compared to the alkali and alkaline earth metals. At constant ionic strength, variations in the concentrations of these cations do not affect the electrode potential.

TABLE 1

Selectivity coefficients of Tl(I) liquid-membrane electrode at ionic strength 0.1

Interfering cation	$K_{Tl/M}$	Interfering cation	$K_{Tl/M}$
Hg^{2+}, Ag^+, Pb^{2+}, Cd^{2+}	>1	Ni^{2+}	$8.3 \cdot 10^{-3}$
H^+	1	Fe^{2+}	$2.0 \cdot 10^{-3}$
Cu^{2+}	0.8	Co^{2+}	$4.4 \cdot 10^{-5}$
Zn^{2+}	$2.9 \cdot 10^{-2}$	Mn^{2+}	$<5 \cdot 10^{-5}$
Cr^{3+}	$1.9 \cdot 10^{-3}$	Be^{2+}, Mg^{2+}, Ca^{2+}, Sr^{2+}	$<10^{-5}$
Al^{3+}	$1.6 \cdot 10^{-3}$	Ba^{2+}, Li^+, Na^+, K^+, Rb^+, Cs^+	

The cations Ag^+, Hg^{2+}, Pb^{2+} and Cd^{2+} form strong complexes with the 0,0'-dialkyldithiophosphoric acids [5] and so interfere.

Analytical application

This thallium(I)-selective electrode can be used practically for the determination of thallium(I) either by direct measurement of the potential and comparison with a working curve, or by potentiometric titration. The direct method can be used in the linear range of the working curve, i.e. 10^{-1}—$5 \cdot 10^{-6}$ M, without interference from the alkaline and alkaline earth metal ions. Direct determinations of thallium(I) in the presence of interfering elements e.g. Pb(I) or Cu(II), were also tested, with EDTA as masking agent. Figure 4 shows the calibration curves obtained for thallium(I) in solutions of 0.1 M $NaNO_3$, and in solutions at pH 5 containing 10^{-3} M lead nitrate with and without 10^{-2} M EDTA. It can be seen that lead(II) after being masked does not influence the electrode potential.

The selectivity of the electrode against some ions and the possibility of masking interfering ions allows direct determinations of thallium in the presence of many accompanying cations.

The electrode can also be used as an indicator electrode in precipitation titrations of thallium(I) with potassium iodide and sodium tetraphenylborate.

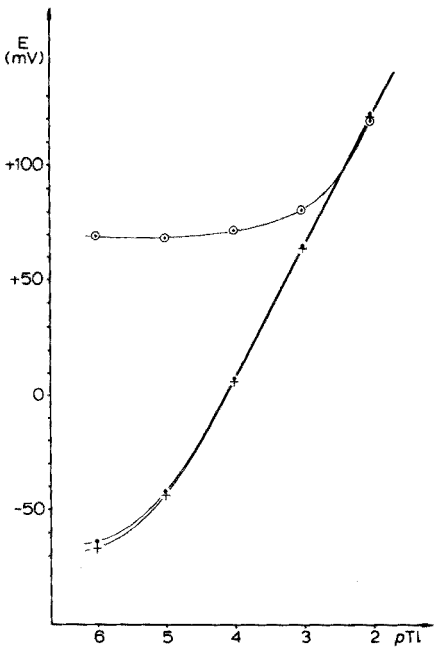

Fig. 4. Calibration curves for thallium(I) in pure solutions (+), in the presence of lead nitrate (⊙), and in the presence of lead nitrate masked with EDTA (•).

Titration curves are presented in Figs. 5 and 6. In all cases the titrant was ten times more concentrated than the titrated solution of thallium(I) nitrate. In the titrations with iodide solutions, good titration curves were obtained for 10^{-1}—10^{-5} M thallium(I) solutions. The poor sensitivity of this titration is due to the relatively high solubility of thallium iodide. When sodium tetraphenylborate was used, 10^{-1}—10^{-4} M thallium(I) solutions could be easily titrated; the curve for 10^{-5} M $TlNO_3$ is less satisfactory, but the end-point of the titration can still be determined. For quantitative characterization of the method, a statistical evaluation was made for the results of titrations of 50 ml of 10^{-4} M $TlNO_3$ with 10^{-3} M sodium titraphenylborate; the end-points were determined graphically from the titration curve. Ten analyses of solutions containing 1.022 mg of thallium(I) gave an average result of 1.018 mg with a standard deviation of 0.004 and a relative standard deviation of 0.36 %; the mean error of the arithmetic mean was 0.0012, and at the 95 % confidence limit, the deviation was ± 0.003 mg.

It is also possible to titrate thallium(I) with sodium tetraphenylborate in the presence of metal cations with high selectivity coefficients if EDTA is used as masking agent. Further analytical possibilities will be described in future publications.

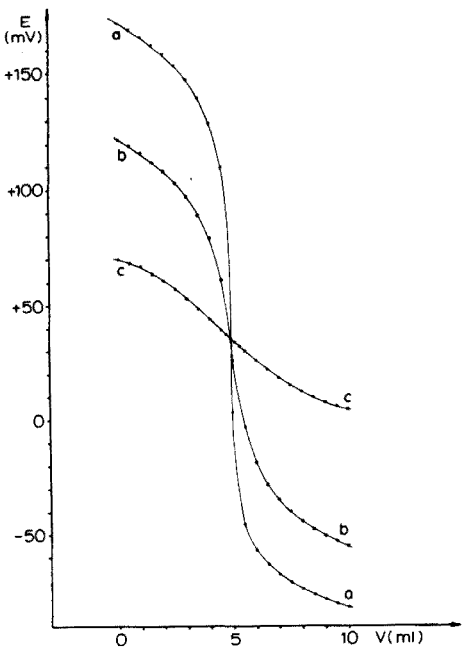

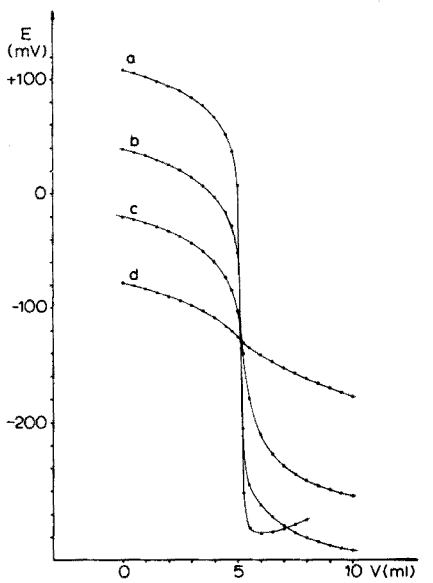

Fig. 5. Titrations of thallium(I) with potassium iodide solutions at pH 10. (a) 10^{-1} M Tl^+. (b) 10^{-2} M Tl^+. (c) 10^{-3} M Tl^+.

Fig. 6. Titrations of thallium(I) with sodium tetraphenylborate solutions. (a) 10^{-2} M Tl^+. (b) 10^{-3} M Tl^+. (c) 10^{-4} M Tl^+. (d) 10^{-5} M Tl^+.

REFERENCES

1 D. E. C. Corbridge, The Structural Chemistry of Phosphorus, Elsevier Scientific Publishing Company, Amsterdam, 1974.
2 A. I. Busev, Synthesis of New Organic Reagents for the Inorganic Analysis, M.G.U., 1972.
3 A. I. Busev and M. I. Ivanjutin, Fr. Kom. Anal. Khim. Akad. Nauk USSR, 11 (1960) 172.
4 K. Ren and W. Szczepaniak, Chem. Anal. (Warsaw), in press.
5 V. F. Toropova, Obshch. Khim. 40 (1970) 1043; 41 (1971) 1673.

Analytica Chimica Acta, 82 (1976) 45—54

A SIMPLE CONTINUOUS METHOD FOR CALIBRATION AND MEASUREMENT WITH ION-SELECTIVE ELECTRODES

G. HORVAI, K. TÓTH and E. PUNGOR

Institute for General and Analytical Chemistry, Technical University, 1502 Budapest XI (Hungary)

(Received 18th August 1975)

SUMMARY

A new, continuous method has been developed for calibration and measurement with ion-selective electrodes. The electrode is immersed into a solution diluted with respect to one of the components which influence the potential of the electrode. The change of potential is followed as a function of diluent volume or dilution time and the results can be used to establish the calibration curve or selectivity data or to determine an unknown concentration value.

Ion-selective electrodes (i.s.e.) are used primarily for the potentiometric measurement of activities and concentrations of ionic species, but in some cases also for that of uncharged particles [1, 2]. Methods suitable for studying the most important parameters of these electrodes, e.g. potential response, selectivity data, etc. are of great practical importance. In this paper, a simple, continuous method which is easy to automate will be discussed in detail.

THEORETICAL

Calibration of i.s.e.

The e.m.f. of a potentiometric cell consisting of an i.s.e. and a suitable reference electrode is described by

$$E = E' + \frac{RT}{z_i F} \ln \left(a_i + \sum_j K_{ij} a_j^{z_i/z_j} \right) \tag{1}$$

where E' involves the activity-independent part of the e.m.f. value, a_i is the activity of the primary ion, a_j is the activity of the j-th interfering ion, and K_{ij} is the selectivity coefficient of the electrode with respect to the j-th interfering ion.

If $\sum_j K_{ij} a_j \ll a_i$, i.e. there is no significant interference, then

$$E = E' + S \log a_i \tag{2}$$

where S has been introduced for the term $RT \ln 10/z_i F$. Empirical S (slope) values are often slightly different from $RT \ln 10/z_i F$ [3]. If the mean activity coefficient $f_{i\pm}$ and the concentration c_i are used, eqn. (2) becomes

$$E = E' + S \log f_{i\pm}\, c_i \tag{3}$$

However, it is well known that if a stirred flow-through cell of constant volume is filled with a solution containing component A at concentration c_0, and "washed out" by passing a solution which does not contain component A, then the concentration of A in the cell will be

$$c = c_0\, e^{-V/V_r} \tag{4a}$$

or

$$c = c_0\, e^{-Wt/V_r} \tag{4b}$$

where V_r denotes the constant volume of solution in the cell, V denotes the volume of solution passed through the cell, t is the time elapsed from the beginning of the "washing-out" period, and W is the flow rate. Equation (4b) holds only if the flow rate W is kept constant.

The concentration of A in the cell, c, is thus a continuous function of V or t. Accordingly, if an electrode sensitive to A is immersed in the cell or built into its outlet, then the potential of the ion-selective electrode measured against a suitable reference electrode will also change continuously with V or t. The variation of E with V or t can easily be recorded; since the variation of c with V or t is known (eqns. (4a) and (4b)), these values can be used to obtain the function E vs. c which can be regarded as a calibration curve. However, E vs. log a curves are most commonly used as calibration curves (see eqn. (2)). Equations (4a) and (4b) are therefore converted to

$$\log c = \log c_0 - \frac{V}{V_r} \log e \tag{5a}$$

and

$$\log c = \log c_0 - t\,\frac{W}{V_r} \log e \tag{5b}$$

If the ionic strength and thus $f_{i\pm}$ is adjusted to a constant value, the E vs. log c function — calculated from E/V and eqn. (5a) or from E/t and eqn. (5b) — can be used as a calibration curve. Thus if E is followed as a function of V or t on a chart recorder, the calibration curve is simply obtained by rescaling the V or t axis in log c units. If one minute is equivalent to h mm on the chart paper, then a change of log c (or log a) by one unit is equivalent to

$$\frac{h\, V_r}{W \log e}\ (\text{mm}) \tag{6}$$

Determination of selectivity coefficients

The calibration method outlined above can also be applied for the measurement of selectivity coefficients, K_{ij}, by using the mixed solution method [4]. Let A_j denote a component which interferes with the measurement of the activity of species A_i, and the activity of which in the cell is kept at a constant value (a_j) by adjusting the activity of A_j to a_j in both the original and the "washing" solution. The calibration technique described above is then applied for A_i; K_{ij} can be determined [4] from the "calibration curve" which has the shape shown in Fig. 1.

Determination of unknown concentrations

The method is also useful in concentration and activity measurements. Three such applications will be discussed: comparison with calibration, standard addition, and a special addition—dilution method.

Comparison with calibration. Calibrations carried out as described above can be used in the same way as any simple (conventional) calibration. Furthermore, they can be employed in fully automated monitoring systems. For example, the sample to be measured is passed in a continuous stream through the cell in which the i.s.e. is immersed, the volume of the solution in the cell is kept constant by using an overflow system, and adequate stirring is done in any convenient way; the e.m.f. against a reference electrode is recorded continuously and compared to the calibration which is carried out at preset time intervals by stopping automatically the sample flow,

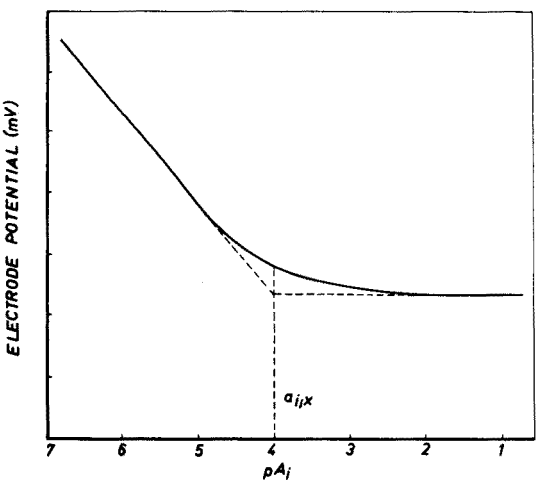

Fig. 1. Diagram used for the determination of the selectivity constant by the mixed solution technique; $K_{ij} = a_i,x/a_j$.

draining the cell, then refilling it with standard solution and diluting the standard with an inert solution of suitable ionic strength. The calibration data can be stored in the memory unit of a computer which compares the e.m.f. values measured in the sample with the calibration data.

The drawback of this method is that it cannot be applied, without further consideration, for electrodes which have long response times. However, if the response times are not too long, they can be compensated for by decreasing the W/V_r term. This will increase the time required for the calibration, but with such electrodes every other calibration method is time-consuming as well.

Standard addition. This method can be used advantageously in computer-controlled automatic monitoring systems. The cell is basically the same as before with the sample streaming continuously through it. Then at a given moment a small volume of standard solution ($V_{add} \ll V_r$) is added and the resulting potential change is followed until the original potential is re-established. The standard is injected near the stirrer and far from the outlet in a short time compared to the half-life of the exponential term in eqns. (4a) and (4b). At the moment of addition the concentration change is

$$\Delta c_0 = c_{add}\, V_{add}/V_r \tag{7}$$

where V_{add} is the volume of the standard solution of concentration c_{add} added to the sample solution. The difference between the actual concentration in the cell and the original sample concentration decreases with V or t according to

$$\Delta c = \Delta c_0\, e^{-\frac{V}{V_r}} \tag{8a}$$

or

$$\Delta c = \Delta c_0\, e^{-\frac{W}{V_r} t} \tag{8b}$$

The e.m.f. (E) is recorded at intervals ΔV or Δt in digital form; the pairs (E;V) or (E;t) can be fed immediately into a digital computer, which transforms the V or t data to Δc values by means of eqns. (7) and (8a) or (8b). The (E;c) pairs obtained in this way can be handled by the methods described in the literature [5, 6].

The advantage of the method is that the results obtained by a single addition are equivalent to those obtained by multiple addition. The standard subtraction method can be applied in the same way.

The following implementation of the multiple standard addition technique is even simpler to carry out. The flow-through cell is initially filled with standard solution which, in turn, is "washed out" by the sample solution. The concentration in the cell can be described as a function of V or t by eqns. (9a) and (9b), respectively:

$$c = c_x + (c_{st} - c_x)\, e^{-\frac{V}{V_r}} \tag{9a}$$

$$c = c_x + (c_{st} - c_x)\, e^{-\frac{W}{V_r} t} \tag{9b}$$

where c_{st} is the concentration of the standard solution. The $(E;V)$ or $(E;t)$ pairs obtained at preset intervals ΔV or Δt can be evaluated by the methods referred to earlier [5, 6]. This method does not involve any restriction such as $V_{add} \ll V_r$, which is a great advantage in some cases when $V_{add} \ll V_r$ requires c_{add} to exceed c by a few orders of magnitude.

Special addition—dilution method. In this method, the cell is filled first with the sample solution and the potential of the cell containing the i.s.e. is measured; then a small volume ($V_{add} \ll V_r$) of standard solution of concentration c_{add} is added. The dilution begins subsequently as described above but this time the diluent is an inert solution with an ionic strength which is approximately equal to that of the sample. The dilution is continued until at least the original potential, i.e. the potential measured in the pure sample, has been attained. However, there is no need to stop the dilution at this particular point; only attaining or passing this point is required. If the volume and time when the original potential is attained or passed are denoted by V_e and t_e, respectively, then the unknown sample concentration, c_x, is given by

$$c_x = (c_x + \Delta c_0)\, e^{-\frac{V_e}{V_r}} \tag{10a}$$

or

$$c_x = (c_x + \Delta c_0)\, e^{-\frac{W}{V_r} t_e} \tag{10b}$$

where Δc_0 is given by eqn. (7). Rearrangement of eqns. (10a) and (10b) gives:

$$c_x = \Delta c_0 \frac{e^{-\frac{V_e}{V_r}}}{1 - e^{-\frac{V_e}{V_r}}} \tag{11a}$$

and

$$c_x = \Delta c_0 \frac{e^{-\frac{W}{V_r} t_e}}{1 - e^{-\frac{W}{V_r} t_e}} \tag{11b}$$

It is obvious from eqns. (11a) and (11b) that the parameters of the electrode, i.e. E' and S, are irrelevant to the results; actually, the electrode does not need to follow the Nernst equation or eqn. (2) at all [7]. The only requirement is that the electrode potential be reproducible at c_x. It is desirable, of course, that the change of potential caused by the concentration change be not too small.

EXPERIMENTAL

Apparatus and chemicals

Conventional calibration was carried out with a Radiometer PHM 64 digital pH/mV meter. In the continuous potentiometric measurements a Keithley Electrometer Type 600 B and a Keithley Differential Electrometer Type 604 were used; in the latter case, recording was done with the recorder unit of a Radelkis OH-102 polarograph, whilst a Solatron—Schlumberger A 233 digital voltmeter, Data Transfer Unit and printer were used to obtain a digital output. The solutions were pumped with a Unipan (Type 304 ELMED) peristaltic pump through PVC and silicone rubber tubing. The reference electrode was a Radelkis SCE (Type OP-810), while the ion-selective electrodes used were silver iodide-based silicone rubber electrodes prepared in this laboratory [8], the Orion cadmium electrode (Mod. 94-48 A) and the Radelkis silver sulphide electrode (Model OP-S-7111-D).

The chemicals used were of p.a. grade (Reanal, Budapest) and deionized water was used. Solutions were prepared by weighing in or by serial dilution. Electrolyte bridges were prepared from agar soaked in 0.1 M KNO_3 and filled into U-shaped glass tubes.

The experimental arrangement is shown in Fig. 2.

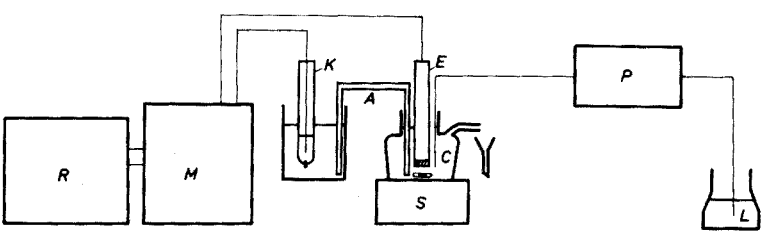

Fig. 2. Schematic diagram of the apparatus: C, Cell with overflow; E, i.s.e.; K, reference electrode; A, electrolyte bridge; S, magnetic stirrer; P, peristaltic pump; L, flask containing the "washing" solution; M, pH—mV — meter or electrometer; R, recording apparatus.

Results

Several ion-selective electrodes were calibrated by the method described. Analog records were compared with conventional calibration curves obtained from potential measurements carried out in a series of unstirred and/or stirred solutions. The results are shown in Fig. 3—6. Time

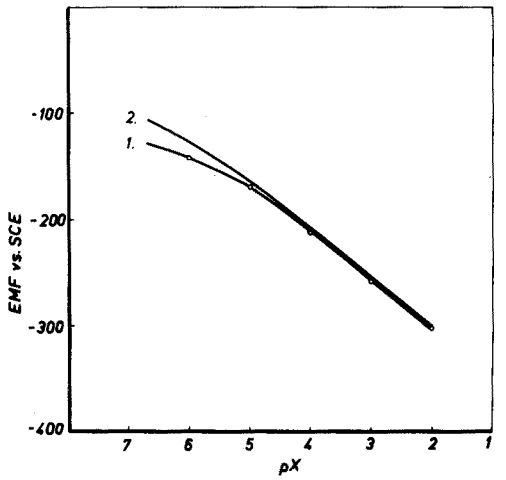

Fig. 3. Calibration curves for a silver iodide-based silicone rubber ion-selective electrode obtained by the conventional (curve 1) and the continuous (curve 2) techniques. $pX = -\log C_{I^-}$.

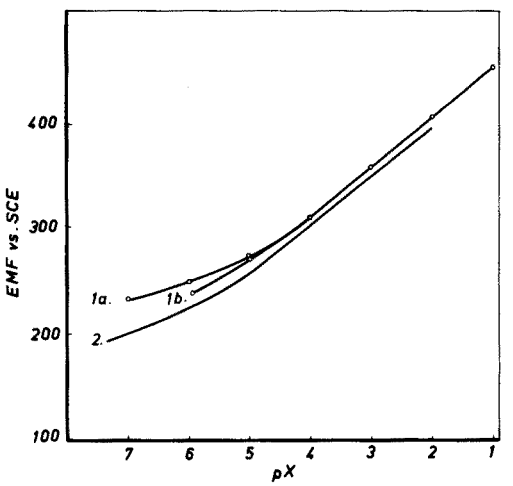

Fig. 4. Calibration curves for the Radelkisz OP-S-7111-D electrode obtained by the conventional (curve 1(a), unstirred solution; curve 1(b), stirred solution) and the continuous techniques (curve 2). $pX = -\log C_{Ag^+}$.

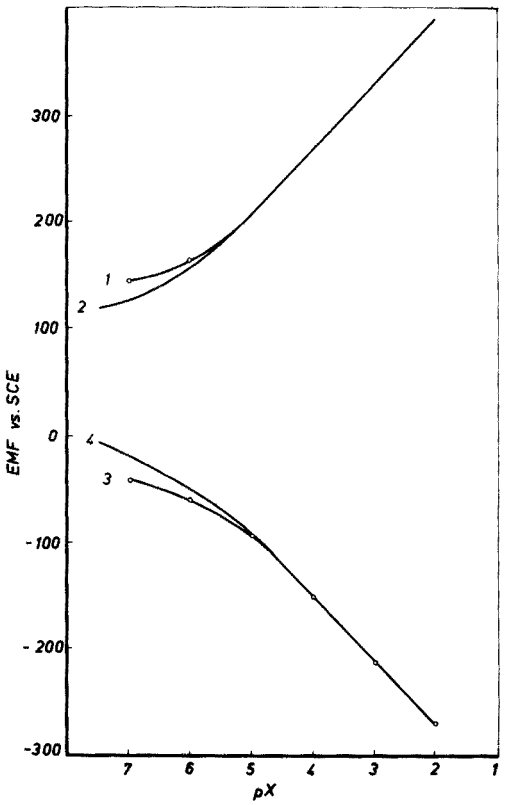

Fig. 5. Comparison of the calibration curves with a silver iodide-based silicone rubber ion-selective electrode for iodide and silver ions obtained by the conventional and the continuous techniques. Curves 1 and 3: conventional calibration. Curves 2 and 4: continuous calibration. $pX = -\log C_{I^-}$ and $pX = -\log C_{Ag^+}$, respectively.

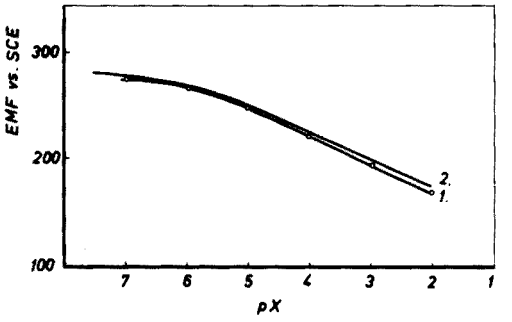

Fig. 6. Calibration curves for the Orion 94-48 A cadmium electrode obtained by the conventional (curve1) and the continuous (curve 2) techniques. $pX = -\log C_{Cd^{2+}}$.

was chosen as the independent variable because the flow rate was kept constant. The diagrams were prepared in the following way: first, the time axis of the recording obtained with the flow-through cell was rescaled in log c units by means of eqn. (6), so that the recording became an E—log c diagram in which the points obtained by conventional calibration were also plotted.

In each flow-through experiment, the concentrations of both the original solution in the cell and the "washing" solution (diluent) were made 0.1 M in potassium nitrate, thus keeping ionic strength and activity coefficients at approximately constant values. In conventional calibration each solution again contained 0.1 M KNO_3.

DISCUSSION

Since most of the methods described in the theoretical part are experimentally based on the same principles as the calibration method described, only a discussion of several experimentally obtained calibration curves seems necessary. From Figs 3—6 it can be seen that the two different calibration techniques result in only slightly different calibration graphs. Two typical differences are observed: first, in the concentration range above 10^{-5} M the two graphs run almost parallel to each other; secondly, the linear parts of the calibration curves obtained by the continuous procedure extend to lower concentrations than those achieved by the conventional method.

The first difference is attributed, at least in part, to the fact that the zero adjustment of the Keithley 600 B Electrometer cannot be done with a greater accuracy in the 1-V range applied than indicated by the differences between the curves. The second difference is probably caused by transient phenomena owing to the relatively fast concentration changes at the surface of the electrodes. This is emphasized by the results of a series of calibration experiments carried out at different flow rates. It was found that the difference between the results of the conventional and the continuous calibration methods increased when the flow rate was increased and when the concentration was lower than 10^{-5} M. In another experiment, the continuous calibration was interrupted at different concentration levels. As long as the concentration was higher than 10^{-5}—10^{-6} M, stable potential values were obtained almost immediately; below that level creeping potential values were observed. However, it should be noted that conventional calibration shows a dependence on the rate of stirring in this concentration range (see Fig. 4).

In conclusion, the advantages and disadvantages of the method can be summarized as follows. Calibrations and selectivity measurements are simple and quick, and serial dilution is circumvented. Several electrodes can be calibrated simultaneously by using a large flow-through cell, and the method can be easily applied with automatic control. However, calibration is possible only by decreasing solution concentrations. For accurate measurements the

value of the exponent in eqn. (4a) or (4b) and other similar equations must be accurately determined.

REFERENCES

1 R. P. Buck, Anal. Chem., 44 (1972) 270 R.
2 R. P. Buck, Anal. Chem., 46 (1974) 28 R.
3 G. J. Moody and J. D. R. Thomas, Talanta, 19 (1972) 623.
4 G. J. Moody and J. D. R. Thomas, Selective Ion-Sensitive Electrodes, Merrow Publishing Co. Ltd., 1971, pp. 13—20.
5 M. J. D. Brand and G. A. Rechnitz, Anal. Chem., 42 (1970) 1172.
6 J. J. Zipper, B. Fleet and S. P. Perone, Anal. Chem., 46 (1974) 2111.
7 H. Matsushita and S. Furuta, Bunseki Kagaku 21 (1972) 1639.
8 E. Pungor, J. Havas, K. Tóth, and G. Madarász, Hung. Pat. 152.106 1963.

Analytica Chimica Acta, 82 (1976) 55—65

THE DETERMINATION OF TOTAL MERCURY IN BIOLOGICAL TISSUES BY A MODIFIED POTASSIUM PERMANGANATE PROCEDURE

JOHN FAWKES, MARGARET FOLSOM and EDWARD O. OSWALD*

Environmental Biology and Chemistry Branch, National Institute of Environmental Health Sciences, P.O. Box 12233, Research Triangle Park, N.C. 27709 (U.S.A.)

(Received 9th July 1975)

SUMMARY

A simple cold-tube atomic absorption method with a silver-mercury amalgam trap and potassium permanganate as oxidizing agent is described for the determination of total mercury in tissue homogenates. Results are presented for animals fed inorganic ($HgCl_2$) and organic (CH_3HgOH) mercury orally at a level of 1 mg Hg kg^{-1}. Data are presented which compare potassium permanganate oxidation of tissue homogenates with whole tissue analysed by cold-tube atomic absorption after digestion with acid, or by neutron activation. For kidney tissue there is good agreement between all three methods for animals fed inorganic and organic mercury. For liver, however, homogenization produced an average loss of about 50 % of the mercury in rats fed mercury(II) chloride. Factors such as adsorption of mercury on sample container walls, bacterial action on the tissue and inadvertent introduction of reducing agents which could reduce the mercury to its elemental state, are not significant. Despite the loss of mercury in the liver by homogenization, rank ordering of mercury values for potassium permanganate—homogenate versus direct neutron activation analyses was essentially the same.

The usual procedure for correlating enzyme activity and total mercury in a given tissue is to homogenize an aliquot for the former analysis and select an intact tissue aliquot for the latter. Objections to this double tissue procedure are that some tissues (e.g. the kidney) may contain an unequal distribution of mercury, and when a limited amount of tissue is available (e.g. in some glandular tissue) it may not be possible to conduct both determinations on the same animal.

In the determination of total mercury by cold-tube atomic absorption, whole biological tissues and biological fluids have most often been prepared by acidic wet digestion [1], oxygen bomb [2], and gas train furnace techniques [3]. The furnace and oxygen bomb methods are not readily adaptable to routine analysis of tissues. Acidic wet digestion seemed to offer the best mode for analysis; however, since relatively large amounts of water were present in a tissue homogenate, the heat developed by the addition of

*Present address: National Environmental Research Center, Environmental Protection Agency, Research Triangle Park, N.C. 27711.

acid to the sample might cause mercury to be lost.

Hatch and Ott [4] used potassium permanganate as the sole oxidant for the preparation of mineral samples. While this procedure has not received wide application to biological tissues, it appeared to be feasible for use with tissue homogenates.

This paper is concerned with exploring the parameters of potassium permanganate concentration and length of oxidation time on rat liver and kidney homogenates from rats fed mercury(II) chloride and methylmercury hydroxide by stomach tube. Spiked sample recoveries were compared with those of acid digested tissues and with samples analyzed directly by neutron activation analysis.

Aliquots of the permanganate-oxidized mercury were reduced with hydroxylamine sulfate to elemental mercury and aerated into a silver wool amalgamator trap as reported by Long et al. [5]. The silver trap was heated and the mercury released into the atomic absorption detector and measured as peak heights on a recorder.

EXPERIMENTAL

Standards and reagents

Mercury standards. Dissolve 13.54 mg of mercury(II) chloride in 100 ml of 1 % nitric acid to obtain a stock solution (100 μg Hg ml^{-1}). Prepare the working solution by diluting the stock solution 100 times with 1 % nitric acid solution.

Prepared standards, with the same reagent volumes as the samples, containing 1—4 μg Hg ml^{-1}, and take aliquots to produce a curve ranging from 10 to 40 ng Hg.

Reagents. The aqueous potassium permanganate oxidizing solution was 5 % (w/v). The sodium chloride and hydroxylamine sulfate solutions were 12 % (w/v). The tin(II) sulfate solution was 25 % (w/v) in 0.25 M sulfuric acid. The compound must be in suspension and should be shaken just before use. Any contaminating mercury in the reducing solution was removed by aeration.

With the exception of pipettes, all glassware was further decontaminated from mercury after initial washing by shaking vigorously with equal volumes (5—10 ml) of 0.01 % dithizone in chloroform and 0.25 M sulfuric acid. The glassware was rinsed thoroughly with deionized water, then with acetone, and oven-dried.

Gas train analytical system

The gas analytical system is shown in Fig. 1. The elemental mercury produced in the gas washing bottle (D) Fisher Cat. no. 3-036B, is flushed with air from the bottle, moisture is removed in a magnesium perchlorate

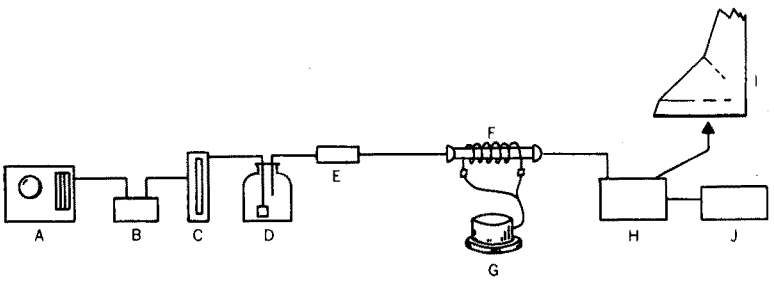

Fig. 1. A, Air pressure regulator. B, Charcoal — Drierite air purifier. C, Manometer. D, Gas aerating bottle — 250 ml. E, Polyethylene drying tube with magnesium perchlorate. F, Silver wool tube with nichrome wire. G, Variac power supply. H, Atomic absorption spectrometer. I, Gas exit tube coupled to exhaust fan. J, Recorder.

drying tube (E) and the mercury trapped on the silver wool (F). The mercury, released by heating the tube, is detected by the atomic absorption instrument.

The gas train was connected initially to the laboratory compressed air line regulated with a Perkin-Elmer 303 Atomic Absorption Pressure Regulator (A). A large gas drying tube (B), Fisher Cat. #9-242A, containing activated coconut charcoal (6-14 mesh) and indicating Drierite (10-20 mesh), removed moisture and other impurities. Air flow was adjusted to 1500 ml min^{-1} with a Kontes "Viz-Flow" Model 221 Meter.

The silver used to pack the tube (Fisher microanalysis grade) was cleaned by heating to 800 °C in a furnace for 2 h. After cooling in a desiccator, 1.0—1.5 g was packed into the tube. The Pyrex tube (3/16 in. i.d. × 4 in.) was wrapped with 100 cm of 22-gauge nichrome wire, and was connected by ball and socket joints. Connections directly from the air line to the aerator and to the atomic absorption instrument were made with short pieces of amber latex surgical rubber tubing. The sample was aerated for 3 min. The air line was disconnected from the aerator and reconnected directly to the line containing the silver amalgam.

Mercury was released from the silver by applying a voltage (25—35 V) to the nichrome wire to heat the wire to redness within 10—15 s. After the mercury trace on the recorder (J) began to decline the power was shut off and the wire cooled with unheated air from an Oster hairdryer. The atomic absorption instrument (H) was vented through a tube connected to an exhaust fan (I). The spectrometer was an Anti-Pollution Technology Corp., Model 2006-1 (used with 10× amplification) with a Perkin-Elmer Model 56 two-pen recorder (200 mV, 5 mm min^{-1} chart speed).

Procedures

Neutron activation analysis. Irradiation for 4 h at 10^3n cm^{-2} s^{-1} was followed after 7 d by counting for 1000 s on a 16-mm Ortec low-energy proton detector (l.e.p.d.) coupled to a computerized ND 2000-Hewlett Packard system (6).

Animal handling. Twelve Sprague-Dawley male rats (200 ± 20 g) were placed into two groups. Six were fed twice with 1 mg Hg kg^{-1} by stomach tube as mercury(II) chloride, 4 d apart; the other six rats were treated similarly, but methylmercury hydroxide was used. The rats were given standard chow and water ad libitum and were sacrificed by decapitation 3 d after the last mercury feeding.

Tissue handling and storage. The kidney and liver were excised as soon as possible after death. Kidneys were weighed immediately. One whole kidney, placed in a 2-ml polyethylene vial with a heat-sealed cap, was used for neutron activation analysis (n.a.a.). The second kidney was stored in a plastic-capped scintillation vial for subsequent homogenization. Both sets of tissues were kept at −10 °C except when required for analysis. After n.a.a. of the kidney, and after radioactivity had subsided to a safe level, mercury was determined again by cold-tube a.a.s. on the same tissue after wet acid digestion.

Similarly, liver samples of about 1 g were prepared for n.a.a. in 5-ml polyethylene containers and heat-sealed. About 3—4 g were weighed at the same time to be homogenized, and a third set of samples (ca. 1 g each) were weighed for the wet digestion method. Tissues were kept at −10 °C until used.

Tissue preparation for analysis. Samples were homogenized in deionized water with a Teflon-Glass Homogenizer; the tissue weight to water volume was 0.1 g ml^{-1}. Samples were cooled in an ice bath before homogenizing. Homogenates were stored in Pyrex glass-stoppered cylinders at −10 °C until used. The Teflon-Glass Homogenizer was rinsed with dithizone-acid solution between samples.

Whole tissue was wet-digested in a sealed glass container at 60 °C in H_2SO_4 : HNO_3 (2 + 1). The final ratio (w/v) of tissue-acid was 1 : 25 or more. Ratios less than this resulted in excessive foaming.

The possibility of mercury loss was reduced by adding the weighed whole tissue to the empty flask along with about 2/3 of the total acid volume and sealing with a silicone-greased glass stopper covered tightly with Parafilm M. The flask was shaken in a reciprocating water bath at 60 °C until the solution became clear or slightly opalescent and evolution of nitrogen oxides ceased. After cooling, the solution was diluted to volume with acid.

When homogenates were wet-digested, the homogenate was added to the flask and frozen with a dry ice—acetone mixture. The acid was added quickly and the solution was kept cool while the sample was thawing. Digestion was then continued as above.

Mercury analysis — Hatch and Ott modification. Aliquots of homogenates were transferred to 200 ml volumetric flasks containing about 100 ml of deionized water. Then 7.5 ml of H_2SO_4 : HNO_3 (2 + 1) acid was added, followed immediately with the specified amount of potassium permanganate. After the solution had been oxidized for the desired length of time, 7.5 ml more

acid was added and the volume brought to 8—10 ml with deionized water. Sufficient hydroxylamine sulfate reagent was added to decolorize the solution completely, and water was added to adjust to the final volume. Aliquots of the wet digestion samples were added in the same manner. More acid was added, if necessary, so that the final volume did not exceed 15 ml.

When the homogenized samples were to be spiked with mercury(II) chloride, the desired aliquot of the homogenate was added directly to the 200-ml volumetric flask followed by the desired concentration of a freshly prepared aqueous mercury(II) chloride solution. After ca. 30 min, 100 ml of deionized water was added. From this point on, the sample was handled in the same manner as the unspiked homogenates.

For analysis, a suitable aliquot taken from the volumetric flask was transferred to the aeration bottle which contained about 50—60 ml of deionized water and 10 drops of 1-octanol, an antifoam agent. Finally 5 ml of tin(II) sulfate reagent was added, and the bottle was attached immediately to the gas train and aerated.

RESULTS

Calibration curves

A typical calibration curve for the range 10—40 ng Hg from standard $HgCl_2$ in 1 % HNO_3, produced a slope of 1.77 and an intercept of 0.2; standard deviations ranged from ± 3.0 % to 1.3 %. The optimum conditions for the release of mercury from the silver by heating were obtained by calibrating with the highest level of mercury. Voltage was increased through the nichrome wire until the rate of heating of the tube containing silver gave maximum peak height. Heating above this value did not increase the peak height appreciably but increased the rate of destruction of the silver wool and shortened the life of the glass tube.

Effects of experimental parameters on Mercury Release

Since potassium permanganate was to be the sole oxidant of mercury in tissue homogenates, the concentration and time necessary to release the maximum amount of mercury had to be determined. Table 1 shows the results when the permanganate concentration was varied from 2 to 30 ml in 200 ml of a sample containing 0.1 g of kidney as an aqueous 10 % homogenate from a methylmercury hydroxide-fed rat. The maximum value occurred when 30 ml of $KMnO_4$ was allowed to react for 48 h. For comparison purposes, this was considered as 100 % released. The same maximum occurred for a liver sample containing 0.3 g of homogenate from a methylmercury hydroxide-fed rat. However, when 0.4 g of homogenate from a mercury(II) chloride-fed rat was oxidized with 30 ml of $KMnO_4$, essentially the same values were obtained at 24, 48, and 72 h.

TABLE 1

Effect of permanganate concentration and time of oxidation on % recovery of mercury from tissue homogenates

$KMnO_4$ (ml)	8h		24h		48h		72h		96h	
	p.p.m.	%	p.pm.	%	p.p.m.	%	p.p.m.	%	p.p.m.	%
Kidney homogenate[a]										
2	2.34	31.0	3.42	45.0	—	—	—	—	4.36	58
3	—	—	4.24	56.0	—	—	—	—	6.63	88.0
4	2.71	36.0	5.16	68.0	—	—	—	—	6.85	91.0
8	2.34	31.0	5.48	72.0	—	—	—	—	6.52	86.0
20	2.93	39.0	5.65	75.0	—	—	—	—	6.80	90.0
30	4.21[b] (± 0.05)	56.0	6.77 (± 0.08)	90.0	7.56 (± 0.05)	100.0	7.10 (± 0.23)	94.0	—	—
Liver homogenate[c]										
30	0.97 (± 0.04)	59.0	1.38 (± 0.04)	84.0	1.64 (± 0.06)	100.0	1.56 (± 0.04)	95.0	—	—
30	—	—	0.11 ± 0.01	—	0.11 ± 0.01	—	0.10 ± 0.01		—	—

[a]Only CH_3HgOH was present; the sample weight was 0.1 g.
[b]The numbers in parenthesis are the standard deviations.
[c]For the liver homogenate, the first sample (0.3 g) contained CH_3HgOH, and the second (0.4 g) contained $HgCl_2$.

The usual procedure was to determine the size of aliquot of the homogenate—$KMnO_4$ solution which, upon analysis, would give mercury values falling near the middle of the standard curve. Variations were made in aliquot size, however, to determine the precision of the mercury values calculated from different portions of the standard curve. Aliquots, in 1-ml increments from 1 to 5 ml, were taken from a 200-ml volume of kidney homogenate containing 0.1 g of tissue. Beginning with a 1-ml aliquot, average values (p.p.m.) of triplicate analyses were as follows: 15.2 ± 0.6, 15.5 ± 0.5, 15.4 ± 0.4, 15.0 ± 0.3 and 14.6 ± 0.4 and the corresponding peak heights were, in arbitrary units, 12.6 ± 0.4, 24.8 ± 0.4, 36.1 ± 1.2, 46.8 ± 0.6 and 56.9 ± 1.6. The average p.p.m. Hg and standard deviation for all samples was 15.1 ± 0.4. It can be concluded that there is no significant difference between each value when aliquots ranged from 1 to 5 ml.

When mercury levels in tissues are low, it is necessary to take larger homogenate aliquots. Samples containing 0.2, 0.4 and 0.8 g of liver homogenate in 200 ml of solution were oxidized with 30 ml of 5 % $KMnO_4$ solution. After 15 h values for the 0.2, 0.4 and 0.8-g samples were 1.06, 0.98 and 0.93 p.p.m. Hg respectively. Within 24 h, maximum values of 1.21 and 1.20 p.p.m. were obtained for the two smaller sample sizes, but, for the

0.8-g samples, a value of only 0.96 p.p.m. Hg was attained. At the end of 48 h the three respective values were 1.23, 1.21 and 1.05 p.p.m. Hg. However, when 40 ml of $KMnO_4$ solution was added to an 0.8-g sample, values of 1.27 and 1.25 were obtained at 24 and 48 h intervals, respectively. These values are essentially equal to those obtained for the smaller sample sizes.

When 30 ml of $KMnO_4$ was added to the 0.8-g liver homogenate, all the permanganate was decolorized after 48 h, but this did not happen when 40 ml of permanganate was used. On the basis of all these experiments, sufficient permanganate was added to the sample solution for it to be colored for at least 72 h.

Control kidney and liver homogenates were spiked with mercury(II) chloride at 1.0, 5.0 and 10 p.p.m. Hg for kidney, and 0.5, 1.0 and 5.0 p.p.m. Hg for liver. The control kidney solution contained 0.064 p.p.m. Hg and the liver control had 0.04 p.p.m. Hg. Subtracting these values from the spiked sample, recoveries from kidney were 1.00 (100 %), 5.06 (101 %) and 10.3 (103 %). For liver, the results were 0.44 (88 %), 1.07 (107 %) and 5.22 (105 %).

Comparison of results by n.a.a. wet digestion and potassium permanganate oxidation

The comparative results of mercury determination in rat kidney and liver by n.a.a. of whole tissue (1 replicate), potassium permanganate oxidation of tissue homogenate (5 replicates), and acid digestion of whole tissue (3 replicates) are shown in Table 2 under the heading designated Method. Tissue samples were derived from rats fed as described. Ratios of the values for homogenate/ n.a.a., wet digestion/n.a.a. and homogenate/wet digestion are also given; finally, rank ordering for sample values obtained from each method is shown, in which the order of numerical increase in p.p.m. from the lowest (No. 1) to the highest value (No. 6) is indicated.

A comparison of the kidney values for the $KMnO_4$—homogenate and wet digestion methods for both inorganic and organic mercury shows the reproducibility, indicated by the average relative standard deviation, to be roughly equivalent for both methods. The homogenates tend to give slightly higher values than wet digestion (average values are 1.04 for inorganic and 1.14 for organic mercury). A similar trend is noted when homogenate and wet digestion methods are compared with n.a.a. It should be noted that the rank ordering values for n.a.a. and homogenate are identical for inorganic mercury but not for organic mercury. For wet digestion, the rank order is relatively randomized compared with either n.a.a. or homogenate for both mercury compounds.

For liver, the reproducibility between $KMnO_4$-homogenate and wet digestion is about the same when average relative standard deviations are compared, although for rats receiving mercury(II) chloride, $KMnO_4$ oxidation of homogenates gave values that were ca. 50 % of those by the wet digestion method. A similar but smaller trend was apparent for values of

TABLE 2

Comparison of results for liver and kidney by n.a.a. and wet digestion of whole tissue, and potassium permanganate oxidation of tissue homogenate

Hg compound	Sample no.	Method					Comparison ratios						Rank ordering		
		N.a.a. p.p.m.	Homogenates p.p.m.	s_r	Wet digestion p.p.m.	s_r	Homog./ n.a.a.	s_r	Wet dig./ n.a.a.	s_r	Homog./ Wet dig.	s_r	n.a.a.	Homog.	Wet dig.
Kidney tissue															
$HgCl_2$	1	10.05	8.38	3.7	8.92	2.8	0.83		0.89		0.94		6	6	6
	2	7.66	7.76	1.8	7.98	7.8	1.01		1.04		0.97		3	3	5
	3	8.86	8.06	2.7	7.40	4.7	0.91		0.84		1.09		5	5	4
	4	6.90	6.23	2.9	5.64	5.3	0.90		0.82		1.10		2	2	2
	5	4.91	4.94	3.2	4.81	7.5	1.01		0.98		1.03		1	1	1
	6	8.52	7.80	1.4	7.25	1.8	0.92		0.85		1.08		4	4	3
	Av.			2.6		5.0	0.93	7.5	0.90	10.0	1.04	6.7			
CH_3HgOH	7	8.12	6.81	3.5	6.09	2.6	0.84		0.75		1.12		4	3	4
	8	8.70	6.93	2.2	5.96	0.5	0.80		0.68		1.16		5	4	2
	9	6.94	6.71	1.6	6.39	1.4	0.96		0.92		1.05		2	1	5
	10	8.00	7.56	3.1	5.80	2.4	0.94		0.72		1.17		3	2	1
	11	8.84	9.27	5.1	—	—	1.05		—		—		6	6	—
	12	6.13	6.94	3.2	5.97	1.2	1.13		0.97		1.16		1	5	3
	Av.			3.1		1.6	0.95	12.6	0.81	16.0	1.13	4.4			

Liver tissue

$HgCl_2$	1	0.29	0.11	9.1	0.18	11.1	0.38		0.62		0.61		6	6	4
	2	0.15	0.083	10.5	0.16	12.5	0.55		1.07		0.52		3	3	3
	3	0.28	0.095	9.5	0.20	5.0	0.35		0.71		0.48		5	4	5
	4	0.24	0.096	5.2	0.21	4.8	0.40		0.88		0.46		4	5	6
	5	0.07	0.062	8.1	0.096	7.3	0.88		1.37		0.64		1	1	1
	6	0.14	0.074	6.8	0.13	7.7	0.50		0.93		0.54		2	2	2
	Av.			8.2		8.1	0.51	39.2	0.93	29.0	0.54	13.0			
$HgCl_2$	3		0.095	9.5	0.093[a]		2.1				1.02				
	6		0.074	6.8	0.071[a]		4.2				1.04				
	Av.										1.03				
CH_3HgOH	7	1.27	1.07	3.7	1.25	7.2	0.84		0.98		0.86		1	3	2
	8	1.32	1.06	4.7	1.58	6.3	0.80		1.20		0.67		2	2	6
	9	1.41	1.10	2.7	1.54	2.6	0.78		1.09		0.71		3	4	5
	10	1.55	1.14	1.8	1.42	5.6	0.73		0.92		0.80		5	5	4
	11	1.43	1.00	4.0	1.11	5.4	0.70		0.78		0.90		4	1	1
	12	1.69	1.64	2.4	1.38	2.9	0.97		0.82		1.19		6	6	3
	Av.			3.2		5.0	0.80	12.5	0.96	14.6	0.86	20.9			

[a]These values were obtained from tissue homogenates. All other values in this column were obtained from whole tissues.

the methylmercury-fed animals.

It is not clear, therefore, whether some of the mercury was not detected, or whether it was lost during the homogenization step and/or subsequent storage. Aliquots of homogenates from two liver samples (nos. 3 and 6 from the mercury(II) chloride-fed rats), from which total mercury levels had been run previously one month earlier by the $KMnO_4$ oxidation method, were analyzed again by the wet digestion procedures. The results of this experiment are shown in Table 2 (data marked in column 6); the ratio of $KMnO_4$—homogenate/wet digestion (homogenate tissue) was 1.02 and 1.04 for samples 3 and 6 respectively, compared with the former values of $KMnO_4$—homogenate/wet digestion (whole tissue) of 0.48 and 0.54 respectively for the same two samples. This information indicates that the mercury was lost mainly during the homogenizing process.

Although ca. 50 % of the mercury is lost during the homogenizing of liver from mercury(II) chloride-fed rats, the rank order sequence is nearly identical to that for n.a.a. values. However, no such similarity of sequence occurs for the methylmercury rats. Even though the wet digestion/n.a.a. values for both mercury compounds are in closer agreement than are the homogenate/n.a.a. values, a comparison of rank ordering sequence between wet digestion and n.a.a. shows a randomized relation for both types of mercury.

DISCUSSION

Inorganic mercury may be lost by adsorption on container walls [7, 8], bacterial conversion to mercury metal [9], and adventitiously added reductants [10]. As much as 60 % of the mercury was lost [7] on the walls of polyethylene containers from natural waters within a few minutes after the addition of mercury(II) chloride at concentrations of 0.5—5.0 p.p.m. Hg, and mercuric chloride spiking solutions gave [8] erratic values (not quantitated) at 1 p.p.m. Hg levels when stored in glass containers.

Magos et al. [9] demonstrated the effect of bacterial action on a 0.1 % kidney homogenate spiked with mercury(II) chloride (0.2—20 p.p.m. Hg). These solutions, when dialysed at 4 °C, lost 10—30 % Hg within 32 h but none was lost when the homogenate was dialysed against a penicillamine solution.

Toribara et al. [10] pointed out that, because of the high oxidation potential of the mercury(II)—mercury(I) system, almost any reducing substance can convert some mercury(II) to mercury(I) and, followed by disproportionation of mercury(I), loss of metallic mercury could occur, particularly at very low concentrations in which a significant amount of mercury(I) remain ionized.

Mercury artefacts produced by any of the conditions mentioned above should produce erratic results from sample to sample. Since the rank ordering of samples in liver, despite the sample loss through homogenization,

remained nearly identical to the rank obtained by n.a.a., the mercury loss probably did not result from these extrinsic factors.

In the oxidation of mercury compounds with potassium permanganate, it would seem more reasonable to add the hydroxylamine directly to a permanganate aliquot in the aeration bottle rather than to perform the reduction on the entire sample in the volumetric flask. When this was tried the results were erratic, probably because some of the mercury adhered to the precipitate that formed.

Addition of the hydroxylamine to the entire sample resulted in some foaming and although it was expected that some elemental mercury would be lost, this was not the case if the glass stopper was kept in the flask. The addition of aliquots by pipette for subsequent aeration had to be done with care, however, so as not to draw the sample into the pipette so rapidly that greatly reduced air pressure and swirling in the pipette took place.

Conclusion

Within the experimental parameters discussed, the potassium permanganate oxidation method for tissue homogenate is satisfactory and is comparable to the wet acid digestion procedure for whole tissue. The evidence presented indicates that the physical process of homogenizing may result in loss of mercury; the magnitude to which this occurs is a function of the kind of tissue and the type of mercury compound administered, and correlations between enzyme activity and mercury level may depend upon whether the mercury data are obtained from homogenized or whole tissue. This effect has not been considered previously. The simpler permanganate procedure is preferred over the wet acid digestion which requires the sample to be pre-cooled to offset the heating effect from the addition of acid. The permanganate oxidation may not, however, be sufficiently vigorous for some compounds of mercury; a preliminary evaluation by both methods is therefore desirable.

REFERENCES

1 J. F. Uthe, F. A. J. Armstrong and M. P. Stainton, J. Fish. Res. Bd. Can., 27 (1970) 805.
2 F. Okuno, R. A. Wilson and R. E. White, J. Assoc. Offic. Anal. Chem., 55 (1972) 96.
3 V. I. Muscat, T. J. Vickers and A. Andred, Anal. Chem., 44 (1972) 218.
4 W. R. Hatch and W. L. Ott, Anal. Chem., 40 (1968) 2085.
5 S. J. Long, D. R. Scott and R. J. Thompson, Anal. Chem., 45 (1973) 2227.
6 J. N. Weaver, Amer. Lab., March, 1973.
7 R. V. Coyne and J. A. Collins, Anal. Chem., 44 (1972) 1093.
8 R. K. Munns and D. C. Holland, J. Assoc. Offic. Anal. Chem., 54 (1971) 202.
9 L. Magos, A. A. Tuffery and T. W. Clarkson, Brit. J. Ind. Med., 23 (1966) 230.
10 T. Y. Toribara, C. P. Shields and L. Koval, Talanta 17 (1970) 1025.

Analytica Chimica Acta, 82 (1976) 67—77

THE DETERMINATION OF URANIUM IN ROCKS BY INDUCTIVELY COUPLED PLASMA-OPTICAL EMISSION SPECTROMETRY

R. H. SCOTT and A. STRASHEIM

National Physical Research Laboratory, C.S.I.R., Pretoria 0001 (South Africa)

M. L. KOKOT

Transterra Mining Ltd., P.O. Box 6521, Johannesburg 2000 (South Africa)

(Received 11th August 1975)

SUMMARY

A method for the determination of uranium in rock samples by emission spectrometry is presented. The rock is dissolved and the uranium content determined by nebulizing the solution into an inductively coupled-plasma optical excitation source. Various spectral lines were investigated. The uranium emission at 378.28 nm was chosen because of its relative freedom from matrix element spectral interferences. For this emission, a practical detection limit of 0.1 p.p.m. in solution was achieved by optimizing source parameters (power, flow-rate, observation height). Results are compared with those obtained by a number of other techniques.

Uranium is generally determined by sensitive fluorimetric or photometric methods, where reagents such as dibenzoylmethane [1], thiocyanate [2], 1-(2-pyridylazo)-2-naphthol (PAN) [3] and arsenazo III [4] are employed. Interference occurs as a result of the presence of many other elements and a prior separation procedure is necessary. A commonly used procedure for the recovery of uranium from aqueous solutions is the extraction of uranyl nitrate in a number of organic solvents, notably diethyl ether. Ion-exchange techniques are also used [5, 6].

The uranyl ion can be determined quantitatively by precipitation as the arsenate [7] or phosphate [8] in the presence of EDTA, followed by dissolution of the precipitate, reduction with lead, and finally titration with cerium(IV) solution. Gravimetric procedures such as precipitation by oxine [9] or cupferron [10] are subject to co-precipitation of a number of interfering elements unless preventative measures are taken. The obvious disadvantages of all of the above methods are that they are tedious and time-consuming.

Strasheim [11] proposed a spectrographic method for uranium determinations in uranium ores, using a d.c. arc. This method could be used for the rapid analysis of ores from 0.01 % U_3O_8 with a reported accuracy of 11%.

Although atomic absorption spectrometry enjoys much popularity as a rapid method of analysis for a number of important elements in geochemical

prospecting, it is particularly insensitive to uranium. This behaviour may be explained by the formation of a refractory compound which binds the free uranium atom, possibly UO [12]. The dissociation energy of UO is 7.76 (±0.3) eV [13]. One method of reducing oxide formation is the use of a reducing flame. In this way, a detection limit of 120 p.p.m. (in solution) was obtained by Amos and Willis [14] with a fuel-rich nitrous oxide—acetylene flame. The determination of uranium by atomic absorption is complicated by significant interference effects and demands critical control of fuel composition and burner adjustment [15]. Because of the above considerations, this technique is considered unsuitable for trace uranium determinations.

A rapid analytical method is x-ray emission spectrometry, which offers a practical lower limit of detection of 0.01 % U_3O_8 and satisfactory accuracy for uranium in exploration samples [16].

This paper deals with an alternative instrumental method which requires sample dissolution. The uranium content is determined spectrometrically by spraying the solution into an inductively coupled plasma [17—20] and measuring the optical emission of the U^+ species formed therein. The plasma temperature of 6000 K [21] is presumably sufficiently high to dissociate the UO molecule.

This plasma has been used previously for Cu, Pb, Zn, Ni and Co determinations in geochemical soil samples [22]. "Standard" plasma operating conditions (see Table 1) were used for these studies. In the present study the influence of source conditions on the spectral line/background intensity ratio and detection limit for uranium was investigated.

A number of rock samples, previously analysed by photometric, fluorimetric, x-ray and radiometric techniques were then analysed with the plasma source and the results were compared.

EXPERIMENTAL

Sample and standards preparation

Core samples were crushed, pulverized, and then split through a chute riffler. A representative sample was then milled to —200 mesh.

TABLE 1

"Standard" operating conditions for plasma

Parameter	Value
Forward r.f. power	1.0 kW
Reflected power	<10 W by tuning
Argon coolant/support gas flow-rate	10.0 l min^{-1}
Height of observation above load coil	20 mm (slit centered)
Argon flow-rate for aerosol transport	1.0 l min^{-1} (stabilized)
Sample solution uptake rate	3.7 ml min^{-1}

Samples were dried at 110 °C, cooled in a desiccator and then 1 or 2 g was weighed and transferred to test-tubes; 5 ml of 18 M HNO_3 and 5 ml of (1 + 1) H_2SO_4 were added. The acidified samples were heated to fumes of sulphur trioxide (about 2 h), then cooled, filtered, and diluted to 100 ml with distilled water.

Aqueous standards were prepared from uranyl nitrate and standardized by precipitating the uranyl solution with ammonia solution as ammonium diuranate. The precipitate was ignited, and weighed as U_3O_8. The final stock solution contained 1000 p.p.m. uranium.

Plasma instrumentation

A description of the instrumental facilities for the plasma study is given in Table 2.

Development of plasma technique

Uranium has a multitude of spectral lines in the wavelength region 200—450 nm, with a marked absence of any significantly strong emitters. The

TABLE 2

Plasma instrumentation

R.f. generator	Frequency 27.12 MHz, stabilized r.f. forward power adjustable from 0-4 kW, 1½ turns load coil. (International Plasma Corp. Model PM 140-27)
Spectrometer	0.5-m Jarrell-Ash monochromator, grating blazed at 300 nm (1st order), ruled 1180 lines mm^{-1}, 1.6 nm mm^{-1} reciprocal linear dispersion, slit width 25 μm × 5 mm slit height
Optics	Plasma imaged in 1:1 ratio onto entrance slit with 16-cm focal length × 5 cm diameter fused quartz lens. Height of observation varied from 10 mm to 25 mm above load coil
Readout	Hamamatsu type R106 photomultiplier (S-19 photocathode response); linear picoammeter with built-in pre-amplifier, zero suppression and variable damping (Keithley Instruments, Model 417); strip chart recorder with 1-s f.s.d. time const. (Hitachi, Model QPD 54)
Plasma torch assembly	Fused quartz with capillary injector [22]
Nebulizer and sample chamber	Teflon and glass pneumatic nebulizer [23] into dual tube sample chamber [20]. No desolvation unit.

choice of a suitable analysis line was therefore made by spraying a 10-p.p.m. uranium aqueous standard, measuring the line-to-background intensity ratio and detection limit for a number of the more intense uranium lines, and examining any spectral interference by possible matrix elements in each case by means of the MIT wavelength tables.

The detection limit is defined as the concentration of uranium (in solution) necessary to produce a signal equal to 3 times the standard deviation (s) of the background signal at the wavelength of the line in question. For practical purposes the background noise "band" recorded on the chart recorder (with a full scale response time constant of 1 s) was used as an estimate of 3 s. Since this noise is a function of the instrumental damping, the detection limit can be lowered by increasing the time constant. If this is increased to 10 s or more, however, the instrumental response is somewhat slow for a practical analytical system.

Standard plasma operating conditions (Table 1) were maintained for these initial studies. Results are given in Table 3. It is remarkable that of a number

TABLE 3

Line to background ratios (L/B) and detection limits (DL) for pure aqueous uranium solutions obtained under standard plasma conditions (Table 1). Possible interfering elements in rock solutions are also given

U^+ spectral line (nm)	L/B for 10 p.p.m. U	DL p.p.m.	Possible interfering elements (from M.I.T. Tables)
434.17	0.57	0.6	Ca, Cr, Ti, Zr
424.44	1.1	0.6	Fe, Zr
424.17	1.1	0.3	Na, V, Zr[a]
417.16	0.90	0.4	Cr, Fe, Ti, V, Zr
411.61	0.76	0.5	Ca, Mn, Ni, V
409.01	1.4	0.2	Cr, Fe, Mn[a], V, Zr
405.00	0.97	0.3	Cr[a], Cu, Fe, Ti, Zr
398.58	1.0	0.3	Fe[a], Li[a], Mn, Ti
393.20	2.8	0.2	Fe, Ti[a]
386.59	0.38	0.8	Fe[a], Mn, Ti, Zr
385.96	1.2	0.2	Ca, Cr, Fe[a], Mg, V
383.15	0.90	0.4	Cr, Fe, Mg, Ni[a], Zr
378.28[b]	1.2	0.3	Ca, Fe, V
374.64	0.78	0.5	Fe[a], Mn, V
370.15	1.2	0.3	Fe[a], Mn, Ti[a]
367.26	0.20	4.1	Ca, Fe[a], V[a], Zr
367.01	3.1	0.1	Ca, Fe[a], Mn
355.22	0.03	10	Ba, Fe[a], Mn, Ni, V, Zr
288.27	0.17	1.3	Mn, Ti, V

[a]Probably a strong interference (estimated on wavelength proximity, relative intensity of the arc lines and the probability of the interfering element being a major or trace component).
[b]Used in this study.

of uranium atomic lines investigated, no line of any significant intensity could be found. The emission from U^+ was predominant. The U^+ emission at 378.28 nm was chosen from the data in Table 3, because of its relative freedom from apparent spectral interferences, while having a reasonably low detection limit. The highest line-to background ratio and lowest limit of detection (0.1 p.p.m.) for standard conditions were obtained at 367.01 nm, but a relatively intense iron line at the same wavelength will cause severe spectral interference if iron is present in varying concentrations in the sample solutions.

With the emission measurement at 378.28 nm, deviations from standard plasma conditions were tested in attempts to optimize conditions to obtain the highest line-to-background ratio and lowest limit of detection for uranium. The parameters studied were r.f. forward power, argon coolant/support gas flow-rate and observation height in the plasma. Other parameters (r.f. reflected power, aerosol transport gas flow-rate, solution uptake rate and spectrometer slit settings) were maintained at the values listed in Table 1.

The results of the above study are shown graphically in Figs. 1—3. Line-to-background ratios are for 10 p.p.m. solutions. The following points should be noted.

(i) Low in the plasma (10 mm above the load coil) the line-to-background ratio is very low for all powers and flow-rates studied.

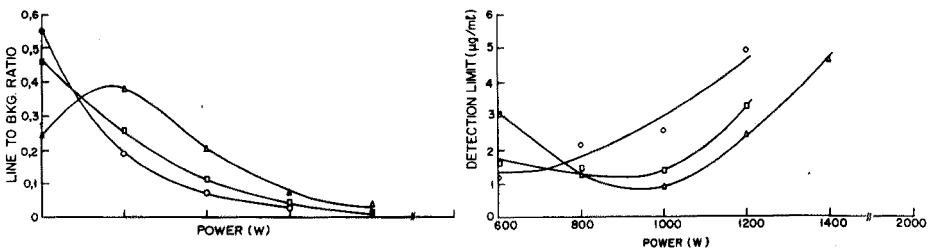

Fig. 1. Line-to-background ratio and detection limit for uranium emission at 378.28 nm, as a function of r.f. power and argon coolant flow-rate, at 10-mm observation height in the plasma. A 10-p.p.m. uranium solution was used for the line-to background ratio determination. (○) 10 l min^{-1}, (□) 15 l min^{-1}, (△) 20 l min^{-1}.

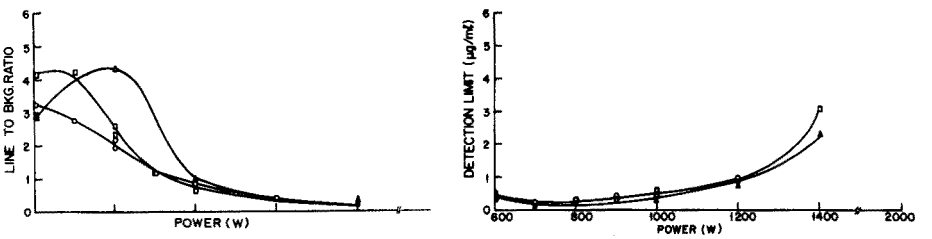

Fig. 2. As in Fig. 1, for 17.5 mm observation height.

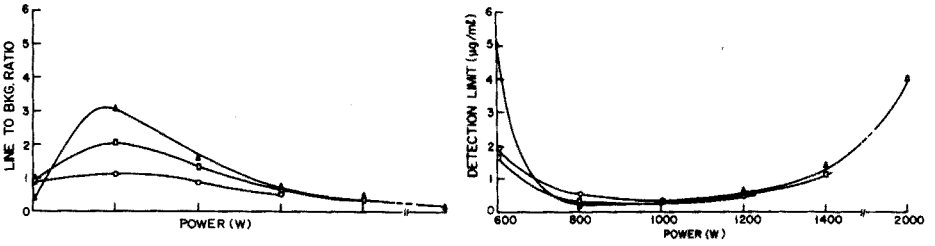

Fig. 3. As in Fig. 1, for 25 mm observation height.

The detection limit is poor and at best equal to about 0.8 p.p.m. for the highest flow-rate studied (20 l min^{-1}) at a forward r.f. power of ca. 950 W. An increase or decrease in power tends to worsen the detection limit.

(ii) Higher in the plasma (17.5 mm) the line-to-background ratio peaks at a power of about 800 W for a flow-rate of 20 l min^{-1}. At lower flow-rates the peak is found at lower powers and only slightly decreased in value. The detection limit does not change significantly for a power change of from 700 to 800 W and is of the order of 0.3 p.p.m. for a flow-rate of 10 l min^{-1}, decreasing to about 0.1 p.p.m. for 20 l min^{-1}. An increase in power, regardless of flow-rate, worsens the detection limit.

(iii) Still higher in the plasma (25 mm) the line-to-background ratio peaks (for all flow-rates studied) at a power of ca. 800 W. The maximum occurs at a flow-rate of 20 l min^{-1}. The peak value decreases significantly as the flow-rate is reduced. An increase in power to 2 kW reduces the line-to-background ratio considerably. No significant change in the detection limit (0.3 p.p.m.) occurs when the power is varied from about 900 to 1100 W, or the flow-rate is varied from 10 to 20 l min^{-1}. A decrease in power to 600 W, or an increase to 2 kW causes a significant deterioration in the limit of detection.

To sum up, the highest value for the line-to-background ratio and the lowest limit of detection occurs at about the same power, flow-rate and height of observation above the load coil. These optimized parameters are given in Table 4, together with the values obtained. The values obtained for standard conditions, and the chosen conditions for the present study, are also listed. A 10 l min^{-1} argon flow-rate was chosen in preference to 20 l min^{-1} purely for economic reasons. It is important to note that:

(i) no highly significant improvement in the detection limit could be obtained by deviating from standard conditions unless the argon flow-rate was doubled, which was uneconomic;

(ii) an increase in r.f. power above 800 W did not improve the detection limit at all; in fact it became increasingly worse. This is contradictory to the generalized statement by Greenfield et al. that higher power plasmas yield greater sensitivity [19].

TABLE 4

Line to background ratios (L/B) and detection limits (DL) obtained for various plasma operating conditions for the uranium line at 378.28 nm

Plasma operating conditions	R.f. power (W)	Ar flow-rate (coolant/support) ($l\ min^{-1}$)	Height of observation (mm)	L/B for 10 p.p.m. U	DL p.p.m.
Optimized	800	20[a]	18—20	4.4	0.1
Standard	1000	10.0	20	1.2	0.3
This study	800	10.0	18	2.2	0.2

[a]Maximum tested.

RESULTS AND DISCUSSION

Study of interferences

Pure aqueous solutions, each containing 1000 p.p.m of a possible concomitant, were sprayed and the apparent uranium concentrations were determined in these solutions by measuring the spectral intensity at 378.28 nm after calibration with aqueous uranium standards (0—5 p.p.m.). Table 5 lists the values measured; there was no reading from Cs, K, Li, Mn, Na or Si, and the interferences are probably due to spectral line overlap. The most important to consider are those of Ca, Fe and V. Of these elements only calcium and iron are major components of the rock samples. These elements would cause an increasingly serious error for uranium determinations from 2 to 0.2 p.p.m. in solution (ca. 200—20 p.p.m. U_3O_8 in the rock samples) if they are present at concentrations exceeding about 500 p.p.m. (5 % in the rock samples).

In a second investigation, the combination of physical and chemical interferences was studied in the following manner. Solutions were made up to contain 25 p.p.m. uranium and 1000 p.p.m. of a possible concomitant,

TABLE 5

Physical interference at 378.28 nm from 1000 p.p.m. of elements in pure solution[a]

Element	Apparent U in soln. (p.p.m.)	Element	Apparent U in soln. (p.p.m.)
Al	0.02	Mg	0.04
Ca	0.36	Sr	0.11
Cr	0.11	V	1.76
Fe	0.17		

[a]Monochromator slit width reduced to 15 μm for this and further investigations.

and these solutions were then analysed; pure aqueous uranium standards were used for calibration. Results are given in Table 6. Most of the concomitants caused a slightly lower emission intensity at 378.28 nm than that measured for the standards. This may possibly be due to ionization suppression of the uranium species in the plasma (and/or lateral diffusion effects) as a result of the presence of the concomitant.

Direct determination of uranium in rock samples

Comparative results for the analysis of a number of ore samples, with pure aqueous uranium solutions for calibrating the plasma system, are presented graphically in Fig. 4. The plasma values are plotted against the average values of 4 independent laboratories. Each laboratory used a different analytical

TABLE 6

Results for the determination of uranium in aqueous solutions containing 25 p.p.m. U and 1000 p.p.m. of various elements

Element	Uranium found[a] (p.p.m.)	Element	Uranium found[a] (p.p.m.)
Al	23.6	Mg	24.4
Ca	24.0	Mn	24.0
Fe	25.0	Si	24.0
K	23.1		

[a]With pure U-standards for calibration. Precision ca. 1 %.

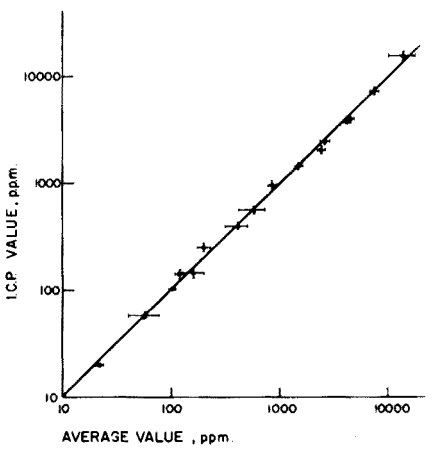

Fig. 4. Comparison between direct inductively coupled plasma results and the average of values from four independent laboratories each using a different technique, for the determination of U_3O_8 in rocks.

technique: x-ray fluorescence spectrometry, radiometry (neutron activation), fluorimetry and ion-exchange photometry. The spread of results for any one sample was rather high. In Fig. 4, the horizontal bars represent ±1 standard deviation for each comparative value, whereas the vertical bars represent the standard deviation for between 4 and 8 repeat determinations by the plasma technique. These repeats included the dissolution procedure, therefore the standard deviations are estimates of the precision of the technique as a whole.

The plasma results in the range 20—200 p.p.m. U_3O_8 were corrected for calcium and iron spectral interference as the uncorrected uranium values tended to be higher than the comparative values. This was done by measuring the calcium and iron concentrations in the sample solutions and correcting for the apparent uranium concentration caused by their presence. These samples are listed in Table 7, together with the results obtained.

A sample analysis rate of about one per minute (allowing for calibration checks) could be maintained with the present readout system.

Ion-exchange—i.c.p. determination of uranium in rock samples

An ion-exchange procedure developed by Strelow for the separation of uranium [24] was used. In this procedure, columns (30 cm long) are packed with AG 1-X8, 100-200 mesh, ion-exchange resin (Bio-rad Labs., Richmond, Calif.), and washed with 1M H_2SO_4 until no positive test is obtained with silver nitrate. The sample solution is then passed through the column, after adjustment of the pH to 1—1.5 with diluted ammonia. The successive eluates obtained with 100 ml of 0.1 M H_2SO_4 and 100 ml 6 M HCl are discarded; the final eluate with 80 ml of 0.1 M HCl is collected and diluted to 100 ml.

These final solutions were then analysed by the plasma source method. A comparison of the plasma values and average values (from other laboratories) is shown graphically in Fig. 5.

TABLE 7

Calcium and iron corrections to i.c.p. results for low U_3O_8 samples

Sample number	Ca concn.[a]	Fe concn.[a]	U_3O_8 in rock (p.p.m.)		
			Apparent value[b]	Corrected value	Average comparative value
1	20	580	10	20	22
2	80	240	7	58	58
3	1070	240	42	108	101
4	670	160	28	142	118

[a]Expressed as p.p.m. in solution

[b]From interference of Ca and Fe.

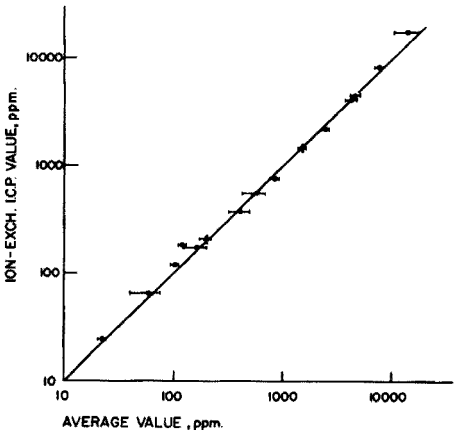

Fig. 5. Comparison as in Fig. 4, for ion-exchange separation of uranium followed by inductively coupled plasma determination.

Conclusion

This study has demonstrated that i.c.p.—o.e.s. can be successfully used for the determination of U_3O_8 in rock and ore samples in the concentration range 0.002—2 % U_3O_8. The technique yields results which are generally within one standard deviation of the results of other methods and is therefore regarded as a good alternative to the more time-consuming methods. Apart from sample dissolution no pre-treatment of the sample is required. No interference corrections seem to be required in the range 0.02—2 % U_3O_8, and pure aqueous uranium standards can be used for calibration. A correction for calcium and iron interference is required to achieve acceptable results on U_3O_8 levels below 0.02%. This correction involves monitoring the Ca and Fe levels in the sample solution, which can be easily accomplished simultaneously if a multi-channel spectrometer is used.

Prior ion-exchange separation of the uranium followed by i.c.p.—o.e.s. analysis did not yield more accurate results than the direct determination. Furthermore, the correction procedure for low U_3O_8 levels in the latter case is simpler than the ion-exchange separation technique, which is time-consuming.

Owing to the long dissolution period (about 2 h) the present technique is best suited to batch determinations where a large number of samples are dissolved simultaneously. These may then be analysed during the preparation of the next batch.

REFERENCES

1 J. H. Yoe, F. Will and R. A. Black, Anal. Chem., 25 (1953) 1200.
2 O. A. Neitzel and M. A. DeSesa, Anal. Chem., 29 (1957) 756.
3 K. L. Cheng, Anal. Chem. 30 (1958) 1027.

4 E. Singer and M. Matucha, Z. Anal. Chem., 191 (1962) 248.
5 F. H. Burstall and R. A. Wells, Analyst (London), 76 (1951) 396.
6 J. Korkisch and G. Arrhenius, Anal. Chem., 36 (1964) 850.
7 V. G. Goryushina and T. A. Archakova, Zavod. Lab., 26 (1959) 789.
8 G. W. C. Milner and J. W. Edwards, Anal. Chim. Acta, 16 (1957) 109.
9 N. R. Sen Sarma and K. Mallik, Anal. Chim. Acta, 12 (1955) 329.
10 B. Bieber and Z. Vecera, Chem. Listy, 52 (1958) 439.
11 A. Strasheim, Spectrochim. Acta, 4 (1950) 200.
12 R. Mavrodineanu, Flame Spectroscopy, Wiley, New York, 1965, pp. 46, 47, 169, 429.
13 G. DeMaria, R. P. Burns, J. Drowart and M. G. Inghram, J. Chem. Phys., 32 (1960) 1373.
14 M. D. Amos and J. W. Willis, Spectrochim. Acta., 22 (1966) 1325.
15 M. J. Martin, Analyst (London), 96 (1971) 843.
16 N. H. Clark and J. G. Pyke, Anal. Chim. Acta, 58 (1972) 234.
17 V. A. Fassel and R. N. Kniseley, Anal. Chem., 46 (1974) 1110A, 1155A.
18 G. F. Kirkbright and A. F. Ward, Talanta, 21 (1974) 1145.
19 S. Greenfield, I. Ll. Jones, H.McD. McGeachin and P. B. Smith, Anal. Chim. Acta, 74 (1975) 225.
20 R. H. Scott, V. A. Fassel, R. N. Kniseley and D. E. Nixon, Anal. Chem., 46 (1974) 75.
21 D. Kalnickey, R. N. Kniseley and V. A. Fassel, submitted for publication.
22 R. H. Scott and M. L. Kokot, Anal. Chim. Acta, 75 (1975) 257.
23 R. H. Kniseley, H. Amenson, C. C. Butler and V. A. Fassel, Appl. Spectrosc., 28 (1974) 285.
24 F. W. Strelow, NCRL, CSIR, South Africa. Personal communication.

Analytica Chimica Acta, 82 (1976) 79—82

THE DETERMINATION OF SOME "TOXIC" METALS IN HUMAN LIVER AS A GUIDE TO NORMAL LEVELS IN NEW ZEALAND PART II. ARSENIC, MERCURY AND SELENIUM

C. A. JOHNSON and J. F. LEWIN

Chemistry Division, DSIR, Private Bag, Petone (New Zealand)

P. A. FLEMING

Animal Health Reference Laboratory, Ministry of Agriculture and Fisheries, Private Bag, Upper Hutt (New Zealand)

(Received 2nd September 1975)

SUMMARY

Results of analyses for arsenic, mercury and selenium in human livers considered to be representative of the population of New Zealand are reported. Procedures are described for the determination of the three elements in liver tissue by colorimetry, flameless atomic absorption spectrometry and spectrofluorimetry respectively.

Part I of this paper [1] reported the levels of bismuth, cadmium, chromium, cobalt, copper, lead, manganese, nickel, silver, thallium and zinc in human liver tissue from autopsies of eleven New Zealanders with no known exposure to metals. The subjects were selected at random from the greater part of the North Island of New Zealand, and in the authors' experience, can be considered representative of the whole country. This study has now been extended to include the levels of arsenic, mercury and selenium in the same livers. The results obtained should serve as a guide for monitoring possible changes of these levels in the future.

The analytical procedures for arsenic, mercury and selenium are diverse. The problem of the volatility of each metal placed considerable importance on the mode of digestion and the method of analysis used. Since the reference methods all required substantial modification for the examination of liver tissue, a considerable amount of methodology is included.

EXPERIMENTAL

Instrumentation

Arsenic determinations were performed on a Beckman Acta CV Spectrophotometer. A Perkin-Elmer Coleman 50 mercury analyser in an open circuit mode was used for the mercury determinations. A Baird Fluorispec Fluorescence Spectrophotometer model S.F. 100 was used with

360-nm excitation and 523-nm emission for the selenium determinations.

Reagents

Glass-distilled water was used for all dilutions. Concentrated sulphuric (36 %) and perchloric (70 %) acids and all chemicals used to prepare standard solutions were analytical grade. Analytical-grade concentrated nitric (70 %) acid was redistilled before use. Redistilled analytical-grade solvents were used where applicable.

Without further purification, 4 g of 2,3-diaminonaphthalene monohydrochloride (Aldrich Chemical Co. Inc.) was dissolved in 1 l of 0.1 M hydrochloric acid for the selenium method.

All other reagents were prepared as described in the original publications.

Standard stock solutions

Arsenic (1 mg As ml^{-1}). Arsenic trioxide was dissolved in sodium hydroxide solution and diluted with distilled water.

Mercury (1 mg Hg ml^{-1}). Mercury(II) chloride was dissolved in nitric acid and diluted with distilled water.

Selenium (1 mg Se ml^{-1}). Sodium selenite was dissolved in 0.1 M hydrochloric acid.

Analytical Procedures

Arsenic. The method used was a modification of that described by Curry [2]. Liver tissue (50 g) was weighed into an acid-washed 250-ml Kjeldahl flask, 50 ml of 70 % nitric acid and 10 ml of 36 % sulphuric acid were added, and the digest was allowed to stand overnight. Gentle heat was then applied with a bunsen burner and concentrated nitric acid was added when necessary to prevent charring. When white fumes were evolved and no further charring occurred, the digest was cooled; 70 % nitric acid was then added and the digest reheated until white fumes were again evolved. Any excess oxides of nitrogen were removed by adding water and heating until white fumes were again evolved. The final solution was diluted to 50 ml with distilled water.

For analysis, a 10-ml aliquot was diluted to 40 ml with distilled water and the arsenic level was determined by the method of Taras et al. [3]. It was found necessary to double the recommended quantities of all reagents except for the pyridine—silver diethyldithiocarbamate (AgDDC) solution. The absorbance of the AgDDC complex was measured at 540 nm within 4 h.

Appropriate amounts of arsenic working standard (10 μg As ml^{-1}) were added to 50-g samples of one particular liver to provide a standard additions

calibration curve in the desired range (usually 0—1 μg As ml^{-1}). These samples were carried through the above procedure.

Mercury. The method used was that of Munns and Holland [4] modified in this laboratory [5] for the analysis of fish. Liver tissue (2 g) was digested in a mixture of 20 ml of 70 % nitric acid and 8 ml of 36 % sulphuric acid in an Erlenmeyer flask with an air condenser at a temperature not greater than 130 °C. The digest was diluted to 40 ml with water.

A 10-ml aliquot was taken for analysis. When the mercury content was high, a smaller aliquot was taken and diluted to 10 ml, so that the volume contained 5 ml of 70 % nitric acid, 2 ml of 36 % sulphuric acid and 3 ml of distilled water. The 10-ml aliquot was diluted to 50 ml with water, and 5 ml of tin(II) chloride—hydroxylamine solution was added. The mercury was flushed from the solution by a stream of air through the spectrophotometer absorption cell.

Selenium. The method used was a modification of the method of Watkinson [6]. A mixture of 3 ml of 70 % nitric acid and 2 ml of 70 % perchloric acid was added to 1 g of liver tissue in a digestion tube. The tubes were placed in boiling water for 1 h, then transferred to a thermostatically controlled heating rack, and heated at 180 °C until white perchloric acid fumes showed that the digestion was complete. The digest was cooled to 100 °C, and after the addition of 1 ml of 1 M hydrochloric acid, allowed to cool for a further 10 min before the sides of the tubes were rinsed down with distilled water.

A drop of cresol red indicator and 0.5 ml of disodium EDTA solution (50 g l^{-1}) were added, and the pH was adjusted to 1.5. After addition of 0.5 ml of 2,3-diaminonaphthalene solution, the solution was diluted to 25 ml with distilled water, shaken, and allowed to stand at 40 °C for 1 h. The selenium complex was extracted from the cooled solution into 5 ml of cyclohexane and the fluorescence measured.

RESULTS AND DISCUSSION

The results of analyses on eleven liver samples for arsenic, mercury and selenium, expressed as micrograms per gram of wet tissue, are presented in Table 1.

The levels of arsenic are similar to the overseas levels reported by Curry [2].

The levels of mercury found in the liver tissue are considerably lower than those indicated by Joselow et al. [7], indicating that the average New Zealander is exposed to less mercury than the subjects analysed by these authors.

The levels of selenium found are consistent with the results of analyses by Money and Rammell [8] on 200 human liver samples, mainly infant, in New Zealand.

TABLE 1

Levels of arsenic, mercury and selenium in human livers expressed as $\mu g\ g^{-1}$ wet tissue

Metal	Range	Mean	S.d.	Lit. range
Arsenic	0.02—0.07	0.05	±0.01	0.03—0.10[2]
Mercury	0.02—0.37	0.16	±0.10	<0.90[8]
Selenium	0.16—0.57	0.30	±0.13	0.10—0.50[9]

The recovery levels for arsenic and selenium were as efficient as those quoted by Morrison and George [9] and Watkinson [6]. Recovery experiments for mercury conducted on human liver samples gave a recovery range of 95—108 % and a mean of 101 %. Analysis of aliquots from the same digest gave a relative standard deviation as high as ± 7 %, indicating that the major source of error occurred at the final stage of the determination in the Coleman 50 mercury analyser.

It was necessary to use the method of standard additions for the determination of arsenic because of sample matrix interference. As the method of standard additions is time-consuming, one sample that had been analysed by this method was used as the standard for direct analysis of the remaining samples.

The above methods of analysis have been used extensively in these laboratories for some years and have been found very satisfactory for toxicological purposes. It is suggested that the mean levels reported in Table 1 be regarded as an indication of normal levels for human liver samples in New Zealand.

Conclusion

The levels of arsenic and mercury found in samples of liver supplied from routine post-mortem investigations are consistent with the limited information on levels found overseas and do not indicate any excessive intake of these metals by New Zealanders. No comparison was possible for selenium since overseas levels do not appear to be available.

REFERENCES

1 C. A. Johnson, Anal Chim Acta, 00 (1975) 000.
2 A. S. Curry, Poison Detection in Human Organs, Thomas, 2nd ed., 1969.
3 M. J. Taras, A. E. Greenburg, R. D. Hoak and M. C. Rands (Eds), Standard Methods for Examination of Water and Waste Water, prepared and published by A.P.H.A., A.W.W.A. and W.P.C.F., 13th edn., 1971.
4 R. K. Munns and D. C. Holland, J. Ass. Offic. Anal. Chem., 54 (1971) 202.
5 I. R. C. McDonald and H. J. W. McGrath, private communication.
6 J. H. Watkinson, Anal Chem., 38 (1966) 92.
7 M. M. Joselow, L. J. Goldwater and S. B. Wemberg, Arch. Environ. Health, 15 (1967) 64.
8 D. F. L. Money and C. Rammell, private communication.
9 J. L. Morrison and G. M. George, J. Ass. Offic. Anal. Chem., 52 (1968) 930.

Analytica Chimica Acta, 82 (1976) 83—92

INVESTIGATIONS OF REACTIONS INVOLVED IN FLAMELESS ATOMIC ABSORPTION PROCEDURES
PART I. APPLICATION OF HIGH-TEMPERATURE EQUILIBRIUM CALCULATIONS TO A MULTICOMPONENT SYSTEM WITH SPECIAL REFERENCE TO THE INTERFERENCE FROM CHLORINE IN THE FLAMELESS ATOMIC ABSORPTION METHOD FOR LEAD IN STEEL

WOLFGANG FRECH and ANDERS CEDERGREN

Department of Analytical Chemistry, University of Umeå, S-901 87 Umeå (Sweden)

(Received 30th August 1975)

SUMMARY

In order to study the interference from chlorine in the flameless a.a.s. method for lead in steel, high-temperature equilibrium calculations were applied to a system containing Fe, Pb, C, Cl, S, H, O, N and Ar. The temperatures as well as the input amounts of elements considered could be varied over a wide range, and a survey of the most important parameters governing the system was thereby obtained. The results indicate that a sample must be ashed in the presence of a sufficiently large amount of hydrogen and at a temperature of about 900 K in order to remove the chlorine from the graphite tube. Otherwise, the volatile lead chlorides $PbCl_2$ and PbCl are formed, which results in a decreased signal from lead.

When flameless atomic absorption devices were introduced it was a common opinion that, in contrast to flame methods, determinations could be made relatively free from interferences caused by the matrix. One of the main reasons for this was that the time for atomization in a graphite furnace is about one thousand times longer than that in a flame. This rather long atomization time makes it easier for refractory compounds to decompose. Furthermore, the highly reducing atmosphere in graphite tubes should facilitate such decomposition.

Several authors have reported results from determinations of minor constituents in heavy matrices which do not cause interferences. For example, Nikolaev [1] determined 10^{-10} g of aluminium in the presence of 10^{-5} g of iron, chromium, nickel, cobalt, titanium or copper. Similar determinations have been reported [2—4].

However, many papers have described interferences from the matrix in flameless atomic absorption spectrometry. Some characteristic examples may be given. A calcium matrix is reported to give a marked increase in sensitivity for the elements Al, Ba, Be, Si and Sn [5] and a severe suppression for the elements Cd, Pb and Zn [6]. Tin gives positive interferences for the determinations of Pb and Bi but negative interferences for the determination

of Ag and Co [7]. Hydrogen has been reported to enhance as well as to decrease the sensitivity [8].

One of the most commonly reported interferences occurs in chloride media. It is assumed that the metal to be determined is lost as a molecule which does not produce any atomic absorption signal. In particular, the presence of chloride together with Na, Fe, Al or Ca gives rise to severe disturbances in the determination of lead [9]. Because chloride is one of the major constituents in several matrices, a study of the rôle of chloride is of considerable interest.

Even when the concentration of components in the sample is small as for example in river water, interferences have been reported [10].

These examples illustrate that results obtained by the flameless technique are often very dependent on the composition of the sample. Many suggestions have been made in order to explain what really happens in the graphite tube during the ashing and atomization processes. However, until now very few theoretical and experimental studies of the mechanisms involved in the graphite tube have been published, possibly because of the complex physical, chemical and spectroscopic parameters which have to be considered. Great difficulties are encountered in the investigation of the chemical reactions because they are likely to be superimposed by physical and spectroscopic phenomena. Moreover, a great number of compounds is involved in the reactions which take place at the high temperatures used; hence, many substances in the solid, liquid and gaseous phases have to be taken into consideration. In addition, the small amounts of sample make it difficult to measure the reaction products during sample treatment in the atomization chamber.

Recently, an investigation which was concentrated on the kinetics of the formation of copper atoms during atomization was described [11]. The model was applied to copper oxide, the form in which the metal was supposed to be present after drying of the sample. Aggett and Sprott [12] made a comparative study between furnaces made of graphite or tantalum. For several elements the lowest temperature at which a significant atomic absorption signal could be detected was determined. For the elements Co, Fe, Ni and Sn, this temperature was found to be significantly lower when the samples were atomized on rods made of graphite rather than tantalum. It was suggested that the metal oxides of these elements, having higher melting points than the pure metal, were reduced to metal by the graphite. This assumption was supported by the fact that these elements had negative values of Gibbs free energy for the reduction of the metal oxide to the metal by graphite. In spite of favourable free energy values, the elements Bi, Cr and Pb appeared at approximately the same temperature in both materials. It was assumed that the reaction rates of the reduction were too slow for these oxides on graphite. Campbell and Ottaway [13] calculated the temperature at which the values of the Gibbs free energy for the reaction changed sign,

$$MeO(s) + C(s) \rightarrow CO(g) + Me(g) \quad (1)$$

and correlated these theoretical values with lowest temperatures at which an atomic absorption signal in the graphite furnace could be detected. Most of the elements were atomized at a temperature which was in agreement with the theoretical results. However, for some elements the experimental results did not fit the theory; for example, tin had to be atomized at a much higher temperature than that thermodynamically predicted. Moreover, the result for tin contradicts the findings of Aggett and Sprott [12] who stated that tin oxide was reduced by the graphite. For the elements lead and chromium Aggett and Sprott reported that carbon did not act as a reducing agent, whereas the results of Campbell and Ottaway compared well with the theoretically evaluated temperatures, i.e., the carbon reduces the metal oxide. Differences in the construction of the atomizing devices and effects from other ions present in the samples used might explain these divergences. Moreover, the models used are simplified and do not account for other possible reactions involved.

In this work a general study of the reactions involved in the determination of lead in steel by means of graphite furnaces has been made. All reasonable reaction products resulting from the reactions between C, H, O, N, S, Fe, Pb, Cl and A have been considered. Because of the great complexity of this system a general data program called SOLGASMIX was applied [14]. The equilibrium compositions in the solid, liquid and ideal gas phases were evaluated. However, in order to perform chemical equilibrium calculations, it is necessary to ascertain that equilibrium in the system has been obtained. Part I of this work deals with the theoretical calculations of the above-mentioned system, whereas Part II deals with the experimental results and shows the relevance of the theoretical calculations.

HIGH TEMPERATURE EQUILIBRIUM CALCULATIONS

The trace determination of lead in steel dissolved in aqua regia as described earlier [15] was selected as an example for the calculations. Chlorides present in a dissolved steel sample are reported to cause interferences [2] in flameless a.a.s. Recently, it was reported that the interferences could be eliminated by ashing the sample at about 900 K in the presence of hydrogen [15]. In the procedure described in the latter paper [15] 1 g of steel is dissolved in 10 ml of 12 M HCl and 5 ml of 16 M HNO_3 and the solution is finally diluted to 100 ml; 1 μl of this solution is pipetted into the graphite tube and dried at about 80 °C in order to remove most of the liquids present (H_2O, HNO_3 and HCl). The amounts of the elements left in the graphite tube after drying were roughly estimated (see Table 1) and provided a basis for the high-temperature equilibrium calculations presented below. Only elements in their standard states are used in the calculations and therefore all elements constituting the sample have been summarized as shown in Table 1.

TABLE 1

Estimated amounts of elements after drying at 80 °C and amounts used in the calculations

Element	Estimated amount after drying (μmol)	Amount used in the calculations (μmol)
Fe	0.07	0.07
Cl_2	0.05	varying
Pb	10^{-4}	10^{-4}
S_2	$7.5 \cdot 10^{-4}$	$7.5 \cdot 10^{-4}$
H_2	1[a]	varying
O_2	0.5[a]	$0.5 \cdot 10^{-3}$
N_2	0.02[b]	—
Ar	—	1.5
C	—	100

[a]Originating from the H_2O adsorbed on the graphite.
[b]Originating from the HNO_3 left in the tube.

In order to investigate the chemical reactions during ashing and atomization, a general computer program called SOLGASMIX [14] for high-temperature equilibria was employed. This program uses the free energy minimization principle which was introduced by White et al. [16]. An introductory book to the field of equilibrium calculations has been written by van Zeggeren and Storey [17]. Recently, a thorough discussion of the SOLGASMIX computer program was given by Eriksson [18]. The system dealt with in this paper contains nine elements (Table 1). The main components in the three phases are represented in Table 2. Substances like $COCl_2$(g), NO(g), HNO(g), CH_2O(g), HCN(g) and PbS(s), which were thought to be possible reaction products, were eliminated because they were not found to be present in such concentrations that they could affect the mass balances. The values of the Gibbs free energy for the formation of compounds like HCl(g), H_2O(g), CO(g),

TABLE 2

Compounds considered in the equilibrium calculations for the three phases

Gaseous			Liquid	Solid	
H_2	Ar	$FeCl_2$	$FeCl_2$	C	FeO
O_2	Cl_2	$FeCl_3$	$FeCl_3$	Fe	FeS
H_2O	CCl_4	COCl	Pb	$FeCl_2$	Pb
CO	HCl	S_2	PbO	$FeCl_3$	PbO
CO_2	Pb	H_2S		Fe_2O_3	$PbCl_2$
CH_4	PbCl	SO_2		Fe_3O_4	
N_2	$PbCl_2$	CS_2			

$Co_2(g)$ are very important for the accuracy of the results. The thermodynamic data for these substances have been determined with very high accuracy; estimates of the quality of the data are available in JANAF [19]. Provided that equilibrium is obtained and that the thermodynamic values used are good, the calculations should give accurate results. It is difficult to predict whether equilibrium can be obtained at a certain temperature, but in general equilibrium is slowly achieved for temperatures below 1000 K; above 1000 K the probability of obtaining a rapid equilibrium situation is normally considered to be high.

All of the equilibrium calculations were performed with the assumption of a constant pressure of 1 atm. Consequently, both the total amount of elements present in the gaseous phase and the temperature will affect the volume of the system. If the volume of the system is changed, the partial pressure of a gaseous compound will be changed if the compound is present only in the gaseous phase. When the compound is present in both the condensed and gaseous phases, the partial pressure of the gaseous compound will be unaffected, but the distribution of the compound between the gaseous and the condensed phases will be changed. For simplicity, however, the total amount of a particular compound is represented in the following figures irrespective of its phase distribution. The input amounts of the elements used in the calculations were chosen so that a volume approximately equivalent to the volume of a graphite tube was obtained at 1500 K.

RESULTS AND DISCUSSION

For the calculations represented in Fig. 1(a—c), it was first assumed that the content of the graphite tube was as specified in Table 1, right column, and that the temperature was 1000 K. Figure 1(a) shows the equilibrium composition when no hydrogen is present for various input amounts of chlorine. It can be seen that even a small amount of chlorine, e.g., 10^{-10} mol, results in redistribution of lead so that it is mainly present in the volatile forms PbCl and $PbCl_2$. In a real situation these molecules will be removed with the flowing argon so that there will be large losses of lead during ashing.

Figures 1(b) and 1(c) show the composition when 0.5 and 50 nmol of hydrogen were assumed to be present from the start. If these diagrams are compared with Fig. 1(a), it can be seen that larger amounts of chlorine can be tolerated before appreciable amounts of lead chloride compounds are formed. The main reaction responsible for the removal of chlorine from the system is

$$FeCl_2(g) + H_2(g) \rightarrow Fe(s) + 2\,HCl(g) \qquad (2)$$

$FeCl_2(g)$ is not removed from the system at 1000 K as will be shown in Part II [20]. The larger the partial pressure of hydrogen the more efficiently will chlorine be removed from the system.

Figure 2 deals with the calculation of the optimum temperature for an

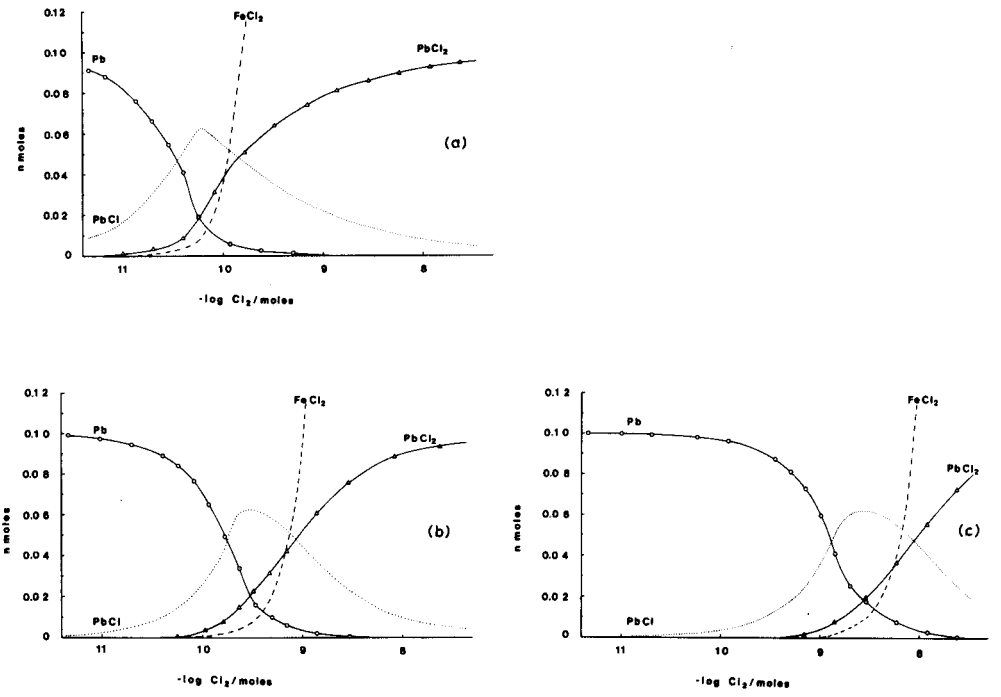

Fig. 1. The distribution of lead compounds and $FeCl_2$ at equilibrium and at a total pressure of 1 atm as a function of the input values of chlorine and hydrogen at 1000 K. The input values used are represented in Table 1, right column. (a) Without H_2. (b) 0.5 nmol of H_2. (c) 50 nmol of H_2.

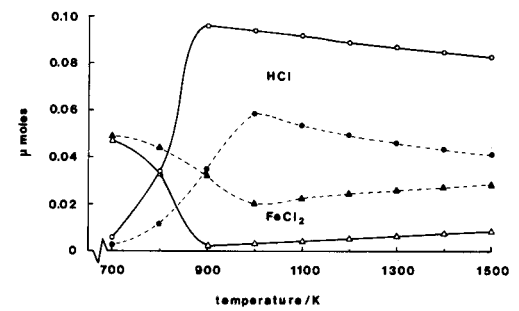

Fig. 2. The distribution of HCl and $FeCl_2$ at equilibrium and at a total pressure of 1 atm as a function of temperature. (△) $FeCl_2$. (○) HCl. Filled symbols: H_2 = 0.055 μmol, Cl_2 = 0.050 μmol. Unfilled symbols: H_2 = 0.5 μmol, Cl_2 = 0.05 μmol. The input values of other elements are represented in Table 1, right column.

ashing procedure. The distributions of HCl and $FeCl_2$ at a total pressure of 1 atm are given as a function of temperature for the input values shown in Table 1. The amount of chlorine used for the calculations was 0.050 μmol.

In Fig. 2 the optimum temperature for the formation of HCl was calculated for 0.50 μmol and 0.055 μmol of hydrogen; as can be seen, the optimum temperature depends on the amount of hydrogen used for the calculations, being 900 K for 0.50 μmol of H_2 and 1000 K for 0.055 μmol of H_2. The temperature at which these maxima occur coincides with the minima on the $FeCl_2$ curves. Consequently, at these temperatures there is a minimum amount of chlorine left in the graphite tube, which according to Figs. 1(a—c) favours the formation of lead atoms. The results shown in Fig. 2 can be better understood if the following equilibrium reactions are considered

$$1/2\ H_2(g) + 1/2\ Cl_2(g) \leftrightharpoons HCl(g) \quad (3)$$

$$Fe(s) + Cl_2(g) \leftrightharpoons FeCl_2(g) \quad (4)$$

At low temperatures, equilibrium reaction (4) is displaced more to the right than reaction (3). At temperatures above 900 K, $FeCl_2$ is more stable than HCl, because at higher temperatures the value of the Gibbs free energy for reaction (4) decreases more rapidly than the value for reaction (3).

If another source of hydrogen, i.e., that produced by the reaction between water and graphite, is considered, the situation presented in Fig. 2 becomes even more complicated. This can be illustrated by considering the water—gas equilibrium

$$CO + H_2O \leftrightharpoons CO_2 + H_2 \quad (5)$$

which is displaced to the left at increasing temperatures, so that the partial pressure of hydrogen is decreased. This in turn results in a displacement of reaction (3) to the left. Consequently, the partial pressure of chlorine increases and the net result is an increase in the amount of $FeCl_2$ formed. The optimum ashing temperature with water as the hydrogen donor can also be calculated by use of the SOLGASMIX program, but because of kinetic aspects and difficulties in estimating the amount of water present, it is better to determine this temperature experimentally [20].

Some of the reaction products have an appreciable vapour pressure at the temperature studied and to simulate the reaction in a graphite tube with flowing gas, a fraction of the gaseous phase was subtracted and the calculations were repeated with the new content. The amounts of the volatile chlorine-containing compounds formed have been measured as will be shown in Part II; only HCl was formed in significant amounts. Other volatile compounds such as carbon monoxide were not subtracted during the calculations because they did not affect the results shown in Fig. 3.

The iterative method for calculation with removal of HCl was used for the equilibrium calculations represented in Fig. 3. This Figure shows the distribution of lead compounds at equilibrium and at a total pressure of 1 atm as a function of temperature. The input values used are shown in Table 1; the amounts of elements not specified in Table 1 were $0.38 \cdot 10^{-1}$ μmol of Cl_2 and 0.5 μmol of H_2. These input values were obtained as follows.

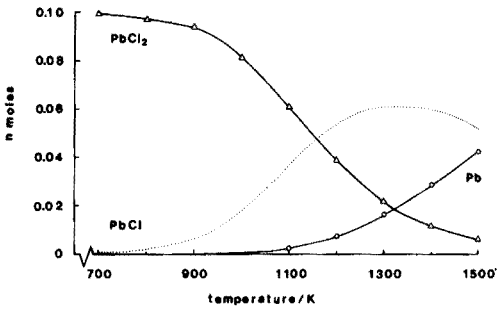

Fig. 3. The distribution of lead compounds at equilibrium and at a total pressure of 1 atm as a function of temperature. The input values for the calculations represented in the figure were obtained after a simulated ashing procedure at 700 K (see text).

The equilibrium composition obtained by use of the amounts of elements present after the drying step at 80 °C (see Table 1, left column, Ar = 1.5 μmol, C = 100 μmol) were calculated for 700 K and a total pressure of 1 atm. The equilibrium amount of chlorine present after the first calculation was distributed between the following species (μmol): $FeCl_2$, $0.47 \cdot 10^{-1}$; PbCl, $0.5 \cdot 10^{-6}$; $PbCl_2$, $0.99 \cdot 10^{-4}$; HCl $0.51 \cdot 10^{-2}$. Other chlorine-containing compounds were present in very small amounts and could be neglected. Eighty per cent of the chlorine present in the form of hydrochloric acid was subtracted from the input amount of chlorine. In this way a new input value for chlorine was obtained and a new equilibrium composition for the system was calculated. This procedure was repeated 6 times. After that the total amount of chlorine present in the system was still as much as $0.38 \cdot 10^{-1}$ μmol. This value was used as input value for Cl_2 for the calculations represented in Fig. 3. If the number of iterations was increased, the amount of chlorine left in the system was only slightly diminished. The results obtained after the six iterations approximately correspond to the experimental results shown in Part II.

These calculations were made for 700 K, because this is the temperature often used in flameless a.a.s. for the determination of lead. The results shown in Fig. 2 suggest that 900 K would be a more suitable ashing temperature than 700 K in the presence of chlorine. Therefore, the equilibrium composition of the system at 900 K was determined with the same initial input values as those used for the calculations at 700 K. The equilibrium amount of HCl present after the first calculation was $0.97 \cdot 10^{-1}$ μmol at 900 K. After subtraction of the chlorine from the total amount and repeated calculations as described above, the chlorine present in the system was (after 6 cycles) $0.45 \cdot 10^{-5}$ μmol. For this input value more than 99 % of lead is present as a metal at all temperatures, and no lead losses should occur.

These results indicate that a sample must be ashed in the presence of a sufficient large amount of hydrogen and at an optimum temperature (900 K) in order to remove the chlorine from the graphite tube during the ashing

procedure. If the sample is ashed at 700 K, the chlorine will not be removed and lead chlorides will be formed at all temperatures. As can be seen in Fig. 3, the amounts of the lead chlorides decrease with increasing temperature. In the atomization step the temperature of the furnace has to be raised from a relatively low temperature to a high preset temperature, thereby scanning part of the temperature range represented in the Figure. The time required to reach the final temperature is important for the distribution of various lead compounds. If the temperature is raised slowly, the formation of the volatile lead chlorides will be more probable than when rapid heating is employed.

Even minor constituents in the sample may affect the results obtained in flameless a.a.s. since the metal to be determined is present in a very low amount. In this study the presence of sulphur can serve as an example. As mentioned above, it was assumed that the amount of sulphur present in the sample was equal to the value given in the certificate of the steel used. In addition, the amount of H_2S liberated from the tube was found to correspond approximately to the amount of sulphur initially assumed. The presence of H_2S in the system discussed here was of considerable interest since it seemed possible that PbS(s) could be formed during the ashing procedure. The melting point of PbS(s) is 1114 °C, which means that a very high ashing temperature could be used without causing any lead losses. However, it was found that in presence of excess of iron the formation of PbS(s) was not thermodynamically possible.

In complex matrices such as blood, urine and sea water, non-specific absorption often affects determinations. However, these effects can be minimized by removing the matrix before the sample is atomized, provided that the metal is not lost during the ashing procedure. In such cases it might be possible to form a stable compound which should make it possible to utilize a higher ashing temperature. In several applications materials other than graphite [21] seem to have advantages. The calculation technique presented here should make it possible to improve some of the flameless procedures used today and to design new procedures.

The authors wish to thank Professor Gillis Johansson and Dr. Gunnar Eriksson for valuable discussions.

REFERENCES

1 G. I. Nikolaev, Zh. Anal. Khim., 20 (1965) 445.
2 F. Shaw and J. M. Ottaway, Analyst (London) 99 (1974) 184.
3 W. Frech, Talanta, 21 (1974) 565.
4 G. K. Pagenkopf, D. R. Neuman and R. Woodriff, Anal. Chem., 44 (1972) 2248.
5 K. C. Thompson, R. G. Fodden and D. R. Thomerson, Anal. Chim. Acta, 74 (1975) 289.
6 R. B. Cruz and J. C. van Loon, Anal. Chim. Acta, 72 (1974) 231.
7 R. Medina, Z. Anal. Chem., 271 (1974) 346.

8 D. E. Shrader, B. Culver and R. Ippolit, Lecture, Pittsburgh Conference, 1975.
9 F. J. Fernandez and D. C. Manning, At. Absorption Newslett., 10 (1971) 65.
10 B. Welz and E. Wiedeking, Z. Anal. Chem., 264 (1973) 110.
11 C. W. Fuller, Analyst (London), 99 (1974) 739.
12 J. Aggett and A. J. Sprott, Anal. Chim. Acta, 72 (1974) 49.
13 W. C. Campbell and J. M. Ottaway, Talanta, 21 (1974) 837.
14 G. Eriksson, Chem. Sch., Chem. Scr., 8 (1975) 100.
15 W. Frech, Anal. Chim. Acta, 77 (1975) 43.
16 W. B. White, S. M. Johnson and G. B. Danzig, J. Chem. Phys., 28 (1958) 751.
17 F. van Zeggeren and S. H. Storey, The Computation of Chemical Equilibria, Cambridge University Press, London, 1970.
18 G. Eriksson, Quantitative Equilibrium Calculations in Multiphase Systems at High Temperatures, Dissertation, Umeå University, Sweden, 1975.
19 JANAF, Thermochemical Tables, Nat. Stand. Ref. Data Ser., Nat. Bur. Std., 1971, 37.
20 W. Frech and A. Cedergren, Anal. Chim. Acta, 82 (1976) 55.
21 R. B. Baird and S. M. Gabrielian, Appl. Spectrosc., 28 (1974) 273.

Analytica Chimica Acta, 82 (1976) 93—102

INVESTIGATIONS OF REACTIONS INVOLVED IN FLAMELESS ATOMIC ABSORPTION PROCEDURES
PART II. AN EXPERIMENTAL STUDY OF THE RÔLE OF HYDROGEN IN ELIMINATING THE INTERFERENCE FROM CHLORINE IN THE DETERMINATION OF LEAD IN STEEL

WOLFGANG FRECH and ANDERS CEDERGREN

Department of Analytical Chemistry, University of Umeå, S-901 87 Umeå (Sweden)

(Received 30th August 1975)

SUMMARY

The rôle of hydrogen in eliminating the interference from chlorine in the flameless a.a.s. method for lead in steel has been experimentally studied with the Perkin-Elmer HGA 72 and Varian-Techtron CRA 63 graphite furnaces. Hydrogen is generated at high temperatures in both systems by the reaction of graphite with water left in the tube after the drying step. The amount of hydrogen formed during the ashing procedure in the Perkin-Elmer tube is about five times larger than that in the Varian tube. The removal of chlorine from graphite tubes containing dissolved steel samples has been determined as a function of temperature for (i) the CRA 63 without hydrogen added, (ii) the CRA 63 with hydrogen added, and (iii) the HGA 72 without hydrogen added. At 950 K, a significant amount of chlorine is left only in case (i); thus the amount of hydrogen formed in the HGA 72 is large enough to remove all of the chlorine through the reaction $FeCl_2(g) + H_2(g) \rightarrow Fe(s) + 2\,HCl(g)$. If a sample is ashed at 950 K, losses of lead as lead chlorides only occur for the case (i) which is in accordance with theoretical prediction. The theoretically predicted optimum ashing temperature range of 900—1000 K is shown to be in good agreement with the experimental results.

As was shown in Part I [1], the presence of hydrogen is necessary to eliminate the interference from chlorine in the flameless a.a.s. method for the trace determination of lead in steel; the interference is eliminated if the chlorine is removed during ashing. Chlorine is removed from the system as a result of the reaction between iron(II) chloride and hydrogen. The theoretical calculations [1] are in agreement with experimentally reported results [2] obtained with the Varian-Techtron system which includes flushing the graphite tube with a mixture of hydrogen and argon during ashing and atomization. In contrast, no hydrogen need be added to the Perkin-Elmer HGA 72 graphite tube [3]. Initially, these findings were unexpected. It was considered possible that water adsorbed on the graphite tubes could react with graphite during ashing of the sample, forming hydrogen. In contrast to the small Varian tube, the large Perkin-Elmer tube might provide sufficient hydrogen to eliminate the interference from chlorine. In fact this was a

reasonable assumption, since it had been noticed earlier that water was difficult to remove from graphite. Therefore, one of the aims of the work presented here was to determine the amount of hydrogen formed in the different graphite tubes during the ashing procedure. These values should be used to check experimentally the relevance of the theoretically predicted optimum ashing temperatures [1]. Another aim was to study the effect of hydrogen on the removal of chlorine from the graphite tube during the ashing procedure by measuring the amount of hydrochloric acid liberated from the tube. As was shown in Part I, this species is produced by the reaction between iron(II) chloride and hydrogen.

EXPERIMENTAL

Instrumentation

Varian-Techtron AA6 and Perkin-Elmer Model 300SG spectrophotometers were used. The Varian instrument was equipped with a CRA 63 furnace and an OmniScribe (Houston Instruments) chart recorder, and the Perkin-Elmer instrument with a HGA 72 furnace and a Hitachi IS recorder. Both instruments were provided with background correctors. The peak absorbance values were measured.

Determination of lead

For measurements with the Varian instrument, 1 g of ultrapure steel (JK 1C) was dissolved in a mixture of 5 ml of 16 M nitric acid and 10 ml of 12 M hydrochloric acid. After the sample had been dissolved, the volume was made up to 100 ml with distilled water. Standard additions of lead were made by adding 2 μl of a 1000 p.p.m. lead standard to 10 ml of this diluted steel solution.

For measurements on the Perkin-Elmer instrument, 0.25 g of ultrapure steel was dissolved in 1 ml of 16 M nitric acid and 2.5 ml of 12 M hydrochloric acid. The dissolved sample was diluted to 100 ml with distilled water; 2 μl of 1000 p.p.m. lead stock solution was added to 40 ml of this sample solution.

The ashing temperature used for determinations with the CRA 63 was measured with a pyrometer. For the experiments with the HGA 72, temperature values were taken from the instrument manual. The instrumental parameters for the determinations are given in Table 1.

Determination of iron

The amount of iron released during the ashing procedure of a steel sample was determined with the Varian-Techtron graphite tube. The dissolved steel sample (1 μl) was injected into the graphite tube and the sample was dried under the conditions shown in Table 1. The graphite tube containing the dried sample was then transferred to a quartz tube which could be

TABLE 1

Instrumental parameters for the determination of iron and lead

	Lead — HGA 72		Lead — CRA 63		Iron — CRA 63	
	Time (s)	Temp[a]	Time (s)	Temp[a]	Time (s)	Temp[a]
Drying step	20	20	15	3	15	3
Ashing step	50	150	30	5.5	25	5.5
Atomization	5	500	3	10	4	8
Outburning	3	999	—	—	—	—
Wavelength (nm)	283.3		283.3		248.3	
Slit width	20 units		50 μm		50 μm	
Lamp current (mA)	6		5		5	
Sample volume (μl)	5		1		2	
Gas flow inert	Gas stop during atom		8[b]		7[b]	
Gas flow hydrogen	Not used		2[b]		Not used	

[a]Temperature in digital units.
[b]Units on flow meter.

heated by means of a furnace regulated by a step transformer. The outlet tip of the tube, which was flushed with 15 ml N_2 min^{-1}, was dipped into an absorption solution (2 ml of 0.7 M nitric acid). The iron content of this solution was determined for ashing times of 18 min at 620 °C and 30 min at 800 °C.

Determination of chloride liberated from the graphite tube during heating

An aliquot (1 μl) of a sample containing 0.07 μmol of iron, 0.42 μmol of HCl, 0.28 μmol of HNO_3 and $1.0 \cdot 10^{-4}$ μmol of lead was transferred into either a Varian Techtron CRA 63 or a Perkin-Elmer HGA 72 graphite tube. Samples were dispensed with a 1-μl 7001 Hamilton syringe with an accuracy of better than 1 %. The graphite tube to be studied was placed in a quartz tube, length 30 cm, diam. 1.5 cm, inserted into an electrically heated oven which was provided with a thermoelement connected to a thermoregulator. The temperature of the graphite tube could be controlled to better than ± 10 °C. In the sample runs the temperature of the oven was normally changed in the following steps: 80, 300, 500, 600, 800 and 1000 °C. A new temperature was reached in about 2 min.

The quartz tube was flushed with 80 ml Ar min^{-1}. The influence of hydrogen on the removal of chlorine from the graphite tube was studied by using a mixture of argon and hydrogen at a flow rate of (80 + 20) ml min^{-1}. The gas stream which passed the graphite tube was bubbled through the electrolyte of the sample compartment of a coulometric cell in which the chloride was absorbed and continuously titrated with silver ions. The coulometric system and the procedure used have been described recently by Cedergren and Fredriksson [4].

Determination of hydrogen

Figure 1 shows the experimental arrangement for the determination of the hydrogen liberated from a graphite tube when heated. An aliquot of 5 μl of a dissolved and diluted steel sample was injected into a Perkin-Elmer HGA 72, and 1 μl into a Varian Techtron graphite tube. The samples were taken from a solution containing 0.25 g of iron, 2.5 ml of 12 M HCl, and 1.0 ml of 16 M HNO_3 per 100 ml of aqueous solution. The graphite tube was placed in the sample compartment as described above (see chloride determination) and was flushed with 80 ml Ar min^{-1}. The water carried along with the argon was absorbed on magnesium perchlorate (dehydrite). The hydrogen present in the sample compartment passed through the dehydrite zone and, after reaction with added oxygen (see Fig. 1) at about 700 °C, formed water in an amount equivalent to the amount of hydrogen. In this way the system was specific for hydrogen. The argon and oxygen gas flow entered a coulometric cell where the amount of water was continuously titrated by a Karl Fischer method [5].

The response and accuracy of the coulometric system were tested by injecting 10 μl and 20 μl of hydrogen (25 °C, 1 atm) successively into the sample compartment (see Fig. 2, points (a) and (d); these volumes are equal to 0.4 and 0.8 μmol, and the experimentally found values were 0.3 and 0.8 μmol of H_2, respectively. In order to confirm the selectivity of this system for hydrogen in presence of water, as much as 300 μmol of water were placed in the sample compartment, the temperature of which was 100 °C. No significant amount of water was detected (see point (b), Fig. 2) which proves that water was effectively absorbed in the zone containing dehydrite. The least amount of water for which a relative standard deviation of 10 % was expected, was estimated to be 0.005 μmol.

After the graphite tube containing the dissolved steel sample had been placed in the sample compartment, about 3 min were required to remove all the oxygen which had entered the compartment with the sample. If oxygen is not completely removed from the sample compartment, low results will be obtained because the oxygen remaining reacts with hydrogen to form water.

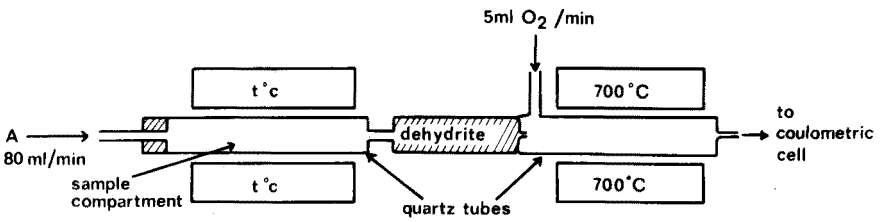

Fig. 1. Schematic experimental arrangement for the determination of hydrogen.

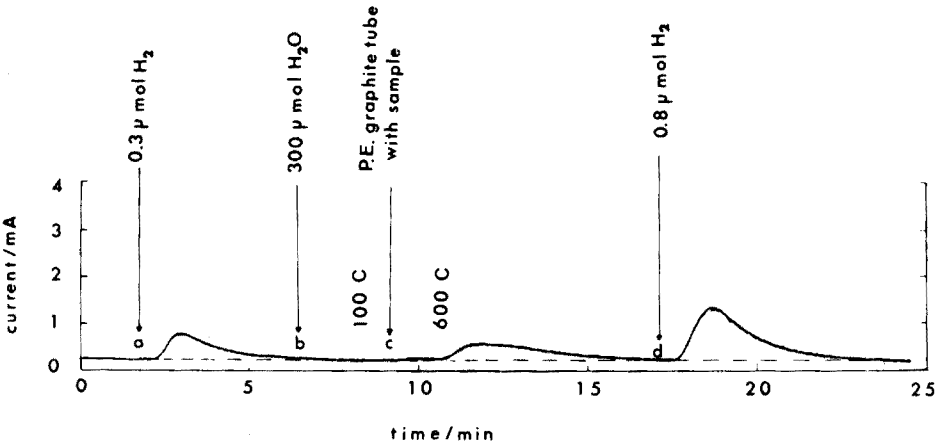

Fig. 2. Recorded coulometric titrations of the amount of hydrogen formed in a Perkin-Elmer graphite tube at the final temperatures 100 °C and 600 °C (see point (c)). 5 μl of a dissolved ultrapure steel sample (JK 1C) was added to the tube. At points (a) and (d) hydrogen was injected into the sample compartment and at point (b) 300 μmol of water was added.

RESULTS

Flameless a.a.s. results

An ultrapure steel, JK 1C with 20 p.p.m. of lead added, was dissolved as described above. Figure 3 shows the peak absorbance values for these samples as a function of ashing temperature for the HGA 72 and CRA 63 graphite furnaces. The instrumental parameters used are shown in Table 1. Each symbol in Fig. 3 represents the mean value of at least two determinations; the standard deviations were about 5 % for ashing temperatures above 800 K and about 15 % for lower ashing temperatures.

The upper curves in Fig. 3 were obtained by making determinations on the HGA 72 without, and on the CRA 63 with, hydrogen added to the inert gas. Both curves are of similar shape, and it can be seen that the sensitivity improves with increased ashing temperatures until a range is attained in which the sensitivity is optimum and unaffected by temperature. In order to attain this optimum, higher temperatures were needed for determinations made on the HGA 72 than on the CRA 63. For determinations with the HGA 72, the sensitivity increased markedly in the region 650—900 K, whereas for determinations with the CRA 63, the effect occurred between 700 and 800 K. As the ashing temperature was increased still further, the sensitivity was unaffected until an upper temperature of about 1000 K was reached; above this temperature the sensitivity was decreased. It should be observed that the samples were ashed for 50 s on the HGA 72 furnace compared to 30 s on the CRA 63. Because of the longer ashing time, the

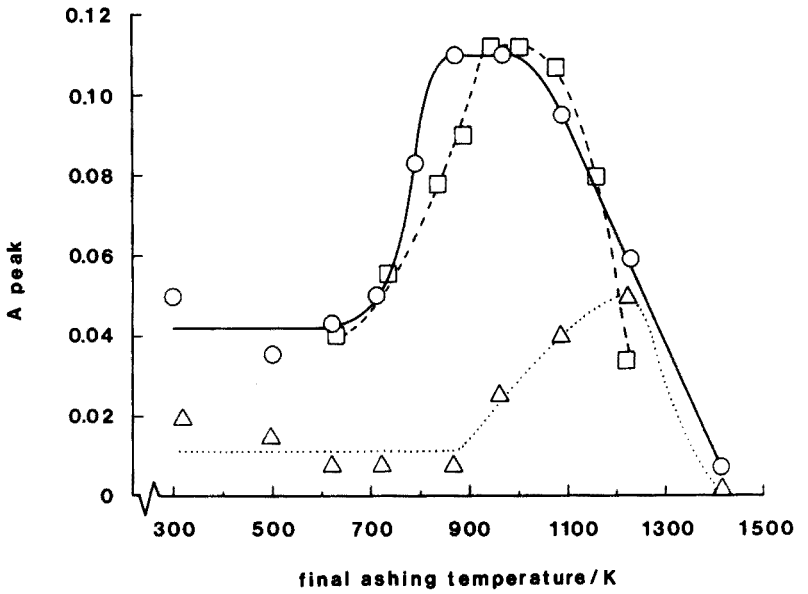

Fig. 3. Peak absorbance values as a function of ashing temperature for an ultrapure steel JK 1C with 20 p.p.m. of lead added. (○) Varian Techtron with H_2, ashing time 30 s. (△) Varian Techtron without H_2, ashing time 30 s. (□) Perkin-Elmer HGA 72 without H_2, ashing time 50 s.

sensitivity decreased more rapidly with the HGA 72 than with the CRA 63 above 1000 K.

The lower curve in Fig. 3 shows the results for samples ashed on the CRA 63 without hydrogen added. In this case the absorbance values were in general very low. Above 900 K, the sensitivity was improved and optimum sensitivity was obtained at about 1250 K.

Table 2 shows that the ashing time has no significant effect on the sensitivity; these results indicate that no lead is lost during ashing at 950 K.

In order to determine the amount of iron released during ashing, 10 μg

TABLE 2

Peak absorbance values for a steel sample containing 15 p.p.m. of lead obtained for various ashing times (The ashing temperature was 950 K. Measurements were made on a CRA 63 graphite furnace with hydrogen added to inert gas)

Ashing time(s)	A peak		Mean
25	0.085	0.076	0.081
60	0.083	0.077	0.080
120	0.079	0.085	0.082
300	0.085	0.087	0.086

of iron were added to a CRA 63 graphite tube. No significant amount entered the absorption solution; the least amount which could be detected was about 10 ng.

Determination of chloride

The amount of chlorine left in the graphite tubes at various temperatures was calculated by subtracting the coulometrically measured amounts of HCl leaving the graphite tube from the amount of chlorine added to the tube at the start of the experiment. Aliquots (1 μl) of a dissolved and diluted steel sample containing 210 nmol of chlorine (Cl_2) were added to the graphite tube, and the following cases were studied: (i) Varian CRA 63 graphite tube flushed with a mixture of hydrogen and argon (1 : 4); (ii) Varian CRA 63 without hydrogen added; (iii) Perkin-Elmer without hydrogen added. When 1 μl of the sample solution was injected directly into the coulometric cell, the mean value found was 417 ± 3 nmol of chloride. The amount of chlorine left in the graphite tubes in the above cases is shown in Fig. 4 as a function of temperature. As can be seen, chlorine is effectively removed from the Varian CRA 63 graphite tube at a rather low temperature when flushed by hydrogen; at ca. 775 K all of the chlorine is removed, but if hydrogen is not added more than 40 nmol is left at this temperature. When the temperature was raised chloride was still liberated but above 1175 K no more chlorine was removed

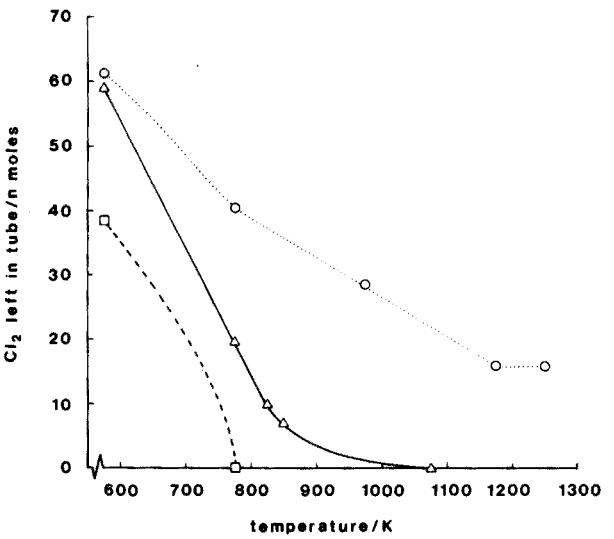

Fig. 4. The amount of chlorine left in the graphite tube as a function of temperature. 1 μl sample containing 210 nmol of chlorine (Cl_2) was added to the graphite tube. (□) Varian CRA 63 with hydrogen added. (○) Varian CRA 63 without hydrogen. (△) Perkin-Elmer HGA 72 without hydrogen.

from the system. When hydrogen was added to the remaining mixture in which about 17 nmol of chlorine was left this amount was totally liberated from the tube. Even when no hydrogen was added, chlorine was easily liberated from the Perkin-Elmer tube. The difference in the results obtained for cases (ii) and (iii) is discussed below.

Figure 5 shows a recorded chloride determination in one of the studies with the Perkin-Elmer tubes. The current—time integral is proportional to the amount of chloride entering the coulometric cell. The accumulated amount of chloride liberated from the tube is given in the legend to Fig. 5. The first and rather sharp peak originates from the excess of HCl in the sample. The other peaks can be regarded as a result of the reaction between $FeCl_2$ and hydrogen. The shape of the peaks gives rough information on the kinetics involved. For example at point (b), i.e., at 300 °C, the reaction seems to be slow because the electrolysis current approaches zero very slowly.

Determination of the amount of hydrogen liberated from the graphite tubes

Hydrogen was liberated from both the Varian CRA 63 and the Perkin-Elmer HGA 72 graphite tubes. In tests with the HGA 72, 5 μl of a steel sample (see Experimental) was added to the tube before it was put in the sample compartment (Fig. 1). The amount of hydrogen liberated from this tube on heating should be somewhat smaller than the total amount of hydrogen formed in the tube because of the reaction with $FeCl_2$. The amount of hydrogen which reacted with $FeCl_2$ at 600 °C was 0.07 μmol. The amount of hydrogen obtained in the sample run in Fig. 2 (point (c)) was 0.3 μmol, which means that the total amount of hydrogen formed was about 0.4 μmol; the mean value of five sample runs for the conditions described in Fig. 2 was 0.3 ± 0.1 μmol.

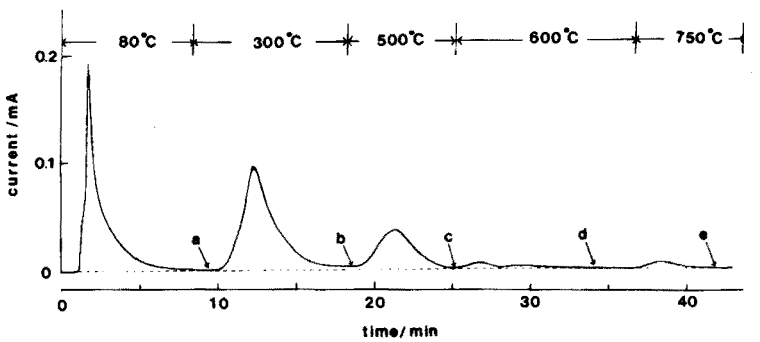

Fig. 5. Coulometric determination of the amount of chloride (equal to the current—time integral on the recorder) liberated from a Perkin-Elmer tube as a function of temperature. 1 μl of the dissolved iron sample containing 0.417 ± 0.003 μmol of Cl^- was used for each experiment. The accumulated amounts of chloride liberated from the tube were at the points indicated: (a) 0.148, (b) 0.302, (c) 0.388, (d) 0.408, (e) 0.418 μmol.

The mean value of the amount of hydrogen liberated from the Varian CRA 63 tube was 0.04 ± 0.02 μmol. Considering the amount of hydrogen which reacted with $FeCl_2$ at 600 °C, the total amount of hydrogen formed in the Varian tube was estimated to be 0.08 ± 0.2 μmol. Experiments with a home-made graphite tube which had a weight about 10 times higher than that of the Perkin-Elmer tube gave values for the amount of hydrogen liberated at least 10 times higher than those obtained with the Perkin-Elmer tube. When the large tube was used, several hours at 600 °C were needed to remove all the water present initially.

DISCUSSION

In Part I [1], the theoretical possibilities of eliminating the interference from chlorine in the flameless a.a.s. method for lead in steel were evaluated. It was shown that the interference should be eliminated by ashing the steel sample in the presence of sufficient hydrogen at a temperature in the range 900—1000 K. Unless the temperature was in this range, too much chlorine was left in the system, and this allowed the formation of volatile lead chloride compounds.

The sensitive coulometric method used here showed that hydrogen is generated in both the Perkin-Elmer and Varian graphite tubes during the ashing procedure. The amount of hydrogen produced in the Perkin-Elmer tube is about five times larger than that produced in the Varian tube, so that the transport of chlorine away from the Perkin-Elmer tube is more effective. Chlorine is liberated from the graphite tubes as hydrogen chloride by the reaction: $FeCl_2(g) + H_2(g) \rightarrow Fe(s) + 2\,HCl(g)$. In the initial studies, it seemed possible that $FeCl_2(g)$ also contributed to the removal of chlorine during ashing and atomization, but the results obtained in the determination of iron showed that less than 0.1 % of the chlorine was transported as $FeCl_2(g)$. The chloride determinations represented in Fig. 4 further supported the assumption that the reaction mentioned is responsible for the removal of chlorine from the system. Obviously, the amount of hydrogen formed in the small Varian tube is too small to remove the chlorine and therefore lead will be lost as lead chlorides. When the Varian CRA 63 tube was flushed with hydrogen during the ashing step all the chlorine was removed at 775 K (Fig. 4). Corresponding results obtained with the Perkin-Elmer tube without hydrogen flushing (Fig. 4) showed that the temperature had to be about 1000 K in order to remove all the chlorine. As can be seen in Fig. 3, a temperature about 100 K higher is needed to obtain optimum sensitivity in the determination of lead for the Perkin-Elmer tube compared to the Varian tube (with hydrogen). In Part I, 900 K was shown to be the optimum ashing temperature for the Varian tube when a large excess of hydrogen was used, and this is in good agreement with the results shown in Fig. 3. The somewhat higher optimum ashing temperature necessary with the Perkin-Elmer system can be explained by the smaller amount of hydrogen present;

this agrees with the theoretical prediction in Part I. The sensitivity of the determination with the HGA 72 without hydrogen, and on CRA 63 with hydrogen, was not changed by a variation of the ashing temperature in the interval 910—1000 K. If an ashing temperature of 950 K is selected, small changes in temperature do not influence the sensitivity and reproducibility. But, if too little hydrogen is present, the sensitivity will be very dependent on a variation of the ashing temperature (see Fig. 3, lowest curve).

Negative as well as positive interferences caused by hydrogen have been reported [6, 7]. The production of hydrogen by the reaction between water and graphite has apparently not been considered before in connection with flameless a.a.s. The present work shows that hydrogen is always present during determinations in graphite tubes, its quantity depending on the type and amount of graphite used. The volume of the sample to be determined as well as the condition of the graphite may also affect the production of hydrogen. The porosity of the graphite normally tends to increase during the course of the determinations, so that the amount of water left after the drying step will also increase, and a greater amount of hydrogen will be formed during subsequent ashing procedures. In such cases the reproducibility of the determinations will, of course, be unsatisfactory. It is reasonable to assume, therefore, that the hydrogen produced in the graphite might also influence the determinations of several other elements.

The authors wish to thank Professor Gillis Johansson and Dr. Gunnar Eriksson for valuable discussions.

REFERENCES

1 W. Frech and A. Cedergren, Anal. Chim. Acta, 82 (1976) 45.
2 W. Frech, Anal. Chim. Acta, 77 (1975) 43.
3 W. Frech, G. Lundgren and S.-E. Lunner, At. Abs. Newslett., submitted for publication.
4 A. Cedergren and S. Å. Fredriksson, Talanta, in press.
5 A. Cedergren, Talanta, 21 (1974) 367.
6 D. E. Shrader, B. Culver and R. Ippolit, Lecture, The Effects of Hydrogen on Flameless Atomic Absorption Analyses, Pittsburgh Conference, 1975.
7 M. D. Amos, P. A. Bennet, K. G. Brodie, P. W. Y. Lung and J. P. Matousek, Anal. Chem., 43 (1975) 211.

Analytica Chimica,Acta, 82 (1976) 103—111

NON-ATOMIC ABSORPTION FROM MATRIX SALTS VOLATILIZED FROM GRAPHITE ATOMIZERS IN ATOMIC ABSORPTION SPECTROMETRY

M. W. PRITCHARD and R. D. REEVES

Department of Chemistry, Biochemistry and Biophysics, Massey University, Palmerston North (New Zealand)

(Received 27 June 1975)

SUMMARY

The non-atomic absorption signals obtained from alkali halides atomized from three types of graphite atomizer are examined. The wavelength dependence of the signals identifies the absorption as that of charge-transfer transitions of the alkali halide molecules. The contribution of light scattering to the total non-atomic absorption signal is shown to be of small significance; the observed light-scattering is not Rayleigh scattering. The temperature dependence of the loss of sodium chloride from a rod atomizer is studied experimentally and compared with calculated vaporization rates based on the kinetic theory of gases.

Non-flame atomizing devices developed recently for atomic absorption spectrometry possess several advantages over conventional nebulizer-flame atomization systems. These advantages include the possibility of carrying out analyses on microlitre samples, the possibility of direct analysis of complex viscous or solid samples (such as biological fluids, lubricating oils and powdered rock specimens) and increased sensitivity.

Atomizers based on electrically-heated graphite rods, furnaces and cuvettes are finding increasing use, such as in the determination of trace levels of various elements in blood [1—5], urine [1, 6, 7], sea water [6, 8], geological and metallurgical samples [9], hydrogeochemical samples [10], crude petroleum [11], used lubricating oils [5, 12—15], and an International Biological Standard [16].

Only in the case of metal particles in used lubricating oils can the sample matrix be described as chemically simple. Removal of the hydrocarbon matrix is achieved by ashing at temperatures well below the atomization temperatures of the elements of interest, and interference effects have not been noted. Many other types of matrix contain moderate or high concentrations of inorganic salts and, in some cases, large proportions of organic matter as well. The ashing process does not necessarily lead to a clean separation of the matrix from the analyte. Difficulties can then arise from non-atomic absorption and from various matrix interference effects.

When poor separation of the analyte from the matrix occurs a non-atomic

component may be superimposed on the atomic absorption signal from the analyte (especially when the matrix is of similar volatility to the analyte). This component may be a result of light scattering or of molecular absorption by volatilized inorganic salts or organic combustion products. The contribution of this relatively broad-band absorption component to the total absorption signal obtained during atomization can be assessed by examining the absorption signal under the same experimental conditions using a continuum source (e.g. hydrogen or deuterium discharge lamp). Correction for non-atomic absorption can then be made by comparison of the continuum and line source absorbances either simultaneously (double beam spectrophotometry) or consecutively (single-beam instrument).

The degree of success attained with this background correction procedure is dependent on the magnitude and the reproducibility of the non-atomic component of the absorption, on the atomizer design, and on the wavelength being used. For example, in the case of sea-water samples atomized in a tubular furnace [8], the compensating ability of a deuterium lamp background corrector was greatly exceeded. Attempts at selective volatilization of the sea-water salts from the elements being determined were largely unsuccessful.

Matrix interference effects lead to a change in the efficiency with which ground-state analyte atoms are produced from the sample. Several different forms can be envisaged for such effects:
(i) loss of volatile compounds of the analyte during ashing or atomization; (ii) failure to break down matrix particles completely during atomization, resulting in incomplete release of analyte atoms; (iii) formation on the atomizer or in the vapour of incompletely-dissociated compounds of the analyte during atomization.

The present work was carried out to establish (1) the nature of the non-atomic absorption produced by some inorganic salts atomized from graphite under a variety of conditions, i.e. whether the absorption is attributable to molecular absorption, light scattering, or both; (2) the conditions of atomizer temperature and heating time under which matrix salts are volatilized from atomizers of various designs.

Because sodium chloride is a major matrix constituent of many samples, including those of biological and marine origin, much of the present work was done with this salt. The conclusions reached have been confirmed by similar studies on other salts.

EXPERIMENTAL

Apparatus

A Varian Techtron Carbon Rod Atomizer (CRA63) was used in conjunction with a Varian Techtron AA-5 Atomic Absorption Spectrophotometer and a fast-response recorder (Model B161, Rikadenki Kogyo Co. Ltd.,

Tokyo, Japan; full-scale deflection less than 0.33 s). Three different types of graphite atomizer were used at various stages: (a) "rod" — a graphite rod with a small sample cavity, similar to that described by Molnar et al. [17], (b) "tube furnace", and (c) "cup" — as supplied with the CRA63, and described elsewhere [18].

The light sources were Varian Techtron single-element hollow-cathode lamps, and a Varian Techtron hydrogen lamp, all operated with the manufacturer's recommended parameters. For all experiments, solutions were dispensed from an Excalibur 5-μl syringe with disposable Teflon tips.

Reagents

All reagents used were analytical grade. Solutions of NaCl and KBr, containing 10000 μg ml^{-1} of the anion, were prepared. Solutions with various concentrations of the anion down to 10 μg ml^{-1} were prepared by dilution with distilled, doubly-deionized water. Solutions containing more than 200 μg ml^{-1} of the anion were stored in polythene bottles. All other concentrations were freshly prepared before use.

General procedure

After samples were placed on the atomizer a three-stage heating cycle was initiated ("dry", "ash", "atomize") with specified voltage and time settings. An argon—hydrogen atmosphere was maintained around the atomizer during the ash and atomize stages only (flow rates: Ar = 3.8 l min^{-1}, H_2 = 2.2 l min^{-1}). All absorption measurements were made at least in triplicate to confirm the reproducibility of the observed behaviour. Estimates of the final temperature reached by the atomizers were made by observing the melting of very small particles of suitable metals.

Studies of the wavelength-dependence of non-atomic absorption were carried out initially using line sources from a variety of hollow cathode lamps. The major part of this work, however, was carried out by a hydrogen continuum source with almost identical results.

RESULTS AND DISCUSSION

Wavelength-dependence of non-atomic absorption

A 5-μl sample of sodium chloride solution (800 μg Cl ml^{-1} was placed in the furnace atomizer, dried for 20 s (~130 °C) and "ashed" for 15 s (~450 °C). Atomization for 2.5 s (to 1450 °C) gave a strong non-atomic absorption which was studied in the range 194—325 nm.

Figure 1(a) shows the absorption spectrum obtained in this way, as well as spectra obtained by previous workers under different conditions. Koirtyohann and Pickett [19] obtained a vapour absorption spectrum from

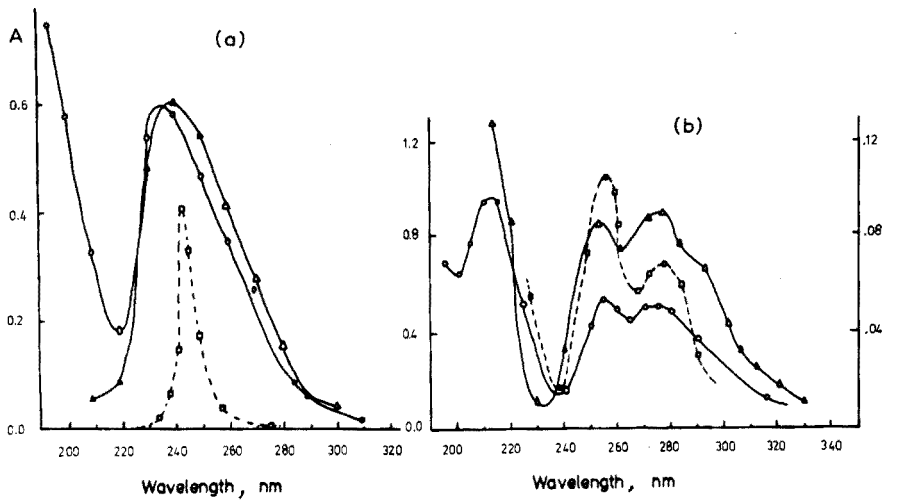

Fig. 1. Wavelength-dependence of non-atomic absorption of (a) NaCl and (b) KBr. (○) Vaporization by graphite tube furnace atomizer (this work); (△) long absorption-path burner (Koirtyohann and Pickett [19]); (□) graphite furnace (Muller [20]). Right-hand ordinate applies to KBr spectrum from Ref. 19.

NaCl solution (10000 μg Na ml^{-1}) aspirated into a hydrogen—oxygen flame with a long-path absorption tube. Earlier work on ultraviolet absorption spectra of alkali halide vapours [20, 21] made use of furnaces maintained at 800—1100 °C.

The general similarity of these spectra indicates that the rapid vaporization of sodium chloride from the graphite furnace under the conditions specified above leads to a high vapour-phase concentration of undissociated NaCl molecules, and the observed absorption can be identified as the charge-transfer spectrum [22] of this species. The spectrum of potassium bromide (Fig. 1(b)) obtained in the same way, shows a pair of peaks at 254 nm and 274 nm, the separation corresponding to that between the $^2P_{3/2}$ and $^2P_{1/2}$ state of the bromine atom, and a further peak at 212 nm, indicating the formation of some potassium ions in an excited state. Similar features can be seen in the spectrum of potassium iodide vapour [21, 23—25] obtained by various means.

If the atomizing conditions for sodium chloride are altered to give faster heating of the furnace (2.5 s to 1800 °C) the general shape of the absorption curve remains, but the peaks are broadened and the absorbances are greatly reduced at all wavelengths, indicating a lower vapour-phase concentration of NaCl molecules. The absorbance at a given wavelength and atomizing temperature is approximately a linear function of the amount of salt atomized. Figure 2 shows the absorbance at 250 nm obtained by atomizing 5 μl of various concentrations of NaCl and KBr aqueous solutions at 1800 °C from the three different types of atomizer. (Because the atomizers have different resistances, the voltage—temperature relation is different for each type, and

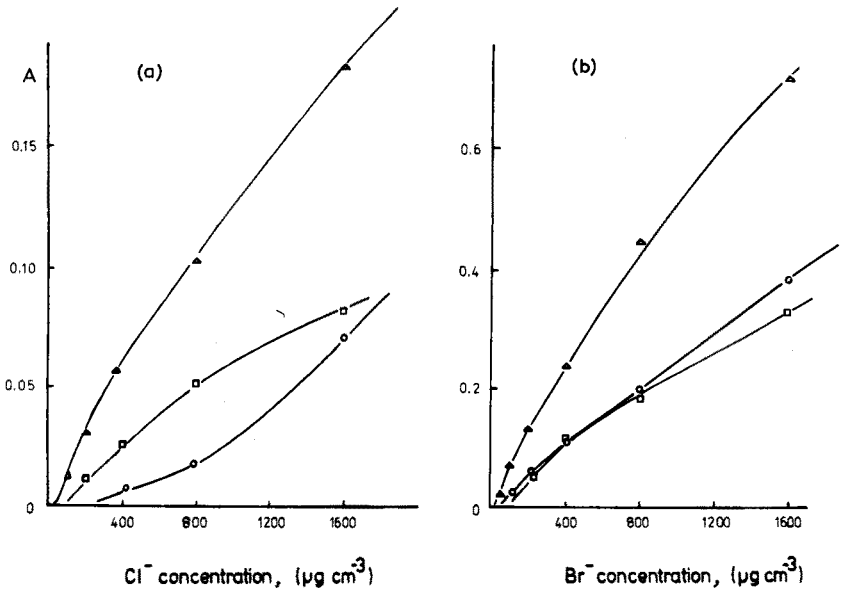

Fig. 2. Non-atomic absorption at 250 nm from different amounts of NaCl (a) and KBr (b) vaporized from furnace (△), cup (○), and rod (□) atomizers. Ashing temperature, 450 °C; atomizing temperature, 1800 °C.

appropriate voltage adjustments must be made to ensure that comparable temperatures are obtained). The higher absorbances obtained with the furnace and cup compared with the rod are probably the result of a greater effective path-length and greater residence time of the vapour in the optical path when these types of atomizer are used.

With ashing at 450 °C (15 s) and atomization at 1800 °C (2.5 s) the amounts of alkali halide at which a non-atomic absorption signal was first detected, with a hydrogen lamp at 250 nm, were as follows:

NaCl : 825 ng (rod), 1440 ng (cup), 250 ng (furnace)

KBr : 750 ng (rod), 187 ng (cup), 187 ng (furnace)

Visible smoke was also first detected at about these levels, indicating condensation of the vapour in the cooler environment away from the atomizer surface.

It is clear from Fig. 1 that molecular absorption rather than light scattering accounts for the major part of non-atomic absorption from alkali halides in furnace-type atomizers, at least at wavelengths above 200 nm. A similar conclusion was reached by Koirtyohann and Pickett [26] with respect to light losses caused by matrix salts (mainly alkali halides) when samples were atomized in a long-path burner. Under similar conditions of temperature and salt concentration, the non-atomic signals from the cup atomizer are similar to those from the furnace (Figs. 3(a), (b)).

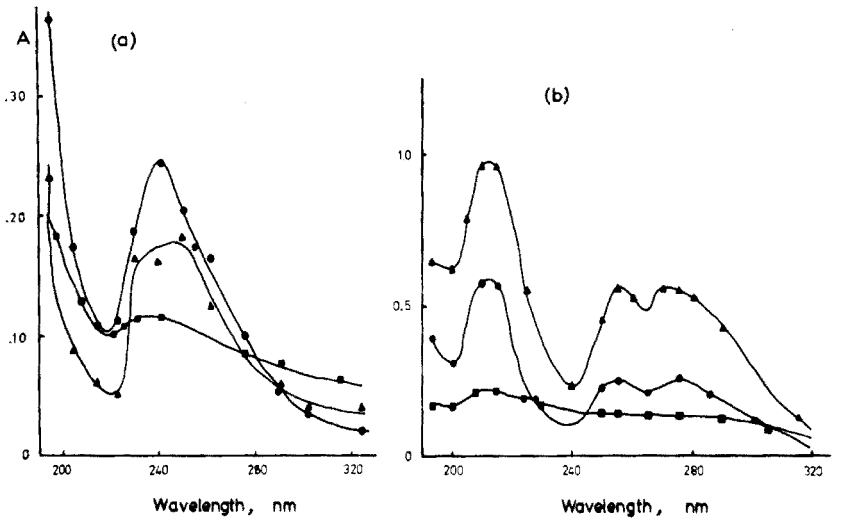

Fig. 3. Wavelength-dependence of non-atomic absorption using furnace (▲), cup (●), and rod (■) atomizers. Ashing temperature, 450 °C; atomizing temperature, 1800 °C. (a) 6.6 μg NaCl. (b) 6.0 μg KBr.

In the case of rod atomizers the non-atomic absorption is generally lower and the structure of the charge-transfer spectrum is almost completely lost, suggesting that light-scattering makes a relatively more important contribution to the non-atomic signal.

When larger amounts of sodium chloride (e.g. 80 μg) are volatilized from a rod at 1800 °C it is possible to detect radiation scattered during the vaporization process, with a hydrogen continuum source, maximum amplifier gain and a slit width of 300 μm (spectral bandpass 1.0 nm). Radiation scattered during the vaporization of a 5-μl sample of NaCl solution (10000 μg Cl ml^{-1}) was observed at 100 ° with respect to the source, this being a convenient angle at which to mount the source. The ratio of scattered radiation intensity to the measured incident radiation from the lamp was virtually constant over the whole wavelength range, as indicated in Table 1.

Scattering by particles much smaller in diameter than the wavelength of the radiation (Rayleigh scattering) shows an inverse fourth-power dependence

TABLE 1

Wavelength dependence of intensity of radiation scattered by volatilized NaCl

Wavelength (nm)	200	220	240	260	280	300	320
Intensity ratio[a]	0.26	0.27	0.29	0.29	0.29	0.26	0.25

[a]These ratios are only proportional to (scattered intensity)/(incident intensity) as different amplifier gains were used for the two sets of measurements.

on the wavelength, although additional criteria are needed to confirm the occurrence of Rayleigh scattering [27, 28]. In the present case, no such dependence is apparent down to 200 nm, either for the scattered radiation or for the non-atomic absorption from the rod atomizer. It appears, therefore, that most of the particles responsible for the scattering are at least comparable in diameter to the wavelength of the incident radiation.

The amount of sodium chloride used here is near the upper limit which would be encountered in analyses with flameless atomizers; amounts less than about 10 μg produced no detectable scattering signal, although strong broad-band absorption occurs at this level. (It would be possible to detect scattered radiation from smaller amounts with an optical system specifically designed for this purpose, but the results would have little relevance to atomic absorption measurements.)

In the optical path above the rod atomizer it is likely that particles occur with a wide range of sizes, from molecules to particles large enough to give a visible smoke and cause detectable light-scattering. The size distribution may depend on the total amount of salt vaporized, and is likely to be both temperature- and time-dependent, varying over the finite diameter of the light beam. We can find no evidence under any conditions for a sufficient population density of particles small enough for Rayleigh scattering to be the predominant cause of light losses.

Volatilization temperatures for NaCl and KBr

The rate of vaporization of sodium chloride from a graphite rod atomizer during an intermediate-temperature "ashing" stage was studied in the following way. A 5-μl sample of solution containing 13.2 μg of sodium chloride was placed on the rod, dried at about 110 °C and then "ashed" with a given voltage applied for 10 s. The rod was then removed and shaken for 3 min in 3 cm^3 of distilled deionized water. The resulting solution was analysed for sodium (flame photometry) and for chloride (chloride-ion electrode). The procedure was repeated at several different applied voltages, i.e. at different ashing temperatures.

The results are shown in Fig. 4. It is clear that very little loss of sodium chloride occurs below about 680 °C, that the loss of chloride parallels that of sodium, and that the loss of most of the 13.2 μg of sodium chloride occurs in 10 s at temperatures above 800 °C.

This situation can be examined in the manner used by L'vov [29] who applied the kinetic theory of gases to the calculation of vaporization rates of metals from atomizer surfaces. For a substance of molecular weight M and saturated vapour pressure P at temperature T, the mass G vaporized in vacuo per unit surface area per unit time is given by

$$G = P \frac{(M)^{\frac{1}{2}}}{(2\pi RT)^{\frac{1}{2}}}$$

L'vov [29] presents evidence that the rate of vaporization at 1 atmosphere pressure is about 60-fold lower than the rate in vacuo. By using this assumption, and the NaCl vapour pressure data of Zimm and Mayer [30] it can be calculated that G has the values 4.2 μg cm^{-2} s^{-1} at 953 K and 55 μg cm^{-2} s^{-1} at 1053 K. The rate of loss from the area of 0.035 cm^2 occupied by the sample after drying is therefore calculated to be 0.15 μg s^{-1} at 953 K and 1.9 μg s^{-1} at 1053 K. These rates are consistent with the observations shown in Fig. 4, i.e. that most of a 13.2 μg sample of sodium chloride is retained on the rod at 680 °C, significant losses occur above 700 °C, and the loss is almost complete at 800 °C. (Since the temperatures recorded in Fig. 4 are those reached at the end of 10 s, the rod has been close to this temperature for a rather shorter period than this.)

It is concluded that sodium chloride is vaporized in microgram amounts from a heated graphite surface in a few seconds at temperatures a little higher than 700 °C. The behaviour of the slightly more volatile potassium bromide is similar, comparable vaporization occurring at temperatures about 30 °C lower than those for sodium chloride.

Vaporization of small amounts of many inorganic halides can occur at temperatures well below their melting points. This point is significant in any discussion of the behaviour of matrix salts in real samples atomized with flameless atomizer systems, and also emphasizes the danger of analyte loss during attempts to separate inorganic matrix salts in the ashing stage. Further work is being carried out on the pre-atomization behaviour of salts of other

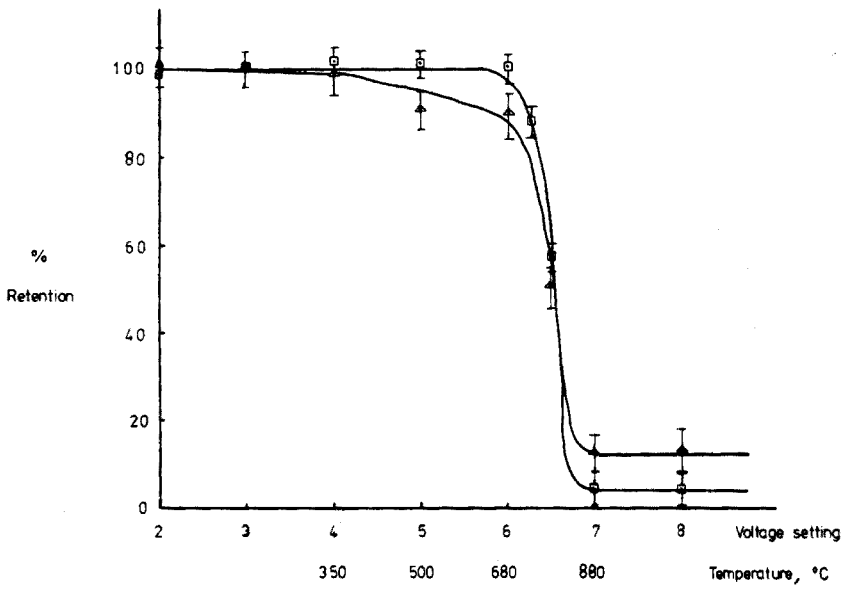

Fig. 4. Loss of NaCl during ashing for 10 s at various applied voltages (final atomizer temperature also shown). (□) Na. (△) Cl.

metals, and indicates that a variety of processes, including hydrolysis and solid-state decomposition, may be important in different cases.

The support of the University Grants Committee for the purchase of the graphite atomizer system is gratefully acknowledged.

REFERENCES

1 M. D. Amos, P. A. Bennett, K. G. Brodie, P. W. Y. Lung and J. P. Matousek, Anal. Chem., 43 (1971) 211.
2 M. T. Glenn, J. Savory, L. P. Hart, T. H. Glenn and J. D. Winefordner, Anal. Chim. Acta, 57 (1971) 263.
3 E. Norval and L. R. P. Butler, Anal. Chim. Acta, 58 (1972) 47.
4 M. T. Glenn, J. Savory, S. A. Fein, R. D. Reeves, C. J. Molnar and J. D. Winefordner, Anal. Chem., 45 (1973) 203.
5 F. S. Chuang, B. M. Patel, R. D. Reeves, M. T. Glenn and J. D. Winefordner, Can. J. Spectrosc., 18 (1973) 6.
6 J. W. Robinson, D. K. Wolcott, P. J. Slevin and G. D. Hindman, Anal. Chim. Acta, 66 (1973) 13.
7 R. T. Ross and J. G. Gonzalez, Anal. Chim. Acta, 63 (1973) 205.
8 D. A. Segar and J. G. Gonzalez, Anal. Chim. Acta, 58 (1972) 7.
9 M. P. Bratzel, C. L. Chakrabarti, R. E. Sturgeon, M. W. McIntyre and H. Agemian, Anal. Chem., 44 (1972) 372.
10 W. M. Edmunds, D. R. Giddings and M. Morgan-Jones, Perkin-Elmer At. Absorption Newslett., 12 (1973) 45.
11 S. Omang, Anal. Chim. Acta, 56 (1971) 470
12 K. G. Brodie and J. P. Matousek, Anal. Chem., 43 (1971) 1557.
13 R. D. Reeves, C. J. Molnar, M. T. Glenn, J. R. Ahlstrom and J. D. Winefordner, Anal. Chem., 44 (1972) 2205.
14 R. D. Reeves, C. J. Molnar and J. D. Winefordner, Anal. Chem., 44 (1972) 1913.
15 J. F. Alder and T. S. West, Anal. Chim. Acta, 58 (1972) 331.
16 P. Schramel, Anal. Chim. Acta, 67 (1973) 69.
17 C. J. Molnar, R. D. Reeves, J. D. Winefordner, M. T. Glenn, J. R. Ahlstrom and J. Savory, Appl. Spectrosc., 26 (1972) 606.
18 J. P. Matousek and K. G. Brodie, Anal. Chem., 45 (1973) 1606.
19 S. R. Koirtyohann and E. E. Pickett, Anal. Chem., 37 (1965) 601.
20 L. A. Müller, Ann. Phys. (Leipzig), 82 (1927) 39.
21 J. Franck, H. Kuhn and G. Rollefson, Z. Phys., 43 (1927) 155.
22 L. E. Orgel, Quart. Rev., Chem. Soc. 8 (1954) 422.
23 S. R. Koirtyohann and E. E. Pickett, Anal. Chem., 38 (1966) 585.
24 T. Takeuchi, M. Yanagisawa and M. Suzuki, Talanta, 19 (1972) 465.
25 B. V. L'vov, Spectrochim. Acta, 24B (1969) 53.
26 S. R. Koirtyohann and E. E. Pickett, Anal. Chem., 38 (1966) 1087.
27 N. Omenetto, L. P. Hart and J. D. Winefordner, Appl. Spectrosc., 26 (1972) 612.
28 P. L. Larkins and J. B. Willis, Spectrochim. Acta, 29B (1974) 319.
29 B. V. L'vov, Spectrochemical Analysis by Atomic Absorption, Israel Programme for Scientific Translations, 1969, pp. 176—8.
30 B. H. Zimm and J. E. Mayer, J. Chem. Phys. 12 (1944) 362.

Analytica Chimica Acta, 82 (1976) 113—119

DETERMINATION OF MANGANESE(II) IN POWDERED BARNACLE SHELLS BY ELECTRON PARAMAGNETIC RESONANCE

STUART C. BLANCHARD and N. DENNIS CHASTEEN

Department of Chemistry, University of New Hampshire, Durham, New Hampshire 03824 (U.S.A.)

(Received 24th June 1975)

SUMMARY

A rapid precise method of determining Mn(II) (as opposed to total manganese) in powdered barnacle shells by e.p.r. is described. The method is based on the linear relationships between the intensity of the first-derivative e.p.r. signal and the weight and Mn(II) concentration in the sample. Atomic absorption was used as a reference method. For eleven samples, the difference between the a.a.s. and e.p.r. methods was, on average, within 3 %; the detection limit was 20 p.p.b. A good correlation between the Mn(II) content of the shell and the position of the animal in an inter-tidal zone was found.

Recently, there has been considerable interest in trace metal analysis of marine systems [1—9]. The exoskeletons of shellfish contain varying amounts of trace metals such as Cu, Cr, Cd, Fe, Mg, Mn, Mo, Ni, Pb, V, Zn, and others. In several instances it appears that the trace metal content is related to the environment of the animal [2, 3, 7—9]. Of the metals mentioned above, manganese is of interest since it is often found to range from less than 1 $\mu g\ g^{-1}$ to greater than 3000 $\mu g\ g^{-1}$ in shellfish exoskeletons, such as barnacles, of the same species [1—3, 5]. The manganese content of the barnacle shell correlates directly with the height of the animal above low tide in an inter-tidal zone [2] and inversely with the salinity of the sea water in an estuarine environment [3].

To date, the analytical techniques employed most frequently for trace metals in shells have been atomic absorption (a.a.s.) [2, 7, 8] and neutron activation [3, 6]. Analysis for manganese by a.a.s. requires the preparation of filtered acidic solutions and suffers from calcium interference (vide infra). Neutron activation analysis (n.a.a.) for manganese utilizes powdered samples; however, access to a nuclear reactor is necessary and "cooling off" periods of 28 d can be required [6].

Electron paramagnetic resonance (e.p.r.) techniques have been developed for the quantitative determination of free Mn(II) in aqueous solution [10—15]. In principle, these could be used to determine Mn(II) in shells, although filtered acidic solutions would still be required. Powdered samples

of shells exhibit intense resonances attributable to Mn(II) substituted for Ca(II) in the $CaCO_3$ lattice (Fig. 1).

This paper reports a method of determining Mn(II) (as opposed to total manganese) in powdered barnacle shells. By weighing the samples in quartz tubes and positioning them carefully in the e.p.r. cavity, the concentration of Mn(II) can be determined from the linear relationship between the intensity of the first-derivative e.p.r. signal and the weight and concentration of Mn(II) in the sample. This technique should be applicable to other shellfish.

EXPERIMENTAL

Five samples of barnacles (*Balanus balanoides*) were collected at Rye North Beach, New Hampshire, from rocks located at five different levels above low tide and labeled as RN001-RN005. Not less than 25 barnacles were pooled to constitute each sample. Animal and other organic matter was removed by boiling the shells in 2.5 % NaOH solution for 15 min, followed by rinsing with several liters of distilled water. The shells were dried at room temperature. Each sample was ground to a fine powder and stored over calcium chloride desiccant. Portions of RN003 powder were immersed in 2.5 % NaOH for 20 min at room temperature, boiled for 15 and 30 min in 2.5 % NaOH, rinsed, dried, and analyzed by e.p.r. to check for possible oxidation of the Mn(II) during the sodium hydroxide treatment. No oxidation was detected.

The analysis for manganese was performed on a Techtron AA-3 instrument, equipped with time-averaging digital read-out, an air—acetylene flame and 100 μm slit, at 279.68 nm [16].

Two solutions of each sample were prepared by weighing ca. 0.5-g samples of the powder into polypropylene beakers, adding water to make a slurry, followed by sufficient 1 M HCl to dissolve the powder. The solution was filtered through a medium porosity sintered glass crucible to remove insoluble

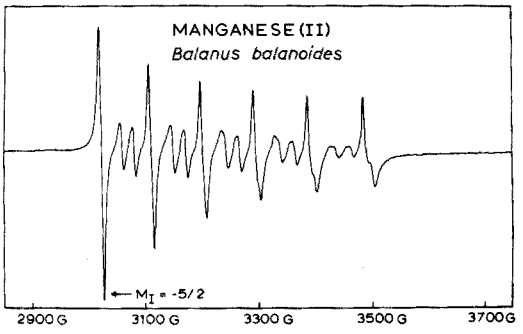

Fig. 1. Room-temperature manganese(II) spectrum of powdered barnacle shell. Power = 20 m W, modulation amplitude = 1.0 G.

proteins from the organic shell matrix, diluted to 50.0 ml with 1 M HCl and stored in acid-washed polypropylene bottles. Standards in the range 0.2—2.0 p.p.m. were prepared from 1000 p.p.m. Mn (Harleco standard) by dilution with 1 M HCl. Samples for standard addition analysis were prepared by adding μl quantities of the 1000-p.p.m. standard to three aliquots (10 ml) of each sample. Random tests with 1 sample replication and 1 instrumental replication demonstrated that sample preparation and instrumental errors were of the same magnitude, the total error being 2—3 % for the analysis by a.a.s.

The quantitative e.p.r. analyses were done with a Varian E-4 single-cavity spectrometer operating at X-band (9.5 GHz) and 100-KHz magnetic field modulation. The g-value and line-width measurements, and the power-saturation and modulation-amplitude effects, were measured on a Varian E-9 dual cavity spectrometer. Strong pitch (g = 2.0028) was used as a g-mark. Both instruments were tuned and operated as recommended by the manufacturer. All samples were placed in selected quartz tubes, 4.00 ± 0.05 mm o.d., and carefully blow-sealed to have uniform, rounded bottoms.

Quartz tubes filled with each sample were analyzed by placing them in a quartz dewar flask in the cavity, tuning the instrument (20 mW power, 1.0 G modulation amplitude) scanning the −5/2 line (1000G/16 min, time constant 0.3 s) and measuring the first-derivative peak-to-peak signal height. Sample RN005 was removed from the tube, ground to a finer powder, returned to the tube, and rescanned to check for reproducibility of sample loading.

For the weighed samples, quartz tubes containing 10—30 mg of the powder were positioned in the cavity by positioning the dewar flask so that the bottom of the quartz tube was 2.5 mm below the center of the cavity; this adjustment was facilitated by marks on the outside of the dewar.

A standard e.p.r. signal *versus* weight curve was obtained for three different weights (10—30 mg) of sample RN002, scanning the −5/2 line as described above. The other samples were run randomly with 1 sample replication and 1 instrumental replication to check for sample preparation and instrumental reproducibilities.

The RN002 sample was assumed to have the concentration of manganese found by a.a.s. The Mn(II) content of the other samples was calculated from the e.p.r. intensity versus weight curve for the standard RN002.

RESULTS AND DISCUSSION

Linear calibration and standard addition curves were obtained for the analyses by a.a.s., but the results calculated from the standard addition curves were up to 10 % higher (Table 1). Analyses of manganese solutions with and without calcium indicated that this resulted from a calcium interference.

Pilkey and Harriss [2] observed that barnacle shells collected at increasing levels above low tide contained increasing concentrations of

TABLE 1

Summary of results for manganese in Rye North Beach samples

Sample	Height (m)	A.a.s. (p.p.m.)[a]		E.p.r. (p.p.m.)[b]		Linewidth[c]	g-value
		A	B	C	D		
RN001	0.0[d]	56 ± 2[e]	62 ± 2[e]	62[f]	61 ± 2[e]	8.30 ± 0.02[e]	2.0011 ± 0.0003[e]
RN002	0.4	64	67	75	67[f]	8.30	2.0008
RN003	1.0	77	83	85	84	8.32	2.0005
RN004	1.7	75	73	59	75	8.36	2.0008
RN005	2.0	88	94	76	78	8.38	2.0008

[a]Columns A and B give the results obtained by the calibration curve and standard addition method, respectively.
[b]Columns C and D give the results obtained by full-tube e.p.r. and weighed e.p.r., respectively.
[c]Peak-to-peak in G.
[d]0.0 m is the observed low tide for June 15, 1974, P.M.
[e]Standard deviation
[f]Based on standard addition a.a.s. value.

manganese, and this was also observed with our samples (Table 1). A plot of the manganese content versus height above low tide gave a correlation coefficient of 0.808 (Fig. 2). The concentrations are lower and the range less than that reported by Pilkey and Harriss [2]. This may result from differences in the salinities of the locations; Rye North Beach is open to the ocean while the locations of Pilkey and Harriss were in an estuary [3].

Figure 1 shows a typical manganese spectrum for powdered barnacle shell. The *g*-value of 2.0008 ± 0.0003 and the hyperfine splitting of −93.8 ± 0.2 G correspond well with those of Mn(II) substituted for Ca(II) in a calcite ($CaCO_3$) lattice [17]. The species detected by e.p.r. is therefore Mn(II), as

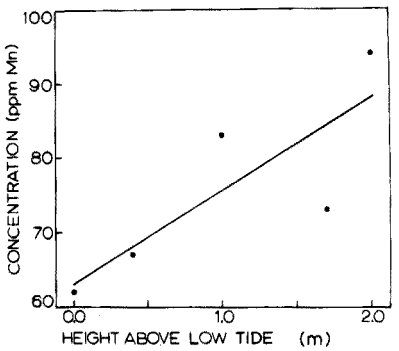

Fig. 2. Correlation of the total manganese content of the shell with the height of the animal above low tide (0.0 m). The linear least-squares line having a correlation coefficient of 0.808 is shown.

opposed to the total manganese content, which would include other oxidation states if present.

The power saturation and modulation amplitude effects on the e.p.r. signal for the $-5/2$ line, obtained in the usual manner [18] (Fig. 3), indicated that at 20 mW power and 1G modulation amplitude the lines were not being partially saturated nor overmodulated. (Subsequent work demonstrated that quantitative analysis at 200 mW and 10.0 G modulation amplitude was also possible, even though the resonance line is distorted under these conditions.)

For the e.p.r. analysis with full tubes, the results were in general agreement with the a.a.s. values (Table 1). Emptying a tube, regrinding the sample to a finer powder, and refilling the tube, gave results, however, that were up to 40 % lower than the original sample. This is attributed either to a decrease in the amount of sample (the finer powders are "fluffy" and do not pack well), or to partial oxidation of Mn(II) by air to give an e.p.r.-silent species.

Since the full tubes are subject to large error, a method of analysis was developed which is essentially free of this problem and is also capable of analyzing much smaller samples.

A profile of microwave intensity against vertical position in the cavity was obtained from the E-4 operation manual (Fig. 4(a)). For a sample positioned over a vertical range the signal intensity was taken to be proportional to the

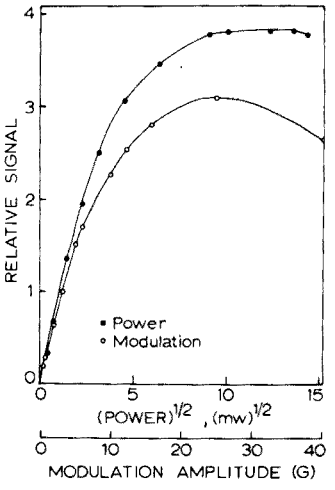

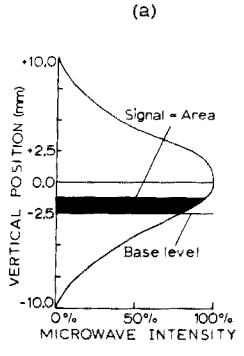

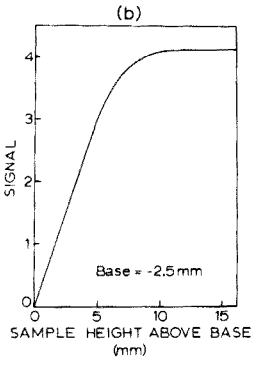

Fig. 3. Power saturation and modulation amplitude curves. The power curve is linear from 0 to 20 mW ((power)$^{\frac{1}{2}}$ = 4.5) and the modulation amplitude curve is linear from 0 to 4 G.

Fig. 4. Microwave intensity profile for the E-4 cavity. The area under the portion of the curve filled by "sample" was taken to be proportional to the signal. Increasing heights of "sample" above -2.5 mm gave the signal versus weight shown to the right.

area under the microwave intensity profile. By selecting base levels (i.e. position of the bottom of the e.p.r. tube) in the cavity and filling the vertical region above that point with increasing "sample" heights and measuring the area under the curve, plots of a signal height against "sample" height could be obtained. That shown in Fig. 4(b) is for a base level (tube bottom) of 2.5 mm below the center of the cavity and is linear up to 5 mm above the base level. This linear range corresponds to sample weights of 0—44 mg. Curves similar to those shown in Fig. 4 were obtained experimentally. Thus for samples in uniform tubes, placed between −2.5 and +2.5 mm in the cavity, the signal is directly proportional to the samle weight and to the concentration of Mn(II).

This relationship may be expressed as

$$\mathrm{Mn(II)}_u = \mathrm{Mn(II)}_k \times \frac{S_u(G_k \times Wt_k)}{S_k(G_u \times Wt_u)} \quad (1)$$

where S is the peak-to-peak e.p.r. signal height, G is the spectrometer gain, Wt is the sample weight, and the subscripts u and k refer to unknown and known respectively. The slope of the linear calibration plot may be substituted, giving

$$\mathrm{Mn(II)}_u = \mathrm{Mn(II)}_k \times S_u/(\mathrm{slope} \times G_u \times Wt_u) \quad (2)$$

The results for the Rye North Beach samples are shown in Table 1. Another series of samples was collected from a piling at Gerrish Island, Maine and analyzed by the standard addition a.a.s. and weighed e.p.r. methods. Table 2 shows two sets of results for the weighed samples. The first are based on standard addition a.a.s. for the Gerrish Island sample GE01; the second are based on a standard curve for RN001, which appears to be the better standard (as will be discussed later). The difference in the results is probably due to the presence of e.p.r.-silent manganese in most of the Gerrish Island

TABLE 2

Summary of results for manganese in Gerrish Island samples

Sample	Height (m)	Standard addn. a.a.s. (p.p.m.)	Weighed e.p.r. (p.p.m.)	Weighed e.p.r. (p.p.m.)
GE01	0.0[a]	65	65[b]	60[c]
GE03	0.4	68	73	68
GE05	0.8	88	88	81
GE07	1.2	79	78	72
GE09	1.6	78	73	68
GE11	2.0	82	76	71

[a] 0.0 m is the observed low tide.
[b] Based on standard addition a.a.s. for GE01.
[c] Based on a standard curve for RN001 similar to that for RN002 in eqn. (2).

samples.

The particularly low e.p.r. results for samples RN005 (Table 1), GE09, and GE11 (Table 2) appear to be real differences between the total manganese content determined by a.a.s. and the e.p.r.-detectable Mn(II). This probably reflects the fact that the environment differs from that of the others. These samples spend the greatest amount of time out of water. Excluding the three low results, the weighed e.p.r. samples agree with the a.a.s. results to within 3 % on average, and are reproducible to within 3 %.

Thus e.p.r. can provide rapid and accurate analyses of Mn(II) in powdered barnacle shells, with a precision and accuracy comparable to that of a.a.s. The detection limit, defined as the concentration at which the signal-to-noise ratio becomes 2 : 1, is 20 p.p.b. at 20 mW and 1.0 G modulation amplitude for a 10-mg sample. The sample preparation time is shorter, requiring fewer steps; with practice, 7 samples per hour, including weighing time, can be analyzed. The only disadvantage is that the manganese content of at least one sample must be determined previously by another method, preferably specific for Mn(II). It is necessary to assume that all manganese in the low tidal level reference sample is Mn(II); this appears to be valid, as only the samples collected at the highest levels above low tide show differences between the a.a.s. (total Mn) and e.p.r. (Mn(II)) methods. This approach might be useful in investigating trace metals in other natural samples.

Acknowledgement is made to the Central University Research Fund of the University of New Hampshire, and the National Science Foundation, Grant #MPS 7503474, for support.

REFERENCES

1 R. R. Brooks and M. G. Rumsby, Limnol. Oceanogr., 10 (1965) 521.
2 O. H. Pilkey and R. C. Harriss, Limnol. Oceanogr., 11 (1966) 381.
3 C. M. Gordon, R. A. Carr and R. E. Larson, Limnol. Oceanogr., 15 (1970) 461.
4 J. H. Martin, Limnol. Oceanogr., 15 (1970) 756.
5 W. E. Segar and J. P. Riley, J. Mar. Biol. Ass. U.K., 51 (1971) 131.
6 K. K. Bertine and E. D. Goldberg, Limnol. Oceanogr., 17 (1972) 877.
7 R. W. Ferrill, T. E. Carville and J. D. Martinez, Environ. Lett., 4 (1973) 311.
8 D. L. Graham, Veliger, 14 (1972) 365.
9 M. Schulzba, Marine Biol., 21 (1973) 98.
10 G. G. Guilbault and G. J. Lubrano, Anal. Lett., 1 (1968) 725.
11 G. G. Guilbault and T. Meisel, Anal. Chem., 41 (1969) 1100.
12 G. G. Guilbault and T. Meisel, Anal. Chim. Acta., 50 (1970) 151.
13 G. G. Guilbault and E. S. Mayer, Anal. Chem., 42 (1970) 441.
14 E. S Moyer and J. W. McCarthy, Anal. Chim. Acta, 48 (1969) 79.
15 E. E. Angino, L. R. Hathaway and T. Worman, Identification of Manganese in Water Solutions by e.p.r. Nonequilibrium Systems in Natural Water Chemistry, Advances in Chemistry Series #106, Amer. Chem. Soc., Washington, D.C., 1971.
16 J. E. Allen, Spectrochim. Acta, 15 (1959) 800.
17 T. R. Wildeman, Chem. Geol., 5 (1969) 167 and references therein.
18 C. P. Poole, Jr., Electron Spin Resonance, Interscience, New York, 1967, pp. 707—708.

Analytica Chimica Acta, 82 (1976) 121—135

INTRA-ELEMENTAL PHOTOELECTRON LINE INTENSITIES AND THEIR SIGNIFICANCE TO QUANTITATIVE ANALYSIS

MARTTI VULLI, MORTEZA JANGHORBANI* and KURT STARKE
F.B. 14, Kernchemie, Philipps-Universität, Marburg-Lahn (Germany)
(Received 5th September 1975)

SUMMARY

Intraelemental relative photoelectron line intensities for 20 pure elements obtained under ultrahigh vacuum ($5 \cdot 10^{-9}$ torr) and high resolution with cleaned surfaces are presented. Theoretical and experimental aspects of relative photoelectron line intensities as well as other characteristics of significance to quantitative analysis are discussed. Experimental data are related to theoretical results and compared with other recent work.

X-Ray photoelectron spectroscopy (x.r.p.s., or e.s.c.a.) has been widely employed for molecular and surface studies, whereas its development as a quantitative tool for analysis is still in its infancy. Wagner [1] was the first to measure e.s.c.a. signal strengths of various elements in different compounds and has shown a monotonously increasing sensitivity as a function of atomic number. Berthou and Jorgensen [2] have compared relative line intensities obtained with Al—Kα and Mg—Kα as excitation sources. Attempts to demonstrate the feasibility of this method for the quantitative determination of lead at trace levels have been made [3, 4]. The quantitative theory of x.r.p.s. is well understood in terms of atomic cross-sections and absorption-edge jump ratios, having been carried over from the more complicated case for x-ray fluorescence analysis [5]. From this theory and the compilation of x-ray cross-sections [6], it is possible to calculate relative inter- and intra-elemental photoelectron line intensities for various elements. In addition, linewidths, effects of surface contamination and matrix on line intensities, as well as other fundamental data must become available if e.s.c.a. is to develop into a quantitative analytical tool.

The purpose of this work has been two-fold: (1) to compile a reference list of intra-elemental relative intensities of photoelectron lines, comparing the experimental measurements with theoretical calculations where possible; and (2) to study the characteristics of each photoelectron line, determining its suitability for quantitative analysis, and testing the feasibility of argon-ion bombardment for cleaning the sample surface for various elements.

---

*To whom correspondence should be directed. Permanent address: Environmental Trace Substances Research Center, Route 3, Columbia, Mo, 65201, U.S.A.

THEORY

If a monoelement sample is irradiated with monochromatic x-radiation, the observed intensity of individual photoelectron lines, $I_{e,d}$, is described by the following approximate relationship [7]:

$$I_{e,d} = k\tau(1 - 1/J_i)\,(1 - \exp(-\csc\phi \cdot \mu_i \rho t))/\mu_i \qquad (1)$$

For the purpose of this discussion, eqn. (1) can be conveniently subdivided into three parts.

1. The parameter k which is only instrument-dependent. It includes such factors as the angle subtended by sample towards both x-ray source and electron analyzer, through-put and detector efficiency for the photoelectron line of interest, instrument geometry, and primary source intensity.
2. The product $\tau(1 - 1/J_i)$, in which τ is the total photoelectric cross-section of the level of interest and all lower (binding) energy atomic levels ($cm^2\ g^{-1}$) [8], and J_i is the absorption-edge jump ratio of the level of interest. The magnitude of this depends on the nature of atoms being analyzed, the specific photoelectron lines of interest, and the energy of exciting radiation, but is independent of sample thickness.
3. The ratio $(1 - \exp(-\csc\phi \cdot \mu_i \rho t))/\mu_i$, where ϕ is the angle between the sample surface and the analyzer, μ_i the mass absorption coefficient of the element for photoelectrons of interest ($cm^2\ g^{-1}$), ρ the sample density ($g\ cm^{-3}$), and t the sample thickness (cm). The magnitude of this ratio depends not only on the nature of atoms, energy of photoelectrons, and excitation energy, but also strongly on sample thickness. The existence of this factor may result in large variations in recorded relative intensities of photoelectron lines of widely differing kinetic energy with varying sample thickness.

The concentration-dependent ratio, G, of any two intraelemental photoelectron line intensities is given by:

$$G = (1 - E_1)\mu_2/(1 - E_2)\mu_1 \qquad (2)$$

where $E = \exp(-\csc\phi \cdot \mu\rho t)$, and subscripts 1 and 2 refer to the two photoelectron lines of the same element. It is quite clear that G approaches the ratio of the two mass absorption coefficients asymptotically as the condition of "infinite thickness" is approached; and unity at the other extreme of thickness. This behavior is shown in Fig. 1 for two electron lines having kinetic energies of 72 and 1403 eV for a gold matrix (the data for electron absorption coefficients are from ref. 9). The consequence of this behavior from the point of view of quantitative analysis is that a low kinetic energy line having high intensity at low concentrations compared to a high kinetic energy line, will exhibit relatively low intensity at higher sample thicknesses. Therefore, in selecting the analytical lines to be used, one should take into account not only the effective atomic cross-sections, i.e. the product $\tau(1 - 1/J_i)$, but also the effect of sample thickness, when considering photoelectron lines of widely differing kinetic energy. A knowledge of

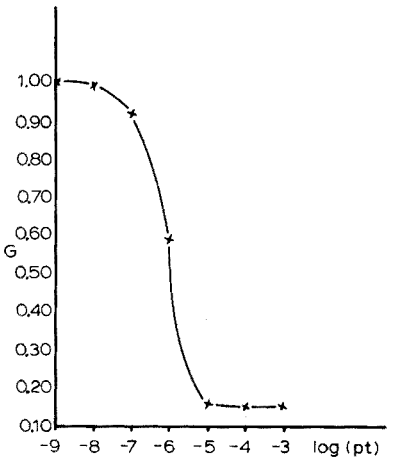

Fig. 1. Effect of concentration on the ratio $\mu_{e,1403}(1 - \exp(-\csc\phi \cdot \mu_{e,72}\rho t))/\mu_{e,72}(1 - \exp(-\csc\phi \cdot \mu_{e,1403}\rho t))$ for two electron lines with kinetic energy 1403 and 72 eV in gold.

mass absorption coefficients of electrons in the energy range of interest for x.r.p.s. will enable evaluation of this effect via eqn. (2). Unfortunately, sufficient reliable data for this purpose do not exist at the present time (see ref. 9 for a summary of data). For close lying photoelectron lines (e.g. the series L_1 to L_3) the differences in the mass absorption coefficients are very likely not great enough to offset the larger effect of effective cross-sections.

The product $\tau(1 - 1/J_i)$ should be the determining factor in the relative intensities of electron lines within a series such as the L-lines. Unfortunately, the compilation of x-ray cross-sections [6] does not include the photoelectric absorption cross-section data for lines whose absorption edges fall below 1 keV, and thus calculation of the effective cross-sections for many lines excited with Al—Kα or Mg—Kα cannot be carried out from reliable data. For elements for which data have been compiled [6], the effective cross-sections calculated with the extrapolation of Giauque et al. [8] and Al—Kα as excitation radiation are given in Table 1. These data clearly show that for the L-series, the most intense line should be L_3, and for the M-series, M_5. Comparison between the L- and M-series for Al—Kα cannot be carried out because of lack of data, but when 10 keV is used as excitation energy, the values placed between parentheses in Table 1 are obtained. It is evident that, in all cases L_3 lines should be more intense than M_5 lines. However, the differences in kinetic energies of the two levels are greater than 5000 eV, and the extent of self-absorption for L_3-lines should therefore be substantially greater than that for M_5 lines. It is quite probable that similar behavior is also operative at the excitation energies employed in x.r.p.s. This would then mean that in cases where both L_3 and M_5-lines can be excited,

TABLE 1

Product $\tau(1 - 1/J_i)$ for some L- and M-lines[a]

Element	Z	$\tau(1 - 1/J_i)$, barns/atom x10^5							
		L_1	L_2	L_3	M_1	M_2	M_3	M_4	M_5
Zn	30	0.8	1.4	2.9					
Ga	31	1.0	1.7	3.3					
Ge	32	1.1	2.0	3.9					
As	33		2.0	4.0					
Se	34		2.3	4.7					
Ba	56				0.7	1.0	2.0		
La	57				0.8	1.2	2.1		
Ce	58				0.8	1.3	2.3		
Nd	60					1.4	2.6		
Pm	61			(22.7)					(4.4)
Sm	62			(24.4)			4.3	4.8	7.4(5.2)
Eu	63			(25.3)					(4.7)
Gd	64			(27.1)				5.1	8.1(5.2)
Tb	65			(31.6)					(5.3)
Dy	66			(31.8)				5.6	9.1(5.5)
Ho	67			(34.5)					(6.0)
Er	68			(39.5)				6.1	10.9(7.2)
Tm	69			(38.2)					(7.0)
Y	70			(36.7)					(6.6)

[a]Data in parentheses are for 10-keV excitation source, others for Al—Kα.

their expected relative intensities cannot be compared without including the effect of self-absorption. This effect may become even more significant in comparisons of electron levels with principal quantum numbers greater than 3 which are often the levels encountered in x.r.p.s. of high-Z elements.

Actual measurement of intra-elemental relative peak intensities for different sample thicknesses is quite difficult for the range of interest in x.r.p.s. because of difficulties associated with sample preparation, whereas measuring the relative intensities of "infinitely thick" samples is not. The expression relating the relative intensities of any two intra-elemental electron lines at any given sample thickness t to that for an "infinitely thick" sample is:

$$I_{e,d,t,1}/I_{e,d,t,2} = (I_{e,d,\infty,1})\ (1 - \exp(-\csc\phi \cdot \mu_1 \rho t))/(I_{e,d,\infty,2})\ (1 - \exp(-\csc\phi \cdot \mu_2 \rho t)) \quad (3)$$

Thus, when the ratio $I_{e,d,\infty,1}/I_{e,d,\infty,2}$ has been measured and the values of μ_1 and μ_2 are known, the expected relative intensities of the two lines can easily be calculated at any sample thickness. This would enable one to know which lines should be sought if the approximate concentration to be expected is known, or when the most intense line cannot be used because of some interference.

It should be emphasized that the above equations are applicable only when

photoelectron peak areas are used, especially in comparisons of electron lines having widely different peak widths. Furthermore, these relations hold only for a monoelement sample. When relative intensities of elements in different compounds are measured, more complicated relations are involved; and basically comparable results from different compounds should not necessarily be expected.

EXPERIMENTAL

Materials

Purity and mode of sample preparations used are given in Table 2.

Instrumentation

The instrument employed was a Vacuum Generator ESCA 3 equipped with sample preparation chamber attached to the ultrahigh vacuum, retarding potential, hemispherical analyzer. In the measurements, the analyzer operating pressure was better than $5 \cdot 10^{-9}$ torr, and that for the sample

TABLE 2

Elemental preparation data

Element	Purity[a]	Preparation
Na	CP	Piece cut from preserved specimen
Mg	CP	Ev[b]., W-coil, $1 \cdot 10^{-6}$
Al	99.99	Ev., W-coil, $5 \cdot 10^{-6}$
V	CP	Sheet
Mn	CP	Ev., Ta-boat, $5 \cdot 10^{-7}$
Ni	99	Ev., W-coil, $3 \cdot 10^{-6}$
Cu	RG	Ev., W-coil, $8 \cdot 10^{-7}$
Zn	99.99	Ev., Ta-coil, $5 \cdot 10^{-7}$
Ge	99	Ev., W-boat, evaporated on Ta-sheet, 3×10^{-5}
Y	99.9	Sheet
Ag	CP	Ev., W-coil, $4 \cdot 10^{-7}$
In	RG	Ev., Ta-boat, $1 \cdot 10^{-6}$
Sb	CP	Ev., Ta-coil, $7 \cdot 10^{-7}$
Ba	99.5	Ev., W-coil, $3 \cdot 10^{-7}$
Ta	EG	Sheet
W	EG	Sheet
Au	99.99	Ev., W-coil, $1 \cdot 10^{-7}$
Pt	EM	Sheet
Pb	99.99	Sheet
Bi	CP	Ev., Ta-boat, $5 \cdot 10^{-7}$

[a]CP: chemically pure; RG: reagent grade; EG: evaporating grade; EM: electrochemical grade.
[b]Ev.: evaporated, with conditions as indicated.

preparation chamber was $5 \cdot 10^{-6}$ torr or better. FWHM of the Au4f7/2 was 1.3 eV. The following settings were maintained during the entire work: x-ray tube at 12 kV and 40 mA, analyzer hemisphere energy at 20 eV, both slits at 2 mm, scan rate at 33 mV s^{-1}, electron multiplier at 3.8 kV, and ratemeter time constant at 3.3 s.

Procedure

In the main experiments, the sample was either sheet cleaned with ethanol or evaporated onto the sample holder tip in the sample preparation chamber of the instrument (Table 2). It was then bombarded with argon ions — typically at 6 kV, 20—25 μA, 1—10 min — and transferred immediately to the analyzer. Immediately, a 1000-eV scan (at 3.3 V s^{-1}) was made to detect any contamination and measure their peak height ratios to that of the most prominent elemental peak (Table 3), and soon thereafter, the spectrum of each line was recorded for all lines of interest in a sequential manner; the sequence was repeated 3—6 times in order to determine residual gas readsorption effect. Peak areas were calculated from the height and the FWHM of the peaks. Total recording time for each element was typically 2 h.

The effect of repetitive argon-ion bombardment on the relative peak

TABLE 3

Ratio of O1s1/2 and C1s1/2 peak heights to the most prominent line of the element immediately after ion bombardment

Element and line	O1s1/2	C1s1/2
	Element line	Element line
Na 1s1/2	0.2	0.01
Mg 1s1/2	0.05	ND[a]
Al 2s1/2	0.6	0.1
V 2p3/2	0.3	ND
Mn 2p3/2	0.09[b]	ND
Ni 2p3/2	0.02	ND
Cu 2p3/2	ND[a]	0.01
Zn 2p3/2	ND	ND
Ge 2p3/2	0.09[b]	0.06[b]
Y 3p3/2	2	1
Ag 3d5/2	ND	0.06[b]
Sb 3d5/2	ND	ND
Ba 3d5/2	0.18[b]	ND
Ta 4d5/2	0.7	ND
W 4d5/2	0.14[b]	0.14[b]
Pb 4d5/2	ND	ND
Bi 4d5/2	ND	ND

[a]ND: not detected.
[b]Ratio is for sample before sputtering.

intensities of lead was studied by bombarding the sample four times (4.5-kV accelerating voltage, 20-μA ion current, 1-min duration) and recording line intensities at the end of each bombardment. For the seven most prominent peaks of lead, the relative peak areas remained constant within a 5 % relative standard deviation. Absolute peak areas also remained invariant within 5 %. It was then concluded that a single sputtering under the above-mentioned conditions sufficed for thorough cleaning of the surface for lead. Whether the same behavior is observed with other elements has not been thoroughly investigated, but has been implicitly assumed from this and our general observations.

Effect of vacuum gas readsorption on relative peak areas

A certain length of time will inevitably elapse during recording of spectra, during which residual gas will be readsorbed on the sample surface. The extent of this adsorption is a function of the nature of the residual gas, its partial pressure, and the type of surface involved. Each element will, of course, behave differently towards the residual gas, and the effect must therefore be taken into account on an individual basis. Typical data for this effect on platinum photoelectron lines are shown in Figs. 2 and 3. In Fig. 2, the per cent change in either peak area or peak height for the 4f7/2 (kinetic energy = 1417 eV) and 4p3/2 (k.e. = 968 eV) lines of platinum is plotted as a function of time elapsed between the end of ion bombardment and the beginning of spectral recording. The experiment was carried out by a single argon-ion bombardment of the platinum sheet followed by six sequential high-resolution recordings which were started each time at the Fermi end of

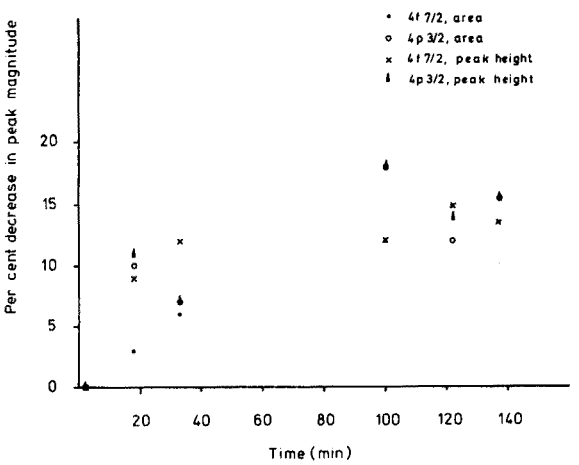

Fig. 2. Per cent decrease in platinum photoelectron peak magnitudes vs. exposure time to residual gas.

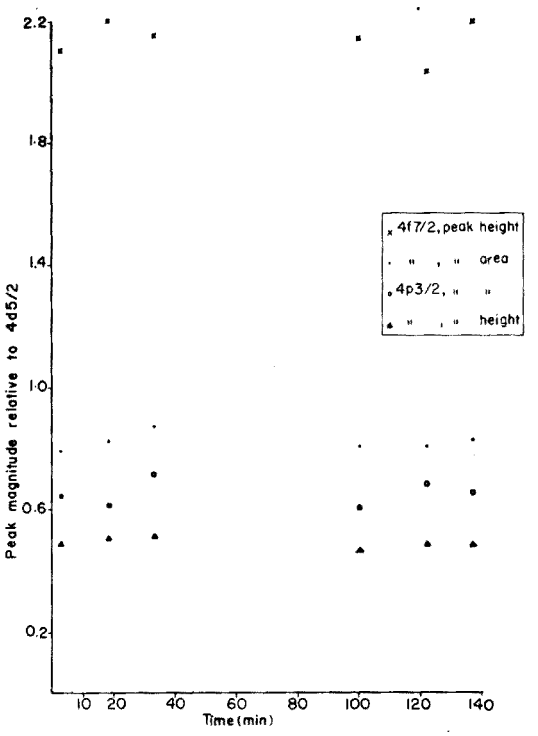

Fig. 3. Variations in relative peak magnitudes vs. exposure time to residual gas.

the spectrum. One entire spectrum was recorded before the next sequence was begun. The time axis refers to the length of time elapsed between the end of ion bombardment and the beginning of each sequence, i.e. the start of recording the 4f7/2 line. The time between each two sequential recordings of individual peaks was kept constant during the entire run so that apart from shifting the origin of the time axis, data are consistent. It is clear from Fig. 2 that even under the ultrahigh vacuum conditions of this experiment ($4 \cdot 10^{-9}$ torr), substantial decreases in peak areas and peak heights occur during the 2.5 h required. There was also a corresponding increase in the magnitude of the C-1s1/2 signal during the experiment, while that of O-1s1/2 peak did not vary systematically, indicating that coverage is probably mostly due to hydrocarbon build-up from the vacuum pump. Therefore, workers interested in quantitative aspects of x.r.p.s. should take due notice if meaningful data are to be obtained. Furthermore, when such work is reported, the vacuum conditions under which the experiments were performed must be explicitly noted. Otherwise, intralaboratory comparisons become meaningless.

Figure 3 shows the relative peak magnitudes (areas and heights) of 4f7/2 and 4p3/2 lines of platinum with respect to its 4d5/2 line as a function of vacuum exposure time. It is evident that no consistent pattern exists between

the two variables of the plots even though the kinetic energies involved are quite different. Therefore, it can be concluded that under the vacuum conditions used, relative peak areas are reproducible to better than 5 % for platinum.

RESULTS AND DISCUSSION

Table 4 summarizes the data on intra-elemental relative peak intensities based on both peak areas and peak heights, individual peak widths, and resolution factor of partially resolved peaks. Each element contains four entries: the first (A) is the relative peak intensity based on peak areas, the second (H) the same parameter based on peak heights, the third ($W_{1/2}$) the measured FWHM of each peak, and the last (R) the separation factor for two adjoining peaks in cases where the parametric value is less than 2.0 (see definition below). The number under each of the first three headings is the average of 3—6 measurements done as outlined above; the uncertainty as measured by the experimental standard deviation of the individual is in the least significant digit of each entry. In general, the relative standard deviations of the intensity ratios based on peak areas were less than 10 %, except for the following lines where the deviations lay between 10 and 15 %: Ni—L_2, Ni—M_2, Cu—M_2, Zn—M_1, Zn—M_2, Ta—N_7, W—N_4, Pb—O_4, Pb—O_5, and Ge—M_2. The relative standard deviations based on peak heights were always less than 10 % and in general somewhat smaller than the corresponding values based on peak areas. Thus, the relative effect of residual gas is under 10 % for the elements studied. Moreover, close scrutiny of standard deviations of individual lines (not listed) revealed no systematic variations for different elements. This observation indicates that the interaction between the residual gas and the cleaned surface is element-independent during the 2 h required for recording the spectra and is within the error limits of these experiments. The relative standard deviation of the half-widths is in general less than 5 %. However, examination of contamination layers (C1s1/2 and O1s1/2) immediately before recording of these high-resolution spectra does show (Table 3) that for some reactive elements such as Na, Al, V, Y, and Ta, rapid build-up of oxygen- and/or carbon-containing layers takes place during the first few minutes after ion bombardment. The quantitative extent of this build-up is currently under investigation. It should also be noted that in general the oxygen contamination peak is much larger than that of carbon, corresponding to easy oxidation of the above mentioned elements. To what extent the measured intra-elemental line intensities of these reactive elements are affected by contamination depends on the thickness of the layers and on the differences of electron kinetic energy.

The relative intensities measured by the two methods are in general quite different, as are the most intense peaks for individual elements. This is due to wide variations occurring in photoelectron linewidths. As pointed out by Berthou and Jorgensen [2], peak heights may be more useful for quantitative

TABLE 4

Data on relative intensities and linewidths of photoelectron lines

Line	Na				Mg				Al				V				Mn			
	A	H	$W^a_{1/2}$	R	A	H	$W_{1/2}$	R	A	H	$W_{1/2}$	R	A	H	$W_{1/2}$	R	A	H	$W_{1/2}$	R
1s1/2	100	100	2.0		100	100	1.6													
2s1/2									100	100	2.2									
2p1/2													31	39	2.6	1.5	29.5	37	3.1	1.8
2p3/2									63	79	1.8		100	100	3.2		100	100	4.0	

Line	Ni				Cu				Zn				Ge				Y			
	A	H	$W_{1/2}$	R	A	H	$W_{1/2}$	R	A	H	$W_{1/2}$	R	A	H	$W_{1/2}$	R	A	H	$W_{1/2}$	R
2p1/2	41	34.0	2.3		49	37	2.0		52	46.5	1.8		51	52.5	1.9					
2p3/2	100	100	1.8		100	100	1.5		100	100	1.6		100	100	1.9					
3s1/2					2.5	1.4	2.8		2.0	1.2	2.9		4.3	3.0	2.8					
3p1/2	8.8	4.4	3.8		3.0	1.7	2.7	0.6	2.1	1.2	2.7	0.6	5.0	3.4	2.9	0.9	64	48.1	3.5	
3p3/2					4.0	2.7	2.2		3.6	2.1	2.8		7.8	6.1	2.4		100	82	3.2	
3d3/2													7.0	8.6	1.6		45	54	2.2	0.5
3d5/2																	90	100	2.4	

Line	Ag				In				Sb				Ba				Ta			
	A	H	$W_{1/2}$	R	A	H	$W_{1/2}$	R	A	H	$W_{1/2}$	R	A	H	$W_{1/2}$	R	A	H	$W_{1/2}$	R
3p1/2	37	13.8	3.3		30	11.8	3.6		25.1	10.1	3.7									
3p3/2	72	26.0	3.3		60	22.6	3.7		43.8	17.3	3.8									
3d3/2	71	69.9	1.2		70	69.1	1.4		64	67.6	1.4		70	70.9	1.9					
3d5/2	100	100	1.2		100	100	1.4		100	100	1.5		100	100	1.9					
4s1/2																				
4p1/2																				
4p3/2													3.6	3.5	2.0		70	38	7.7	
4d3/2					12.4	8.7	2.0		6.5	6.4	1.5	0.5	5.7	6.5	1.7	0.9	59	43	5.7	1.2
4d5/2									7.1	8.1	1.3		7.9	9.1	1.7		100	72	5.9	
4f5/2																	61	100	2.6	0.5
4f7/2																	38	95	1.7	

Line	W				Pt				Au				Pb				Bi			
	A	H	$W_{1/2}$	R	A	H	$W_{1/2}$	R	A	H	$W_{1/2}$	R	A	H	$W_{1/2}$	R	A	H	$W_{1/2}$	R
4p3/2	62	30	5.9		65	22.8	6.5		58	17.4	5.5		57	14.3	5.9		48	11	5.4	
4d3/2	56	36	4.5	1.6	77	30	5.8	1.9	71	24	4.8		60	20.0	4.4		61	17.1	4.4	
4d5/2	100	62	4.7		100	47	4.9		100	36.6	4.5		100	32.7	4.5		98	29	4.2	
4f5/2	47	82	1.7	0.8	76	87	2.0	1.1	67	81	1.4	1.6	72	77	1.4		79	79	1.2	
4f7/2	59	100	1.7		82	100	1.8		82	100	1.3		89	100	1.3		100	100	1.2	
5d3/5													9	9.3	1.4	1.2	8.3	8.3	1.2	1.5
5d5/2													11	12.4	1.3		12.0	12.1	1.2	

[a]As eV.

analysis, if simple non-computer methods are employed; this is the prime reason for their inclusion in Table 4. However, it must be emphasized that peak area data should be used for any interline intensity correlations.

The term resolution, R, is defined as: $R = (dE)/(0.852(W_{1/2} + W'_{1/2}))$, where dE is the peak separation, and $W_{1/2}$ and $W'_{1/2}$ are the FWHM values of the two peaks; this definition is standard for describing the separation of two Gaussian peaks. All doublets with $R \leqslant 1.5$ have been deconvoluted by measuring the peak height of the more energetic member and the leading half of its FWHM, thereby calculating the Gaussian peaks under the doublet. Some representative doublets with $R \leqslant 1.5$ are shown in Fig. 4. It is clear that peaks with $R \geqslant 1.5$ can be considered fully resolved.

When intra-elemental intensities are compared, then in all cases the measured intensities of L_3- lines are higher than those for L_2-lines. This is quite consistent with calculated values of $\tau(1 - 1/J_i)$ for the two levels (Table 1). If the effect of differences between the mass absorption coefficients of L_2- and L_3-levels is ignored (which is quite justifiable for the elements whose L_2- and L_3-lines are excited with Al—Kα), the intensity ratios for zinc and germanium can be calculated from the data in Table 1, to be 2.1 and 2.0, respectively. The measured ratios obtained from Table 4 are 1.9 and 2.0, respectively. The agreement is good to within 10 %. When the study was extended to other elements for which the ratios can be calculated from compiled data [6], the calculated ratios were generally found to lie around 2.0 (Table 5), whereas the measured ratios of present work varied between 1.9 and 3.4. Whether or not the measured values for lighter elements are too high, cannot be established at this time. However, it was observed that when these ratios are calculated for an x-ray excitation energy of 3 KeV, they generally

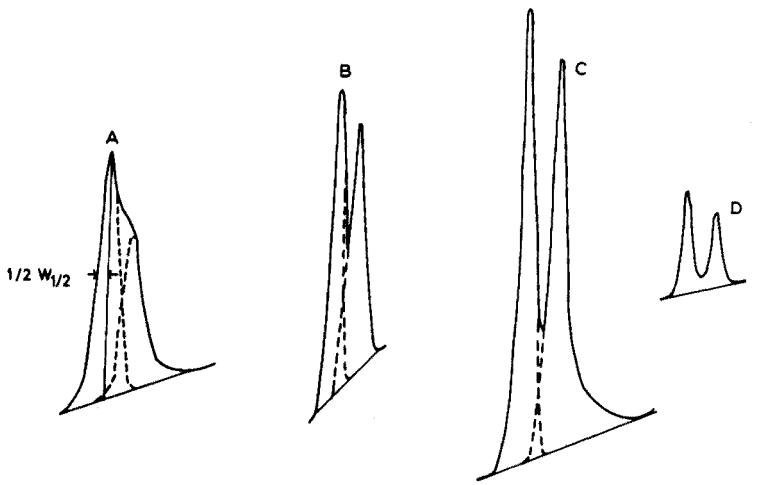

Fig. 4. Photoelectron peaks and their deconvolutions for typical doublets with $R \leqslant 1.5$. A, Cu 3p 1/2, 3/2, R = 0.6; B, W 4f 5/2, 7/2, R = 0.8; C, Pt 4f 5/2, 7/2, R = 1.1; C, Bi 5d 3/2, 5/2, R = 1.5.

TABLE 5

Ratios of L_3/L_2 lines for Al—Kα as excitation source

Element	Z	L_3/L_2	
		Measured	Calculated
V	23	3.2	
Mn	25	3.4	
Ni	28	2.4	
Cu	29	2.0	
Zn	30	1.9	2.1
Ga	31		2.0
Ge	32	2.0	2.0
As	33		2.0
Se	34		2.0

[a]Calculated from data in Table 1.

decrease as Z is increased, yielding extrapolated values of 2.5 for the elements vanadium and manganese.

When the M-level intensities are examined for any given element, a general increase in intensity is observed as the levels become farther from the nucleus. The only exception seems to be for yttrium, the M_3-level of which is the most intense. The general trend observed is in agreement with that calculated in Table 1. Generally, M_5-levels are about 1.5—2 times more intense than M_4, while M_4- and M_3-lines have about the same intensities. For the purpose of quantitative analysis, M_5- and M_4-levels are by far the most suitable because of their narrow linewidths.

The intensities of N-lines do not seem to follow any simple pattern. In almost all cases, the 4d5/2-line is the most intense, while the 4f7/2-level has the highest peak magnitude. Unfortunately, reliable data on the N-level cross-sections and jump ratios are not available, so that comparisons between the measured values and those expected cannot be made at present.

Berthou and Jorgensen [2] have also reported relative photoelectron line intensities, but for unspecified compounds instead of pure elements. The results of the present work are compared with theirs in Table 6. It is clearly seen that fair agreement is obtained in some cases (both sets of data compared are based on peak heights). In several cases, however, the ratios obtained in the present work are much larger than theirs, and in only one case is the ratio smaller. It is also clear that in cases where agreement is observed the levels involved have the same principal quantum number. These levels are, of course, characterized by small differences in the kinetic energies of their photoelectrons as shown by the data of Table 6. It should be noted that in all cases, except germanium, the greater the difference between the kinetic energy of the two levels involved, the larger the magnitude of the disagreement between our results and theirs. Berthou and Jorgensen used

TABLE 6

Comparison between relative intra-elemental intensities of this work and those of ref.2

Element	Lines	Intensity ratios[a]			Difference in kinetic energy (eV)
		1	2	3	
Al	L_1/L_3	1.2	1.3	1.6	44.8
Bi	N_7/O_5	7	8	8	132.7
Y	M_3/M_5	0.9	0.8	1.1	142.9
Ag	M_3/M_5	0.3	0.3	0.7	204.7
Pt	N_5/N_7	0.5	0.5	1.2	242.7
Au	N_5/N_7	0.4	0.4	1.2	249.8
Pb	N_5/N_7	0.3	0.3	1.1	276.6
Bi	N_5/N_7	0.3	0.3	1.0	282.9
Sb	M_5/N_5	6	12.4	14.1	496.1
Ba	M_5/N_5	4	11.0	8.9	690.8
Ni	L_3/M_3	5	22.7	11.4	730.4
Cu	L_3/M_3	5(CuI) 8(CuII)	37.0	25.0	857.5
Ge	L_3/M_3	10	16.4	12.8	1095.9

[a] 1: Calculated from data of ref. 2.
2: Present data based on peak heights.
3: Present data based on peak areas.

unspecified compounds and apparently employed no surface cleaning method in order to avoid decomposition of their compounds. Furthermore, their instrument operating pressure was not specified, and may have been higher than the pressure used here. The discrepancies can be explained satisfactorily by assuming electron absorption in the surface contamination layers, and perhaps matrix effects, in the earlier work. This comparison serves to emphasize the important point that with the very small penetration depths of the photoelectrons of interest in x.r.p.s. (typically 10—20 Å), quantitative measurements of intensities are quite meaningless unless matrix and surface effects have been dealt with. Furthermore, in order to enable interlaboratory comparison of intensity data, peak areas should be reported even though peak heights may be more convenient for analysis. There is no consistency between ratios reported in terms of peak areas and those for peak heights (Table 4) unless peak widths are also reported.

CONCLUSIONS

Reliable data on intra-elemental photoelectron line intensities have been presented for the case of "infinitely thick" monoelement samples for 20 elements. Similar data are needed for other elements. Moreover, such effects as sorption of residual gas, which have not received primary emphasis in this work, and their significance in quantitative aspects of x.r.p.s. should be investigated more thoroughly. It has been shown that the effects of surface

contamination and compound type on relative line intensities may be large. These effects are probably even more pronounced for individual line intensities, but more work is needed to establish the effects, perhaps even quantitatively. It has been indicated that, via access to electron mass absorption coefficients, the present and similar results can be extended to thicknesses of interest in trace analysis. Therefore, pertinent data are needed. In this work, Auger lines have not been considered, but they are certainly present and should be taken into account. Finally, the availability of compilations covering the atomic levels of interest in x.r.p.s. would greatly advance comparative understanding between theoretical and experimental aspects.

This work was supported by the Bundesministerium für Forschung und Technologie under Contract SN 7023 and the Fonds der Chemischen Industrie. The authors also thank K. K. Janghorbani for her assistance with the literature search.

REFERENCES

1 C. D. Wagner, Anal. Chem., 44 (1972) 1050.
2 H. Berthou and C. K. Jorgensen, Anal. Chem., 47 (1975) 482.
3 J. S. Brinen and J. E. McLure, J. Electron Spectrosc. Rel. Phenom., 4 (1974) 243.
4 D. M. Hercules, L. E. Cox, S. Onisick, C. D. Nichols and J. C. Carver, Anal. Chem., 45 (1973) 1973.
5 H. Ebel and M. F. Ebel, X-Ray Spectrometry, 2 (1973) 19.
6 W. H. McMaster, N. Kerr Del Grande, J. H. Mallett and J. H. Hubell, Compilation of X-Ray Cross-sections, UCRL-50174-S2, Lawrence Radiation Laboratory, Univ. Cal., Livermore, 1969.
7 M. Janghorbani, M. Vulli and K. Starke, Anal. Chem., 47 (1975) 2200,
8 R. D. Giauque, F. S. Goulding, J. M. Jacklevic and R. H. Pehl, Anal. Chem., 45 (1973) 671.
9 C. R. Brundle, J. Vac. Sci. Technol., 11 (1974) 212.

Analytica Chimica Acta, 82 (1976) 137—144

FLOW INJECTION ANALYSIS
PART V. SIMULTANEOUS DETERMINATION OF NITROGEN AND PHOSPHORUS IN ACID DIGESTS OF PLANT MATERIAL WITH A SINGLE SPECTROPHOTOMETER

J. W. B. STEWART* and J. RŮŽIČKA**

Centro de Energia Nuclear na Agricultura (CENA), C.P. 96, 13400 Piracicaba, S.P. (Brasil)

(Received 4th August 1975)

SUMMARY

The rapid simultaneous determination of nitrogen and phosphorus in a single acid digest of plant material based on the Berthelot and phosphomolybdate colorimetric methods, respectively, has been adapted to Flow Injection Analysis with a dual-channel manifold. A routine sampling rate of 200 determinations per hour can be achieved with a single spectrophotometer; evidence is presented that 400 determinations per hour are possible with two spectrophotometers. The effect of sample volume on absorbance, and the methods of obtaining different proportions of sample split are discussed.

A valuable feature of continuous flow analysis is the possibility of splitting the sample into two or more aliquots and performing automatically a separate analysis on each of them. This type of multiple analysis is of great importance in clinical analysis, where up to twelve different determinations are routinely made on a single sample of blood serum, and instrumentation intended to accommodate up to forty different tests is being developed. All these analyzers are based on the concept of continuous measurement on the air-segmented stream, originated by Skeggs [1], and are marketed by Technicon. Splitting of the sample on stream seems a straightforward idea, but much effort had to be spent on its technical perfection. After the development of a single instrument [2] and experience with a two-channel system for determinations of glucose and urea, it took several years before the eight-channel analyzer was developed [3], followed by a twelve-channel commercial version [4, 5]. During the last ten years Sequential Multichannel Analyzers (SMA) have become a very important part of the clinical laboratory of any large hospital, where the work load is often so high that even further development of this instrument into a fully computerized version (SMAC)

*Present address: Department of Soil Science, University of Saskatchewan, Saskatoon, Canada.

**Present address: Chemistry Department A, The Technical University of Denmark, Building 207, 2800 Lyngby, Denmark.

[6—8] became justified.

In other fields, like agriculture, food and water analysis, environmental studies, industrial applications and in small clinical laboratories, two-, four- and six-channel analyzers remain most useful as they are more versatile, and easier to operate and purchase, than multichannel instruments. However, for these moderate work loads, yet another approach, Flow Injection Analysis [9], based on a substantially higher sampling rate than the Auto Analyzer, could be visualized. As the manifold used in Flow Injection has a small hold up, and can be rapidly replaced or altered, a two-channel system might easily be reprogrammed to accommodate the same number of determinations during the same period of time as four- or even six-channel continuous flow analyzers of the conventional type. Whether Flow Injection Analysis [9] can be operated in such a way depends primarily on the reproducibility of sample splitting into required aliquots. However, the approach to this must be different from the AutoAnalyzer system, where the sample is split before it enters the pump and the size of the aliquots is regulated by the choice of the pump tube diameters. In Flow Injection Analysis, the sample is injected into the carrier stream after the pump, as the well defined sample plug created by injection would otherwise be broadened during passage through a pump tube. It was learned previously [10] in analysis of water for chloride that the size of the aliquots in the Flow Injection Analysis technique could be regulated by the flow resistance of the individual branch lines, and that the length and inner diameter of these could also determine the residence time and allow phasing of the output signal. In the present case, however, reproducible splitting would be more difficult to achieve, because two-component analysis requires branches which are independent and have different flow rates when additional reagents are added downstream from the point of splitting.

The important need for simultaneous nitrogen and phosphorus determinations in most agricultural research is well documented, and many methods have been developed for the simultaneous determination of nitrogen and phosphorus in plant digests [11—14]. For instance, at this institution (CENA) some 15000 plant samples have to be analyzed annually to service soil fertility and plant breeding experiments. Therefore it was decided to adapt the Flow Injection methods [15, 16] for phosphorus and nitrogen to give simultaneous determinations on the same sample. As in both cases spectrophotometric measurement of a blue colour is employed, it was possible to use a single spectrophotometer with two identical flow-through cells placed in the same optical path.

EXPERIMENTAL

The instrumentation used in this work was exactly the same as reported in Part IV of this series [10], except that a temperature-controlled water bath (Tecam, Temporar, Techne Inc., USA) became available and two identical

flow-through cuvettes of 10-mm light path were aligned in the optical path of the sample beam. As reference, 2 M KCl solution was used.

The plant material and digestion procedure were identical with those analyzed and described previously [16] and computations were made in the same way.

Reagents for nitrogen analysis, i.e. solutions of alkaline hypochlorite and alkaline phenol, were identical with those used previously [16].

For the phosphate determination, a single reagent solution consisting of 0.01 M ammonium molybdate in 0.02 M H_2SO_4, 1.0 % (w/v) ascorbic acid and 0.025 % (w/v) potassium antimony tartrate was used. The solution was prepared fresh daily; ascorbic acid and the antimony tartrate had to be dissolved first in a small volume of distilled water and then added to the acid molybdate solution which was then made up to volume with 0.02 M H_2SO_4.

The 0.04 M sulphuric acid solution used as the carrier stream into which the sample was injected, contained 0.05 % of nonionic neutral commercial laboratory detergent (Triplex, Struers A/S, Denmark).

The standards for nitrogen and phosphorus were made in 0.4 M H_2SO_4 from $(NH_4)_2SO_4$ and KH_2PO_4 so that samples 1—6 contained 1, 2.5, 5.0, 7.5, 10.0 and 12.5 μg P ml^{-1}, respectively, and the equivalent of 0.25, 0.50, 1.0, 2.0, 3.0 and 3.5 % N in the assayed plant material, respectively, taking into consideration sample size and digestion procedure [14, 16].

RESULTS AND DISCUSSION

Design of the two-channel Analyzer

The two-channel Flow Injection Analyzer (Fig. 1) consisted of a phosphorus line (top), injection and split line (middle) and nitrogen line (lower), the latter being the longest one. For simplification, the coils in the following description are referred to by their function or by their lengths, but it should be understood that the lengths stated comprise not only that part of the tubing wound into a coil (approximately 80 %) but also the transmission tube to the next joint, flow cell, etc. Thus, following the sample injection point (S), the 66-cm long split delay coil was inserted to avoid the effect of variations of the injection speed on sample splitting. In this way, the sample zone reaches the split point only when the flow rates have been reestablished after the injection, and the splitting is therefore effected only by pumping action. The sample, split in the ratio 4:1 (P:N) at the split point, proceeds through a short transmission line (5 cm) into the phosphate branch and through the 470-cm phasing coil into the nitrogen line. The ratio of splitting is effected by two means: by enlarging the diameter of the 265-cm hypochlorite coil in the nitrogen line, and by increasing the flow resistance of the phosphate branch by placing a brake coil (400 cm long) behind the phosphate flow cell. This arrangement proved

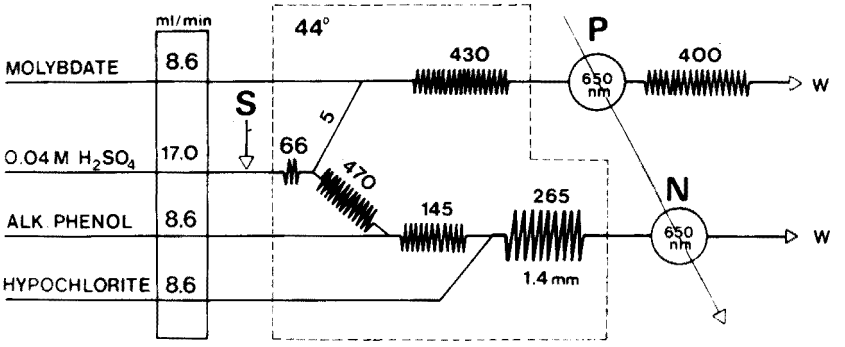

Fig. 1. Flow diagram of the dual-channel manifold used in the simultaneous spectrophotometry of phosphorus and nitrogen by flow injection. S is the point of sample injection, P and N represent the phosphorus and nitrogen flow-through cuvettes, respectively. All tube lengths are expressed in cm and the i.d. of all tubes was 1.0 mm unless otherwise stated. The part of the manifold enclosed by the dotted line was immersed in a thermostated water bath kept at 44 °C.

to be highly versatile and effective, considering not only the various pump rates used to supply the branches, but also the large difference in viscosity between the phenol solution and the other reagents. While the variations in the length and diameter of the hypochlorite coils were used as a coarse regulator, the length of the brake coil effected the fine trimming.

The role of the 470-cm phasing coil was to delay the passage of the sample plug in the nitrogen line until the sample zone in the phosphate line passed the flow cell and cleared the optical path below the 1 % absorbance level.

Flow parameters and sample volume

As the composition of the reagents, line length, influence of temperature and the shapes of calibration curves had been investigated previously [15, 16] for both the nitrogen and phosphate methods, only the influence of flow parameters and of sample volume are given here, as these are of importance in a two-channel analyzer.

The splitting of the sample and the formation of phosphomolybdenum blue and indophenol blue in the respective branches of the manifold, results in the formation of two peaks (Fig. 2) which, from right to left, correspond to phosphate and nitrogen, respectively. There is a 16-s interval between the injection point S_1 and the phosphate readout P, followed by an 18-s interval to the nitrogen readout N. Thus, when 2 s is allowed between the readout N and the next injection S_2, for a reliable readout, a total of 36 s must elapse between two successive injections, so that the maximum sampling rate is 100 samples per hour and the analysis rate is 200 determinations per hour. Obviously, if a dual-channel spectrophotometer had been used, the phasing coil could have been left out, and the sampling as well as

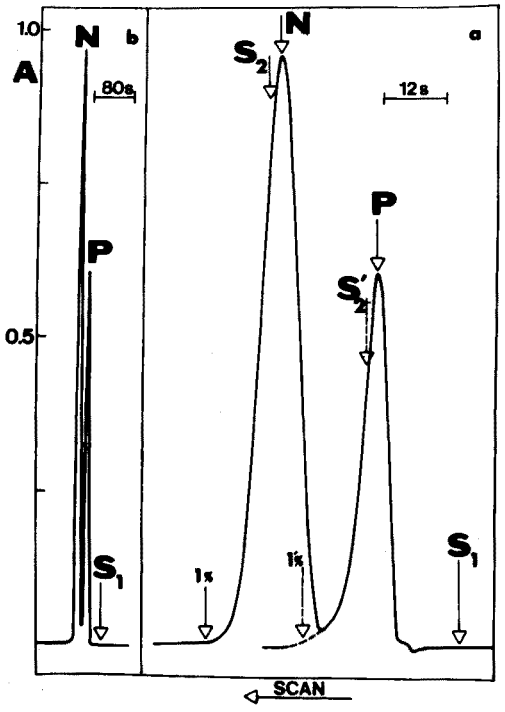

Fig. 2. Flow parameters of the dual-channel manifold recorded at (a) high and (b) low paper speed with standard S and a sample volume of 0.4 ml. S_1, S_2 and S'_2 are injection points. P and N are the phosphorus and nitrogen peaks, respectively, and 1 % is the time at which 1 % of the maximum absorbance colour of the previous peak is left in the flow cell. Diagram (a) was used to establish the flow parameters, whereas diagram (b) is the type of recording used in normal analyses. (See also Fig. 4.)

determination rates could have been doubled; with a separate readout the second sample could have been injected at the point S'_2 with a time gap between successive injections of only 18 s. All these considerations are based on the requirement that at most only 1 % of the colour belonging to the previous peak may remain in the optical path during each readout.

The absorbances for both the phosphate and nitrogen channels increase linearly with the volume of the injected sample (Fig. 3), which is advantageous if the sensitivity of the determination must be altered to accommodate a change in the type of the sample material. If for any reason the ratio of the N and P readouts has to be adjusted, this can be achieved, on a single-channel spectrophotometer by lowering the ethanol content in the phenol solution and by changing the sample volume, spectrophotometer sensitivity or both.

The calibration curve and part of the following routine readout obtained with 0.4 ml of injected plant digest sample are shown in Fig. 4. All standards and samples were injected in triplicate, each injection resulting in a double peak (compare Fig. 2b) of which the first readout belongs to phosphorus and

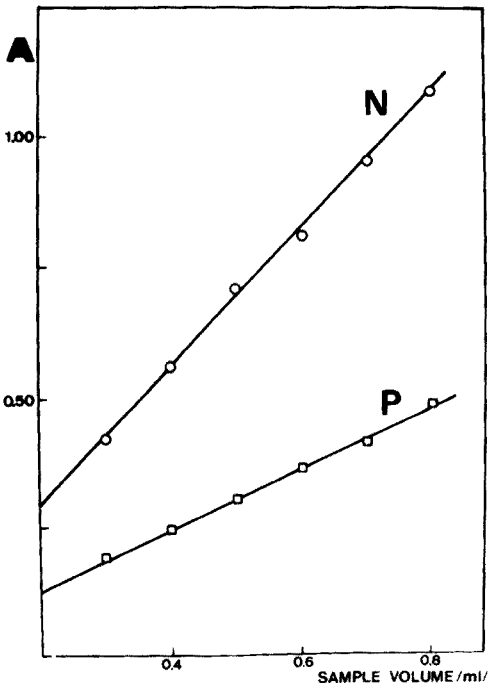

Fig. 3. The influence of the sample volume (0.3—0.8 ml) on the sensitivity of the N and P absorbances obtained with sample 4.

the second one to nitrogen. It was observed as before [15, 16] that the phosphorus standard graph was linear and that the nitrogen standard graph was curved. It should be noted that, in contrast to the previously reported methods for phosphorus and nitrogen by the Flow Injection method [15, 16], both the slopes of the calibration curves and the baseline positions remain unchanged during a series of routine analyses, regardless of the number of determinations performed. This is due to the use of a constant-temperature bath (kept at 44 °C) and the addition of the detergent to the carrier stream of diluted sulphuric acid; the latter improved the wash out and thus avoided formation of deposits in the flow cell and tubing of the manifold.

No significant statistical difference could be found between the nitrogen and phosphate analyses made on the same digests by dual-channel and single-channel Flow Injection Analysis. As twenty of these samples were also analyzed by conventional methods [15, 16], it can be inferred that the two-channel technique can be used for reliable and accurate routine screening.

CONCLUSION

Sample splitting effected after injection into a continuously moving stream yields reproducible results even if the split zones are not re-routed through the same flow cell as was the case in the determination of chloride [10]. The

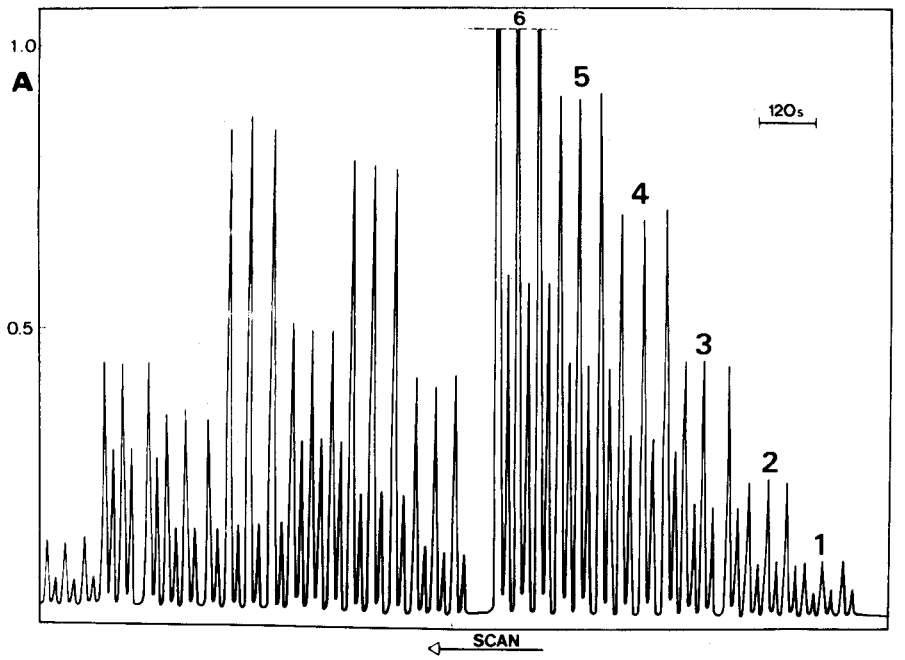

Fig. 4. Calibration graph and part of the routine plant digest analysis for nitrogen and phosphorus, showing from right to left dual standards 1—6 followed by sample analysis. All samples (0.4 ml) were injected in triplicate with (from right to left) the first peak of each sample being phosphorus and the second nitrogen.

aliquoting of the sample zone, effected by a difference in flow rates in the individual branches of the manifold, can be done reproducibly and, if required, easily altered. This allows the simultaneous determination of phosphorus and nitrogen in a single digest of plant material, at a higher sampling rate than any previously reported. The extremely short residence time of the sample in the analyzer, makes both analytical readouts available 32 s after the sample has been injected. The simplicity of manifold construction and its adaptability to virtually any type of peristaltic pump and recording spectrophotometer makes the system widely accessible.

It is interesting to note that the line length through which the aliquot for nitrogen analysis is transported towards the detector is nearly 9 m long, yet the sample plug remains well preserved during the complete passage despite further addition of reagents downstream, and the use of a wider diameter in the last coil. This certainly indicates that even slower and more complex analytical methods, requiring longer lines and sequence of reagents can be adapted to Flow Injection, performed on a continuous stream unsegmented by air.

As to the further adaptation of methods for two- or even multi-channel Flow Injection Analysis, a number of clinical analyses could now be contemplated, as most frequently a fixed combination of two or several determinations is required. The main obstacle to flow injection in this field,

however, is the necessity of using continuous dialysis, as this separation technique might spoil the flow pattern of the injected sample to the degree that the advantages of flow injection would be lost. These aspects are the subject of continuing studies.

The authors would like to acknowledge the help and assistance given to them by Dr. A. Cervellini, Director, and the staff of CENA. They also are indebted to A. Růžičková for preparation of the diagrams.

REFERENCES

1 L. T. Skeggs, Clin. Chem., 2 (1956) 241.
2 L. T. Skeggs, Amer. J. Clin. Pathol., 28 (1957) 311.
3 L. T. Skeggs and H. Hochstrasser, Clin. Chem., 10 (1964) 918.
4 E. C. Whitehead, Technicon Symp. Aut. Anal. Chem., 1965, p. 437.
5 W. J. Smythe, M. H. Shamos, S. Morgenstern and L. T. Skeggs, Technicon Symp. Aut. Anal. Chem., 1967, p. 105.
6 J. Israeli and W. Smythe, Technicon Symp. Aut. Anal. Chem., vol. 1, 1972, p. 13
7 H. Diebler and M. Pelavin, Technicon Symp. Aut. Anal. Chem., vol. 1, 1972, p. 19.
8 S. Morgenstern, R. Rush and D. Lehman, Technicon Symp. Aut. Anal. Chem., vol. 1, 1972, p. 33.
9 J. Růžička and E. Hansen, Anal. Chim. Acta, 78 (1975) 145.
10 J. Růžička, J. W. B. Stewart and E. A. G. Zagatto, Anal. Chim. Acta, 81 (1976) 387.
11 C. H. Williams and J. R. Twine, CSIRO, Div. of Plant Industry Tech., Paper 24 (1967).
12 W. D. Basson, D. A. Stanton and R. G. Boehmer, Analyst (London), 93 (1968) 166.
13 J. V. O'Neill and R. A. Webb, J. Sci. Food Agr., 21 (1970) 217.
14 J. A. Parkinson and S. E. Allen, Commun. Soil Sci. and Plant Anal., 6 (1975) 1.
15 J. Růžička and J. W. B. Stewart, Anal. Chim. Acta, 79 (1975) 79.
16 J. W. B. Stewart, J. Růžička, H. Bergamin Filho and E. A. G. Zagatto, Anal. Chim. Acta, 81 (1976) 371.

Analytica Chimica Acta, 82 (1976) 145—153

EINE THERMOMETRISCH—KINETISCHE METHODE ZUR BESTIMMUNG VON KUPFER UND CYANID MIT HILFE DER KUPFER-KATALYSIERTEN ZERSETZUNG VON WASSERSTOFFPEROXID

HERBERT WEISZ, SIEGBERT PANTEL und WOLFGANG MEINERS

Lehrstuhl für Analytische Chemie, Chemisches Laboratorium der Universität Freiburg, Freiburg i. Br. (BRD)

(Eingegangen den 1 September 1975)

ZUSAMMENFASSUNG

Der durch Kupfer katalysierte Zerfall von Wasserstoffperoxid wird durch Cyanid verzögert. Die Oxidation des Cyanid durch H_2O_2 ist gleichfalls Kupfer-katalysiert. Der Reaktionsverlauf der Zersetzung von H_2O_2 wird thermometrisch verfolgt. Daher lässt sich bei bekannter Kupfer-menge die unbekannte Cyanid-menge aus der Verzögerungszeit bestimmen; ebenso lässt sich aber auch umgekehrt bei bekannter Cyanid konzentration aus der Verzögerungszeit eine unbekannte Kupfer-menge bestimmen. Darüber hinaus kann nach Ablauf der Verzögerungszeit aus dem entsprechenden Anstiegswinkel der Temperaturkurve (tgα) gleichfalls die Kupfer konzentration ermittelt werden. Es wurden Kupfer im Bereich von 4—40 μg und Cyanid im Bereich von 3—30, 6—60 und 8—80 μg bestimmt.

SUMMARY

The copper-catalyzed decomposition of hydrogen peroxide is retarded by cyanide. The oxidation of cyanide by hydrogen peroxide is likewise catalyzed by copper ions. The decomposition reaction of H_2O_2 can be followed thermometrically. Therefore, at a known copper concentration an unknown amount of cyanide can be determined from the retardation time; and an unknown amount of copper can be determined by adding a known amount of cyanide. Moreover, after the end of the retardation time, unknown copper concentrations can also be determined from the slope of the temperature curve (tanα). Copper was determined in the range 4—40 μg, and cyanide in the ranges 3—30, 6—60 and 8—80 μg.

Kupfer(II) katalysiert in Form seines Tetramminkomplexes in ammoniakalischem Medium den Zerfall von Wasserstoffperoxid [1—4]. Diese Reaktion ist exotherm und daher thermometrisch gut zu indizieren. Auf diese Weise wurde bereits mit Hilfe einer katalytisch—kinetischen Differenzmethode Kupfer im μg-Bereich bestimmt [5].

Ist in einem Reaktionssystem aus Wasserstoffperoxid und Ammoniak ausser Kupfer zusätzlich noch Cyanid anwesend, so wird der Beginn der Zerfallsreaktion des Wasserstoffperoxids, hier indiziert als Temperaturanstieg, um eine Zeit Δt verzögert. Die Verzögerung dauert so lange bis das Cyanid

zu Cyanat oxidiert ist. Während der Verzögerungszeit liegt der Katalysator Kupfer offenbar in einer Form vor, in der er für die Katalyse des Wasserstoffperoxid-Zerfalles total inhibiert, aber für die Oxidation des Cyanids katalytisch aktiv ist. Dies ist z.B. dadurch denkbar, dass Cyanid die für den Wasserstoffperoxid-Zerfall katalytisch aktiven Zentren am Kupfertetramminkomplex besetzt. Die Frage, ob und wie das Cyanid die Ammoniakliganden am Kupferion verdrängt, ist für die gefundenen kinetischen Verhältnisse nicht wichtig. Das Cyanid ist aber durch die Fixierung am Kupfer offenbar leichter zu oxidieren. Ungewöhnlich ist der Fall, dass es entweder eine totale oder aber keine Inhibition des Wasserstoffperoxid-Zerfalles zu geben scheint. Zur Erklärung ist folgende Vorstellung möglich.

Das am Kupfer fixierte Cyanid wird durch Oxidation abgebaut und solange durch Cyanid aus der Lösung ersetzt, bis ein Molverhältnis Cu:CN von etwa 1:1 erreicht ist (extrapoliert aus der nichtlogarithmierten Eichkurve). Das restliche Cyanid wird wesentlich schneller (innerhalb weniger Sekunden) oxidiert, wie es der Temperaturverlauf zeigt (innerhalb des kleinen Bogens vor dem linearen Temperaturanstieg, vergl. Abb. 2).

Erst nach Ende der Verzögerungszeit Δt steht praktisch das gesamte Kupfer als Katalysator der exothermen Indikatorreaktion zur Verfügung. Das bedeutet, dass — unabhängig von der Cyanidkonzentration — die von der Kupferkonzentration abhängige Steigung des Temperaturanstiegs ($tg\alpha$) durch den Wasserstoffperoxid-Zerfall konstant bleibt.

$$CN^- + H_2O_2 \xrightarrow{Cu} OCN^- + H_2O$$

$$2\,H_2O_2 \xrightarrow{Cu} H_2O + O_2$$

Die Kinetik der Wasserstoffperoxid-Zerfallsreaktion selbst wird nach Ende der Verzögerungszeit nicht beeinträchtigt, so dass aus ihr immer noch die Kupferkonzentration bestimmt werden kann. Messgrösse ist dazu der $tg\alpha$ des Temperaturanstiegs. Konsequenterweise ist aber auch die Dauer des Cyanidabbaus bei jeweils gleicher Cyanidmenge eine Funktion der Kupferkonzentration, damit ist also auch Kupfer auf diese Weise zu bestimmen.

Musha et al. [6] haben bereits Cyanid dadurch bestimmen können, dass es die durch Kupfer katalysierte Reaktion von Luminol mit Wasserstoffperoxid verzögert.

EXPERIMENTELLER TEIL

Messanordnung

Als Reaktionsgefäss (Abb. 1) wurde ein 25 ml Dewar (a), innenversilbert und eingebettet in Styropor (b), verwendet. Zum Verschluss des Gefässes diente ein dreifach durchbohrter Teflonstopfen (c). Durch zwei Bohrungen

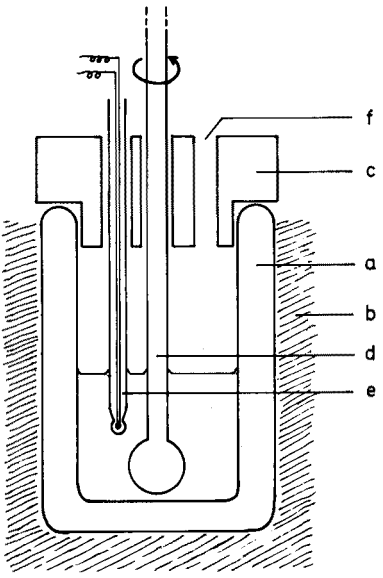

Abb. 1. Das Reaktionsgefäss.

wurden ein motorgetriebener Glasrührstab (d) und ein Glasrohr als Träger des Thermistors (e) geführt. Die dritte Bohrung (f) diente zum Einpipettieren der Startlösung. Die temperaturabhängige Widerstandsänderung eines Messheissleiters (ITT/SEL F 23 D, 2.0 KOhm Widerstand bei 20 °C) wurde durch die Verstimmung einer Wheatstone-Brücke in eine Spannungsänderung umgewandelt, die dann mit einem Kompensationsschreiber (Metrawatt, Servogor RE 541) gegen die Zeit (Papiervorschub 120 mm min^{-1}) registriert wurde.

Ausführung der Cyanidbestimmung

Die Verzögerungszeit Δt ist bei sonst gleichen Reaktionsbedingungen eine Funktion der Kupfer- und der Cyanidkonzentration. Sie ist umso länger, je höher die Cyanid- und je kleiner die Kupferkonzentration ist. Für die Auswertung ist es günstig, wenn die Verzögerungszeit zwischen 5 Sek und 10 Min liegt. Bei jeweils gleicher Kupferkonzentration ist die Verzögerungszeit Messgrösse für die Cyanidkonzentration. Allerdings ist bei einer einzigen Kupferkonzentration der Bestimmungsbereich für Cyanid klein. Erst bei zusätzlicher Aenderung der Kupferkonzentration ist der Bestimmungsbereich zu erhöhen. Cyanid ist bei einer Katalysatorkonzentration von 20 μg Cu/10,5 ml im Bereich von 6—30 μg und bei 40 μg Cu im Bereich von 20—60 μg zu bestimmen.

Die eingesetzte Kupfermenge sollte 4 μg nicht unterschreiten, da sonst das Ende der Verzögerungszeit wegen zu geringer Richtungsänderung der Schreiberkurve (Temperaturanstieg) nicht auszuwerten ist.

Für den Bereich von 6—60 μg CN^-/10,5 ml wurde folgendermassen verfahren:

In das Reaktionsgefäss werden 2 ml 2 M Ammoniaklösung einpipettiert und mit 100 bzw. 200 μl einer Kupferacetatlösung mit 200 μg Cu ml^{-1} versetzt (Eppendorfpipette). Nun werden zur Aufstellung der Eichkurve 6—60 μg Cyanid bzw. die zu bestimmende Cyanidlösung zugegeben und mit bidestilliertem Wasser auf 10 ml aufgefüllt.

Gestartet wird die Reaktion mit 0,5 ml einer Wasserstoffperoxid-Lösung (10 mg H_2O_2 ml^{-1}), die mittels einer Eppendorfpipette durch die Bohrung (f, Abb. 1) zugegeben wird. Ergibt eine erste Messung mit 40 μg vorgelegtem Kupfer eine zu kurze Verzögerungszeit, so wird die Messung mit 20 μg Kupfer wiederholt.

Auswertung

Die Verzögerungszeit in Sekunden wird aus dem Abstand des Knicks der Temperaturkurve (k) vom Startpunkt (S) auf dem Schreiberpapier abgelesen, Abb. 2.

Die Logarithmen der Verzögerungszeiten aufgetragen gegen die Cyanidkonzentration, ergeben eine Gerade. Abbildung 3 zeigt die beiden so erhaltenen Eichkurven aus dem zuvor beschriebenen Ansatz. Auf diese Weise wurden unbekannte Cyanidproben bestimmt; einige Ergebnisse sind in Tab. 1 wiedergegeben.

Der Anteil an unkatalysierter Reaktion zwischen Cyanid und Wasserstoffperoxid kann innerhalb der Messzeit vernachlässigt werden. Erst nach frühestens 10 Min ist ein schwacher Abfall der Cyanidkonzentration zu beobachten, nach frühestens 2 Stunden ist das Cyanid oxidiert.

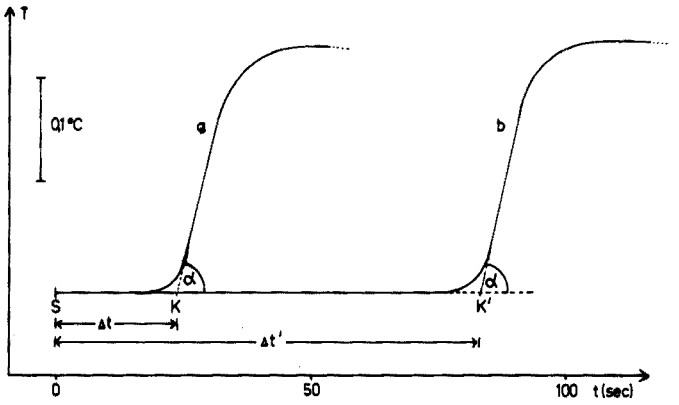

Abb. 2. Beispiele registrierter Schreiberkurven für (a) 35 und (b) 48 μg CN^- bei jeweils 40 μg Cu.

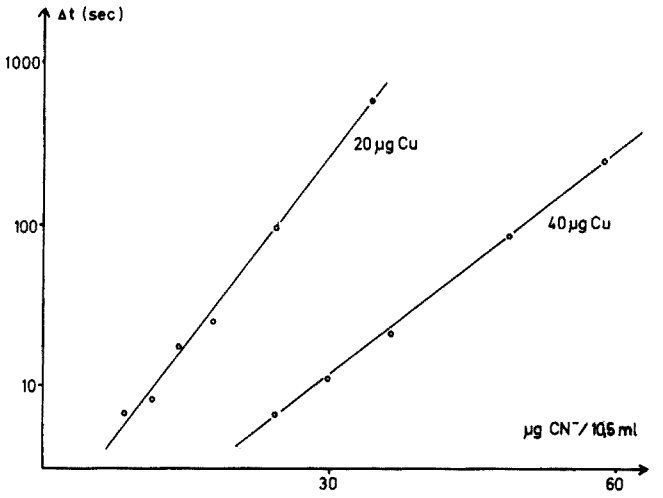

Abb. 3. Eichkurven zur Cyanid-Bestimmung.

TABELLE 1

Bestimmung von Cyanid
(Ergebnisse in µg CN/10,5 ml)

Gegeben	6,8	11,7	12,4	23,8	24,6	35,2	43,5	48,4	53,2	58,0
Gefunden	6,9	10,5	11,3	21,8	23,8	36,4	43,7	49,0	52,4	57,8
% rel Fehler	+1,5	−10,2	−8,9	−8,4	−3,3	+3,4	+0,5	+1,2	−1,5	−0,4

Ausführung der Kupferbestimmung

Wie schon erwähnt, ist die Verzögerungszeit Δt bei konstanter Cyanidmenge von der Kupferkonzentration abhängig. Aus den gleichen Gründen wie bei der Cyanidbestimmung sind für einen Bestimmungsbereich von etwa 4—40 µg Cu/10,5 ml drei verschiedene Vorlagen an Cyanid nötig

Vorlage an Cyanid (µg)	Messbereich für Kupfer (µg/10,5 ml)
6	4—15
12	8—20
24	15—40

Ausserdem ist Kupfer als Katalysator des Wasserstoffperoxidzerfalls, dessen Beginn — wie erwähnt — das Ende der Verzögerungszeit Δt indiziert, im selben Reaktionsansatz zu bestimmen. Die Kinetik der exothermen

Wasserstoffperoxid-Zerfallsreaktion wird durch den Anstieg der Temperatur charakterisiert. Die Auswertung erfolgt nach der Tangentenmethode [7]. Messgrösse ist die Steigung des Temperaturanstiegs als Tangens des abzulesenden Steigungswinkels. Der Temperaturanstieg ist unabhängig von der Dauer der vorangegangenen Verzögerungszeit.

Wird der tgα gegen das Quadrat der Kupferkonzentration aufgetragen (Abb. 4), erhält man eine lineare Eichkurve. Zur Bestimmung des Kupfers aus der Verzögerungszeit wird jeweils deren Logarithmus gegen die Kupferkonzentration aufgetragen und liefert gleichfalls eine lineare Eichkurve, Abb. 5. Die Ergebnisse der Bestimmung unbekannter Kupferproben, gewonnen nach beiden Verfahren, zeigt Tab. 2.

Die Reproduzierbarkeit der mit Hilfe der Verzögerungszeit bestimmten Werte erwies sich als etwas schlechter. Für einen Wert von 20 μg Cu/10,5 ml wurde eine Standardabweichung von 20,0 ± 0,68 μg (3,5 %) gefunden. Die Bestimmung aus dem tgα ergab für den gleichen Wert 20,0 ± 0,29 μg (1,5 %).

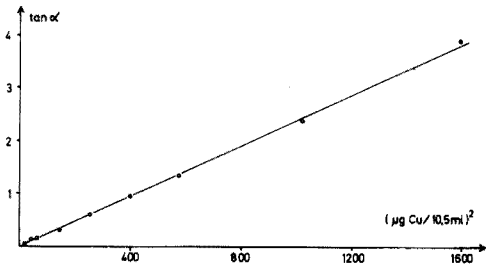

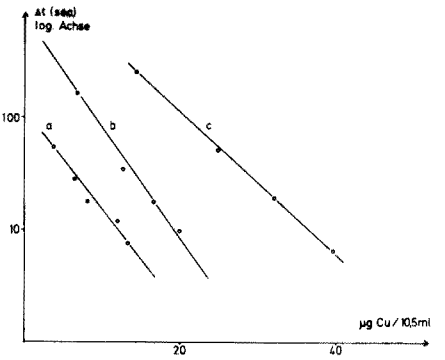

Abb. 4. Eichkurve zur Kupfer-Bestimmung aus der Steigung des Temperaturanstiegs.

Abb. 5. Eichkurven zur Kupfer-Bestimmung aus der Verzögerungszeit für verschiedene Cyanid-Mengen: a, 6 μg; b, 12 μg; c, 24 μg.

TABELLE 2

Bestimmung von Kupfer
(Ergebnisse in μg Cu/10,5 ml)

Gegeben	7,0	8,3	9,3	13,4	15,8	16,4	32,4	34,5	36,5
Gef. aus Δt	7,3	9,6	10,3	13,5	15,8	18,4	33,6	33,5	36,8
% rel. Fehler	+4,3	+15,7	+10,8	+0,7	±0	+12,2	+3,7	−2,9	+0,8
Gef. aus tg α	6,4	8,1	8,9	11,8	15,5	18,5	34,4	34,8	40,5
% rel. Fehler	−8,6	−2,4	−4,3	−12,0	−1,9	+12,8	+6,2	+0,9	+11,0

Cyanidbestimmung mit Variation der Katalysatorkonzentration während der Reaktion

Für die Cyanidbestimmung im Bereich von 6—60 μg/10,5 ml waren mit der vorher beschriebenen Methode zwei verschiedene Kupfermengen vorzulegen. Das bedeutet, dass sehr häufig zwei Messungen gemacht werden müssen. Nun ist es aber auch möglich, während eines Reaktionsablaufs die Konzentration von Kupfer diskontinuierlich mit einer Eppendorfpipette oder kontinuierlich mit einer Motorkolbenbürette zu erhöhen.

Diskontinuierliche Arbeitsweise

Es wird die Reaktion entsprechend der bisher beschriebenen Arbeitsweise mit einer niedrigen Kupferkonzentration (10 μg) gestartet. Falls der Wasserstoffperoxid-Zerfall innerhalb einer bestimmten Zeit (z.B. 1 Min) nicht einsetzt (erkennbar am Ausbleiben des Temperaturanstiegs), wird durch Zugabe von weiterem Kupfer die Reaktion beschleunigt. Die Katalysatorzugabe ist natürlich auch mehrmals möglich, nur sind dabei die für die Eichung des Verfahrens gewählten Zeitabstände streng einzuhalten.

Zur Bestimmung von Cyanid im Bereich von 2,8—35 μg/10,5 ml war folgende Arbeitsweise günstig. Die Reaktion wird mit einer Kupfermenge von 10 μg im Ansatz gestartet. Nach genau einer Minute wird die Kupfermenge mit einer Eppendorfpipette um 10 μg auf 20 μg erhöht. Falls nötig (bei hohen Cyanidkonzentrationen), wird die Kupfermenge nach genau 3 Min noch ein zweitesmal um 10 μg auf insgesamt 30 μg erhöht.

Abbildung 6 zeigt einige Schreiberkurven, die auf die oben beschriebene Weise erhalten wurden. Die Eichkurve dazu zeigt Abb. 7. Damit wurden unbekannte Cyanidproben bestimmt; einige Ergebnisse sind in Tab. 3 wiedergegeben.

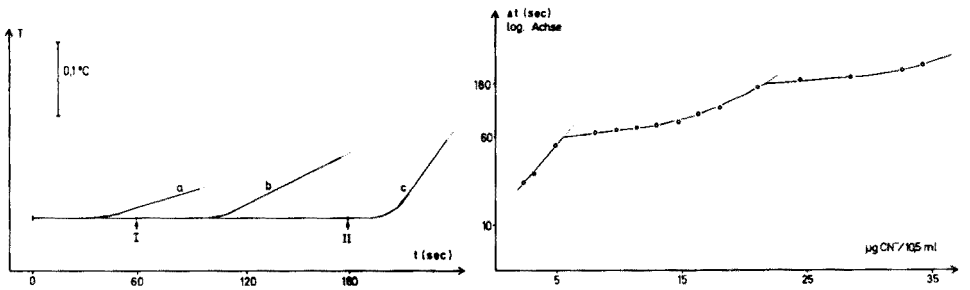

Abb. 6. Schreiberkurven für die Cyanid-Bestimmung mit Katalysatorzugabe während der Reaktion (diskontinuierliche Arbeitsweise) Bei I und II Zugabe von je 10 μg Cu. a, 4 μg CN^-; b, 16 μg CN^-; c, 26 μg CN^-.

Abb. 7. Eichkurve zur Cyanid-Bestimmung (diskontinuierliche Arbeitsweise).

TABELLE 3

Bestimmung von Cyanid
(Ergebnisse in μg CN/10,5 ml)

Gegeben	2,75	4,24	7,2	15,0	15,5	17,0	22,0	29,2	35,2
Gefunden	2,5	4,15	6,5	15,5	15,9	17,6	21,1	29,8	34,8
% rel. Fehler	−10,0	−2,1	−9,7	+3,3	+2,6	+3,5	−4,1	+2,1	−1,1

Kontinuierliche Arbeitsweise

Eine Cyanidbestimmung im Bereich von 8—90 μg/10,5 ml wurde folgendermassen ausgeführt: 5 ml 0.6 M Ammoniaklösung werden mit 8—90 μg CN^- zur Aufstellung der Eichkurve bzw. mit der CN^--Probelösung versetzt und mit bidestilliertem Wasser auf 10 ml aufgefüllt. Die Reaktion wird mit 0.2 ml einer Wasserstoffperoxid-Lösung (30 mg H_2O_2 ml^{-1}) gestartet; gleichzeitig wird der Zulauf einer Kupfer(II)-acetatlösung mit 100 μg Cu ml^{-1} (Motorkolbenbürette) mit 0,15 ml min^{-1} Zugabeschwindigkeit gestartet.

Abbildung 8 zeigt Beispiele für Schreiberkurven, die auf diese Weise erhalten wurden. Die Auswertung der Verzögerungszeit erfolgt wie bisher. Beim graphischen Auftragen von Δt gegen die Cyanidkonzentration ergibt sich eine lineare Abhängigkeit.

Die Ergebnisse der Bestimmung unbekannter Cyanidproben nach dieser Methode sind in Tab. 4 wiedergegeben.

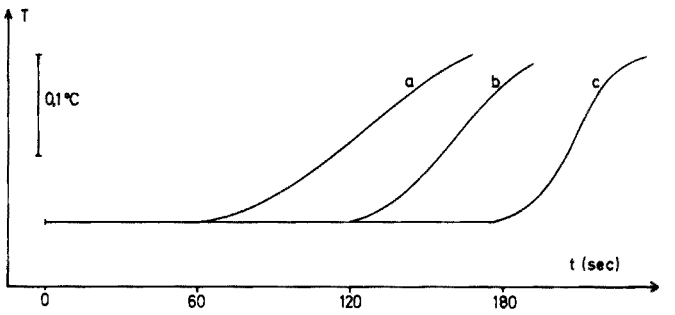

Abb. 8. Schreiberkurven für die Cyanid-Bestimmung mit Katalysatorzugabe während der Reaktion (kontinuierliche Arbeitsweise). a, 20 μg; b, 40 μg; c, 60 μg.

TABELLE 4

Bestimmung von Cyanid
(Ergebnisse in μg CN/10,5 ml)

Gegeben	8,0	12,9	21,0	30,6	45,6	60,0	63,0	72,0	84,0	90,0
Gefunden	8,2	13,5	20,5	32,8	47,0	62,0	56,5	73,0	84,0	87,0
% Rel. Fehler	+2,5	+4,6	−2,4	+7,2	+3,1	+3,3	−10,3	+1,4	±0	−3,3

LITERATUR

1 A. Quartaroli, Gazz. Chim. Ital., 61 (1931) 466; Chem. Abstr., 26 (1932) 24.
2 L. A. Nikolaev, Vestn. Mosk. Univ., 2 (1946) 105; Chem. Abstr., 42 (1948) 3653.
3 B. Kirson, Bull. Soc. Chim. Fr., (1952) 957.
4 H. Erkut, Rev. Fac. Sci. Univ. Istanbul, Ser. A, 18 (1953) 153; Chem. Abstr., 48 (1954) 31.
5 S. Pantel and H. Weisz, Anal. Chim. Acta, 68 (1974) 311.
6 S. Musha, M. Ito, Y. Yamamoto and Y. Inamori, Nippon Kagaku Zasshi, 80 (1959) 1285; Chem. Abstr., 55 (1961) 5228.
7 K. B. Yatsimirskii, Kinetic Methods of Analysis, Pergamon Press, Oxford, 1966.

Analytica Chimica Acta, 82 (1976) 155—167

BEITRÄGE ZU KINETISCH-KATALYTISCHEN ANALYSENMETHODEN UNTER VERWENDUNG OFFENER SYSTEME

H. WEISZ und K. ROTHMAIER

Lehrstuhl für Analytische Chemie, Chemisches Laboratorium der Universität Freiburg i. Br. (German Federal Republic)

(Eingegangen den 1. September 1975)

ZUSAMMENFASSUNG

Zunächst werden drei grundlegende Möglichkeiten zur Anwendung "offener Systeme" bei kinetisch-katalytischen Untersuchungsmethoden kurz diskutiert, nämlich steady state-, Stat- und Durchflussmethoden. Über zwei weitere Möglichkeiten wird berichtet: Die gleichzeitige Zugabe eines Reaktanten und eines Katalysators mit konstanter Geschwindigkeit einerseits, und die zur Aufrechterhaltung eines vorgegebenen Zustandes vom System her selbst geregelte Zugabe des Gemisches, bestehend aus einem Reaktenten und dem zu bestimmenden Katalysator andererseits. Zu beiden Methoden werden einige Beispiele beschrieben, die sowohl mit photometrischer als auch potentiometrischer Verfolgung, bzw. Steuerung arbeiten.

SUMMARY

Three basic possibilities for the application of "open systems" in catalytic-kinetic analytical methods are discussed: steady-state, stat and continuous-flow methods. Two further possibilities for such methods are reported: (1) the simultaneous addition of one reactant and the catalyst at constant speed; (2) the simultaneous addition of one reactant and the catalyst at a speed, regulated by the system itself, necessary to keep constant a preset potential or absorbance. Some examples of both methods are described.

Kinetisch-katalytische Analysenmethoden, bei denen während des Ablaufs einer Reaktion ständig von aussen Eingriffe vorgenommen werden, sei es durch Hinzufügen von Reaktionspartnern, katalytisch aktiven Substanzen oder beiden, sei es durch Wegnahme von Reaktionsprodukten, oder sei es durch gleichzeitiges Zu- und Abführen von Reaktionspartnern und Reaktionsprodukten, werden als "offene Systeme" bezeichnet. Bei den in der analytischen Chemie verwendeten katalysierten Reaktionen, die in homogener flüssiger Phase ablaufen, reagieren meist nur zwei Partner miteinander

$$A + B \xrightarrow{K} P$$

Zur Bestimmung der katalytisch aktiven Substanz K stehen logischerweise folgende Möglichkeiten zur Verfügung, die alle in Abb. 1 systematisch dargestellt sind.

Bei der sogenannten "steady state"-Methode [1] (Abb. 1(a)) wird ein Reaktionspartner (A) mit konstanter, bei jeder Bestimmung jeweils gleicher Geschwindigkeit zu einer Lösung, die den zweiten Reaktionspartner B in hoher Konzentration und den zu bestimmenden Katalysator K enthält, hinzugefügt. Die Reaktion läuft nach dem Start nur sehr langsam ab, da zu diesem Zeitpunkt nur eine geringe Konzentration des Partners A vorhanden ist. Wird der Reaktionspartner A durch die ablaufende Reaktion nicht vollständig verbraucht, so wird seine Konzentration und damit auch die Reaktionsgeschwindigkeit erhöht. Schliesslich wird ein "stationärer" Zustand in Bezug auf A erreicht, in dem die Zugabegeschwindigkeit der Reaktionsgeschwindigkeit gleich wird, d. h. in dem der kontinuierlich zugeführte Reaktant eben durch die ablaufende Reaktion verbraucht wird. Die Konzentration von A in diesem stationären Zustand ist ein Mass für die Geschwindigkeit der katalysierten Reaktion und somit ein Mass für die zu bestimmende Katalysatorkonzentration.

Bei den Strömungsmethoden (Abb. 1(d)) werden sowohl beide Reaktanten als auch der zu bestimmende Katalysator laufend mit konstanter Geschwindigkeit zugeführt und unverbrauchte Anteile (A, B) ebenso wie das Reaktionsprodukt P und der Katalysator K (in Abb. 1(d) insgesamt als P bezeichnet) abgeführt. Zur Gewinnung kinetischer Daten werden hier im allgemeinen ebenfalls Konzentrationsmessungen von Reaktanten oder auch von Produkten in einem stationären Zustand, der vom System her selbst aufgebaut wird, vorgenommen. So wird über eine "continuous flow"-Methode berichtet, bei der die Konzentration eines Reaktionsproduktes an zwei verschiedenen

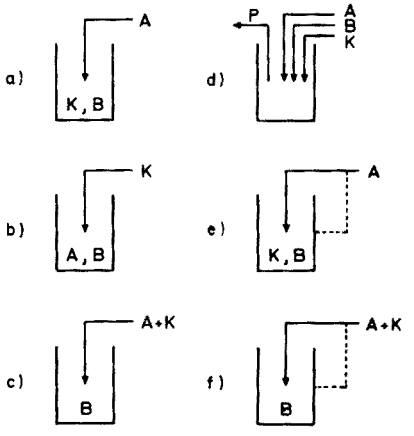

Abb. 1. Versuchsanordnungen bei offenen Systemen (A, B = Reaktanten, P = Reaktionsprodukte, K = Katalysator).

Stellen eines Strömungsrohres (Methode ohne Rückvermischung) gemessen wird [2], wobei sich aus der Differenz der beiden gemessenen Konzentrationen die unbekannte Katalysatorkonzentration ermitteln lässt. Bei Verwendung einer Durchflusszelle (Methode mit völliger Rückvermischung) ist die dort herrschende stationäre Konzentration eines Reaktionspartners oder Reaktionsproduktes ein Mass für die Katalysatorkonzentration [3, 4].

Bei der sogenannten "steady state"-Methode und den Strömungsmethoden wird der stationäre Zustand also vom reagierenden System her selbst aufgebaut. Bei den "Stat"-Methoden (Abb. 1(e)) dagegen wird ein bestimmter Zustand des Systems (z. B. Konstanthaltung der Konzentrationen von A, P oder A/P) willkürlich von aussen vorgegeben. Die kinetischen Daten erhält man hier aus der messenden Verfolgung der zur Aufrechterhaltung eines vorgewählten Zustandes gerade benötigten Zugabegeschwindigkeit des Reaktanten A (oder eines Hilfsreagenz R, welches überschüssige Mengen an Reaktionsprodukt P jeweils entfernt), wobei jede kontrollierbare (physikalische) Eigenschaft des Systems zur Steuerung (in Abb. 1(e) und 1(f)) strichliniert angedeutet) herangezogen werden kann. So sind bisher pH-Staten [5, 6], Potentiostaten [7—10], Biamperostaten [11], Absorptiostaten [9, 12] und Luminostaten [13] beschrieben worden.

Ein Blick auf Schema 1 zeigt, dass noch weiter Möglichkeiten existieren müssen. So kann man den zu bestimmenden Katalysator K zusammen mit einem Reaktionspartner (A) zum zweiten in hoher Konzentration vorliegenden Partner B mit konstanter, bei jeder Bestimmung gleicher Geschwindigkeit zugeben (Abb. 1(c)) wie dies bei der sogenannten steady state-Methode üblich ist (siehe Abb. 1(a)). Es ist auch möglich das Katalysator-Reaktanten-Gemisch (A + K) in dem Masse zum Reaktionsansatz zuzugeben, wie dies zur Aufrechterhaltung eines bestimmten vorgegebenen Zustandes (vgl. Stat-Methode Abb. 1(e)) gerade nötig ist (Abb. 1(f)). Zu beiden Verfahren werden im weiteren Verlauf dieser Arbeit einige Anwendungsbeispiele beschrieben.

Eine weitere Möglichkeit (Abb. 1(b)) besteht darin, lediglich den Katalysator K mit konstanter bei jeder Bestimmung jeweils gleicher Geschwindigkeit zu einem Reaktionsansatz zuzugeben, der die beiden Reaktanten A und B enthält. Hierzu liegen einige Anwendungsbeispiele vor, über die später gesondert berichtet werden soll.

Allen diesen zuletzt erwähnten neuen Verfahren gemeinsam ist, dass man hier verdünntere Katalysatorlösungen durch längerdauernde Zugabe zum Reaktionsansatz bestimmen kann, da bei diesen Methoden kein von vornherein festgelegtes Katalysatorvolumen angewendet werden muss.

GEMEINSAME ZUGABE VON KATALYSATOR UND REAKTANT MIT KONSTANTER GESCHWINDIGKEIT

Bei dieser Methode wird wie schon erwähnt ein Katalysator—Reaktanten-Gemisch mit konstanter, bei jeder Bestimmung gleicher Geschwindigkeit zum zweiten in hoher Konzentration vorliegenden Reaktionspartner zugefügt.

Selbstverständlich können Katalysator und Reaktant auch getrennt mit gleicher oder auch unterschiedlicher Geschwindigkeit zum zweiten Reaktionspartner zugegeben werden.

Werden die Konzentrationsänderungen des solchermassen mit konstanter Geschwindigkeit zugefügten Reaktanten im Reaktionsgemisch mit einer geeigneten Messmethode laufend verfolgt, dann beobachtet man nach dem Start der Reaktion zunächst eine rasche Konzentrationszunahme, da der Reaktant durch die vorerst noch langsam ablaufende Reaktion nicht vollständig verbraucht wird. Durch die Zunahme der Konzentration des Reaktanten und durch die des Katalysators im Reaktionsgemisch, der ja definitionsgemäss durch die Reaktion nicht verbraucht wird, nimmt die Reaktionsgeschwindigkeit im weiteren Verlauf der Reaktion ständig zu, d. h. in der Zeiteinheit wird immer mehr Reaktant umgesetzt als zu Beginn der Reaktion. Schliesslich wird ein vorübergehender Zustand erreicht, bei dem die zufliessende Menge des Reaktanten gerade durch Reaktion verbraucht wird. Danach beobachtet man eine Abnahme der Konzentration des Reaktanten, da dieser nun schneller umgesetzt wird, als er durch die vorgegebene Zugabegeschwindigkeit nachgeliefert werden kann, bedingt durch die jetzt höhere Katalysatorkonzentration. Die so erhaltenen Reaktionskurven weisen daher ein Maximum auf. Die Höhe des Maximums stellt dann bei stets gleichbleibender Konzentration des zugefügten Reaktionspartners ein Mass für die unbekannte zu bestimmende Katalysatorkonzentration dar; es ist keinesfalls nötig den gesamten Kurvenverlauf nach dem Maximum zu registrieren.

Bestimmung von Osmium(VIII) unter Verwendung der Reaktion von Cer(IV) mit Arsen(III)

Die Reaktion zwischen Cer(IV) und Arsen(III) wird durch Osmium(VIII) katalysiert [14]:

$$2\,Ce(IV) + As(III) \xrightarrow{Os(VIII)} 2\,Ce(III) + As(V)$$

Experimentelles

Zur Verfolgung des Reaktionsablaufes wurde ein Photometer ("Universal-Kolorimeter Modell J", Lange, Berlin) benutzt. Die Absorption der gelb gefärbten Cer(IV)-Lösung wurde bei 415 nm gemessen. Die Küvette hatte eine Schichtlänge von 20 mm und war zur Konstanthaltung der Temperatur mit einem temperierbaren Mantel umhüllt. Die Temperatur des Thermostaten betrug 35 °C. Zur Durchmischung der Lösungen diente ein Magnetrührer. Die Zugabe des Katalysators und des Reaktanten, bzw. des Katalysator—Reaktanten-Gemisches erfolgte hier und bei allen anderen Bestimmungen mit dieser Methode durch eine Motorkolbenbürette ("Dauerinfusionsgerät Unita I", Braun, Melsungen).

Cer(IV)sulfatlösung (0.05 M in 0.5 M Schwefelsäure). Dieser Lösung (aus einer 0.1 M Cer(IV)sulfat-Stammlösung in 0.5 M Schwefelsäure hergestellt) wird die zu bestimmende Osmiummenge beigefügt (Osmiumkonzentration in dieser Lösung: 2.5—50 ng Os ml^{-1}). Osmium-Stammlösung, 1 mg Os ml^{-1} (OsO_4).

Arsenitlösung (0.2 M) 9.892 g As_2O_3 werden in 200 ml 1 M NaOH gelöst, mit 35 ml 10 M H_2SO_4 versetzt und mit Wasser auf 500 ml aufgefüllt.

Durchführung. In die Küvette werden 1 ml Arsenitlösung, 1 ml 4 M Schwefelsäure und 7.5 ml Wasser einpipettiert. Das Gesamtvolumen beträgt 9.5 ml. Nach zehn Minuten wird die Bürettenspitze (Glaskapillare) in die Lösung eingetaucht. Anschliessend wird die Cer(IV)—Osmiumprobelösung mit einer Geschwindigkeit von 10 μl min^{-1} zum Reaktionsgemisch zugegeben. Die zeitliche Änderung der Absorption wird durch einen Schreiber registriert. Einige der so erhaltenen Kurven sind in Abb. 2 dargestellt.

Auswertung und Ergebnisse

Zur Auswertung wird aus der registrierten Kurve die Absorption im Maximum A_{max} (%) graphisch entnommen.

Zur Aufnahme einer Eichkurve (Abb. 3) wurden Messungen mit folgenden Osmiumkonzentrationen durchgeführt: 2.5, 5.0, 10.0, 20.0, 30.0, 40.0 und 50.0 ng Os ml^{-1}. Die entsprechenden A_{max} - Werte werden gegen die Katalysatorkonzentration aufgetragen.

Einige Ergebnisse sind in Tab. 1 aufgeführt.

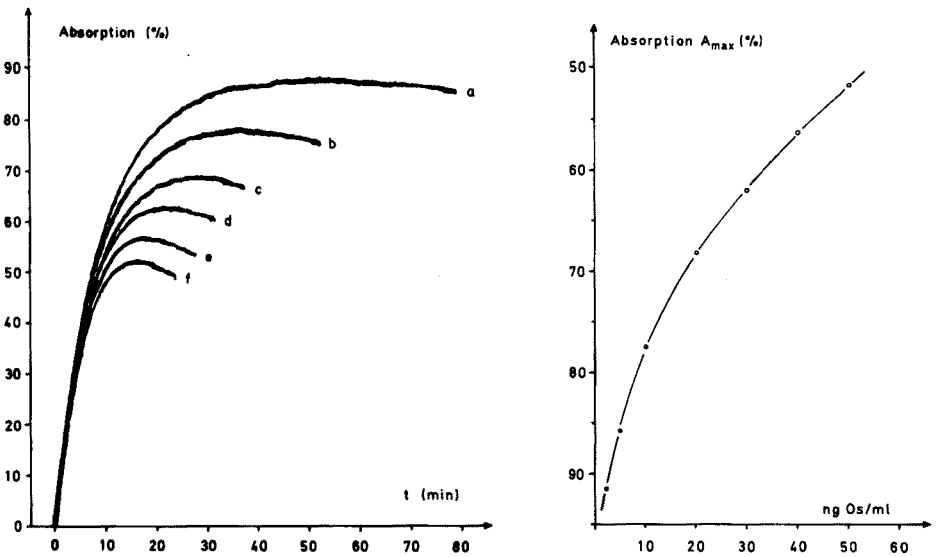

Abb. 2. Abhängigkeit der Absorption von der Zeit für verschiedene Osmiumkonzentrationen. (a) 5, (b) 10, (c) 20, (d) 30, (e) 40, (f) 50 ng Os ml^{-1}.

Abb. 3. Eichkurve zur Bestimmung von Osmium.

TABELLE 1

Bestimmung von Osmium
(Ergebnisse in ng Os ml^{-1})

Gegeben	3.00	5.00	10.75	15.00	25.00	33.00	35.00	45.00	50.00
Gefunden	3.00	5.00	10.00	15.25	25.25	32.25	35.25	47.25	48.50
% rel. Fehler	±0.0	±0.0	−6.5	+1.7	+1.0	−2.3	+0.7	+5.0	−3.0

Bestimmung von Kupfer(II) unter Verwendung der Reaktion von Eisen(III) mit Thiosulfat

Die Reaktion von Eisen(III) mit Thiosulfat wird durch Kupfer(II) katalysiert [15].

$$2\ Fe^{3+} + 2\ S_2O_3^{2-} \xrightarrow{Cu(II)} 2\ Fe^{2+} + S_4O_6^{2-}$$

Die Änderungen der Eisen(III)-Konzentration wurden hier mit Hilfe des intensiv rotviolett gefärbten Eisen(III)-Sulfosalicylat-Komplexes [16] photometrisch verfolgt (512 nm). Die zu bestimmende Kupferlösung und die Eisen(III)-sulfosalicylatlösung werden bei dieser Methode getrennt, aber mit gleicher Geschwindigkeit zu einer in hoher Konzentration vorhandenen Thiosulfatlösung zugegeben. Die Badtemperatur des Thermostaten beträgt hier 25 °C.

Experimentelles

In die Küvette werden 2 ml 0.1 M Natiumthiosulfatlösung und 7.5 ml bidest. Wasser einpipettiert. Das Gesamtvolumen beträgt 9.5 ml. Die weitere Durchführung gleicht derjenigen bei der Osmiumbestimmung. Die Zugabegeschwindigkeit der Eisen(III)-sulfosalicylatlösung (7.5 g $FeCl_3 \cdot 6\ H_2O$ und 10 g 5-Sulfosalicylsäure ad 500 ml) und der Kupferprobelösung beträgt jeweils 6.25 $\mu l\ min^{-1}$. Der Kurvenverlauf ist dem in Abb. 2 dargestellten ähnlich.

Auswertung und Ergebnisse

Zur Auswertung wird auch hier aus der registrierten Kurve die Absorption im Maximum A_{max} (%) graphisch entnommen. Die Eichkurve ähnelt der in Abbildung 3 dargestellten. Dazu wurden Messungen mit 0, 10, 30, 50, 75 und 100 $\mu g\ Cu\ ml^{-1}$ ($CuSO_4 \cdot 5\ H_2O$) durchgeführt.

Einige Ergebnisse sind in Tab. 2 aufgeführt.

TABELLE 2

Bestimmung von Kupfer
(Ergebnisse in μg Cu ml^{-1})

Gegeben	10.00	20.40	40.00	50.00	60.00	67.10	80.00	90.30	100.00
Gefunden	10.25	19.80	40.50	47.00	59.50	70.50	80.25	87.00	105.50
% rel. Fehler	+2.5	−2.9	+1.2	−6.0	−0.8	+5.1	+0.3	−3.7	+5.5

Bestimmung von Molybdän(VI) unter Verwendung der Reaktion von Jodid mit Wasserstoffperoxid

Die Reaktion zwischen Wasserstoffperoxid und Jodid wird durch Molybdän(VI) katalysiert [17]

$$H_2O_2 + 2\,J^- + 2\,H^+ \xrightarrow{Mo(VI)} J_2 + 2\,H_2O$$

Experimentelles

Der Reaktionsverlauf wurde hier potentiometrisch verfolgt. Die Potentialmessung erfolgte hier und in der nachfolgenden Bestimmung von Kupfer mit einer jodid-selektiven Elektrode (Orion, Typ 94-53) als Indikatorelektrode, einer ges. Kalomel-Bezugselektrode und dem Präzisions pH-Meter "pH 34" der Fa. Knick, Berlin.

Jodidlösung. 10^{-2} M, täglich frisch aus einer 0.1 M Kaliumjodid-Stammlösung hergestellt.

Molybdat-Stammlösung. 100 μg Mo/ml ($Na_2MoO_4 \cdot 2\,H_2O$).

Durchführung. In ein temperierbares Becherglas (Volumen ca. 35 ml) werden 1 ml Wasserstoffperoxidlösung (0.21 M, täglich frisch aus einer 30 %igen Wasserstoffperoxidlösung hergestellt), 3 ml 0.5 M Schwefelsäure und 11 ml bidest. Wasser gegeben. Das Gesamtvolumen beträgt 15 ml. Nach 10 Min (Temperatur des Thermostaten: 25 °C) werden die Bürettenspitzen und die Elektroden in die Lösung eingetaucht. Anschliessend werden die Jodidlösung und die Katalysatorlösung gesondert und mit unterschiedlicher Geschwindigkeit zum Reaktionsgemisch zugegeben, und zwar erstere mit 10 μl min^{-1} letztere mit 100 μl min^{-1}. Die Reaktionskurven sind den in Abb. 2 dargestellten ähnlich.

Auswertung und Ergebnisse

Zur Auswertung wird hier das Potential im Maximum U_{max} (mV) graphisch aus der registrierten Kurve ermittelt. Die Eichkurve wurde durch Auftragen der U_{max}-Werte gegen die Katalysatorkonzentration hergestellt. Dazu wurden Messungen mit folgenden Molybdänkonzentrationen

durchgeführt: 1, 2, 3, 4, 5, 7.5, 10, 15 und 20 μg Mo ml^{-1}. Die Eichkurve ist der in Abb. 3 dargestellten ähnlich.

Einige Ergebnisse sind in Tab. 3 zusammengestellt.

TABELLE 3

Bestimmung von Molybdän
(Ergebnisse in μg Mo ml^{-1})

Gegeben	1.20	3.60	4.70	5.85	8.15	10.85	12.40	14.75	17.70
Gefunden	1.41	3.45	4.76	5.42	8.75	10.70	12.83	14.20	16.78
% rel. Fehler	+17.5	−4.2	+1.3	−7.3	+7.4	−1.4	+3.5	−3.7	−5.2

Bestimmung von Kupfer(II) unter Verwendung der Reaktion von Jodid mit Peroxodisulfat

Die Reaktion zwischen Jodid und Peroxodisulfat wird durch Kupfer(II) katalysiert [18]

$$S_2O_8^{2-} + 2\,J^- \xrightarrow{Cu(II)} 2\,SO_4^{2-} + J_2$$

Zur Bestimmung von Kupfer wurde die gleiche potentiometrische Messanordnung wie bei der Molybdänbestimmung benutzt.

Experimentelles

Jodidlösung. $4 \cdot 10^{-2}$ M, tägl. frisch aus einer 0.1 M Kaliumjodid-Stammlösung hergestellt.

Kupfer-Stammlösung. 100 μg Cu/ml ($CuSO_4 \cdot 5\,H_2O$).

Durchführung. In das Reaktionsgefäss werden 8 ml Peroxodisulfatlösung (7 g $K_2S_2O_8$ und 0.5 g K_2SO_4 zur Stabilisierung [19] ad 250 ml; tägl. frisch hergestellt) und 2 ml 0.5 M Schwefelsäure einpipettiert. Das Gesamtvolumen beträgt 10 ml. Die weitere Durchführung gleicht derjenigen bei der Molybdänbestimmung. Die Zugabegeschwindigkeit der Jodidlösung beträgt 10 μl min^{-1}, die der Kupferprobelösung 100 μl min^{-1}.

Auswertung und Ergebnisse

Zur Auswertung wird auch hier das Potential im Maximum U_{max} (mV) graphisch aus der registrierten Kurve ermittelt. Die Eichkurve ist der in Abb. 3 dargestellten ähnlich. Dazu wurden Messungen mit 0.5, 1, 2, 4, 5, 7.5 und 10 μg Cu ml^{-1} durchgeführt.

Tab. 4 gibt einige Ergebnisse wieder.

TABELLE 4

Bestimmung von Kupfer
(Ergebnisse in μg Cu ml^{-1})

Gegeben	0.50	0.90	1.60	2.35	3.10	5.40	7.20	8.50	9.95
Gefunden	0.54	0.87	1.55	2.46	2.85	5.05	6.50	9.00	10.00
% rel. Fehler	+8.0	−3.3	−3.1	+4.7	−8.1	−6.5	−9.7	+5.9	+0.5

GEMEINSAME ZUGABE VON KATALYSATOR UND REAKTANT MIT EINER VOM SYSTEM GEREGELTEN GESCHWINDIGKEIT

Bei diesem Verfahren wird ein Katalysator—Reaktanten-Gemisch (A + K) in dem Masse zum zweiten in hoher Konzentration vorliegenden Partner B zugegeben, wie dies zur Aufrechterhaltung eines bestimmten Zustandes, z. B. der Konzentration von A nötig ist (vgl. Stat-Methoden [5—13]). Voraussetzung dabei ist, dass sich Katalysator und Reaktant A gegenseitig nicht beeinflussen. Bei Zugabe dieser Lösung zum zweiten Partner B nimmt die Konzentration des Katalysators im Reaktionsgemisch ständig zu. Damit erhöht sich laufend die Reaktionsgeswindigkeit und damit auch die Zugabegeschwindigkeit des Katalysator—Reaktanten-Gemisches, was wiederum zu einer weiteren Erhöhung der Konzentration des Katalysators im Reaktionsgemisch führt. Da sich die Reaktionsgeschwindigkeit ständig erhöht, können die Reaktionskurven nicht linear sein, sondern müssen eine Krümmung aufweisen (s. Abb. 4).

Die in jedem Punkt der Kurve gerade herrschende Zugabegeschwindigkeit der Reagenzlösung (A + K) entspricht einer bestimmten im Reaktionsansatz eben vorhandenen Katalysatorkonzentration [K]. Daher könnte die zu bestimmende Katalysatorkonzentration in der Reagenzlösung (A + K) auch aus deren Zugabegeschwindigkeit bei einem bestimmten zugegebenen Volumen ermittelt werden. Dazu müsste eine Tangente in diesem Punkt der registrierten Kurve angelegt werden. Einfacher auszuwerten ist aber eine Steigung (ctgα) zwischen zwei geeigneten, durch Vorversuche ausgewählten Volumina der Reagenslösung (A + K) (vgl. Abb. 4).

Bestimmung von Molybdän(VI) unter Verwendung der Reaktion von Jodid mit Perborat

Molybdän, das bei der Oxydation von Jodid mit Wasserstoffperoxid als Katalysator wirkt (s. oben), beschleunigt auch die Reaktion von Jodid mit Natriumperborat

$$2\,J^- + BO_3^- \xrightarrow{Mo(VI)} J_2 + BO_3^{3-}$$

Bei dieser Methode wird, gesteuert von einem Potentiostaten [7—10], zu einem Reaktionsansatz, in welchem Natriumperborat in hoher Konzentration vorliegt, eine definierte Jodidlösung, welche die zu bestimmende Menge an

Molybdän enthält, in dem Masse zugegeben, wie es gerade nötig ist, um ein vorgegebenes Potential und damit — bei Verwendung einer Platin-Indikatorelektrode — ein bestimmtes Verhältnis $[J_2]/[J^-]^2$ aufrechtzuerhalten.

Experimentelles

Zur Bestimmung von Molybdän diente der schon früher beschriebene "Potentiostat [7—10]", bestehend aus einem Steuergerät (Impulsomat), einem mV/pH-Meter, einer Motorkolbenbürette (alle Geräte vereinigt im "Combititrator 3D", Metrohm, Herisau, Schweiz), einer Platinindikator-elektrode und einer ges. Kalomel-Bezugselektrode.

Kaliumjodidlösung. $2 \cdot 10^{-3}$ M. Dieser Lösung (täglich frisch aus einer 0.1 M KJ-Stammlösung hergestellt) wird die zu bestimmende Molybdänmenge zugefügt (Molybdänkonzentration in dieser Lösung: 0.1—1.5 μg Mo ml^{-1}).

Molybdän-Stammlösung. 1 mg Mo ml^{-1} ($Na_2MoO_4 \cdot 2\,H_2O$).

Durchführung. Vor Beginn der Bestimmung werden am Combititrator folgende Einstellungen vorgenommen: Dauerimpulsbegrenzung "ΔE" 5 mV, Anpassung $dE/dVol$ 7 Skalenteile, Zugabegeschwindigkeit der Motorkolbenbürette (10 ml-Bürette) 6 Skalenteile, Schreibervorschub 15 mm min^{-1}. Der Sollwert wird so eingeregelt (ca. 435 mV), dass der Dauerimpuls nach Zugabe von etwa 1.5—2.0 ml Jodid/Molybdänlösung unterbrochen wird.

Zur Bestimmung werden 3 ml 0.05 M Natriumperboratlösung und 2 ml 2 M Salzsäure in das Reaktionsgefäss [7] einpipettiert. Die Lösung wird mit bidest. Wasser auf 50 ml aufgefüllt. Um ein reproduzierbares Ausgangspotential (512 mV) zu erhalten, werden 0.1 ml Jod/Jodidlösung ($5 \cdot 10^{-4}$ M $J_2/1.2 \cdot 10^{-3}$ M KJ) zugefügt (Gesamtvolumen der Lösung: 50.1 ml). Die Umwälzpumpe des Thermostaten (Badtemperatur 24 °C) wird nach Einführung der Elektroden und der Bürettenzuleitung in Gang gesetzt. Nach 10 Min wird die Reaktion durch Zugabe der Jodid/Molybdänprobelösung gestartet, indem man das Steuergerät (Impulsomat) einschaltet. Der Verbrauch dieser Lösung in Abhängigkeit von der Zeit wird vom Schreiber registriert (s. Abb. 4).

Auswertung und Ergebnisse

Zur Auswertung wird die Zeit t (s), die erforderlich ist, um 4 ml der Jodid/Molybdänprobelösung zwischen 6.00 und 10.00 ml zu verbrauchen, graphisch aus der registrierten Kurve entnommen. Der Cotangens des Steigungswinkels α wird wie folgt berechnet: $ctg\alpha = 4\ (ml)/t\ (s)$.

Zur Aufstellung einer Eichkurve werden die $ctg\alpha$-Werte für 0.1, 0.5, 1.0, 1.2 und 1.5 μg Mo ml^{-1} bestimmt und gegen die entsprechende Molybdänkonzentration aufgetragen. Mit Hilfe dieser so erhaltenen annähernd linearen Eichkurve werden die unbekannten Molybdänkonzentrationen bestimmt; einige Ergebnisse sind in Tab. 5 aufgeführt.

TABELLE 5

Bestimmung von Molybdän
(Ergebnisse in μg Mo ml^{-1})

Gegeben	0.106	0.280	0.385	0.460	0.581	0.717	0.938	1.193	1.425
Gefunden	0.102	0.300	0.373	0.485	0.620	0.740	0.948	1.185	1.500
% rel. Fehler	−0.3	+7.1	−3.1	+5.4	+6.7	+3.5	+1.1	−0.7	+5.3

Bestimmung von Mangan(II) unter Verwendung der Reaktion von Malachitgrün mit Perjodat

Die Oxydation von Malachitgrün durch Perjodat zu farblosen Produkten unbekannter Konstitution wird durch Mangan(II) katalysiert [20]

$$JO_4^- + \text{Malachitgrün} \xrightarrow{\text{Mn(II)}} JO_3^- + \text{Oxydationsprodukte}$$

Bei dieser Methode wird unter Verwendung eines "Absorptiostaten" (Extinktiostat) [9, 12] zu einem Reaktionsansatz, in dem Perjodat in hoher Konzentration vorliegt, eine definierte Malachitgrünlösung, welche die zu bestimmende Menge an Mangan enthält, in dem Masse zugegeben, wie es gerade nötig ist, um einen vorgegebenen Absorptionswert und damit eine bestimmte Malachitgrünkonzentration aufrechtzuerhalten.

Experimentelles

Der zur Bestimmung von Mangan verwendete Absorptiostat [9, 12] besteht aus dem Combititrator 3D und einem Photometer (s. oben). Die verwendete Küvette hatte eine Schichtlänge von 23 mm und ein Volumen von ca. 75 ml. Die Absorption der Malachitgrünlösung wurde bei 617 nm gemessen.

Malachitgrünlösung. 0.05 mg Malachitgrün/ml. Zu dieser Lösung, die aus einer Stammlösung (1 mg Malachitgrün/ml) angesetzt wurde, fügt man die zu bestimmende Manganmenge (Mangankonzentration in dieser Lösung: 0.1—1.0 μg Mn ml^{-1}).

Pufferlösung. 69 g $NaH_2PO_4 \cdot H_2O$ und 30 ml Eisessig ad 250 ml. Zu dieser Lösung gibt man 57.5 ml 0.1 M Natronlauge.

Manganchlorid-Stammlösung. 1 mg Mn ml^{-1}.

Durchführung. Am Combititrator werden vor Beginn der Bestimmung folgende Einstellungen vorgenommen: Dauerimpulsbegrenzung "ΔE" 8 mV, Anpassung dE/dVol 11 Skalenteile, Zugabegeschwindigkeit der Motorkolbenbürette (10 ml-Bürette) 2 Skalenteile, Schreibervorschub 15 mm min^{-1}. Das Ausgangspotential wird mit Hilfe der Irisblende des Photometers auf 600 mV (entsprechend 0 % Absorption) eingestellt (Verstärkung: Z_f/Z_i = 330

$k\Omega/1000\Omega$). Der Sollwert (ca. 20 mV) wird so eingeregelt, dass der Dauerimpuls nach ungefähr 3—4 ml Malachitgrün/Manganlösung unterbrochen wird.

In die Küvette werden 2 ml Natriumperjodatlösung (2 % ig) und 2 ml Pufferlösung einpipettiert. Diese Lösung wird mit bidest. Wasser auf 45 ml aufgefüllt. Nach Einführung der Bürettenspitze wird die Umwälzpumpe des Thermostaten (Badtemp. 30 °C) eingeschaltet. Nach 10 Min wird die Reaktion durch Zugabe der Malachitgrün/Manganprobelösung gestartet, indem man das Steuergerät (Impulsomat) einschaltet. Der Verbrauch dieser Lösung in Abhängigkeit von der Zeit wird vom Schreiber registriert. Die erhaltenen Reaktionskurven sind der in Abb. 4 dargestellten ähnlich.

Auswertung und Ergebnisse

Zur Auswertung wurde hier die Zeit t (s), die erforderlich ist, um 5 ml der Malachitgrün/Manganprobelösung zwischen 5.00 und 10.00 ml zu verbrauchen, graphisch aus der registrierten Kurve entnommen. Der Cotangens des Steigungswinkels α (vgl. Abb. 4) wird nach $\mathrm{ctg}\alpha = 5\ (\mathrm{ml})/t\ (\mathrm{s})$ berechnet.

Zur Aufstellung der Eichgeraden wurden vier Messungen mit bekannten Mangankonzentrationen (0.1, 0.4, 0.7 und 1.0 μg Mn ml^{-1}) durchgeführt. Die entsprechenden $\mathrm{ctg}\alpha$-Werte werden graphisch gegen die Mangankonzentra-

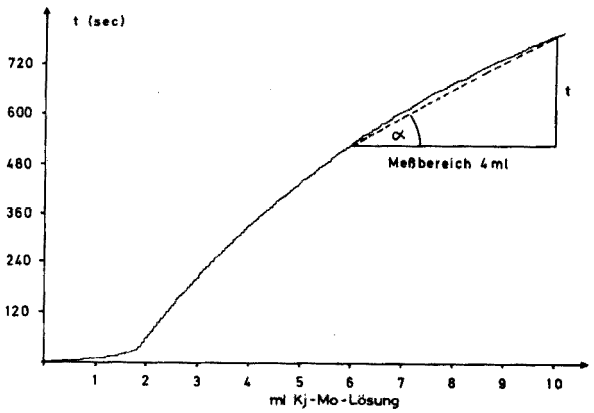

Abb. 4. Reaktionskurve für 1.2 μg Mo ml^{-1}.

TABELLE 6

Bestimmung von Mangan
(Ergebnisse in μg Mn ml^{-1})

Gegeben	0.100	0.125	0.250	0.340	0.500	0.622	0.750	0.910	1.000
Gefunden	0.103	0.117	0.247	0.320	0.500	0.613	0.763	0.893	1.010
% rel. Fehler	+3.0	−6.4	−1.2	−5.9	±0.0	−1.4	+1.7	−1.9	+1.0

tion aufgetragen.

Einige Ergebnisse von Einzelbestimmungen gibt Tab. 6 wieder.

Wir danken Herrn B. Schoch, Freiburg, für die Durchführung eines Teiles dieser Versuche.

LITERATUR

1 H. Weisz und H. Ludwig, Anal. Chim. Acta, 60 (1972) 385.
2 A. M. Wilson, Anal. Chem., 38 (1966) 1784.
3 H. Weisz und H. Ludwig, Anal. Chim. Acta, 62 (1972) 125.
4 H. Ludwig, H. Weisz und T. Lenz, Anal. Chim. Acta, 70 (1974) 359.
5 K. M. Møller, Biochim. Biophys. Acta, 16 (1955) 162.
6 H. V. Malmstadt und E. H. Piepmeier, Anal. Chem., 37 (1965) 34.
7 H. Weisz, D. Klockow und H. Ludwig, Talanta, 16 (1969) 921.
8 D. Klockow, H. Ludwig und M. A. Giraudo, Anal. Chem., 42 (1970) 1682.
9 D. Klockow, H. Weisz und K. Rothmaier, Z. Anal. Chem., 264 (1973) 385.
10 H. Weisz, K. Rothmaier und H. Ludwig, Anal. Chim. Acta, 73 (1974) 224.
11 S. Pantel und H. Weisz, Anal. Chim. Acta, 70 (1974) 391.
12 H. Weisz und K. Rothmaier, Anal. Chim. Acta, 75 (1975) 119.
13 S. Pantel und H. Weisz, Anal. Chim. Acta, 74 (1975) 275.
14 R. D. Sauerbrunn und E. B. Sandell, Mikrochim. Acta, (1953) 22.
15 A. C. Oudemans, Z. Anal. Chem., 6 (1867) 129.
16 J. Bognár und O. Jellinek, Anal. Chim. Acta, 29 (1963) 395.
17 K. B. Yatsimirskii, Kinetic Methods of Analysis, Pergamon Press, Oxford, 1966, S. 96.
18 A. V. Kiss und L. V. Zombory, Rec. Trav. Chim. Pays-Bas, 46 (1927) 225.
19 Gmelins Handbuch der Anorganischen Chemie, Kalium (System Nr. 22), Verlag Chemie, Berlin, 1937, S. 761.
20 A. A. Fernandez, C. Sobel und S. L. Jacobs, Anal. Chem., 35 (1963) 1721.

Analytica Chimica Acta, 82 (1976) 169—174

2-[2-(5-BROMOPYRIDYL)AZO]-5-DIMETHYLAMINOPHENOL; A NEW SENSITIVE REAGENT FOR CADMIUM

SHOZO SHIBATA, EIJIRO KAMATA and RYOZO NAKASHIMA

Government Industrial Research Institute, Nagoya, Hirate-machi, Kita-ku, Nagoya (Japan)

(Received 9th June 1975)

SUMMARY

Cadmium(II) reacts with 2-[2-(5-bromopyridyl)azo]-5-dimethyl-aminophenol (5-Br-DMPAP) in aqueous solution; the complex can be extracted with organic solvents such as chloroform, 3-methyl-1-butanol and methyl isobutyl ketone at pH 8—10.5 to give a red solution which absorbs at 525—555 nm. The absorbance in organic solvents is stable and the system conforms to Beer's law; the optimal range in 3-methyl-1-butanol for measurement in 1.00-cm cells is 0.01—1 p.p.m. cadmium. Moderate amounts of many cations and anions do not interfere, and interfering cations such as zinc, copper, manganese and nickel can be separated by extraction with dithizone. The 5-Br-DMPAP method is one of the most sensitive procedures available for the determination of cadmium; the molar absorptivity in a 3-methyl-1-butanol extract is $1.41 \cdot 10^5$ $1\ mol^{-1}\ cm^{-1}$ at 555 nm.

A study of some azo compounds containing various heterocycles has been made [1—8] with the object of preparing sensitive organic reagents which have molar absorptivities of the order of 10^5 for different metals; such organic reagents were very rare until a few years ago. Previously, the authors reported [3] that the molar absorptivities of the copper, zinc and nickel complexes of 2-[2-(5-bromopyridyl)azo]-5-dimethylaminophenol (5-Br-DMPAP) in alcoholic aqueous solution were 1.0, 1.33 and $1.28 \cdot 10^5$ $l\ mol^{-1}\ cm^{-1}$, respectively. This compound was observed to give with cadmium a red complex which is soluble in various organic solvents. This paper describes the use of 5-Br-DMPAP as an extraction—photometric reagent for cadmium; its sensitivity is compared with other typical reagents for the determination of cadmium in Table 1.

EXPERIMENTAL

Reagents

5-Br-DMPAP solution

An ethanolic solution (0.05 %) was prepared; this was stable for several months when stored in a refrigerator. The reagent was prepared by coupling *m*-dimethylaminophenol with the diazotate of 5-bromo-2-aminopyridine in alcoholic solution.

TABLE 1

Sensitivity of some reagents for cadmium

Reagents		Molar absorptivity (10^4 l mol^{-1} cm^{-1})
1	Diphenylcarbazone (Bu_3PO_4)	4.0 at 530 nm
2	5-Cl-PAN($CHCl_3$) [5]	7.0 at 560 nm
3	PAN($CHCl_3$) [8]	4.9 at 555 nm
4	Dithizone(CCl_4) [9]	8.8 at 520 nm
5	Pyrrolidinedithiocarbamate [10]	3.5 at 262 nm
6	Glyoxal bis(2-hydroxy-anil) [11]	2.6 at 610 nm
7	PAR [12]	8.4 at 495 nm
8	6-Bromobenzthiazolyl-(2-azo-1)-2-naphthol(BBTAN) [13]	6.35 at 595 nm
9	Thiodibenzoylmethane (Benzene) [14]	3.0 at 406 nm
10	Calmagite [14]	1.2 at 530 nm
11	5-Br-DMPAP(3-Methyl-1-butanol)	14.1 at 555 nm

Buffer solutions

Mixtures of 0.1 M sodium chloride and 0.1 M hydrochloric acid and of 0.1 M ammonium chloride and 0.1 M ammonia were used to adjust pH.

Standard cadmium solution, $1.00 \cdot 10^{-2}$ M

0.562 mg of 99.99 % cadmium metal was dissolved in 30 ml of 12 M hydrochloric acid. This solution was concentrated to about 10 ml, cooled, and diluted to 500 ml in a volumetric flask with distilled water.

Organic solvents were purified by standard methods. All solutions were prepared with twice-distilled water from analytical-grade chemicals.

Apparatus

Absorbance curves were measured with a Model 323 Hitachi recording spectrophotometer with 1-cm cells: absorbances were measured with a Model 139 Hitachi spectrophotometer with 1-cm cells. A Hitachi-Horiba M5 type pH meter was used.

General procedure for the determination of cadmium

Transfer an aliquot of the slightly acidic sample solution containing 0.5—10 μg of cadmium to a 50-ml separatory funnel, and dilute to about 20 ml with water. Add 0.7 ml of ethanolic 0.5 % 5-Br-DMPAP solution and 5 ml of pH 9 buffer solution. Mix well, and add 10 ml of 3-methyl-1-butanol. Shake vigorously for 1 min. Transfer the organic phase to a glass-stoppered conical flask, and dehydrate with anhydrous sodium sulfate. Measure the absorbance at 555 nm in 1-cm cells against a reagent blank carried through the same procedure.

RESULTS AND DISCUSSION

Optimal conditions and sensitivity

The effects of several solvents on the absorbance of the extracted complex are shown in Table 2. 3-Methyl-1-butanol was chosen as the solvent for extraction because of the relatively high molar absorptivity found although MIBK is probably the most suitable solvent for atomic absorption analysis.

The addition of 5-Br-DMPAP to a solution containing cadmium causes the immediate formation of a red complex which is sparingly soluble in water. The absorbance curves of the reagent and of its cadmium complex in various solvents are shown in Fig. 1. The absorbance of the reagent is very small at the wavelength of maximum absorbance of its cadmium complex.

To establish the optimal pH, standard amounts of cadmium and 5-Br-DMPAP solution were buffered at various pH values. The final pH of each aqueous solution was measured after extraction and the absorbance was measured at 555 nm. A plot of absorbance against pH showed that although the maximum absorbance was constant over the range pH 8—10.5, the absorption decreased sharply from pH 6.5—8 and pH 10.5—13. Subsequent determinations were carried out at pH 9.

The absorbances of a series of solutions containing known amounts of cadmium and various amounts of 0.5 % dye solution were measured at pH 9. It was found that 0.7 ml of the dye solution sufficed to complex 10 μg of cadmium; with higher concentrations the absorbance was essentially constant. The time for the absorbance of the complex to reach a stable value was only a few minutes at room temperature.

The calibration graph was linear over the range 0.01—1 p.p.m. cadmium. The molar absorptivity of the complex is shown in Table 1.

TABLE 2

Effect of solvent on sensitivity

Solvents	λ_{max} (nm)	Sensitivity (μg Cd cm^{-2})	Molar absorptivity ($\cdot 10^5$ l mol^{-1} cm^{-1})
Chloroform	525	0.00095	1.18
Ethyl acetate	525	0.00084	1.33
Chlorobenzene	525	0.00098	1.14
1,2-Dichloroethane	525	0.00097	1.16
4-Methyl-2-pentanone (MIBK)	525	0.00117	0.96
Ether	555	0.00255	0.44
1-Pentanol	555	0.00080	1.40
3-Methyl-1-butanol	555	0.00079	1.41
1-Butanol	555	0.00087	1.29

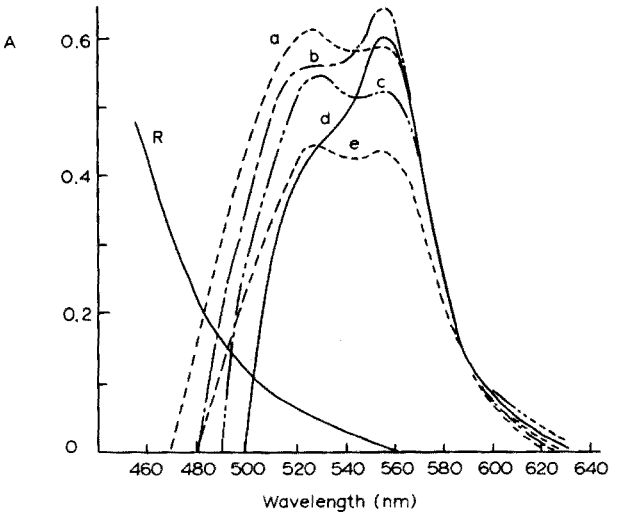

Fig. 1. Absorption spectra of cadmium—5-Br-DMPAP complex in (a) ethyl acetate, (b) 3-methyl-1-butanol, (c) chloroform, (d) 1-butanol, (e) 4-methyl-2-pentanone (MIBK). 5.6 μg Cd/10 ml, reagent in excess, versus reagent blank. (R) Reagent in chloroform.

Effect of foreign ions

The analytical method was applied to a fixed amount of cadmium in the presence of various amounts of other ions (Table 3). Copper, manganese, nickel and zinc react with the reagent to give intense colour complexes that interfere in the general procedure for determining cadmium. A preliminary separation is therefore necessary.

Procedure for the determination of cadmium in the presence of interfering metals

Transfer an aliquot of the slightly acidic sample solution containing 1—6 μg of cadmium to a 100-ml separatory funnel and dilute to 50 ml with water. Add 5 ml of 20 % sodium potassium tartrate and 1 ml of 20 % hydroxyammonium chloride solution, and then add 5 ml of 25 % sodium hydroxide solution. Add 5 ml of dithizone—chloroform solution (20 mg l^{-1}) and shake vigorously for 1 min. If the aqueous phase is brownish-yellow, add another 10 ml of the dithizone—chloroform solution to the aqueous phase and shake vigorously for 1 min. This procedure is repeated until the aqueous phase is brown. Combine all organic phases in a 100-ml separatory funnel and add 5 ml of dithizone—chloroform solution (200 mg l^{-1}). Wash the organic phase with 50 ml of water, and transfer the organic phase to a 50-ml separatory funnel which contains 20 ml of pH 2 buffer solution. Shake vigorously for several minutes and discard the organic phase. Wash

TABLE 3

Effect of foreign ions (5.70 μg of cadmium taken)

Ion	Amount added (μg)	Cd found (μg)	Error (μg)	Ion	Amount added (μg)	Cd found (μg)	Error (μg)
Al^{3+}	104	5.59	−0.11	Ni^{2+}	0.25	6.15	+0.45
	208	5.59	−0.11		0.5	6.59	+0.89
	416	5.48	−0.22	Pb^{2+}	5	5.77	+0.07
Bi^{3+}	5	5.70	±0.00		10	6.37	+0.67
	20	5.92	+0.02	Sn^{4+}	2.5	5.70	±0.00
Co^{2+}	1	7.04	+1.39		5	5.25	−0.45
	0.5	6.26	+0.57	Th^{4+}	10	5.70	±0.00
Cr^{3+}	1	5.53	−0.17		15	5.48	−0.22
	2	5.35	−0.34		20	4.82	−0.88
	3	5.14	−0.56	Tl^{+}	50	5.70	±0.00
Cu^{2+}	0.1	5.81	+0.11		200	5.48	−0.22
	0.25	6.15	+0.45	W^{6+}	200	5.70	±0.00
	0.5	6.48	+0.78		400	5.70	±0.00
Fe^{3+}	10	5.48	−0.22	Y^{3+}	5	6.26	+0.56
	20	5.35	−0.34	Zn^{2+}	0.16	5.70	±0.00
	40	4.70	−1.00		0.25	6.04	+0.34
Hg^{2+}	5	5.93	+0.23		0.41	6.71	+1.01
	10	6.37	+0.67	Zr^{4+}	1	5.70	±0.00
La^{3+}	10	4.70	−1.00		5	5.60	−0.10
Mn^{2+}	0.25	6.37	+0.67		10	5.37	−0.33
	0.5	6.71	+1.01		20	5.25	−0.45

the aqueous phase with small amounts of dithizone—chloroform solution. Transfer the aqueous phase into a 50-ml separatory funnel, add 0.7 ml of ethanolic 0.5 % 5-Br-DMPAP solution, and adjust to pH 9 with buffer. After several minutes add 10 ml of 3-methyl-1-butanol and shake vigorously for 1 min. Transfer the organic phase to a glass-stoppered conical flask and dehydrate with anhydrous sodium sulfate. Measure the absorbance at 555 nm in 1-cm cells against a reagent blank. Results obtained by this method for cadmium in the presence of various ions that normally interfere are shown in Table 4. A photometric method for determining cadmium directly in the organic phase by dithizone after the separation of cadmium from metals such as nickel, cobalt, copper, zinc, aluminium, iron, chromium, manganese and magnesium by extraction with a solution of tribenzylamine in dichloroethane from a 0.3 M hydrobromic acid medium has been described [15]. This procedure may also be useful for the 5-Br-DMPAP method.

TABLE 4

Elimination of interfering ions by dithizone method (5.00 μg of cadmium taken)

Ion	Amount added (mg)	Cd found (μg)	Error (μg)
Cu^{2+}	0.01	5.2	+0.2
	0.025	5.4	+0.4
	0.05	5.9	+0.9
Zn^{2+}	0.4	4.9	−0.1
	1.0	5.5	+0.5
Pb^{2+}	0.1	5.0	±0.0
	0.2	5.5	+0.5
	0.5	6.4	+1.4
Ni^{2+}	0.2	4.9	−0.1
	0.5	4.7	−0.3
Co^{2+}	0.05	5.0	±0.0
	0.1	5.3	+0.3

Nature of complex

The epirical formula of the complex was studied by the continuous variation and mole ratio methods. A typical plot showed unequivocally that a stable 1:2(Cd:R) complex is formed at pH 9, λ_{max} = 555 nm.

REFERENCES

1 S. Shibata, M. Furukawa and Y. Ishiguro, Anal. Chim. Acta 55 (1971) 231.
2 S. Shibata, M. Furukawa and K. Goto, Anal. Chim. Acta, 71 (1974) 85.
3 S. Shibata, M. Furukawa and K. Toei, Anal. Chim. Acta, 66 (1973) 397.
4 S. Shibata, M. Furukawa and E. Kamata, Anal. Chim. Acta, 73 (1974) 107.
5 S. Shibata, M. Furukawa and Y. Ishiguro, Mikrochim. Acta, (1972) 721.
6 S. Shibata, K. Goto and E. Kamata, Anal. Chim. Acta, 45 (1969) 279.
7 S. Shibata, M. Furukawa, E. Kamata and K. Goto, Anal. Chim. Acta, 50 (1970) 439.
8 S. Shibata, Anal. Chim. Acta, 25 (1961) 348.
9 R. E. Stanton, A. J. McDonald and I. Carmichel, Analyst (London), 87 (1962) 134.
10 M. B. Kalt and D. F. Boltz, Anal. Chim., 40 (1968) 1096.
11 N. Oi, Bunseki Kagaku, 9 (1960) 770.
12 M. Kitano and J. Ueda, Nippon Kagaku Zasshi, 91 (1970) 760.
13 D. A. Drapkina, W. G. Bruds, K. A. Smirnowa and I. H. Doroschina, Zh. Anal. Khim., 17 (1962) 940.
14 B. Schuhknecht, G. Robisch and E. Uhlemann, Anal. Chim. Acta, 69 (1974) 329.
15 A. I. Vasyutinskii, N. A. Kisel and E. N. Matveeva, Zh. Anal. Khim., 23 (1968) 1847.

Analytica Chimica Acta, 82 (1976) 175—185

ANALYSIS OF THE PHOSPHOLIPID COMPOSITION OF *PLASMODIUM KNOWLESI* AND RHESUS ERYTHROCYTE MEMBRANES*

S. McCLEAN**, W. C. PURDY, A. KABAT, J. SAMPUGNA and R. DeZEEUW***

Department of Chemistry, University of Maryland, College Park, Maryland 20742 (U.S.A.)

G. McCORMICK

Department of Endocrinology and Metabolism, Division of Medicine, Walter Reed Army Institute of Research, Washington, D.C. 20012 (U.S.A.)

(Received 30th June 1975)

SUMMARY

Methods for the separation and analysis of the phospholipid classes have been studied. The lipid extracts of normal and *Plasmodium knowlesi*-infected rhesus erythrocytes and of the parasite itself have been examined for phospholipid composition on an animal-to-animal basis. Several differences were apparent between the phospholipids of parasites and infected host cells. Phosphatidylinositol, phosphatidylcholine, and phosphatidylethanolamine represented larger percentages in the parasite than in the host; the average phosphatidylinositol content was 1.8 % in infected host cells and 4.3 % in parasites. Sphingomyelin and phosphatidylserine were also strikingly different in the two membranes; in the parasite they averaged less than 20 % and 33 % respectively of their level in the infected red blood cell.

Almost one-half of the mass of plasma membranes of mammalian cells is lipid [1, 2]; in human erythrocytes phospholipids account for about 60 % of the total lipid content [3]. The major phospholipids so far detected in mammalian erythrocytes are phosphatidylcholine (PC), phosphatidylethanolamine (PE), phosphatidylserine (PS), sphingomyelin (SM) and phosphatidylinositol (PI). These account for over 90 % of the total phospholipids in all species for which data are now available [4].

That host lipids might be important to malarial parasites was indicated by early studies which showed that growth of *Plasmodium knowlesi* in monkeys resulted in increased levels of phospholipids in parasitized cells [5, 6]. These findings were supported by the investigation of Angus et al. [7] who reported that *Plasmodium knowlesi* cells contain up to 5 times as much phospholipid as non-parasitized cells.

---

*This is publication no. 1316 in the Army Research Program in Malaria.

**Present address: Clinical Laboratories, Clinical Center, National Institutes of Health, Bethesda, Md. 20014.

***Present address: Laboratory for Pharmaceutical and Analytical Chemistry, State University, Groningen, The Netherlands.

Initial work by Rock et al. [8] on the composition of these phospholipids indicated a number of differences between the membranes of parasite and host. This work was continued on pooled samples by deZeeuw et al. [9]. Their work produced much smaller standard deviations for individual phospholipids than did the work of Rock et al. [8]. However, their results showed large variations between pooled samples. This paper reports analyses done on an animal-to-animal basis; normal and infected samples from the same animal have been examined and the results are essentially in agreement with those of Rock et al. [8]. However, some differences which were only suggested by their pooled samples appear more definite in samples from individual monkeys.

EXPERIMENTAL

The adenosine diphosphate solution was made by dissolving 100 mg of adenosine-5′-diphosphate, monosodium dihydrate in 10 ml of normal saline. The solution was stored at 4 °C.

The column for removing platelets used glass beads of 0.11-mm diameter. After each use the beads were rinsed from the column into a large beaker and washed several times with water to remove most of the residual blood. Adsorbed protein was removed by stirring the beads for 6—18 h with 6 M HCl. The beads were rinsed several times with distilled water until the rinse water had a neutral pH, then dried at 100 °C. A small plug of glass wool was used to keep the beads in place. For each 1-ml of whole blood expected 1.5 g of beads were used. After packing, the column was tamped gently on a soft surface for about 1 min to allow the beads to settle into place.

The cellulose powder column was packed with Whatman column chromedia fibrous cellulose powder, with a plug of glass wool to hold the powder in place. For every 10 ml of whole blood 1.5 g of powder was poured into the column and tamped gently for 1—2 min to settle.

MgCa—NS solution was made by adding 1.0 ml each of 0.1 M $MgCl_2$ and 0.1 M $CaCl_2$ to 1 l of normal saline solution.

The 0.2 % saponin solution was prepared by adding 0.1 M $MgCl_2$ to 1 l of normal saline; this solution was used to dissolve 0.5 g of saponin in a 250-ml volumetric flask.

The chloroform—methanol solution used for extraction contained 10 mg of 2,6-di-(tert) butyl-*p*-cresol for every 1 l of 2:1 chloroform—methanol.

The wash solution contained 480 ml of methanol, 470 ml of water and 30 ml of chloroform.

The procedure for fractionation of blood and lipid extraction was similar to that of Rock et al. [8], but differs in a number of details.

Rhesus monkeys were inoculated intravenously with *Plasmodium knowlesi*. Beginning about three days following inoculation, parasitemia was monitored by daily smears. When parasitemia was between 20 and 60 %, whole blood was collected by cardiac puncture into sodium heparin (1 volume of heparin

to 25 volumes of blood). Blood samples from normal animals were also obtained by cardiac puncture. Inoculation with *Plasmodium knowlesi* did not occur until at least 1 month after drawing the normal sample.

The sample was incubated at room temperature for 15 min with 1 ml of adenosine diphosphate solution to promote platelet aggregation. Following incubation the sample was spun at 500 G for 10 min. The resulting plasma supernate was saved for future lipid extraction and the pellet resuspended to the original volume with CaMg—NS. This mixture was then filtered under 5—8 p.s.i. nitrogen pressure through a column of glass beads to remove platelets. Leukocytes were removed by filtering the effluent from the first column through a cellulose powder column again with 5—8 p.s.i. nitrogen pressure.

This filtrate from the second column was separated into 4 tubes, diluted with an equal volume of CaMg—NS and centrifuged at 500 G at 4 °C for 10 min. The supernate was discarded and the washing repeated once more. CaMg—NS was added to each tube along with an equal volume of 0.2 % saponin in Mg—NS. The tubes were incubated at 37 °C for 30 min then centrifuged at 500 G for 10 min. The supernate containing the lysed erythrocytes was saved for use below. The parasite pellet was washed with 20 volumes of CaMg—NS and recentrifuged. Finally the parasite pellet was resuspended in CaMg—NS for storage.

The red cell membranes were recovered by centrifugation at 23600 G for 15 min. The red cell membranes were washed twice with an equal volume of ice cold CaMg—NS and spun at 23600 G between washings.

Both parasites and RBC membranes were stored at −20 °C until lipid extraction. Extraction was done in a series of glass screw cap tubes. To each tube were added 2 ml of sample and 8 ml of chloroform—methanol. The tubes were capped, shaken for 3 min, then centrifuged for 30 min at 1086 G. The upper phase was removed by aspiration and an equal amount of wash solution added. The lower phase was washed by shaking it with the wash solution, centrifuging, then removing the upper phase by aspiration. This wash step was performed twice. The lower phase was concentrated by evaporation to 3—5 ml for storage. Prior to separation of the phospholipids the extract was further reduced in volume to about 250 μl, of which 10—20 μl would be used for spotting each t.l.c. plate.

The procedure used for the separation and analysis of phospholipids was essentially that described by Nelson [10]. Phospholipids were separated by two-dimensional thin-layer chromatography with chloroform—methanol—ammonia (65:33.5:5.5,v/v) in the first dimension and chloroform—acetone—methanol—acetic acid—water (50:20:10:10:5,v/v) in the second. The developed chromatogram was visualized with iodine vapor and the individual spots transferred from the plate to reaction tubes. A 2:1 mixture of 85 % sulfuric acid and 60 % perchloric acid was used to digest each phospholipid. Following digestion, the resulting inorganic phosphorus was treated with ammonium molybdate to form the blue phosphomolybdate complex,

and the absorbance was read at 795 nm.

Phospholipid samples which contained less than 0.5 μg of lipid phosphorous received one fifth as much of all reagents as did samples which contained more than 0.5 μg. The final volume for the large samples was about 5 ml; the final volume for the small samples was 1 ml. An inorganic standard was run with each of the two groups to determine the exact ratio between the groups. This ratio was then used to adjust the absorbance reading of one group to that of the other for calculation of percent composition.

RESULTS

Several checks were made on the colorimetric procedure. Standard curves were run with both an inorganic phosphorus standard and a phospholipid control. With either 1-ml or 5-ml samples, both standards gave linear plots of absorbance vs. amount of phosphorous up to an absorbance of 1. Figure 1 indicates the extent of the deviation above unit absorbance. As is explained later, the use of standard curves could be avoided by diluting large samples with reagent blank to read between 0 and 1 absorbance units; quantitative color development for amounts of phosphatidylcholine less than 1200 μg was found.

Chen et al. [11] reported a curve showing the effect of acidity on the absorbance of the phosphomolybdate complex with ascorbic acid as the reducing agent. The use of 1-amino-2-naphthol-4-sulfonic acid (ANSA) as

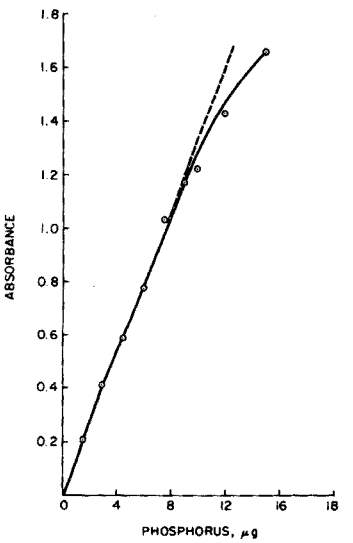

Fig. 1. Absorbance at 795 nm of 5-ml samples of phosphate standard, $Na_2HPO_4 \cdot 7H_2O$. Digestion and color development in the presence of silica gel HR. The data were taken on 5 different days over a period of 40 d. The points below unit absorbance represent averages of 4 measurements, the points above 1 are single measurements.

the reducing agent gives a similar curve, shown in Fig. 2; a plateau region occurs at 1.6—2.7 sulfuric acid instead of 0.4—1.0 N. Chen et al. [11] refer, however, to calculated values for the sulfuric acid concentration after color development; for Fig. 2, the values are based on titrations of those solutions with sodium hydroxide. Since the color development must take place within a certain pH range, it was decided to check the effect on acidity of large amounts of PC in order to determine whether significant amounts of acid might be consumed during the digestion and result in a color change. PC, in amounts of 257—2,570 μg, was added directly to flasks and digested, and the color developed. These samples were diluted sufficiently with water to give a reading below 1 absorbance unit and then read on the spectrophotometer against an appropriate blank diluted with a like amount of water. Figure 3 shows the resulting calibration curve which indicates that, even for large amounts of lecithin, significant amounts of acid were not consumed; if appreciable acid were consumed the calibration curve would be concave upward on the basis of Fig. 2. The apparent break in the slope above 6 absorbance units Fig. 3 indicates that samples should be kept small enough to give an absorbance below 6. The reason for this break at 6 is not known presently. It may be an indication that the rate-controlling step of the phosphorus-catalyzed reduction of molybdic acid undergoes a change with increasing phosphorus concentrations, or it might simply be that

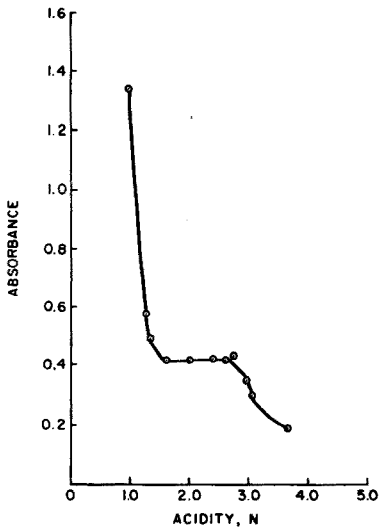

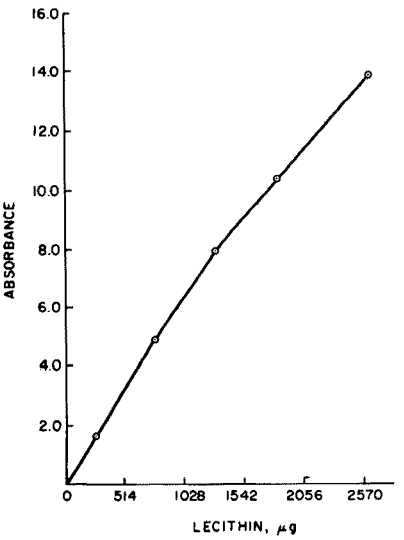

Fig. 2. Effect of acidity on the absorbance at 795 nm of the phosphomolybdate complex given by ANSA as the reducing agent. Samples were run in duplicate and titrated with standardized sodium hydroxide after color development.

Fig. 3. Effect of large amounts of lecithin on the linearity of the calibration curve. Samples were diluted with sufficient water to yield an absorbance below 1 and corrected by the dilution factor before plotting.

larger amounts of various reagents need to be added.

That significant amounts of acid were not consumed was further verified by titrating each of the samples with sodium hydroxide; for weights of PC ranging from 0—2770 μg, the average normality found was 2.38 ± 0.02.

The limit of detection for samples measured in a final volume of 5 ml was 0.075 μg of phosphorus; for 1 ml samples the limit was 0.015 μg. To verify whether measuring the major phospholipids in the 5-ml volume and the minor phospholipids in the 1-ml volume was worth the extra time required, standard deviations were determined for both combinations. Table 1 (A) indicates the variance for each phospholipid when all phospholipids were measured in a 5-ml volume. Part B of Table 1 shows the variance when the major and minor components were reacted in different volumes. With the exception of PC, the relative standard deviations were diminished by analyzing the smaller components with the more sensitive assay. If the standard deviation of PC had been computed on the 7 closest values, it would be ±0.56 %. Although handling the major and minor components differently gave more trouble, the improved precision seemed worth the increased effort; thus, when the percent composition of a component was expected to be below 6 %, it was measured in a 1-ml volume.

Table 2 contains phospholipid levels of erythrocytes before and after infection. Trends apparent in this table are increases in PC (and probably PI) and decreases in PE and SM with infection. Parasitemias for the various monkeys are listed in Table 3.

Since infected monkeys were sacrificed when parasitemia was between 20 and 60 %, the erythrocytes from infected animals were, at best, a mixture of uninfected and infected cells. However, saponin lysis can result in most of the infected RBC membranes remaining with the parasites and the erythrocyte fraction being composed primarily of uninfected cells [12]. Thus the differences in phospholipid composition seen in Table 2 between erythrocyte fractions from normal and parasitized animals may be due either to differences between normal and uninfected cells or normal and infected cells. It may also be possible that both uninfected and infected cells in the parasitized animal differ from cells in the normal animal.

Table 4 shows the phospholipid composition of infected RBC's and parasites from the same monkey. PC and PE levels were higher in the parasite than in the RBC membrane, sometimes by as much as 25—30 %. Phosphatidylinositol was much higher in the parasite than in the erythrocyte; its level in the parasite was usually at least double that in the RBC. The levels of SM and PS in the parasite, on the other hand, were about 20 % and 33 % respectively of what they were in the host cell. Most, if not all, methods for removal of parasites from host cells are believed either to damage the parasite membrane or not to remove the host membrane. Saponin lysis, which was used in the preparation of our samples, falls in the latter group [13]. Despite the almost certain contamination of the parasite fraction by host cells, the differences found between these fractions are considered to be real

TABLE 1

Standard deviation of two methods of phospholipid determination

A. All components reacted in same volume				B. Major and minor components reacted in different volumes		
Component	Monkey L719, normal RBC-8 trials			Monkey L248, normal RBC-8 trials		
	Percent composition	s	s_r	Percent composition	s	s_r
PE	32.7	1.05	3.2	32.4	0.89	2.7
PC	37.1	0.50	1.3	38.2	1.06	2.8
SM	17.9	0.64	3.6	17.4	0.25	1.4
PS	9.4	0.65	6.9	8.8	0.21	2.4
PI	1.1	0.18	15.8	1.5	0.14	9.3
PA	0.8	0.14	18.0	0.8	0.06	7.9

TABLE 2

Composition of phospholipids in rhesus red blood cell membranes before and after infection with *plasmodium knowlesi*

Sample	Tissue	Percentage of total phospholipid								
		n[a]	PC[b]	PE	SM	PI	PS	PA	LPC	UNK
L248	Normal RBC	8	38.2	32.4	17.4	1.5	8.8	0.8	0.6	0.2
	Infected	4	39.8	30.6	13.6	2.0	12.0	1.2	0.1	0.7
L497	Normal	3	36.1	32.7	17.1	2.2	10.0	0.8	0.3	0.8
	Infected	3	45.4	20.2	23.0	1.1	4.7	1.2	0.5	0.5
L331	Normal	3	40.6	30.8	16.8	1.3	8.6	0.7	0.5	0.6
	Infected	3	43.0	26.3	15.5	1.5	11.4	1.1	0.7	0.5
H348	Normal	3	35.7	31.3	18.8	1.7	9.1	0.8	1.5	0.6
	Infected	3	43.4	30.1	12.7	2.0	10.0	1.4	<0.1	0.5
L492	Normal	3	39.0	29.1	19.0	1.3	9.0	0.9	1.1	0.4
	Infected	3	41.0	29.8	14.9	2.7	9.8	0.8	0.4	0.4
L727	Normal	4	36.0	30.8	17.0	1.5	11.5	1.2	0.2	1.5
	Infected	4	42.4	21.7	18.5	1.6	9.1	2.0	1.6	3.1
M621	Normal	3	34.5	30.8	18.2	1.8	10.9	1.0	1.0	1.8
	Infected	3	41.3	27.2	14.6	1.9	11.4	1.4	0.3	1.6

[a]n = Number of separations and analyses performed on each extract.
[b]PC = Phosphatidylcholine; PE = phosphatidylethanolamine; SM = sphingomyelin; PI = phosphatidylinositol; PS = phosphatidylserine; PA = phosphatidic acid; LPC = lysophosphatidylcholine.

TABLE 3

Parasitemias at time of sacrifice

Monkey	Parasitemia %	Monkey	Parasitemia %
L248	26	L234	28
L497	46	K815	48
L331	4[a]	L727	34
H348	60	M621	20
L241	27		

[a]Resistant to infection.

because of their consistency and magnitude. If the fractions were pure, the differences would undoubtedly be even more pronounced.

DISCUSSION

This work on individual animals has shown that differences exist between these membrane fractions; study on an animal-to-animal basis rather than of pooled samples makes these differences much more apparent and also enabled

TABLE 4

Composition of phospholipids in infected rhesus red blood cell membranes and in *plasmodium knowlesi*[a]

Sample	Tissue	Percentage of total phospholipid								
		n	PC	PE	SM	PI	PS	PA	LPC	UNK
L248	Infected RBC	4	39.8	30.6	13.6	2.0	12.0	1.2	0.1	0.7
	Parasite	3	49.0	41.9	2.1	5.0	1.8	0.1	—	0.2
L497	Infected RBC	3	45.4	20.2	23.0	1.1	4.7	1.2	0.5	0.5
	Parasite	4	51.7	38.7	2.5	4.6	2.1	0.4	0.1	0.1
L331	Infected RBC	3	43.0	26.3	15.5	1.5	11.4	1.1	0.7	0.5
	Parasite	3	43.0	36.9	9.3	4.5	6.7	0.4	0.2	0.3
H348	Infected RBC	3	43.4	30.1	12.7	2.0	10.0	1.4	<0.1	0.5
	Parasite	4	50.2	41.6	1.9	4.3	1.6	0.1	0.2	0.2
L241	Infected RBC	3	45.9	29.2	14.2	0.9	7.8	1.3	0.1	0.7
	Parasite	3	46.6	42.2	2.5	4.2	3.2	0.7	0.1	0.5
L234	Infected RBC	3	38.0	35.2	14.8	1.8	8.6	0.8	0.1	0.7
	Parasite	3	51.0	37.8	3.0	3.8	3.7	0.3	0.2	0.2
K815	Infected RBC	3	41.2	31.0	13.1	1.7	10.6	1.2	0.1	1.0
	Parasite	3	47.0	43.1	2.0	5.2	2.3	0.2	<0.1	0.2
L231	Infected RBC	3	43.6	31.8	11.6	2.8	8.5	1.0	0.4	0.1
	Parasite	3	50.1	38.9	2.1	5.0	2.9	0.4	0.4	0.2
L492	Infected RBC	3	41.0	29.8	14.9	2.7	9.8	0.8	0.4	0.4
	Parasite	3	49.4	42.2	2.3	3.6	2.0	0.4	—	0.2
L727	Infected RBC	4	42.4	21.7	18.5	1.6	9.1	2.0	1.6	3.1
	Parasite	4	45.2	40.5	2.6	3.5	3.9	0.1	0.5	3.7
M621	Infected RBC	3	41.3	27.2	14.6	1.9	11.4	1.4	0.3	1.6
	Parasite	3	48.2	38.2	3.0	3.8	2.8	0.9	0.2	2.9

[a]For abbreviations, see Table 2.

particularly interesting animals to be investigated.

The L331 monkey was found to be resistant to infection; 12 d after infection it showed only 4 % parasitemia, whereas most monkeys die within a week of infection. There are two interesting points to note; the levels of SM and PS in the L331 parasite fraction were much higher than for other monkeys, and the infected RBC fraction from L331 shows as large a change compared with the normal L331 fraction as do any of the other normal-infected fraction pairs. Since the low parasitemia would mean that the L331 RBC fraction contained essentially only uninfected RBC's, it would appear that uninfected cells do undergo a change in the parasitized animal.

The normal RBC fraction came from uninfected animals and can be considered to be composed essentially of normal erythrocytes. The infected RBC fraction, of course, came from infected animals, and because the animals were about 50 % parasitized this fraction contained at least 50 % uninfected cells. However, uninfected cells are not necessarily the same as cells from uninfected animals. Both uninfected and parasitized erythrocytes exhibit abnormal osmotic fragilities [14] and the rate of hemolysis in malaria

exceeds that expected from the number of infected cells [15]. The parasite fraction, as previously explained, contained both infected RBC's and parasites. Several investigators [12, 15, 16] have found PE slightly higher in cells from *Plasmodium berghei*-infected mice compared with uninfected mice. Our work with *Plasmodium knowlesi*-infected monkeys, on the other hand, shows a decrease in PE for infected cells, but a relatively high level of PE for the parasite fraction which contained infected cells as well as parasites. In the case of the other phospholipids the level of each in the infected cells and parasites changed in the same direction when compared to the normal RBC fraction. Thus it is difficult to make any statement about what could be expected of a pure fraction. The different directions of change for PE indicate that, for a pure parasite fraction, PE would probably represent a higher percentage of the total phospholipids than it does in the parasite fraction as prepared in this work.

Although these results do not allow prediction of what might be expected of a pure fraction for the other phospholipids, they do indicate the direction for future research. In the parasite fraction the levels of certain phospholipids, particularly SM, PE and PS, were quite different from their levels in the normal host-cell fraction. This large variation indicates that either the cells in the infected animal are quite different from those in a uninfected animal or the membranes of the parasite are very different from the host's. If the former is true, the change in the host cell might be either a result of the host's response to infection or be a result of the parasite's drain on the host's resources. If the latter is true, and the parasite is very different from the host, this may give a key to understanding the parasite better.

The ideal way to proceed experimentally would be to prepare pure parasite fractions, but that is not yet possible. The alternative is to find some means of gauging the degree to which the parasite fraction is contaminated with host cells, and couple this knowledge with an analysis of pure infected-host cell preparations. Other investigators have had some success with selective labels for erythrocyte [17, 18] and one of these might be used for estimating contamination in the parasite fraction. Preparation of an infected host-cell fraction free of non-infected cells is now possible [19]; its analysis would allow stronger statements about the parasite to be made.

This work was supported in part by the U.S. Army Medical Research and Development Command under contract no. DADA-17-73-C-3014.

REFERENCES

1 M. Bretscher, Science, 181 (1973) 622.
2 J. Dodge, C. Mitchell and D. Hanahan, Arch. Biochem. Biophys., 100 (1963) 119.
3 G. Nelson, Blood Lipids and Lipoproteins: Quantitation, Composition and Metabolism, Wiley—Interscience, New York, 1972, p. 320.
4 G. Nelson, Blood Lipids and Lipoproteins: Quantitation, Composition and Metabolism, Wiley—Interscience, New York, 1972, p. 331.

5 E. Ball, R. McKee, C. Anfinsen, W. Cruz and Q. Geiman, J. Biol. Chem., 175 (1948) 547.
6 D. Morrison nad H. Jeskey, Fed. Proc., 6 (1947) 279.
7 M. Angus, K. Fletcher.and B. Maegraith, Ann. Trop. Med. Parasitol. 65 (1971) 429.
8 R. Rock, J. Standefer, R. Cook, W. Little and H. Sprinz, Comp. Biochem. Physiol., 32B (1971) 225.
9 R. deZeeuw, J. Wijsbeek, R. Rock and G. McCormick, Proc. Helminthol. Soc., 39 (1972) 412.
10 G. Nelson, Blood Lipids and Lipoproteins: Quantitation, Composition and Metabolism, Wiley-Interscience, New York, 1972, pp. 51—73.
11 P. Chen, T. Toribara and H. Warner, Anal. Chem., 28 (1956) 1756.
12 C. W. Lawrence and R. J. Cenedella, Exp. Parasitol., 26 (1969) 181.
13 R. Cook, M. Aikawa, R. Rock, W. Little and H. Sprinz, Mil. Med., 134 (Suppl.) (1969) 866.
14 B. J. Fogel, C. D. Shields and J. von Doenhoff, Amer. J. Trop. Med. Hyg., 15 (1966) 269.
15 E. Weidekamm, D. F. H. Walloch, P. S. Lin and J. Hendricks, Biochim. Biophys. Acta, 323 (1973) 539.
16 K. N. Rao, D. Subrahmanyam and S. Pakrash, Exp. Parasitol., 27 (1970) 22.
17 T. Seed, M. Aikawa and C. Sterling, J. Protozool., 20 (1973) 603.
18 M. Weintraub, K. Gerson and R. Silber, Blood, 13 (1974) 549.
19 L. Miller, Private communication, NIH, 1974.

Analytica Chimica Acta, 82 (1976) 187—201

POTENTIOMETRIC DETERMINATION OF THE STABILITY CONSTANTS OF THE FLUOROBORATE—DYE COMPLEXES USED IN COLORIMETRIC ANALYSIS FOR BORON

PIER LUIGI BULDINI

C.N.R., LAMEL Laboratory, Via de'Castagnoli 1, 40126 Bologna (Italy)

(Received 14th July 1975)

SUMMARY

An extensive bibliography on the determination of boron by means of tetrafluoroborate—dye complexes is given. The stability constants of the fluoroborate—dye complexes are calculated from potentiometric measurements with an Orion fluoroborate ion-selective electrode, for the following nineteen dyes: methylene blue, methylene green, new methylene blue N, thionine, toluidine blue O, malachite green, brilliant green, crystal violet, fuchsine, methyl green, methyl violet, Victoria blue B, brilliant cresyl blue, Nile blue A, rhodamine B, rhodamine 6G, pyronine Y, safranine T and Janus green B. The solubilities of these dyes have been determined by spectrophotometry.

In the past two decades, many papers have described spectrophotometric methods for the determination of boron, based on the reaction of tetrafluoroborates with dyes. Generally, the samples used are brought into solution, and the boron is converted to tetrafluoroborate by the addition of hydrofluoric acid; a solution of the dye is then added and the resulting complex extracted with an inert solvent. The tetrafluoroborate complex has the formula $(BF_4)R$, where R is the monovalent cation of the coloured organic dye.

Three main groups of dyes have been used in these determinations — thiazine, triphenylmethane and oxazine – but some use has also been made of xanthene and phenazine dyes.

Some general reviews of analysis for boron are available [1—9], most of which were issued during the sixties, but few of these give much consideration to the fluoroborate methods, thus it seems worthwhile to give an extensive bibliographic list of these papers, according to the organic dye used.

In Tables 1—5, the dyes are described; the Colour Index [10] features and the official formulae derived from Chemical Abstracts are given, to avoid the various, obsolete or technical names which often bewilder the reader.

Two factors must be evaluated when one of these organic dyes is selected for the determination of boron: (1) the stability constant of the fluoroborate—dye complex; (2) the partition coefficient between the aqueous phase and the organic solvent used. Stability constants may be determined by various methods; potentiometry is convenient if a fluoroborate-selective electrode is available.

TABLE 1

Thiazine dyes

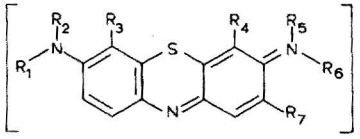

Azure A	$R_3 = R_4 = R_5 = R_6 = R_7 = H$ $R_1 = R_2 = CH_3$
Azure B	$R_3 = R_4 = R_6 = R_7 = H$ $R_1 = R_2 = R_5 = CH_3$
Azure C	$R_1 = R_3 = R_4 = R_5 = R_6 = R_7 = H$ $R_2 = CH_3$
Methylene blue	$R_3 = R_4 = R_7 = H$ $R_1 = R_2 = R_5 = R_6 = CH_3$
Methylene green	$R_3 = R_7 = H$ $R_4 = NO_2$ $R_1 = R_2 = R_5 = R_6 = CH_3$
New methylene blue	$R_1 = R_6 = R_7 = H$ $R_2 = R_5 = C_2H_5$ $R_3 = R_4 = CH_3$
Thionine	$R_1 = R_2 = R_3 = R_4 = R_5 = R_6 = R_7 = H$
Toluidine blue O	$R_3 = R_4 = R_5 = R_6 = H$ $R_1 = R_2 = R_7 = CH_3$

Common name	Colour index name and number	Extensive formula	References
Azure A	— (52005)	3H-Phenothiazine,7-(dimethylamino)-3-iminohydrochloride	11—13
Azure B	— (52010)	3H-Phenothiazine,7-(dimethylamino)-3-methyliminohydrochloride	11, 12
Azure C	— —	3H-Phenothiazine,7-methylamino-3-iminohydrochloride	11—14
Methylene blue	Basic blue 9 Solvent blue 8 (52015)	3,7-Bis(dimethylamino)phenazathionium chloride	11, 12, 15—56
Methylene green	Basic green 5 (52020)	3,7-Bis(dimethylamino)-4-nitrophenazathionium chloride	11, 12, 57
New methylene blue N	Basic blue 24 (52030)	3,7-Bis(ethylamino)-2,8-dimethylphenazathionium chloride (zinc chloride salt)	11, 12
Thionine	— (52000)	3H-Phenothiazine,7-amino-3-imino-3,7-diaminohydrochloride	11, 12
Toluidine blue O	Basic blue 17 (52040)	3-Amino-7-dimethylamino-2-methylphenazathionium chloride	11, 12

The stability constant of the fluoroborate—dye complex may be defined as

$$K = \frac{[BF_4 \cdot Dye]}{[BF_4^-][Dye]} \quad (1)$$

where $[BF_4^-]$ is the fluoroborate concentration at equilibrium (the value given by the electrode). $[BF_4 \cdot Dye]$ can be calculated from the difference between the fluoroborate ion added and that found at equilibrium. [Dye] can be calculated from the difference between the known amount added and the amount complexed, i.e. $[BF_4 \cdot Dye]$.

Because many of the dyes contain chloride or sulfate ions as components of the molecule, the requisite quantity of 0.1 M sodium chloride was added in order to achieve the same ionic strength in all solutions to be measured. This addition is necessary, because the fluoroborate electrode is somewhat sensitive [86] to chloride and sulfate ions ($K_{BF_4^-, Cl^-} = K_{BF_4^-, SO_4^{2-}} = 10^{-3}$).

EXPERIMENTAL

Apparatus

An Orion fluoroborate-selective electrode (Model 92-05) and an Orion single-junction Ag/AgCl electrode (Model 90-01) were used. The reference electrode was filled with 0.1 M KCl solution saturated with silver chloride.

Potentials were measured (within 0.5 mV) on a Knick Model pH 35 mV/pH meter. Every potential measurement was made under moderate magnetic stirring, to obtain electrode equilibrium within a few minutes even in dilute solutions. Response time and equilibrium potentials were defined by recording the electrode signal with an Amel Model 867 potentiometric recorder.

All solutions containing fluoroborate were prepared and stored in polyethylene bottles.

Small volumes were precisely measured with an SB-2 syringe microburet (Micrometric Instrument Co., Cleveland) having a capacity of 1 ml (0.001-ml divisions).

The spectrophotometric measurements to determine the solubilities of the dyes were carried out on a Perkin-Elmer Model 323 spectrophotometer.

Reagents

For the standard (0.1 M) fluoroborate solution 11 g of sodium fluoroborate (B.D.H) were dissolved in 1 l of water and this solution was diluted as required.

0.1 M sodium chloride was RPE (C. Erba).

Dye solutions were obtained by dissolving J. T. Baker (safranine T, crystal violet, brilliant green, Victoria blue B, brilliant cresyl blue, pyronine Y, new

TABLE 2

Triphenylmethane dyes

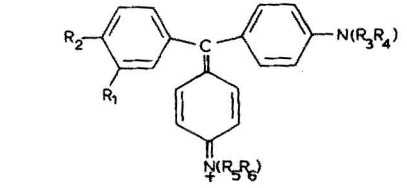

Malachite green	$R_1 = R_2 = H$ $R_3 = R_4 = R_5 = R_6 = CH_3$
Brilliant green	$R_1 = R_2 = H$ $R_3 = R_4 = R_5 = R_6 = C_2H_5$
Crystal violet	$R_1 = H$ $R_2 = N(R_3R_4)$ $R_3 = R_4 = R_5 = R_6 = CH_3$
Ethyl violet	$R_1 = H$ $R_2 = N(R_3R_4)$ $R_3 = R_4 = R_5 = R_6 = C_2H_5$
Fuchsine	$R_3 = R_4 = R_5 = R_6 = H$ $R_2 = N(R_3R_4)$ $R_1 = CH_3$
Methyl green	$R_1 = H$ $R_2 = NC_2H_5(CH_3)_2Br$ $R_3 = R_4 = R_5 = R_6 = CH_3$
Methyl violet	$R_1 = R_6 = H$ $R_2 = N(R_3R_4)$ $R_3 = R_4 = R_5 = CH_3$

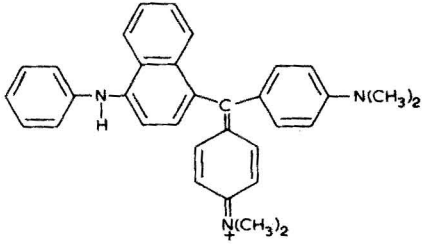

Victoria blue B (K?)

Common name	Colour index name and number	Extensive formula	References
Malachite green	Basic green 4 Pigment green 4 (42000)	4-[*p*-(Dimethylamino)-α-phenylbenzylidene-2,5-cyclohexadien-1-ylidene] dimethylammonium chloride	17, 58
Brilliant green	Basic green 1 Pigment green 1 (42040)	(4-[*p*-(Diethylamino-α-phenylbenzylidene)]-2,5-cyclohexadien-1-ylidene) diethylammonium hydrogen sulfate	16, 59—63
Crystal violet	Basic violet 3 (42555)	[4-[Bis[*p*-(dimethylamino)-phenyl] methylene]-2,5-cyclohexadien-1-ylidene] dimethylammonium chloride	17, 43, 64—67

TABLE 2 (continued)

Common name	Colour index name and number	Extensive formula	References
Ethyl violet	Basic violet 4 (42600)	[4-[Bis[*p*-(diethylamino)-phenyl] methylene]-2,5-cyclohexadien-1-ylidene] dimethylammonium chloride	68
Fuchsine	Basic violet 14 (42510)	2-Methyl-4,4'-[(4-imino-2,5-cyclohexadien-1-ylidene)methylene] dianiline hydrochloride	17
Methyl green	— (42590)	[4-[*p*-(Dimethylamino)-α-[*p*-(dimethylamino)phenyl]benzylidene]-2,5-cyclohexadien-1-ylidene]dimethylammonium chloride ethobromide	96
Methyl violet	Basic violet 1 Pigment violet 3 (42535)	4-[Bis[*p*-(dimethylamino)phenylmethylene]-2,5-cyclohexadien-1-ylidene] monomethylammonium chloride	16, 17, 63, 65, 69—75
Victoria blue B (K?)	Basic blue 26 Pigment Blue 2 (44045)	[4-[α-(4-Anilino-1-naphthyl)-*p*-(dimethylamino)-benzylidene]-2,5-cyclohexadien-1-ylidene dimethylammonium chloride	16

TABLE 3

Oxazine dyes

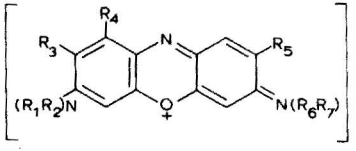

Brilliant cresyl blue
Capri blue GON

$R_1 = R_2 = R_3 = H \quad R_5 = CH_3 \quad R_4 = NH_2 \quad R_6 = R_7 = C_2H_5$
$R_4 = R_5 = H \quad R_3 = R_6 = R_7 = CH_3 \quad R_1 = R_2 = C_2H_5$

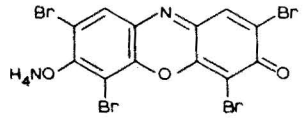

Lacmoid

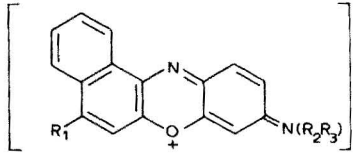

Meldola's blue
Nile blue A

$R_1 = H \quad R_2 = R_3 = CH_3$
$R_1 = NH_2 \quad R_2 = R_3 = C_2H_5$

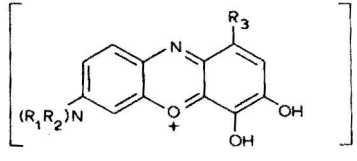

Celestine blue
Gallamine blue
Gallocyanine

$R_1 = R_2 = C_2H_5 \quad R_3 = CONH_2$
$R_1 = R_2 = CH_3 \quad R_3 = CONH_2$
$R_1 = R_2 = CH_3 \quad R_3 = COOH$

Common name	Colour index name and number	Extensive formula	References
Brilliant cresyl blue	— (51010)	3H-Phenoxazine, 7-(diethylamino)-3-imino-8-methyl hydrochloride	76
Capri blue GON	— (51015)		76

TABLE 3 (continued)

Common name	Colour index name and number	Extensive formula	References
Lacmoid	— (51400)		76
Meldola's blue	Basic blue 6 (51175)	9-(Dimethylamino)benzo[a]-phenazoxonium chloride	76
Nile blue A	Basic blue 12 (51180)	5-Amino-9-(diethylamino)benzo[a]phenazoxonium hydrogensulfate	17, 76—80
Celestine blue	Mordant blue 14 (51050)	1-Carbamoyl-7-(diethylamino)-3,4-dihydroxyphenazoxomium chloride	76
Gallamine blue	Mordant blue 45 (51045)	1-Carbamoyl-7-(dimethylamino)-3,4-dihydroxyphenazoxonium chloride	76
Gallocyanine	Mordant blue 10 (51030)	1-Carboxy-7-(dimethylamino)-3,4-dihydroxyphenazoxonium chloride	76

TABLE 4

Xanthene dyes

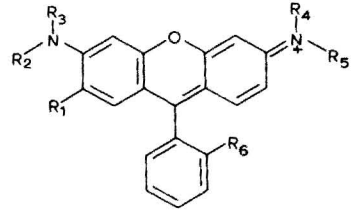

Rhodamine B — $R_1 = H$ $R_2 = R_3 = R_4 = R_5 = C_2H_5$ $R_6 = COOH$
Rhodamine 3B (3S?) — $R_1 = H$ $R_2 = R_3 = R_4 = R_5 = C_2H_5$ $R_6 = COOC_2H_5$
Rhodamine 6G — $R_3 = R_4 = H$ $R_2 = R_5 = C_2H_5$ $R_1 = CH_3$ $R_6 = COOC_2H_5$

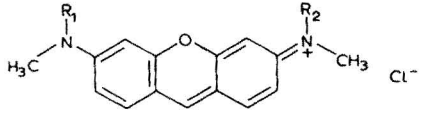

Pyronine Y — $R_1 = R_2 = CH_3$
Acridine red — $R_1 = R_2 = H$

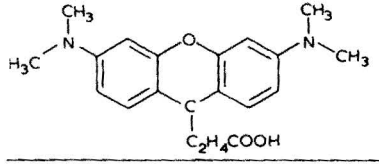

Rhodamine S

Common name	Colour index name and number	Extensive formula	References
Rhodamine B	Basic violet 10 Pigment violet 1 Food red 15 (45170)	[9-(*o*-Carboxyphenyl)-6-(diethylamino)-3H-xanthen-3-ylidene] diethylammonium chloride	17, 81, 82
Rhodamine 3B (3S?)	Basic violet 11 Pigment violet 2 (45175)	[9-(*o*-Carboxyphenyl)-6-(diethylamino)-3H-xanthen-3-ylidene] diethylammonium chloride ethyl ester	83
Rhodamine 6G	Basic red 1 Pigment red 81 (45160)	(Ethyl-*o*-[6-(ethylamino)-3-(ethylimino)-2,7-(dimethyl)-3H-xanthen-9-yl]-benzoate monohydrochloride	17, 81

TABLE 4 (continued)

Common name	Colour index name and number	Extensive formula	References
Pyronine Y	— (45005)	[6-(Dimethylamino)-3H-xanthen-3-ylidene]dimethylammonium chloride	17
Acridine red	— (45000)		17
Rhodamine S	Basic red 11 (45050)	[9-(2-Carboxyethyl)-6-(dimethylamino)-3H-xanthen-3-ylidene] dimethylchloride	17
Butylrhodamine	— —	Butyl ester of rhodamine B	81, 83, 84

TABLE 5

Phenazine dyes

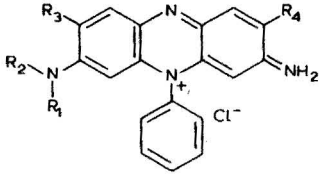

Safranine T $R_1 = R_2 = H \quad R_3 = R_4 = CH_3$
Safranine bluish $R_3 = R_4 = H \quad R_1 = R_2 = CH_3$

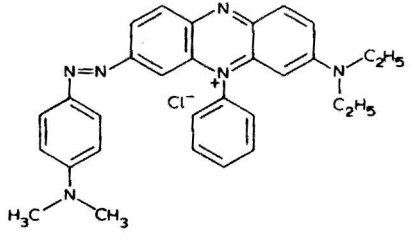

Janus green B

Common name	Colour index name and number	Extensive formula	References
Safranine T	Basic red 2 (50240)	3,7-diamino-2,8-dimethyl-5-phenyl-phenazinium chloride	17, 83
Safranine bluish	Basic violet 5 (50205)		17
Methylene violet			
Janus green B	— (11050)	3-(diethylamino)-7-[(*p*-(dimethyl-amino)-phenyl)azo]-5-phenylphena-zinium chloride	85

methylene blue N, methyl green), Merck (methylene blue, methyl violet, toluidine blue O, fuchsine), Kuhlmann R.A.L. (malachite green, Nile blue A, methylene green), B.D.H. (rhodamine 6G, Janus green B) and C. Erba (thionine, rhodamine B) products in sufficient amounts to give 0.1 M or more concentrated solutions. Saturated solutions were avoided.

Determination of solubility

Concentrated solutions were used to ensure a large excess of the organic dye. As a result, the solubility of the dyes had to be calculated, when values were lacking in the literature, in order to avoid possible error in determining the stability constant.

The solubility was determined by spectrophotometric measurements, a known standard solution of the dye (10^{-5} M) being compared with a saturated solution suitably diluted. The saturated solution was obtained by agitating water and an excess of dye crystals. The vessel and its contents were heated to 60—70 °C and then cooled to room temperature. Fifteen days later (to ensure that equilibrium had been reached), an aliquot of the liquor was centrifuged and suitably diluted. After the final dilution, the dye solution contained also 10^{-3} M HCl to ensure the same acidity in the known and unknown solutions.

Table 6 gives the solubilities found.

TABLE 6

Solubility of the dyes in water at 20—25 °C

Dye	Solubility (g/100 ml H_2O)	Ref.
Methylene blue	4.36	87
Methylene green	1.6	
New methylene blue N	3.9	
Thionine	0.2	
Toluidine blue O	3.82	88
Malachite green	4.0	
Brilliant green	9.7	
Crystal violet	0.1	
Fuchsine	0.265	87
Methyl green	4.2	
Methyl violet	3.3	
Victoria blue B	6.5	
Brilliant cresyl blue	5.5	
Nile blue A	3.1	
Rhodamine B	1.2	
Rhodamine 6G	5.4	
Pyronine Y	8.96	88
Safranine T	2.9	
Janus green B	3.2	

Procedures

Calibration curve. To three or four polyethylene vessels, add suitable quantities of the standard fluoroborate solution with a microsyringe, selecting the boron concentrations so as to bridge the concentration range expected after formation of the complex with the organic dye. Add the necessary quantity of 0.1 M sodium chloride, in order to obtain the same concentration of interfering ion as in the solutions containing the dye. Read the potential obtained while stirring, and check the equilibrium potential attained by recording.

Prepare a calibration graph from the points obtained with the standard solution.

Complex potentials. Prepare several (4—5) solutions in the same way but vary the known dye or fluoroborate concentration. Measure the potential as described above and determine the fluoroborate concentration from the calibration graph. Calculate the stability constant of the fluoroborate—organic dye complex from eqn. (1). All potential measurements were carried out at room temperature (20—25 °C).

Table 7 gives the results of a typical experiment. The calibration graph for the fluoroborate electrode was essentially Nernstian in the fluoroborate range 10^{-2}—10^{-5} M, the points measured lying on a very gradual curve. Although the electrode response shows good reproducibility, the calibration curve should be checked before each experiment.

RESULTS AND DISCUSSION

Table 8 shows the results obtained for the stability constants of the complexes of the nineteen organic dyes at our disposal.

TABLE 7

Results of a typical experiment with methylene blue
(All solutions were made 0.01 M in chloride for final measurements)

Vessel no.	0.1 M $NaBF_4$ (ml)	0.1 M NaCl (ml)	0.1 M Dye (ml)	H_2O (ml)	$[BF_4^-]$ M in.	[Dye] M	mV	K	log K
1	10	10	—	80	0.01	—	25	—	—
2	1	10	—	89	0.001	—	83	—	—
3	0.1	10	—	89.9	0.0001	—	138	—	—
4	0.01	10	—	90	0.00001	—	188	—	—
A	1	5	5	89	0.001	0.005	90	91	1.96[a]
B	1	0	10	89	0.001	0.01	97	89	1.95[a]
C	0.1	5	5	89.9	0.0001	0.005	148	108	2.03[a]
D	0.1	0	10	89.9	0.0001	0.01	156	104	2.01[a]

[a]Mean value 2.0 (± 0.05).

TABLE 8

Stability constants for the fluoroborate—dye complexes

Dye	log K	Dye	log K
Methylene blue	2.0 ± 0.05	Methyl violet	2.6 ± 0.1
Methylene green	1.7 ± 0.05	Victoria blue B	3.7 ± 0.1
New methylene blue N	1.6 ± 0.2	Brilliant cresyl blue	1.1 ± 0.05
Thionine	2.0 ± 0.1	Nile blue A	1.6 ± 0.1
Toluidine blue O	1.3 ± 0.05	Rhodamine B	1.6 ± 0.1
Malachite green	2.0 ± 0.1	Rhodamine 6G	2.4 ± 0.2
Brilliant green	2.6 ± 0.1	Pyronine Y	0.7 ± 0.1
Crystal violet	3.2 ± 0.1	Safranine T	1.5 ± 0.1
Fuchsine	2.0 ± 0.1	Janus green B	2.2 ± 0.05
Methyl green	1.8 ± 0.2	Ferroin	1.3 ± 0.05

In addition to the dyes described above, two other fluoroborate complexes have been used for the determination of boron: the tetraphenylarsonium fluoroborate complex [89—92] and the tris(1,10-phenanthroline)iron(II) fluoroborate complex [93, 94]. The tetraphenylarsonium complex has been thoroughly studied by Smith and Manahan [95], who used the same Orion ion-selective electrode. In order to complete this research, it seemed useful to determine the stability constant of the ferroin—fluoroborate complex; the value found was log K = 1.3 (Table 8).

The author is grateful to Prof. Pietro Lanza for his encouragement and helpful suggestions, and to Prof. Giovanni Semerano, Director of the "G. Ciamician" Chemical Institute of the University, where this work was carried out.

REFERENCES

1 R. Capelle, Chim. Anal. (Paris), 45 (1963) 303.
2 J. F. Epstein and L. Pásztor, Jonas and Laughlin Steel Co. Res. and Dev. Dept., Sect. A, B et C. P. W 1300 (21 XI 1958 and 3 VIII 1959).
3 A. G. Fogg, C. Burgess and D. Thorburn Burns, Talanta, 18 (1971) 1175.
4 G. W. Goward and V. R. Wiederkehr, Anal. Chem., 35 (1963) 1542.
5 M. W. Lerner, Rep. At. Energy Comm., U.S., TID-25190 (1970).
6 A. A. Nemodruk and Z. K. Karalova, Analytical Chemistry of Boron, I.P.S.T., Jerusalem, 1965.
7 F. Rab, Chem. Listy, 55 (1961) 919.
8 F. Vlacil and K. Drbal, Chem. Listy, 62 (1968) 1371.
9 P. Ya. Yakovlev and G. V. Kozina, Zavod. Lab., 29 (1963) 920.
10 Colour Index, The Society of Dyers and Colourists, London, 2nd ed., 1956.
11 L. Pásztor and J. D. Bode, Anal. Chim. Acta, 24 (1961) 467.
12 L. Pásztor and J. D. Bode, Anal. Chem., 32 (1960) 1530.
13 C. C. Weir, J. Sci. Food Agri., 21 (1970) 545.
14 B. L. Goydish, Microchem. J., 15 (1970) 572.
15 T. Adachi, Denki Seiko, 32 (1961) 268.

16 A. K. Babko and P. V. Marchenko, Zavod. Lab., 26 (1960) 1202.
17 A. Banno and T. Sawaya, Technol. Rep. Tohoku Imp. Univ., 25 (1961) 163.
18 E. S. Beskova and G. I. Zhuravlev, Zh. Anal. Khim., 28 (1973) 1411.
19 E. S. Beskova, G. I. Zhuravlev and V. I. Dorofeeva, Zavod. Lab., 40 (1974) 935.
20 O. P. Bhargava and W. G. Hines, Talanta, 17 (1970) 61.
21 D. Blazejak-Ditges, Z. Anal. Chem., 247 (1969) 20.
22 R. Capelle, Document AFNOR, A — 06 — f — doc 182.
23 C.E.A.- CETAMA, Report No. 66, September, 2nd edn. 1961.
24 A. G. Coedo and J. L. J. Seco, Rev. Met. (Madrid), 4 (1968) 447.
25 L. Ducret, Anal. Chim. Acta, 17 (1957) 213.
26 Yu. G. Eremin and P. N. Romanov, Zavod. Lab., 29 (1963) 420.
27 N. Fukushi and Y. Kakita, Bunseki Kagaku, 15 (1966) 553.
28 H. Gotô and S. Takeyama, J. Jap. Inst. Metals, Sendai, 25 (1961) 588.
29 O. Holwech and O. B. Skaar, unpublished work.
30 A. Isozaki and S. Utsumi, J. Chem. Soc. Jap., Pure Chem. Sect., 88 (1967) 741.
31 O. Kammori, I. Taguchi and T. Ishiguro, Bunseki Kagaku, 15 (1966) 1376.
32 Z. K. Karalova and A. A. Nemodruk, Zh. Anal. Khim., 18 (1963) 615.
33 V. I. Klitina, Tekhnol. Legk. Splavov. Nauch.-Tekh. Byul. VILS, (1970) 65.
34 V. I. Klitina and V. F. Bakurova, Tekhnol. Legk. Splavov. Nauch.-Tekh. Byul. VILS, (1971) 105.
35 P. Lanza and P. L. Buldini, Anal. Chim. Acta, 70 (1974) 341.
36 M. Kh. Mikheev, God. Sôfii. Univ. Fiz.-Mat. Fak., 52 (1959) 113.
37 J. Mroziński, Chem. Anal. (Warsaw), 12 (1967) 93.
38 H. Onishi and H. Nagai, Bunseki Kagaku, 18 (1969) 164.
39 L. Pásztor, J. D. Bode and Q. Fernando, Anal. Chem., 32 (1960) 277.
40 R. Rosotte, Chim. Anal. (Paris), 44 (1962) 208.
41 I. G. Shafran, Sb. Khim. Reakt. (Moskva), i preparaty, Goskhimizdat (1961).
42 O. B. Skaar, Anal. Chim. Acta, 28 (1963) 200.
43 J. Slama and H. Tuma, Hutn. Listy, 26 (1971) 137.
44 Jung You So, Youg Hwan Jang and Chae Ok Song, Punsok Hwahak, 9 (1971) 104.
45 R. D. Srivastava and H. Gesser, J. Prakt. Chem., 38 (1968) 262.
46 R. E. Stanton and A. J. McDonald, Analyst (London), 91 (1966) 775.
47 N. V. Stashkova and L. A. Ozornina, Tr. Vses Nauch. Issled. Inst. Stand. Obraztsov Spektral. Etalonov, 7 (1971) 106.
48 E. Sudo and S. Ikeda, Bunseki Kagaku, 17 (1968) 1197.
49 S. Takeyama and H. Gotô, Sci. Rep. Res. Inst. Tôhoku Imp. Univ., Ser. A, 15 (1963) 144.
50 A. S. Tenney, J. Electrochem. Soc., 120 (1973) 1284.
51 S. Utsumi and A. Isozaki, J. Chem. Soc. Jap., Pure Chem. Sect., 88 (1967) 545.
52 S. Utsumi, S. Ito and A. Isozaki, J. Chem. Soc. Jap. Pure Chem. Sect., 86 (1965) 921.
53 F. Vernon and J. M. Williams, Anal. Chim. Acta, 51 (1970) 533.
54 C. C. Weir and R. L. Jones, Trop. Agr., Trinidad, 47 (1970) 261.
55 T. S. West, Ind. Chem., 39 (1963) 379.
56 A. N. Zaidel, N. I. Kaliteevskii, L. V. Lipis and M. P. Chaika, Emission Spectrum Analysis of Atomic Materials, U.S. At. Energy Comm., 1963.
57 V. M. Tarayan, E. N. Ovsepyan and S. R. Barkhudaryan, Dokl. Akad. Nauk Arm. SSR, 48 (1969) 52.
58 I. M. Korenman and L. V. Sidorenko, Tr. Khim. Khim. Tekhnol., (1964) 431.
59 I. L. Barbanlÿ and T. R. Mizeyova, Azerb. Khim. Zh., (1961) 115.
60 Z. K. Karalova and A. A. Nemodruk, Zh. Anal. Khim., 17 (1962) 985.
61 Zh. Kuus and A. Lust, Uch. Zap. Tartu. Gos. Univ., (1970) 122.
62 P. V. Marchenko, Zavod. Lab., 27 (1961) 801.
63 I. Muraki, K. Hiiro, H. Fukuda and E. Miyade, Bull. Osaka Ind. Res. Inst., 11 (1960) 44.

64 K. A. Abashidze, Tr. Inst. Sadovod. Vinograd. Vinodel. Gruz. SSR, 22 (1973) 153.
65 I. A. Blyum, T. K. Dushina, T. V. Semenova and I. Ya. Shcherba, Zavod. Lab., 27 (1961) 644.
66 I. A. Blyum, T. V. Semenova, I. Ya. Shcherba and T. I. Shumova, Metody Khim. Anal. Miner. Syr'ya, (1963) 21.
67 Z. E. Delkova, Dokl. Mosk. Sel'skokhoz.-Khoz. Akad. (1965) 465
68 Gh. Banateaun, T. Popovici and A. Schiopescu, Bull. Inst. Petrol, Gaze Geol., 19 (1972) 221.
69 M. P. Babkin and R. D. Sechan, Izv. Vyssh. Ucheb. Zaved. Khim. Khim. Tekhnol., 5 (1962) 847.
70 B. Ya. Kaplan and A. E. Gorbatkina, Byull. VIMSa, 17 (6) (1960) 206.
71 E. I. Lerman, Sb. Tr. Vses. Nauch.-Issled. vatel. Inst. Upravlen Proizvodstvom Gos. Zuakov Monet.; Ordenov (1957) 243.
72 I. Muraki, K. Hiiro, H. Fukuda and E. Miyade, Bull. Osaka Ind. Res. Inst., 11 (1960) 52.
73 I. Muraki, K. Hiiro, H. Fukuda and E. Miyade, Bunseki Kagaku, 9 (1960) 71.
74 N. S. Poluetkov, L. I. Kononenko and R. S. Lauer, Zh. Anal. Khim., 13 (1958) 396.
75 Wu Jae Rim and Il Youg Kim, Punsok Hwahak, 9 (1971) 81.
76 O. B. Skaar, Anal. Chim. Acta, 32 (1965) 508.
77 E. Gagliardi and E. Wolf, Mikrochim. Acta, (1968) 140.
78 E. Gagliardi and W. Höllinger, Mikrochim. Acta, (1972) 136.
79 E. Mainka and W. Coerdt, Report USAEC—EURATOM KFK 1360 EURFNR 909, Karlsruhe, 1971.
80 R. A. Nicholson, Anal. Chim. Acta, 56 (1971) 147.
81 A. K. Babko and Z. I. Chalaya, Ukr. Khim. Zh. 30 (1964) 268.
82 H. Onishi and H. Nagai, Bunseki Kagaku, 17 (1968) 345.
83 V. I. Kuznetsov and I. V. Seryakova, Moskva Izdal'stvo ANSSSR 1956.
84 A. K. Babko, Z. I. Chalaya and E. D. Voronova, Zavod. Lab., 31 (1965) 157.
85 I. K. Guseinov, I. L..Bagbanly and A. K. Posadovskaya, Azerb. Khim. Zh., (1970) 122.
86 Orion Ionalyzer, Instruction Manual Fluoroborate Electrode 92-05, 1968.
87 Beilsteins Handbuch der Organischen Chemie, Berlin, 1918.
88 The Merck Index, Merck Rahway, 8th edn., 1968.
89 H. E. Affsprung and V. S. Archer, Anal. Chem., 36 (1964) 2512.
90 J. Coursier, J. Huré and R. Platzer, Anal. Chim. Acta, 13 (1955) 379.
91 L. Ducret and P. Seguin, Anal. Chim. Acta, 17 (1957) 207.
92 S. Hirano, H. Kamada and T. Nishiya, Kogyo Kagaku Zasshi, 62 (1959) 622.
93 V. S. Archer, F. G. Doolittle and L. M. Young, Talanta, 15 (1968) 864.
94 M. Nishimura and S. Nakaya, Bunseki Kagaku, 18 (1969) 148.
95 M. J. Smith and S. E. Manahan, Anal. Chim. Acta, 48 (1969) 315.
96 I. Paralescu and V.V. Cosofret, Rev. Chin. (Bucharest) 25 (1974) 923.

Analytica Chimica Acta, 82 (1976) 203—205

Short Communication

A DOUBLE-FUSION METHOD FOR THE TOTAL ELEMENT ANALYSIS OF SOILS AND ROCKS CONTAINING CHROMITE

M. S. CRESSER and R. HARGITT

Soil Science Department, Aberdeen University, Old Aberdeen, AB9 2UE (Scotland)

(Received 16th August 1975)

Procedures recommended for the decomposition of chrome spinels have been critically reviewed by Rodgers [1], who concluded that many of the available methods were unnecessarily complicated and time-consuming, or failed to yield consistent and reproducible results. Rodgers found the sodium peroxide fusion method of Rafter [2] most satisfactory, although there is a slight attack on platinum, and pyroxenes may require separate treatment [1]. The attack on platinum may be minimized by limiting the fusion to a short period at a temperature below 540 °C [2], or by using silver or zirconium crucibles [1, 3]. Recently we required a fusion method suitable for small samples of soils containing chromite and wide ranges of other minerals. A method was developed based on rapid sequential fusion with sodium hydrogensulphate and sodium carbonate.

Experimental

Soils with a high iron-oxide content must be digested with acid before fusion to prevent damage to platinum ware. Extract the ignited soils (200 mg) with 20 ml of a (2 + 1) mixture of 12 M hydrochloric acid and 16 M nitric acid mixture for 2 h at 50—150 °C. Graduated test tubes (25 ml) are ideal for this digestion, if heated in a suitable dri-block; thermal contact between the tubes and the block may be improved by wrapping metal foil around the tubes before inserting them in the holes in the block. Cool each digest, and dilute to ca. 40 ml. Filter directly into a 250-ml volumetric flask, and add washings from the tube and precipitate to give a final volume of ca. 100 ml. Dry the residue and filter paper, and ignite in a platinum crucible over a Meker burner to ash the paper.

To each residue obtained as above, or to a 200-mg portion of ground rock or ignited soil (low in free-iron oxide), add sodium hydrogensulphate (2.00 g, analytical reagent grade). Gently heat the mixture over a Meker burner to fuse, and to remove water. Slowly increase the heating rate until evolution of white fumes ceases, after about 20 min. Allow the crucible to cool, and add sodium carbonate (4.00 g, analytical reagent grade). Heat the

mixture, slowly at first, and then strongly for 30 min. Allow the crucible contents to cool to room temperature, place the crucible in a 50-ml beaker, and add ca. 30 ml of water. The fusion flux normally breaks away from the crucible in 1 h, and may be dispersed thoroughly in water; the mixture should not be heated strongly at this stage, or precipitation may occur subsequently. Transfer the dispersed mixture and washings slowly, with intermittent swirling, through a funnel into the volumetric flask containing the diluted acid digest, or, if digestion was unnecessary, a corresponding amount of diluted, boiled HCl : HNO_3 mixture. Eventually a clear solution should be obtained. Dilute to volume, and use the solutions thus obtained for the determinations of Si, Al, Fe, Mg and Ca by flame atomic absorption spectrometry in a nitrous oxide—acetylene flame. Chromium and manganese may also be determined in the same flame, and potassium may be determined by flame emission or atomic absorption in an air—acetylene flame, if required. All standards must be prepared in a fusion blank matrix.

Results and discussion

As a check on the accuracy of the method, five B.C.S. standard materials were analysed in duplicate by the procedure outlined, without the acid pre-extraction. The results obtained (Table 1) clearly indicate that the proposed method is suitable for the dissolution of a wide range of materials. The method has now been applied by five people in this laboratory to the analysis of a range of soils and clay, silt, and sand fractions, containing widely varying amounts of chromite and other minerals. No difficulty has been experienced with the method, and clear solutions have been obtained in every instance.

The precision attainable by atomic absorption spectrometry is poorer than that of the more time-consuming classical procedures, particularly for silicon.

TABLE 1

Comparison of certified values and values found by suggested method (mean of duplicates)

Sample	Result	SiO_2	Al_2O_3	Fe_2O_3	MgO	CaO
B.C.S. 269 Firebrick	B.C.S.	56.7	33.9	3.31	0.93	0.22
	This work	56.0	34.2	3.33	0.94	0.20
B.C.S. 309 Sillimanite	B.C.S.	34.1	61.1	1.51	0.17	0.34
	This work	33.8	60.8	1.49	0.165	0.35
B.C.S. 370 Magnesite-chrome	B.C.S.	3.01	12.2	7.24	61.8	1.54
	This work	2.9	12.0	7.20	61.4	1.50
B.C.S. 375 Soda feldspar	B.C.S.	67.1	19.8	0.12	0.05	0.89
	This work	67.5	19.5	0.12	0.045	0.91
B.C.S. 376 Potash feldspar	B.C.S.	67.1	17.7	0.10	0.03	0.54
	This work	66.3	17.8	0.10	0.033	0.55

However, the analysis of seven replicates of B.C.S. 375 soda feldspar for silicon (as SiO_2) gave a range of only 66.2 to 67.7 %, with a mean of 67.0 % and a relative standard deviation of 0.99 %, which is quite adequate for most purposes. One advantage of the flame spectrometric method is that where sample availability is limited, as is sometimes the case when soil particle-size fractions are analysed, the fusion technique can be applied to samples of only 40 mg. In this case 400 mg of sodium hydrogensulphate and 800 mg of sodium carbonate are used, and the mixture is diluted to a final volume of only 50 ml of acid solution. No significant loss in precision or accuracy was observed provided that a representative sample is employed.

It should be pointed out that, although the attack on platinum by sodium pyrosulphate (formed from the hydrogensulphate) is less than the attack by potassium pyrosulphate [1], slight attack still occurs at orange heat. The mean loss in weight per crucible was 1.2 mg per fusion, based on twelve fusions; this seems quite acceptable for substances which may otherwise be difficult to bring into solution.

REFERENCES

1 K. A. Rodgers, Mineral. Mag., 38 (1972) 882.
2 T. A. Rafter, Analyst (London), 75 (1950) 485.
3 J. I. Dinnin, Bull. U.S. Geol. Surv., 1084-B (1959).

Analytica Chimica Acta, 82 (1976) 207—211

Short Communication

VERGLEICHENDE UNTERSUCHUNGEN ZUR PHOTOMETRISCHEN BESTIMMUNG VON ALUMINIUMSPUREN MIT CHROMAZUROL S

G. RÖBISCH

Sektion Chemie/Biologie, Pädagogische Hochschule "Karl Liebknecht" Potsdam, Potsdam-Sanssouci (Deutsche Demokratische Republik)

(Eingegangen am 25 Juli 1975)

Wir suchten eine möglichst selektive, gut reproduzierbare und sehr empfindliche spektralphotometrische Methode zur Bestimmung von Aluminiumspuren (bis 10^{-5} %) vorzugsweise in natürlichen Mineralsalzen und in Solen. Unter Berücksichtigung der neueren vergleichenden Arbeiten [1, 2] haben wir zwölf Reagenzien untersucht (Alizarin S, Aluminon, Arsenazo, Brenzkatechinviolett, Calmagit, Chromazurol S, Eriochromcyanin R, Hämatoxylin, 8-Hydroxychinolin, Methylthymolblau, Stilbazo, Xylenolorange) und dabei mit Chromazurol S die besten Resultate erzielt.

Chromazurol S (Trinatriumsalz der 2'',6''-Dichloro-3''-sulfo-3,3'-dimethyl-4-oxyfuchson-5,5'-dicarbonsäure, Chromoxan-Reinblau BLD, Alberon, Solochrombrillantblau B, Polytropblau R, Eriochromazurol S) wurde als komplexim etrischer Indikator für Aluminium eingeführt [3] und für die photometrische Aluminiumbestimmung vorgeschlagen [4]. Das Aziditätsverhalten von Chromazurol S in wässriger Lösung untersuchte Malat [5], seine Komplexbildung mit Aluminium Nishida [6].

Erhebliche Widersprüche zwischen Angaben verschiedener Bearbeiter und unerwartete Misserfolge bei der Anwendung von Chromazurol S veranlassten die analytische überprüfung der spektrophotometrischen Bestimmung von Aluminiumspuren mit Chromazurol S.

Voruntersuchungen

Unter den analytisch interessierenden Bedingungen bilden Aluminium und Chromazurol S (H_4L) in Abhängigkeit vom pH—Wert zwei verschiedene Komplexe (s. Spektren der Abb. 1). Das Spektrum mit λ_{max} = 570 nm (pH 2,9) ist dem Komplex AlHL, das mit λ_{max} = 545 nm (pH 6,4) dem Komplex AlL_2^{5-} zuzuordnen [6]. Abbildung 1 zeigt ausserdem im interessierenden Bereich die Spektren der bei pH 2,9 (H_3L^-) und pH 6,4 (HL^{3-}) vorliegenden Chromazurol S-Formen (Zuordnung nach Malat [5]).

Nach Pakalns [7] (Abb. 2, Kurve I) ist die Abhängigkeit der Extinktion vom Säuregrad der Lösung ausserordentlich ungünstig. Kurve II (Abb. 2) wurde von uns erhalten, wenn das molare Verhältnis Al:H_4L = 1:6 war und

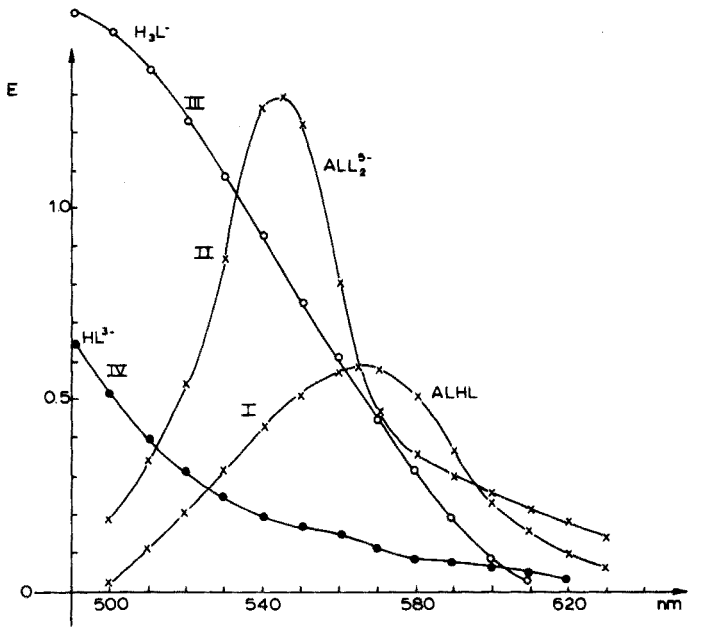

Abb. 1. Absorptionsspektren (I, II) von Lösungen, die Aluminium und Chromazurol S enthalten, gemessen gegen Blindlösung. [Al] = $0{,}04 \cdot 10^{-3}$ M; [H_4L] = $0{,}32 \cdot 10^{-3}$ M; d = 0,5 cm. I, pH 2,9; II, pH 6,4. Absorption der Blindlösung (III, IV), gemessen gegen Wasser. III, pH 2,9; IV, pH 6,4.

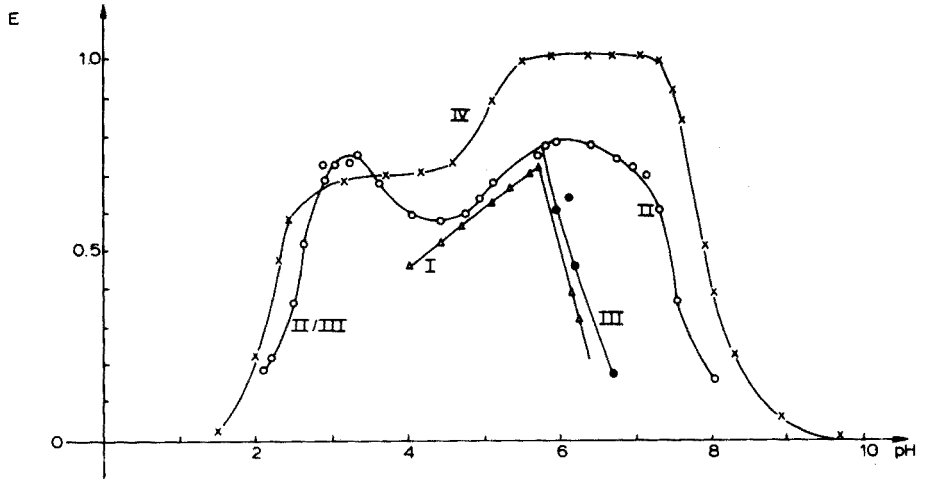

Abb. 2. Abhängigkeit der Extinktion vom Säuregrad. I: Nach Pakalns [7]. II: [Al] = $0{,}06 \cdot 10^{-3}$ M, [H_4L] = $0{,}35 \cdot 10^{-3}$ M; d = 0,5 cm; λ = 568 nm; gemessen gegen Blindlösung. Lösung acetatfrei. III: Wie II, Lösung acetathaltig. Bis zum pH 6 decken sich die Kurven II und III. IV: Wie II und III, aber [H_4L] = $1{,}20 \cdot 10^{-3}$ M.

zur Einstellung des Säuregrades nur Salzsäure und Natronlauge verwendet wurden, Kurve III unter den gleichen Bedingungen, aber bei Anwesenheit von Acetat/Essigsäure. Kurve IV erhielten wir bei einem molaren Verhältnis $Al:H_4L = 1:20$; hierbei wird der Verlauf der Kurve durch die Gegenwart von Acetat nicht beeinflusst.

Ein wenigstens zwanzigfacher molarer Überschuss an Chromazurol S ist erforderlich zur Erzielung der maximalen und vom weiteren Wachsen des Reagenzüberschusses unabhängigen Extinktion. Sie erreicht ihren höchsten Wert 10 min nach Reagenzzugabe und ist dann über mehrere Stunden unabhängig von der Zeit und der Lichteinwirkung unter normalen Laborbedingungen.

Aufgrund der Spektren (Abb. 1) und der pH—Abhängigkeit der Extinktion (Abb. 2) sollte die spektralphotometrische Bestimmung von Aluminium möglich sein bei pH ≈ 3 und 570 nm sowie bei pH ≈ 6,5 und 545 nm. Bei pH 4,6 (vgl. Pakalns [7]), müsste die Extinktion wegen des bedingungsabhängigen Gleichgewichtes zwischen zwei Komplexen bei der Wellenlänge des isosbestischen Punktes (568 nm) gemessen werden, damit die Erfüllung des Beerschen Gesetzes erwartet werden kann.

Die Erprobung des Verfahrens

Wir haben das Verfahren getestet bei pH 4,6 und 568 nm (vgl. Pakalns [7]), bei pH 2,9 und 568 nm, bei pH 6,4 und 568 nm sowie bei pH 6,4 und 545 nm. Da (erwartete) echte Selektivitätsunterschiede bei Variation des Säuregrades nicht auftraten, fällt der Gesichtspunkt der Selektivität bei der Festlegung der optimalen Bedingungen weg. Die grösste Empfindlichkeit (ϵ = 42000 bis 47000 l mol^{-1} cm^{-1}) ist bei pH 6,4 und 545 nm zu erzielen, jedoch ist das Beersche Gesetz unter diesen Bedingungen jeweils nur innerhalb eines halben Zehnerpotenzbereiches der Aluminiumkonzentration gültig. Die Erwartung, dass der Einfluss des vorzugsweise bei pH ≈ 3 existierenden AlHL—Komplexes bei pH 6,4 vernachlässigbar klein wäre, erfüllte sich demnach nicht. Als optimale Bedingungen wurden festgestellt pH 6,4 und 568 nm sowie ein wenigstens zwanzigfacher Reagenzüberschuss. Günstig ist pH 6,4 auch deshalb, weil bei pH < 5,3 die Extinktion der Blindlösung sehr hoch wird (Abb. 1).

Zu bemerken ist, dass bei pH 2,9 bei Verwendung von Glykokollpuffer die Extinktion insgesamt sinkt und ausserdem von der Pufferkonzentration abhängig wird. Citrat maskiert Aluminium bei pH 2,9 völlig. Das trifft auch zu für Phosphat (geprüft bei pH 6,4) und für Äthylendiamintetraacetat im pH—Bereich 3—7.

Versuche, das Aluminium—H_4L—System z.B. in Form des neutralen Komplexes AlHL bei pH 3 mit Chloroform, MIBK oder Amylalkohol bzw. in Form des anionischen AlL_2^{5-} — Komplexes bei pH 6,5 als Ionenassoziat oder durch flüssigen Ionenaustausch (unter Verwendung quaternärer Amine) zu extrahieren, waren bisher erfolglos.

Die photometrische Aluminium—Bestimmung mit Chromazurol S wurde im wesentlichen nach Gottschalk [8] ausgewertet.

EXPERIMENTELLES

Geräte. Spektralphotometer VSU 1 (VEB Carl Zeiss, Jena); pH-Meter MV 84 (VEB Präcitronic, Dresden), mit Glas- und Kalomelelektrode.

Aluminiumstandardlösung. Als Standardsubstanz diente $Al(NO_3)_3 \cdot 9\ H_2O$ reinst (VEB Berlin-Chemie). Entsprechende Einwaagen wurden im 1 l-Masskolben in 0,05 M Salpetersäure gelöst.

Chromazurol S-Lösung. 0,9 g Chromazurol S (Merck) wurden in 500 ml Aqua bidest. gelöst. (Nach Tagen dunkelblaue Ablagerungen an den Glaswänden.)

Pufferlösung. Ammoniumacetatlösung (1 M), deren Säuregrad durch Essigsäurezusatz auf pH 6,4 eingestellt war.

Arbeitsbedingungen. In einem 100 ml-Masskolben gibt man zu a ml (a = 1, 2, 4, 6, 8, 10) Aluminiumstandardlösung (0,1 mM), 8 ml Chromazurol S-Lösung, 40 ml Pufferlösung und füllt dann mit Aqua bidest. auf. Nach 10 min misst man die Extinktion bei einer Schichtdicke von 3 cm und der Wellenlänge 568 nm gegen Blindlösung. Es ist auch die Bestimmung der zehnfachen Aluminiumkonzentration möglich, wenn die Chromazurol S-Konzentration entsprechend erhöht und die Schichtdicke von 0,5 cm verwendet wird.

Ergebnisse

Das Beersche Gesetz ist jeweils erfüllt, die Berechnung der Aluminiumkonzentration erfolgt nach $[Al] = \omega \cdot E$ (Tab. 1). Der Versuch bei pH 6,4 und 545 nm wurde wegen der eingeschränkten Gültigkeit des Beerschen Gesetzes nicht statistisch ausgewertet.

Der Einfluss der im folgenden aufgeführten Ionen wurde untersucht. Keine

TABELLE 1

Versuchsergebnisse bei verschiedenen Bedingungen

Arbeitsbereich (μ mol ml^{-1})	0,01—0,10[a]	0,0012—0,012[b]	0,001—0,010[c]
ω (μ mol ml^{-1})	0,0852	0,0135	0,0103
ϵ (l mol^{-1} cm^{-1})	23470	24630	32480
s (μ mol ml^{-1})	±0,00110	±0,00020	±0,00009
s_r (%)	±(1,1—11,0)	±(1,7—17,2)	±(0,9—9,3)

[a] V = 100 ml, d = 0,5 cm, pH 4,6.
[b] V = 100 ml, d = 3 cm, pH 4,6.
[c] V = 100 ml, d = 3 cm, pH 6,4

Störung ergeben bis zu dem angegebenen molaren Überschuss: 10000: Na, K, SO_4^{2-}, Cl^-, ClO_3^-; 1000: Cu, Fe, Ca, Mg, Zn, Cd; 100: Ni, Co, Cr(III), Sn(II), Pb, OCl^-;10: Mn, W(VI); 1: Hg, Mo(VI).

Bei Kupferanwesenheit ist ein Zusatz von Natriumthiosulfat als Maskierungsreagenz erforderlich. Bei Eisen(III)—Anwesenheit muss Ascorbinsäure (oder bei kleinen Mengen Thioglykolsäure, die auch kleine Kupfermengen maskiert) zugesetzt werden.

Dem VEB Chemiekombinat Bitterfeld danken wir für die gewährte Unterstützung.

LITERATUR

1 J. A. Corbett und B. D. Guerin, Analyst (London), 91 (1966) 490.
2 W. N. Tichonow, Zh. Anal. Khim., 19 (1964) 1204.
3 M. Theis, Z. Anal. Chem., 144 (1955) 106.
4 E. A. Kaschkowskaja und I. S. Mustafin, Zavod. Lab., 24 (1958) 1189.
5 M. Malat, Anal. Chim. Acta, 25 (1961) 289.
6 H. Nishida, Bunseki Kagaku, 19 (1970) 972.
7 P. Pakalns, Anal. Chim. Acta, 32 (1965) 57.
8 G. Gottschalk, Statistik in der quantitativen chemischen Analyse, Enke—Verlag, Stuttgart, 1962.

Analytica Chimica Acta, 82 (1976) 213—215

Short Communication

IMPROVEMENT IN THE FLUORIMETRIC DETERMINATION OF SELENIUM IN PLANT MATERIALS WITH 2,3-DIAMINONAPHTHALENE

CHRIS C. Y. CHAN

Air Quality Laboratory, Ontario Ministry of the Environment, Toronto, Ontario (Canada)

(Received 14th July 1975)

Submicrogram quantities of selenium can be determined fluorimetrically with 2,3-diaminonaphthalene [1—4]. When plant materials are analyzed for selenium, a problem arises in the partial loss of selenium during digestion. In attempts to avoid volatilization losses, reflux condensing devices have been used. Hoffman [5] employed a Kjeldahl flask. Hall and Gupta [6] used a digestion flask fitted with a reflux adapter and controlled the temperature by heated silicone oil following a very lengthy procedure for complete digestion. Only a few samples can be digested simultaneously in such a complex fashion.

This communication reports a rapid digestion procedure with a modified fluorimetric method for the determination of selenium in vegetation. It has advantages over previous methods that are commonly tedious and time-consuming, being suitable for routine analyses of large numbers of samples.

A batch of samples is digested at a controlled temperature with nitric—perchloric acid mixture in test tubes in an aluminum block. Potential interferences are masked with EDTA, and selenium is complexed with 2,3-diaminonaphthalene and measured fluorimetrically after extraction into n-hexane.

Experimental

Apparatus. A Turner Model 110 fluorimeter fitted with a No. 7-60 (365 nm) primary filter and a combination of No. 58 (525 nm) and No. 2A-15 (520 nm) secondary filters, was used with matched 12 × 75-mm, cuvettes. A Corning Model 12 pH meter with glass and reference electrodes was used in pH adjustment.

Reagents. All reagents were analytical grade, unless otherwise specified.

For the stabilizing solution, dissolve 9.306 g of Na_2-EDTA and 25 g of hydroxylammonium chloride in 1 l of water.

For the 2,3-diaminonaphthalene solution [4], add 0.25 g of reagent to 25 ml of 12 M hydrochloric acid and dilute to 250 ml with water. Extract this solution with 10-ml portions of *n*-hexane several times until the fluorescence of the extract is negligible. Store the aqueous reagent under a

layer of n-hexane in a brown bottle in a refrigerator.

For the standard selenium solution, dissolve 0.1634 g of reagent-grade selenious acid in water and dilute to 1 l (100 μg Se ml^{-1}). Prepare 0.10, 0.20, 0.30 and 0.40 μg Se ml^{-1} working standards by dilution of the stock standard with 0.1 M hydrochloric acid.

Procedure. Digest 0.5 g of vegetation sample in a test tube (15 × 150 mm) with 4 ml of a (3 + 1) mixture of nitric acid (*d*,1.42) and perchloric acid (70 %). This tube is placed in a close-fitted hole in an aluminum block heated on a hot plate at a controlled temperature; a block can hold fifty samples. Add one glass bead and one drop of kerosene as a defoamer to the tube. Heat the sample at 40°—50 °C, for about 1 h. Increase the temperature to 70 °C and digest for about 6 h. Raise the temperature to 125 °C and digest further overnight.

Cool the solution and dilute with water. Filter the solution with rinsing into a 100-ml graduated beaker. Make up to 20 ml with water. Add 3 ml of stabilizing solution. Adjust the solution to pH 1.5 with 8 M ammonia solution and 6 M hydrochloric acid. Then add 2 ml of 2,3-diaminonaphthalene solution in dim light. Heat the solution just to the boil. Cool for 1—2 h in the dark. Transfer to 125-ml separatory funnel (Teflon stopcock), add 6.0 ml of Spectrograde n-hexane and shake vigorously for 30 s. Leave for 5 min for phase separation. Discard the aqueous portion and transfer the n-hexane extract by means of a disposable pipet into the cuvette. Read the fluorescence of the extract against a reagent blank.

Calculate the selenium content by comparing with standards which have been taken through the entire procedure, including the digestion. For adequate fluorimetric work, all glassware should be cleaned by rinsing with methanol and warm tap water followed by distilled water.

Results and discussion

Loss of selenium was observed when the temperature was too high during the initial digestion, probably because of entrainment by the nitrogen oxide fumes which surge rapidly. If the temperature is held first at 40 °C, and increased step by step, appreciable loss of selenium can be avoided. Recoveries were studied by adding known amounts of selenium to 0.5-g samples of mixed vegetation, and were found to be satisfactory (Table 1).

TABLE 1

Recovery of selenium added to mixed vegetation sample

Se added (μg)	—	0.040	0.200	0.400
Se found (μg)[a]	0.045	0.086	0.237	0.440
Recovery (%)	—	103	96	99

[a]Mean of 3 results.

The effect of shaking time on extraction of the selenium complex was studied for 0.30 μg Se standards. Quantitative extraction was attained after shaking for 10 s; time was not critical in this aspect, and it was unnecessary to prolong extraction beyond 30 s.

Calibration curves constructed by plotting fluorescence intensity against selenium concentration were linear in the range 0.05—0.40 μg Se.

To test the method, quadruplicate analyses were done on a variety of vegetation samples; standards were always analyzed simultaneously. The method shows good precision (Table 2). The blanks (contributed by the reagents taken through the entire procedure) are so low and reproducible, corresponding to 0.02—0.03 μg Se, that the method is reliable even at levels of 0.04 p.p.m. Se.

TABLE 2

Determination of selenium in vegetation samples
(The results are the mean and relative standard deviation for 4 determinations)

Sample	Se content p.p.m.[a]	s_r	Sample	Se content p.p.m.[a]	s_r
Birch	0.225	4.2	Aspen	0.731	5.4
Fern	0.043	6.8	Pine	0.469	6.1
Maple	0.088	4.6	Spruce	0.176	2.7
Grass	0.107	5.5	Orchard leaves (NBS standard)[a]	0.077	6.9

[a]Certified value is 0.08 ± 0.01 p.p.m. Se.

REFERENCES

1 W. H. Alloway and E. E. Carry, Anal. Chem., 36 (1964) 1359.
2 J. H. Watkinson, Anal. Chem., 38 (1966) 92.
3 I. Hoffman, J. Ass. Offic. Anal. Chem., 50 (1967) 917.
4 J. B. Wilkie and M. Young, J. Agr. Food Chem., 18(5) (1970) 944.
5 I. Hoffman, J. Ass. Offic. Anal. Chem., 51(5) (1968) 1039.
6 R. J. Hall and P. L. Gupta, Analyst (London), 94 (1969) 292.

Analytica Chimica Acta, 82 (1976) 217—221

Short Communication

DETERMINATION OF THE ACTIVITY COEFFICIENT OF TRICAPRYLMETHYLAMMONIUM CHLORIDE AND THE STABILITY CONSTANTS OF THE AQUEOUS COMPLEXES FORMED IN THE EXTRACTION OF ZINC(II) FROM HYDROCHLORIC ACID SOLUTIONS

TAICHI SATO and SHIGERU MURAKAMI

Department of Applied Chemistry, Faculty of Engineering, Shizuoka University, Hamamatsu (Japan)

(Received 24th April 1975)

The activity coefficient of a solute is very important in studies of the chemical properties of solutions. Activity coefficients for various compounds are available [1—4] but the values obtained are limited. In the present work, the activity coefficient of a long-chain alkylammonium salt in benzene was determined by means of a vapour pressure method, and the stability constants of the complexes formed in the aqueous phase in the extraction of zinc(II) from hydrochloric acid solutions by Aliquot-336 were calculated.

Experimental

Tricaprylmethylammonium chloride (General Mills, Aliquat-336, $R_3R'NCl$) was purified by washing with aqueous sodium chloride solution and n-hexane [5]. For aqueous solutions of zinc(II), zinc chloride was dissolved in hydrochloric acid of the required concentration. Other chemicals used were of analytical reagent grade.

Distribution coefficients were determined as described previously [5], except that zinc in the organic phase was stripped with 1 M nitric acid solution. Zinc was determined by titration with EDTA and xylenol orange indicator [6].

A Hitachi Model 115 isothermal molecular-weight apparatus equipped with a vapour meter based on a thermistor detector was used.

The chloride ion in the aqueous solution after extraction, was determined with a Toa model IM-1A ion-densitometer equipped with a chloride-selective electrode (CL-125).

The stability constants of the complexes formed in the solvent extraction system were calculated with a FACOM 230-45 S computer.

Determination of activity coefficient of Aliquat-336

The molecular weight apparatus used is based on the vapour-pressure method, hence

$$\Delta T_b = -\frac{RT_0^2}{\Delta h_0^0} \ln a_0 \quad (1)$$

where ΔT_b is the difference in the boiling points of sample solution and pure solvent, Δh_0^0 the latent heat of the pure solvent, R the gas constant, T_0 the temperature of measurement, and a_0 the activity of the solvent. In this work, ΔT_b values for benzene solutions of Aliquat-336 were measured for varying concentrations of the solute at 42.7°C (T_0); the Δh_0^0 value used for benzene was 7.8 kcal mol^{-1} [7, 8]. The results are shown in Table 1.

The Gibbs—Helmholtz equation for the relationship between the solvent and solute can be written

$$x_0 \frac{\partial \ln a_0}{\partial x_1} + x_1 \frac{\partial \ln a_1}{\partial x_1} = 0 \quad (2)$$

where x_0 and x_1 are the mole fractions of solvent and solute, respectively. Suitable substitution and integration yield the form

$$\ln (a_1/x_1) = \ln \gamma_1 = -\int_0^x (1 - x_1)/x_1 \, \mathrm{d} \ln \gamma_0 \quad (3)$$

where γ_0 and γ_1 are the activity coefficients of the solvent and solute, respectively, in the sample solution. As the activity coefficient of benzene in the solution of Aliquat-336 can be determined from eqn. (1), the activity coefficient of Aliquat-336 in benzene can be obtained by graphical integration of the curve $(1 - x_1)/x_1$ vs. $\ln \gamma_0$ (Fig. 1). The relationship between the activity coefficient and the molarity of Aliquat-336 in benzene is given in Fig. 2; molarity is used here (cf. Table 1) because the density of Aliquat-336 can be ignored at the low concentrations used. Figure 2 shows that the activity coefficient decreases steeply as the concentration of Aliquat-336 increases to about 0.02 M, and then more gradually until it reaches almost

TABLE 1

Data for varying the concentration of Aliquat-336 in benzene

$[R_3R'NCl]$ ($\cdot 10^{-2}$ mol kg^{-1})	$\frac{1-x_1}{x_1}$	ΔT_b ($\cdot 10^{-2}$ K)	$\ln a_0$ ($\cdot 10^{-4}$)	$\ln \gamma_0$ ($\cdot 10^{-3}$)
1.09	1174	0.65	−2.580	0.434
1.92	665.7	0.88	−3.466	1.260
2.86	433.8	1.20	−4.720	1.831
3.82	334.1	1.65	−6.496	2.346
5.08	250.9	2.11	−8.307	3.087
6.41	199.0	2.44	−9.606	3.879
8.26	154.0	2.78	−10.945	5.605

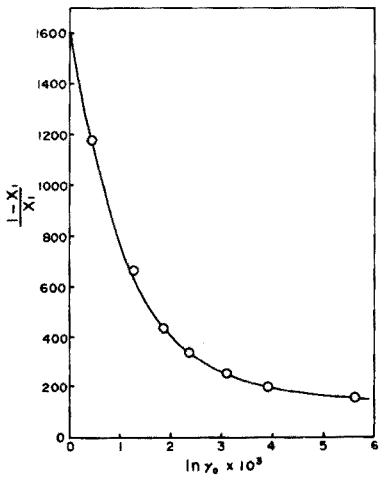

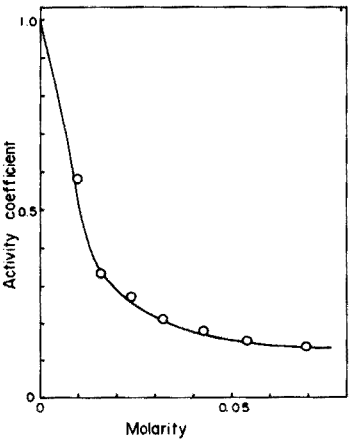

Fig. 1. Variation in the values of $(1 - x_1)/x_1$ vs. $\ln \gamma_0$.

Fig. 2. Activity coefficient of Aliquat-336 in benzene.

a limiting value. It appears that if Aliquat-336 is to be used in quantitative analyses without activity coefficient corrections, its concentration should be below 0.001 M ($\gamma_1 \approx 1$) or above 0.05 M (γ_1 becomes nearly a constant).

Determination of stability constants in the extraction system

The extraction of $7.1 \cdot 10^{-3}$ M zinc(II) from aqueous solutions containing hydrochloric acid of varying acidity with solutions of Aliquat-336 in benzene at 20 °C gave the results shown in Fig. 3. The distribution coefficient passes through a maximum at initial HCl concentrations of ca. 2 M. However, when part of the hydrochloric acid, which competes for association with Aliquat-336, is replaced by lithium chloride, the decrease in the distribution coefficient at higher aqueous acidities is checked; this implies that the controlling factor for extraction is the total chloride concentration. In the extraction of zinc chloride solutions ($7.1 \cdot 10^{-3}$ M) containing 2 M HCl or 0.2 M HCl in the presence of 1.8 M lithium chloride by 0.1 M Aliquat-336 in benzene, the zinc molarity in the organic phase as a function of initial aqueous zinc molarity approached a limiting value of ca. 0.05. For those organic phases, the mole ratio of the chloride molarity to the molarity of zinc extracted reached a limiting value of 4. This suggests that the zinc complex in the organic phase contains zinc : chloride : $R_3R'N^+$ in the molar ratio 1 : 4 : 2, indicating the formula $(R_3R'N)_2ZnCl_4$.

After formation of tetrachlorozincate ions in the aqueous phase, the extraction system can be represented [5, 9] by

$$ZnCl_4^{2-}\ (a) + 2\ R_3R'NCl\ (o) \rightleftharpoons (R_3R'N)_2ZnCl_4\ (o) + 2\ Cl^-\ (a) \qquad (4)$$

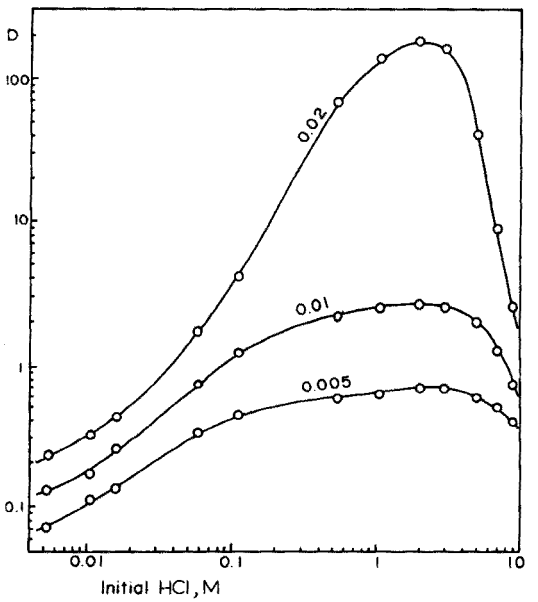

Fig. 3. Extraction of zinc(II) from hydrochloric acid solutions by Aliquat-336 in benzene. (The numbers on the curves are the Aliquat-336 molarities when multiplied by the factor 1.0978.)

where (a) and (o) indicate the aqueous and organic phases, respectively. Thus

$$K = \frac{[(R_3R'N)_2ZnCl_4]_{(o)}}{[Zn^{2+}]_{(a)}[Cl^-]_{(a)}[R_3R'NCl]^2_{(a)}} \tag{5}$$

and

$$D = \frac{K[Cl^-]^2_{(a)}[R_3R'NCl]^2_{(o)}}{1 + \sum_{j=1}^{N} \beta_j [Cl^-]^j_{(a)}} \tag{6}$$

where K is the equilibrium constant, D the distribution coefficient, β_j the over-all stability constants, viz. $[ZnCl_j^{2-j}]_{(a)}/[Zn^{2+}]_{(a)}[Cl^-]^j_{(a)}$, and the subscripts (a) and (o) denote the equilibrated concentrations of the aqueous and organic phases, respectively. In eqn. (6), $[R_3R'NCl]_{(o)}$ is corrected by using the activity coefficient obtained from eqn. (3). Since eqn. (6) can be considered as a function containing five parameters and two variables, the parameters can be determined by iterative techniques. The distribution data for the aqueous species formed in the extraction of $7.1 \cdot 10^{-3}$ M zinc chloride solutions at different hydrochloric acid concentrations, which were used in calculation, are listed in Table 2. The stability constants of the aqueous zinc complexes formed in this extraction system were found to be: $\beta_1 = 3.07$, $\beta_2 = 1.01$, $\beta_3 = 8.25$ and $\beta_4 = 1.04$.

TABLE 2

Distribution data for calculation of β_j

Initial $[R_3R'NCl]$ (· 1.0987 M)	Initial aq.[HCl] (M)	D	$[Cl^-]_{(a)}$ (M)	$[R_3R'NCl]_{(o)}$ (M)
0.02	0.112	4.16	0.0927	0.0103
	0.0584	1.77	0.0504	0.0128
	0.0159	0.430	0.0191	0.0177
	0.0106	0.320	0.0150	0.0185
	0.00532	0.224	0.00826	0.0207
0.01	0.537	2.20	0.534	0.00101
	0.112	1.27	0.0949	0.00278
	0.0584	0.771	0.0498	0.00466
	0.0159	0.258	0.0181	0.00802
	0.0106	0.170	0.0144	0.00886
	0.00532	0.131	0.00993	0.00930
0.007	0.112	0.690	0.1028	0.00188
	0.0584	0.475	0.0570	0.00312
	0.0159	0.174	0.0214	0.00558
	0.0106	0.128	0.0170	0.00608
	0.00532	0.0760	0.0120	0.00668
0.005	0.112	0.440	0.0798	0.00105
	0.0584	0.333	0.0498	0.00189
	0.0159	0.134	0.0185	0.00379
	0.0106	0.115	0.0147	0.00399
	0.00532	0.0730	0.00960	0.00451
0.0035	0.107	0.250	0.0935	0.00100
	0.0534	0.198	0.0460	0.00150
	0.0108	0.0664	0.0160	0.00296
	0.00553	0.0471	0.0125	0.00320
	0.00128	0.0352	0.00973	0.00336
	0.000744	0.0320	0.00931	0.00346
	0.000213	0.0305	0.00897	0.00342

REFERENCES

1 M. Davies and D. K. Thomas, J. Phys. Chem., 60 (1956) 41.
2 C. F. Baes, Jr., J. Phys. Chem., 66 (1962) 1629.
3 A. S. Kertes and G. Markovits, Proc. Symp. Thermodyn. Nucl. Mater., 1967, Vienna, p. 227 (1968).
4 E.g., F. J. C. Rosssotti and H. Rossotti, The Determination of Stability Constants, McGraw—Hill, New York, 1961, pp. 17—37; and the literature cited therein.
5 T. Sato and H. Watanabe, Anal. Chim. Acta, 49 (1970) 463.
6 J. Körbl and R. Pribil, Chemist—Analyst, 45 (1956) 102.
7 J. H. Matthews, J. Amer. Chem. Soc., 48 (1926) 562.
8 M. L. Bradford and G. Thodos, J. Chem. Eng. Data, 12 (1967) 373.
9 T. Sato, J. Inorg. Nucl. Chem., 34 (1972) 3855.

Analytica Chimica Acta, 82 (1976) 223—226

Short Communication

A CARBON FIBRE pH ELECTRODE FOR ACID—BASE TITRATIONS

V. J. JENNINGS and P. J. PEARSON

Department of Chemistry and Metallurgy, Lanchester Polytechnic, Coventry, CV1 5FB (England)

(Received 20th July 1975)

It has recently been reported that the potential of a single carbon fibre electrode 1 cm long and 7—8 μm in diameter varies linearly with pH changes in aqueous solutions [1]. The Nernst slope factor is about —50 mV per pH unit at 20 °C. The present communication describes the fabrication and use of such electrodes for the detection of the end-point in titrations of hydrochloric, acetic and orthophosphoric acids. The advantages of such a pH indicator electrode are its low cost, low impedance, and suitability for micro-volume pH measurements; the electrode is viable for a pH range of at least 1—13.

Experimental

Preparation of carbon fibre electrodes. The electrodes were prepared by soldering a 1.5-cm length of carbon fibre (Courtaulds Ltd., low-temperature, 8-μm diameter (Type AS) to a 0.028-in. (tin coated) single strand copper wire. The solder joint was coated with an epoxy resin (Araldite) and sealed into a borosilicate glass tube (8 cm long, 3 mm i.d., 6 mm o.d.) with the same resin. The resin was then allowed to harden at room temperature for 24 h. About 1 cm of the carbon fibre was exposed. As an alternative to Araldite, a quicker drying polyester—polystyrene resin (Isopon) was also used.

Reagents and solutions. Reagents were of analytical grade. Phthalate, phosphate and borate buffer solutions were prepared by standard procedures [2]. Standard solutions of 0.1 M hydrochloric acid and 0.1 M sodium hydroxide with pH values of 1.11 and 12.99, respectively, were also used.

Potential measurements. The potential of the carbon fibre electrode was measured against a calomel electrode (EIL SCE/4) with a Corning EEL model 109 digital pH meter used in its mV mode. It was necessary to use a screened coaxial lead to connect the copper wire terminal of the carbon fibre electrode to the pH meter, because any stray leakage currents caused potential instability. The carbon fibre and SCE electrodes were immersed in a 100-ml beaker containing 50 ml of buffer solution, which was stirred magnetically.

Nitrogen containing less than 10 p.p.m. oxygen (B.O.C. Ltd. White spot grade) was bubbled through the solution during potential measurements. The pH of each solution was measured with an Activion Glass pH electrode with a stated alkaline error at 25 °C of about 0.005 pH in 0.1 M sodium hydroxide, and a negligible acid error down to pH 0.

Potentiometric titrations. Standard solutions of hydrochloric, acetic and orthophosphoric acids were prepared with concentrations of 1.0, 1.0 and 0.5 M, respectively. Aliquots (25 ml) of each of these solutions were titrated with 1.0 M sodium hydroxide solution. The potential was measured, under conditions similar to those described above, at 1,2 and 3-min intervals after each increment of titrant from a 50-ml burette had been added. The volumetric glassware was of Grade A quality.

Results and discussion

Table 1 shows typical values obtained for the rate of potential change with time of a carbon fibre electrode in the various buffered solutions at 20.8 ± 0.2 °C. Potentials stable to about 1 mV were established within 5 min, except for 0.1 M sodium hydroxide for which times of 10 min were required.

The carbon fibre electrode used had been stored previously in distilled water for a period of 7 weeks. A graphical plot of the results in Table 1 showed a slope of about −49 mV per pH unit, though this electrode had a slope of −54 mV per pH unit at 19°C during the first 3 weeks after its fabrication; there was therefore some deterioration in response with age. However, another electrode which had been stored in distilled water for 15 days gave a response of −45 mV per pH, but a response of −51 mV per pH unit after a further two days in distilled water; this suggests that some form of activation by pH variation is required by the carbon fibre.

Some experiments were done with a carbon fibre electrode which had

TABLE 1

Rate of potential equilibration of a carbon fibre electrode vs. SCE in various buffered solutions

Buffer	Measured pH	Potential (mV) after (min)					
		0	1	2	3	4	5
0.10 M HCl	1.19	340	342	342	343	343	343
0.05 M COOH C_6H_4COOK	4.00	169	177	180	182	184	186
0.025 M KH_2PO_4 0.025 M Na_2HPO_4	6.90	44	40	43	45	47	48
0.0087 M KH_2PO_4 0.030 M Na_2PO_4	7.43	30	28	29	30	31	32
0.010 M $Na_2B_4O_7$	9.30	−50	−54	−55	−54	−54	−54
0.10 M NaOH	12.99	−207	−197	−190	−186	−186	−181

been dried in a silica gel desiccator. The potential of this electrode was initially unstable in a pH 4 buffer, and declined from 274 mV to 250 mV in about 10 min; but the potential variation with time was much less when the other buffer solutions were used. Accordingly, the electrodes must be stored in aqueous solutions.

Table 2 shows the potential variation given by 6 freshly prepared electrodes in a pH 4.00 buffer solution. Two of these electrodes (3 and 6) were made in a loop form so that only the surface of the longitudinal axis of the fibre was exposed to the solution; it is of interest that their potentials are almost identical. The cross-sectional surface of the carbon fibre used for this work is structurally very different from the longitudinal surface. Scanning electron micrographs have shown that some carbon fibres have sheath-like elements concentric to the fibre axis [3], and this effect could account for the difference in potential found for the different 1-cm single-strand carbon fibre electrodes shown in Table 2.

Figures 1, 2 and 3 are typical potentiometric titration graphs for hydrochloric, acetic and phosphoric acids, respectively; for comparison the pH glass electrode titration curves are also shown. The end-points found with the two electrodes agreed to within 0.1 ml. The potential of the carbon fibre electrode was read at 1, 2 and 3 min after each addition of titrant. Figure 1 shows that a plot of the results obtained after 1 min does not affect the position of the end-point though the potentials become more negative after the 3-min intervals. The slight kinks in the graphs indicate some irreversible electrode behaviour immediately before the end-point. A similar effect was observed in the titration of sulphuric acid. The effect may be due to a slower response to pH changes in strong acid solutions. Repeated titrations gave similar potential readings, as shown in Fig. 3. for the titration of phosphoric acid.

The response of the carbon fibre to pH changes is believed to be due to the ionization of carboxylic acid groups formed on the surface of carbon by surface reactions with atmospheric oxygen [1]. Preliminary results suggest that a carbon fibre electrode can also detect end-points in redox and argentimetric titrations, analogously to the graphite electrode of Růžička et al. [4].

We thank the Carbon Fibres Unit of Courtaulds Limited, Coventry for the gift of the carbon fibres.

TABLE 2

Potentials of freshly prepared carbon fibre electrodes vs SCE after equilibration for 10 min in a pH 4.00 buffer

Electrode	1	2	3[a]	4	5	6[a]
mV (vs. SCE)	215	204	182	172	187	181

[a]Loop type.

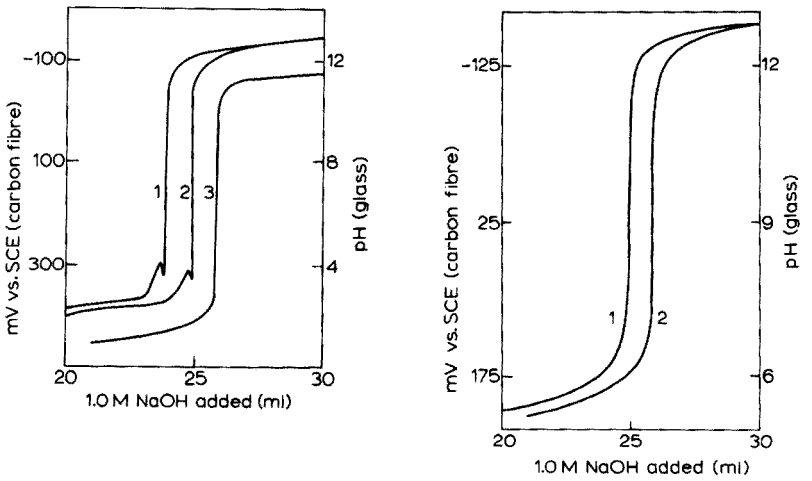

Fig. 1. Potentiometric titration of 25 ml of 1.0 M hydrochloric acid with 1 M sodium hydroxide. Curves 1 and 2: carbon fibre electrode; potentials after 1 min and 3 min respectively. Curve 3: pH with glass electrode. For clarity of presentation, curves 1 and 3 have been offset by 1.0 ml from curve 2.

Fig. 2. Potentiometric titration of 25 ml of 1.0 M acetic acid with 1.0 M sodium hydroxide. Curve 1: carbon fibre electrode, potential after 3 min. Curve 2: pH with glass electrode. The scale has been offset by 1 ml for curve 2.

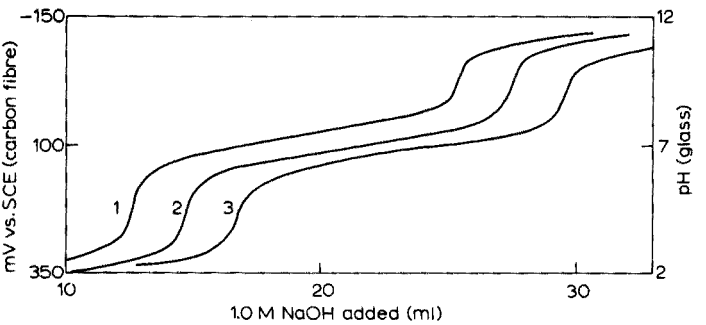

Fig. 3. Potentiometric titration of 25 ml of 0.5 M orthophosphoric acid with 1.0 M sodium hydroxide. Curves 1 and 2: carbon fibre electrode, potential after 3 min; curve 2 has been offset by +2 ml for clarity. Curve 3: pH with glass electrode; this curve has been offset by +4 ml from curve 1 for clarity.

REFERENCES

1 V. J. Jennings and P. J. Pearson, Nature (London), 256 (1975) 31.
2 R. G. Bates, J. Res. Natl. Bur. Stand. (USA), 66A (1962) 179.
3 M. Stewart, M. Feughelman and L. M. Gillen, Nature (London) 235 (1972) 274.
4 J. Růžička, C. G. Lamm and J. C. Tjell, Anal. Chim. Acta, 62 (1972) 15.

Analytica Chimica Acta, 82 (1976) 227—229

ANNOUNCEMENTS

Vorschau auf Veranstaltungen der Gesellschaft Deutscher Chemiker 1976 und 1977

1976

29—31 März	*Jahrestagung der GDCh-Fachgruppe "Makromolekulare Chemie"* Bad Nauheim.
29 März—2 April	*Chemiedozententagung veranstaltet von ADUC, verbunden mit einer GDCh-Festsitzung,* Regensburg.
4—9 April	*EUCHEM-Konferenz "Organic Liquids: Structures, Dynamics and Chemical Properties"* Schloss Elmau b. Mittenwald.
9—13 April	*ANALYTIKA* veranstaltet von der Deutschen Gesellschaft für Klinische Chemie, der Gesellschaft Deutscher Chemiker mit den Fachgruppen "Analytische Chemie" und "Lebensmittelchemie und gerichtliche Chemie" und der Gesellschaft für Biologische Chemie, München.
21—23 April	*Sixth Annual Symposium on Recent Advances in the Analytical Chemistry of Pollutants* mitveranstaltet von der GDCh-Fachgruppe "Analytische Chemie", Wien.
26—29 April	*Osterreichisch-Deutsches Chemikertreffen* gemeinsam veranstaltet von Verein Österreichischer Chemiker und Gesellschaft Deutscher Chemiker, Salzburg.
24—26 Mai	*Jubiläumstagung der GDCh-Fachgruppe "Wasserchemie"* zum 50 jährigen Bestehen, verbunden mit einer GDCh-Festsitzung am 24 Mai 1976, Kiel.
20—26 Juni	*ACHEMA —XVIII Ausstellungstagung für chemisches Apparatewesen und Europäisches Treffen für Chemische Technik.* Frankfurt/Main. GDCh-Festsitzung am 23 Juni 1976.

5—9 Juli	*IMEBORON III—Third International Meeting on Boron Chemistry* verbunden mit einer GDCh-Festsitzung aus Anlass des 100. Geburtstages von Alfred Stock am 5 Juli 1976, München und Ettal.
12—16 Juli	*VIIth International Symposium on Organic Sulphur Chemistry*, Hamburg.
25—31 Juli	*Tenth International Congress of Biochemistry* veranstaltet von der Gesellschaft für Biologische Chemie, organisiert von der GDCh, Hamburg.
6—10 September	*XVIIth International Conference on Coordination Chemistry - ICCC*, Hamburg.
13—17 September	*5th International Conference on Modern Trends in Activation Analysis* unter Mitwirkung der GDCh-Fachgruppen "Analytische Chemie" und "Kern-, Radio- und Strahlenchemie", München.
2 Septemberhälfte	*Vortragstagung der GDCh-Fachgruppe "Medizinische Chemie"*, Münster.
20—21 September	*Tagung des Arbeitskreises Chromatographie* in der GDCh-Fachgruppe "Analytische Chemie" mit der British Chromatography Discussion Group und der französischen GAMS, Baden-Baden.
20—23 September	*GDCh-Festsitzung* im Rahmen der 109. Versammlung der Gesellschaft Deutscher Naturforscher und Ärzte, Stuttgart.
22—25 September (voraussichtlich)	*Jahrestagung der GDCh-Fachgruppe "Chemieunterricht"*,
27 Sept.—1 Okt.	*VI. Internationales Farbensymposium*, Freudenstadt/ Schwarzwald.
29 Sept.—1 Okt.	*Deutscher Lebensmittelchemikertag* veranstaltet von der GDCh-Fachgruppe "Lebensmittelchemie und gerichtliche Chemie", Münster.

6—8 Oktober	*Vortragstagung der GDCh-Fachgruppe "Anstrichstoffe und Pigmente"*, Aachen.
7—8 Oktober	*Vortragstagung der GDCh-Fachgruppe "Angewandte Elektrochemie" über 'Elektroden in der Elektrochemie'* Erlangen.
7—8 Oktober	*Vortragstagung der GDCh-Fachgruppe "Waschmittelchemie"*, Aachen.
Herbst	*Gemeinsame Tagung der GDCh-Fachgruppe "Analytische Chemie" mit den Chemikerausschüssen von VDEh und GDMB.*
18—19 November	*Vortragstagung der GDCh-Fachgruppe "Photochemie"*, Göttingen.

1977

28 März—1 April	*VI Europäisches Fluorsymposium*, Dortmund.

Unterlagen bei der GDCh-Geschäftsstelle, D-6000 Frankfurt/M 90, Postfach 90 04 40, angefordert werden können.

INTERNATIONAL CONFERENCE ON MODERN TRENDS IN ACTIVATION ANALYSIS

edited by **T. BRAUN,** Institute of Inorganic and Analytical Chemistry, L. Eötvös University, and **E. BUJDOSÓ,** Head of the Isotope Laboratory, Research Institute for Non-ferrous Metals, Budapest.

Reprinted from the Journal of Radioanalytical Chemistry.

1974. 933 pages. US$93.75/Dfl. 225.00. ISBN 0-444-99879-9

CONTENTS:

Elsevier Scientific Publishing Company

P.O. Box 211

Amsterdam, The Netherlands

A 1507E

(Continued from page 4 of cover)

Printed in The Netherlands

VOL. 82 No. 1 ANALYTICA CHIMICA ACTA MARCH 1976

CONTENTS

(continued on inside page of the cover)